ELECTRICAL AND OPTICAL PROPERTIES OF CHALCOGENIDE GLASSES

BY

Kenneth Hulls, B.Sc.

A thesis submitted for the degree of
Doctor of Philosophy of the
University of Warwick

School of Physics,
University of Warwick

December 1970

To my wife, whose love and patience
have been a continual source of
encouragement, and to my parents.

ACKNOWLEDGEMENTS

I am grateful to Dr P. W. McMillan for his supervision, continued interest and encouragement throughout the duration of this work, and for his careful reading of the manuscript. I should also like to thank Professor A.J. Forty for allowing me to use the facilities of the School of Physics, and Dr H. Harper, for his help and valuable discussions concerning all aspects of the work.

The project could not have been completed without the considerable aid of the members of the mechanical and glass workshops, whose assistance in the construction of apparatus I gratefully acknowledge. In particular I should like to thank Mr James Huckfield for the application of his skill in the construction of the Infra-Red cryostat.

Mr John Francis made the measurements of section 8.03 which proved so useful. Miss Sylvia Alexander of the School of Engineering Science carefully prepared the typescript and Mrs Christine Allsopp the diagrams.

Finally I should like to thank the English Electric Nelson Laboratories of Stafford, for the provision of funds for my own maintenance and also for equipment.

MEMORANDUM

This dissertation is submitted to the University of Warwick in support of my application for admission to the degree of Doctor of Philosophy. It contains an account of my own work performed at the School of Physics of the University of Warwick in the period October 1967 to September 1970 under the general supervision of Dr P.W. McMillan. No part of it has been used previously in a degree thesis submitted to this or any other university. The work described in this thesis is the result of my own independent research except where specifically acknowledged in the text.

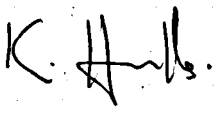

K. Hulls

ABSTRACT

A number of chalcogenide glasses, representing the complete glass forming regions of the three binary systems Selenium-Arsenic, Selenium-Tellurium, and Tellurium-Arsenic were prepared in bulk form.

For each of the glasses in each of the three systems, measurement of d.c. conductivity over a large temperature range, and optical absorption also over a large temperature range were completed. The Hall effect was looked for in the glasses from the Tellurium-Arsenic system. Other supporting experiments, namely, space charge limited current measurements in representative glasses from two systems, and density measurement of all glasses were carried out. X-Ray diffraction tests were used to identify each material as amorphous.

A description is given of the material and specimen preparation techniques, as are details of experimentation.

A consideration of some current theoretical ideas is shown to point to a density of states model which should apply to a large range of amorphous semiconductors.

Based upon this model certain computer calculations are made:

The temperature dependence, of the density of free carriers in the conduction and valence bands, and the position of the Fermi energy as a function of temperature are determined. The calculations assume, acceptor, and donor, character for the localized states (proposed in the model) associated with the conduction and valence bands respectively.

A second group of calculations is made to determine the variation of optical absorption coefficient with incident photon energy, assuming band to band transitions to be the dominant absorption mechanism.

A comparison between the calculated and empirically determined functions for the above two cases, plus those of the space charge limited current measurement is made so that a number of conclusions can be drawn. These include amongst others, the 'universal' nature of the density of states model, the existence and role of localized states, the nature of the conductivity, i.e. intrinsic or extrinsic, and the validity of the calculations.

An anomolous low temperature, conductivity - temperature - electric field, characteristic is found in annealed specimens of certain glasses. This effect is discussed and is thought to be associated with 'hopping conduction'.

Other questions concerning, variation of properties with composition, the difference bulk and thin film produced samples, and quality of electrical contacts are raised and discussed.

CONTENTS

CHAPTER 1

GENERAL INTRODUCTION

1.01.0 CHALCOGENIDE GLASSES AND AMORPHOUS SEMICONDUCTORS

Chalcogenide glasses, being those glasses based on one or more of the elements Sulphur, Selenium and Tellurium, form a large and important group, of a class of materials known as amorphous semiconductors. They are distinguished from other groups in that they are solid, as opposed to liquid, do not contain oxygen, and are easily produced in bulk from the melt and do not require the more rapid quenching processes entailed in thin film production.

Throughout this work the term chalcogenide glass is considered synonomous with term amorphous semiconductor. The justification for this is that many of the aspects discussed, particularly in relation to the band structure are expected to apply to other groups of disordered materials.

The expression semiconductor as used in this work requires defining. In the simplest terms, it refers to any material which conducts electronically (rather than ionically), the conductivity of which over any temperature interval will be governed by a characteristic activation energy, or energies. This energy, will often be associated with a region of forbidden energy in the band structure of the material.

It is immediately obvious that this definition is further reaching than that used for crystalline semiconductors. As defined here a material with a conductivity of 10^{-16} ohm^{-1} cm^{-1} may still be semiconducting. Such a value for the conductivity of a crystalline material would require it to be in the class of an insulator, although a characteristic activation energy may still govern the temperature dependence of the conductivity. A more appropriate term for many of these materials may be semi-insulating.

The term amorphous should also be defined. It is here meant only to imply the absence of any long range order (over $\triangleq$ 100 Å or more) in the atomic structure of the material. Hence for example such materials as two phase glasses, polycrystalline solids with crystallite size >100 Å will still be classed as amorphous.

1.02.0 HISTORICAL NOTE

With the exceptions of amorphous selenium and arsenic tri-sulphide, chalcogenide glasses were not generally known, and considered as a separate group of materials until the latter part of the 1950's. At this time work began to be published, principally from the U.S.S.R. by Kolomiets, Goryunova et al (see for example [1] - [3]) and also by Pearson et al ([4][5]). These works reported mainly new glasses, and glass forming limits, but also the initial findings of fundamental physical properties. A number of review articles summarize this work ([6] - [9]).

As theoretical interest in disordered solids increased and the materials became established in their own right, more work was published, primarily on theoretical predictions and electrical and optical properties (specific references to some of this work is made in the introduction to chapter 3).

In 1965 the first International Conference on Liquid and Amorphous Semiconductors took place. Since then two further conferences have been held, the most recent being in 1969. In the published proceedings of the 1969 Conference [10] there are a number of review articles summarizing various aspects of amorphous semiconductors.

1.03.0 THE IMPORTANCE OF AMORPHOUS SEMICONDUCTORS

With established crystalline semiconductors satisfying the vast majority of the needs of the electronics industry the question of the importance, and need for amorphous semiconductors becomes in many ways a valid one.

There are several possible answers to this question, some of which even by themselves would require work to be done on this group of materials. Some of these points will now be briefly discussed. The order in which they are considered is not intended to imply any scale of importance.

From the physicist's point of view, these materials form an easily obtainable and reproducible class of disordered solids, and as more and more of the problems concerned with electronic properties of materials with ordered lattices are solved, it is reasonable that theoreticians and experimentalists, should begin to consider the more difficult problems of disordered structures. Ioffe and Regel [9] first pointed out one of the most important aspects of these materials: From a theoretical viewpoint a regular crystalline potential (implying long range order) is a necessary condition for the band structure of allowed electron states. But from the first investigations on amorphous semiconductors it was apparent that the concept of a band structure still applied. Short range order and the prevailing form of the chemical bond then become the requisites for a band structure, and an understanding of these becomes important. The chalcogenide glasses (as a class of amorphous solids) many of which have reasonable conductivities provide a potential source of data, upon which a phenomenological theory can be based, or which could be used to verify other theoretical predictions.

From a technological point of view, amorphous semiconductors have an apparently vast potential, which stems from a number of properties: In particular they can transmit in the infra red to considerably longer wavelengths than oxide glasses, and of course many are truly semiconducting, as regards the actual magnitude of the conductivity. It also became apparent even from early investigations [11] that impurities do not generally affect the electronic properties so drastically as is the case

for crystalline semiconductors. Any relaxing of the high specifications of purity in manufacturing processes would obviously be advantageous.

The apparently insatiable requirements of the electronics industry for new and improved devices also created interest in properties peculiar to these materials: Firstly many of the materials are reported to show an anomolous switching behaviour (see[20][21] of chapter 6) where a simple two terminal device can change its resistance state merely by the application of an appropriate voltage. The switching occurs very rapidly, and some 'devices' are capable of staying in the switched state, exhibiting a form of memory function. Also since the materials are already highly disordered they are impervious to even excessive radiation doses [12].

The understanding and exploitation of these properties could be of great technological importance.

These and other points not mentioned, can be seen to place amorphous semiconductors in the class of materials for which a much greater understanding is required.

1.04.0 DEFINING THE PROJECT

Bearing in mind the 'state of the art' at the commencement of the project, there were a number of paths which a study of the fundamental properties of amorphous semiconductors conductors could have taken.

One of the initial decisions, taken almost immediately, was to work exclusively on bulk produced materials as opposed to thin vacuum deposited films. Two reasons are put forward to explain the choice; (a) Owing to the different evaporation rates and melting temperatures of the initial constituents, the proportions of these constituents in the final (thin film) product cannot be accurately known. The same problem does not occur with bulk materials. (b) There are considerable difficulties in the

reproducible production of thin films. Such parameters as substrate temperature, ambient pressure and residual gases must be very carefully controlled to obtain any reproducibility. Also the actual structure of a thin film may differ from the melt, due to the far more rapid quenching processes that are operative.

Two more factors further defined the project. Firstly it was decided to investigate a range of glasses in an attempt to determine if any general features of amorphous semiconductors(strictly chalcogenide glass) exist (This statement anticipates to some extent the discussion in chapter 3, where it becomes obvious that a model containing features which should be common to all materials, is arguable). Secondly the glasses would only be simple binary glasses. In fact up till 1967 the great majority of chalcogenide glasses reported were very complex, containing as many as five and six elemental components([1] - [5]). In using binary glasses any quantitative analysis of the results would become much simpler (Note: Only one elemental glass exists, this being amorphous selenium).

The final decision, as to which glasses, or glass systems were to be investigated, was left until a preliminary investigation of the glasses and glass forming systems had been undertaken.

The final choice, was to investigate glasses made from binary combinations of Selenium,Tellurium and Arsenic. The criteria on which the decision was based were (a) conductivity and range of conductivity of these glasses, (b) the compositions comprised all binary glasses from a ternary system, (c) difficulty of manufacture, (d) reproducibility. Other glasses that were made, were from the systems As-S, Ge-Se, Ge-S, Si-Te, Si-Se.

1.04.1 CHOICE OF EXPERIMENTS

The choice of the measurements to be made was in some ways straight-

forward. A new branch of semiconducting materials required the basic measurements of semiconductor physics to be applied. Hence the experiments initially proposed were d.c. conductivity as a function of temperature, optical absorption (in particular the fundamental absorption edge), Hall effect, and thermoelectric e.m.f.

The first two of the experiments would provide information about the band structure of the materials, principally the size of the energy gap, and possibly the density of states function at the band edges. The second two would give evidence concerning the type of charge carrier and mobility and scattering mechanism.

Having stated this it is necessary to say that in fact measurements of thermoelectric e.m.f's were not possible. All of the experimental apparatus had to be built, and time did not allow the development of the apparatus required for this measurement. It remains an experiment from which much useful information is still to be obtained.

Emphasis was placed on the measurement of d.c. conductivity. Special measures were taken to allow the measurements to be made over as large a temperature and conductivity range as possible. It had been claimed that conduction in these materials was always intrinsic (see review articles quoted), but this conclusion was based almost entirely on data obtained above room temperature. To determine if there were any extrinsic regions, measurements must obviously be made over the whole range of temperature for which the conductivity is measurable.

During the course of the work it became obvious certain other supporting experiments would be useful. These were all carried out on a smaller scale than those described above. The reasons for each of them will be explained in the text.

1.05.0 PLAN OF THESIS

The project consisted of four approximately equal parts (a) preparation of materials and fabrication of experimental specimens, (b) construction of experimental apparatus and establishing of experimental techniques, (c) measurement, (d) computation and interpretation of results.

Chapters 2 and 3 serve to give a brief introduction to crystalline and amorphous semiconductors. The theories briefly discussed in chapter 3 are not intended to provide a summary of all the theoretical work completed on disordered solids. Instead a brief review of three of the more phenomenological theories currently used in discussion of amorphous semiconductors is presented.

Chapters 4 and 5 deal with (a) (b) (c) as above, whilst chapters 6 - 9 deal with (d).

Chapter 10 is a statement of the conclusions.

REFERENCES CHAPTER 1

(1) Goryunova N.A., et al. Sov. Phy.-Tech. Phys. 3, p.912, 1958

(2) Kolomiets B.T. and Goryunova N.A., Zhur.Tek. Fiz. U.S.S.R. 25, p. 984, 1955.

(3) Goryunova N.A., Kolomiets B.T., Sov. Phy.-Tech. Phys. 3, p. 1766, 1958.

(4) Flaschen S. et al, J. Appl. Phys. 31, p. 219, 1960.

(5) Pearson A.D. et al, Advances in Glass Technology, p. 357, Plenum Press, 1967.

(6) Pearson A.D., Modern Aspects of the Vitreous State 3, Butterworths, 1964.

(7) Rawson H., Inorganic Glass Forming Systems, Academic Press, 1967.

(8) Kolomiets B.T., Phys. Stat. Sol. 7, p.713, 1964.

(9) Ioffe A.F. and Regel A.R., Prog. in Semicond. 4, p. 237, 1960.

(10) Proceedings of Inter. Conf. Liquid and Amorphous Semicond., Cambridge, 1969, Printed in Journal of Non. Cryst. Sol. 4, 1970.

(11) Kolomiets B.T. and Nazarova T.S., Sov. Phys. Solid State 2, p. 159, 1960.

(12) Fagen E.A., Fritzsche H., J. Non. Cryst. Sols. 2, p. 170 and 180 1970.

CHAPTER 2

CRYSTALLINE SEMICONDUCTORS

2.01.0 INTRODUCTION

Despite the fact that amorphous materials have no long range order, (a necessary condition for band structure) results obtained for them are often discussed in terms of band structure. The theoretical justification for this will be discussed in chapter 3, but in this chapter, the essential features of the band structure for crystalline semiconductors, partly for their own sake, but also as a prelude to chapter 3, are outlined.

The chapter is written with special reference to the experiments to be described later, and in particular, for the effect of space charge limited currents, a complete semi-quantitative theory is given.

2.02.0 ENERGY BANDS

When a number of atoms are brought together as in a solid, the state of the electrons of individual atoms change. The obvious illustration is that of two hydrogen atoms. When the atoms are close enough together for the wave functions to overlap, then it is found that combinations of ψ_A and ψ_B, the wavefunctions of the individual atoms, describe the new wavefunctions. The two different combinations have different energies.

A similar effect occurs with an assembly of N similar atoms. Electrons which on individual atoms had the same energy, now split into bands, so that there will be bands of allowed and forbidden energy levels, just as for the individual atoms there are only certain allowed energy levels, see fig. 2.1. The difference in energy levels within a band decreases as N increases. For a simple band, because of the two spin states available

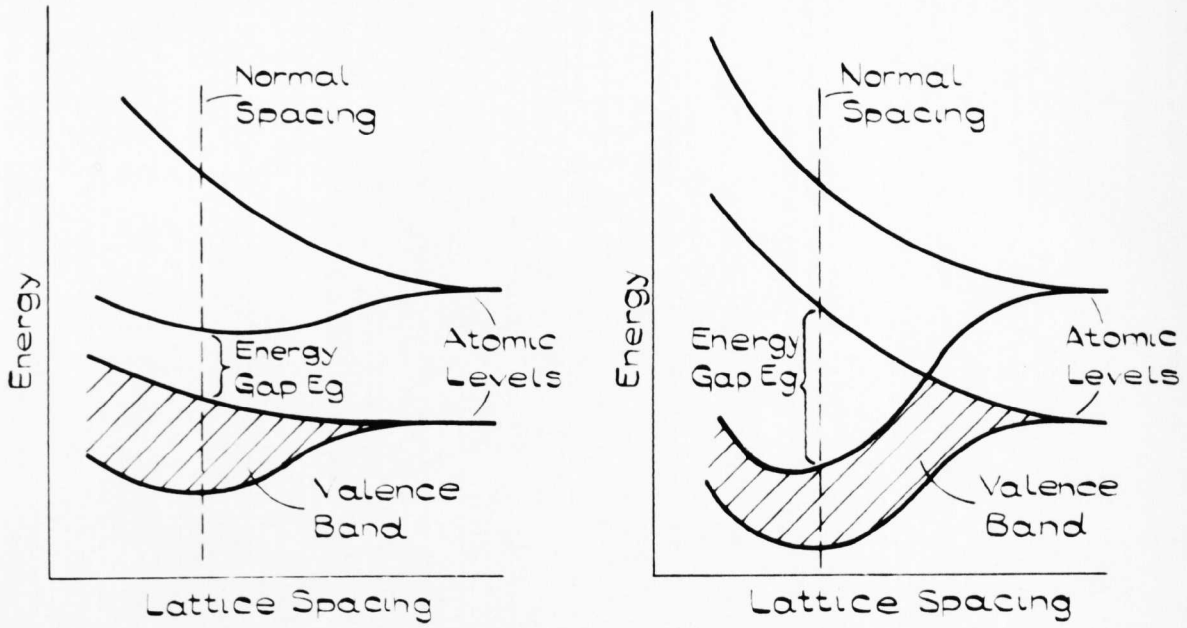

FIGURE 2.1

POSSIBLE ENERGY BAND DEVELOPMENTS

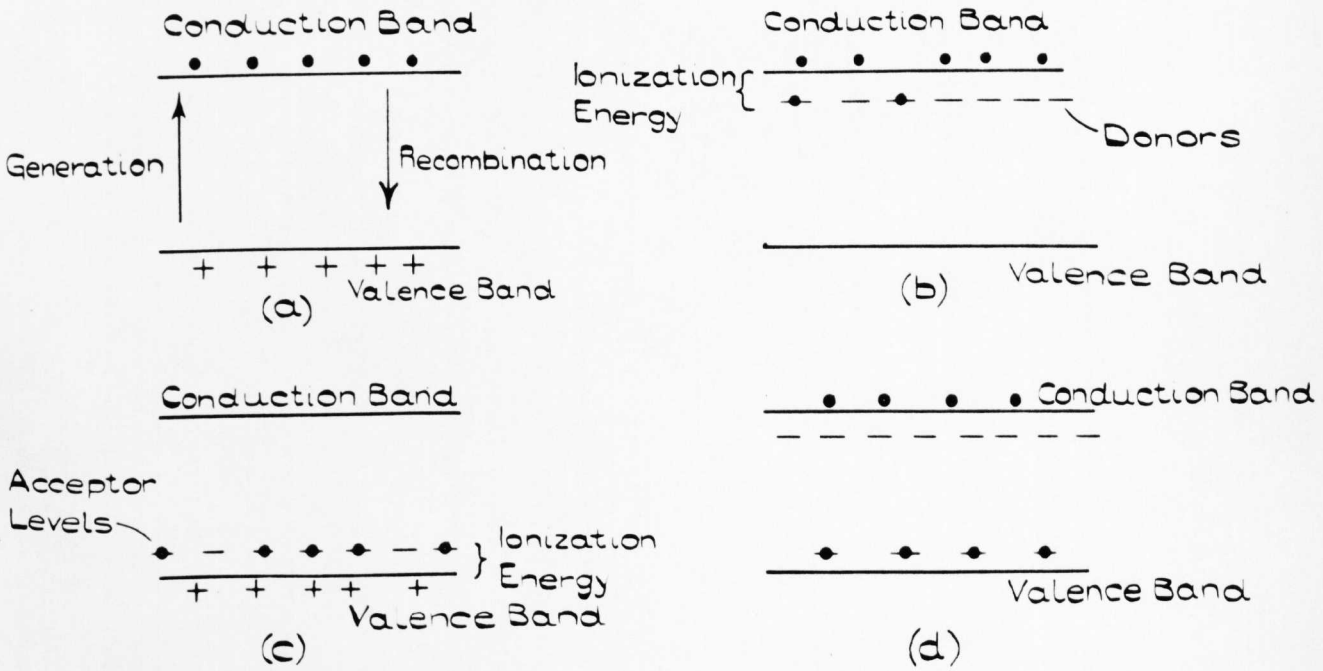

FIGURE 2.2.

ENERGY LEVELS FOR (a) INTRINSIC SEMICONDUCTORS (b) DONORS (c) ACCEPTORS (d) PARTIAL COMPENSATION g IN CRYSTALLINE SEMICONDUCTORS

to each electron, 2N electrons are required to fill each band. In the event of two bands overlapping this condition will be modified.

The highest, filled band is associated with those electrons which form the covalent bands in the usual chemical bond picture, and for this reason is referred to as the valence band. The next highest band, part filled or empty is the conduction band, since electrons in this band are less tightly bound and are free to move throughout the crystal.

Another approach to the problem of electrons in solids and one which shows up further features of the band structure is the nearly free electron model. In this model the electrons are treated as almost free, but being perturbed weakly by the periodic potential of the ion cores.

For the free electron the wave function obeys the wave equation

$$\nabla^2\psi = \frac{2mE}{\hbar^2}\psi \qquad \text{2.02.1}$$

the solutions of which are travelling waves, with wave vector

$$\underline{k} = \frac{2\pi}{\lambda} \qquad \psi = Ae^{i\underline{k}\underline{r}} + Be^{-i\underline{k}\underline{r}} \qquad \text{2.02.2}$$

The energy in the one dimensional case is

$$E = \frac{\hbar^2}{2m}k^2 \qquad \text{2.02.3}$$

which on comparison with the de-Broglie relation shows the momentum to be

$$p = \hbar k \qquad \text{2.02.4}$$

i.e. directly dependent on the wave number.

The case of an electron moving in a periodic potential was first solved by Bloch, who found that solutions were of the form

$$\psi_{\underline{k}} = U_{\underline{k}}(x)\, e^{i\underline{k}x} \qquad \text{2.02.5}$$

where $e^{i\underline{k}x}$ represents a plane wave, and $U_k(x)$ is a function periodic in the crystal lattice.

The dependence of E vs $\underline{k}$ is modified from the free electron case, discontinuities appearing at integer values of π/a for $\underline{k}$ where a is the interatomic distance for the lattice. The discontinuities can be seen (e.g. [13]) to be the result of Bragg reflections in the lattice, since they occur when the wave vector equals an integal number of interatomic spacings. Because of the Bragg reflections, two standing waves are generated having different energies, thus causing the discontinuity.

2.02.1 BRILLOUIN ZONES

The region of $\underline{k}$ space bounded by $\pm\pi/a$ is referred to as the first Brillouin zone, that between $\frac{-\pi}{a} - \frac{-2\pi}{a}$ and $\frac{\pi}{a} - \frac{2\pi}{a}$ as the 2nd Brillouin zone and so on. However because of the form of equation 2.02.5 it can be shown [1], the wave numbers differing by integer values of $\frac{\pi}{a}$ are equivalent, so that all waves can be reduced to the 1st Brillouin zone, which representation is termed the reduced zone scheme.

In three dimensions, Bloch functions are of the form

$$e^{i\underline{k}\underline{r}} U_{\underline{k}}(\underline{r}) \qquad \text{2.02.6}$$

The Brillouin zones now become polyhedra and in the extended zone scheme the volumes lying between polyhedra. The $\underline{E}$ vs $\underline{k}$ surfaces will depend on the exact crystal structure and in general are quite complicated functions.

2.03.0 INSULATORS AND SEMICONDUCTORS

If the valence electrons completely fill one or more bands and the next highest band is empty then the crystal will be an insulator. This arises simply because all the states within an energy band are occupied so that an applied electric field is unable to alter the net momentum (see equation 2.02.4) of the band.

In a semiconductor, the width of the forbidden band, and temperature, (see 2.06.0) are such that there is a finite probability of electrons from the valence band being thermally excited into the conduction band. Now under the influence of an applied electric field there will be a net change in momentum for each band so that charge transport can occur. The actual magnitude of the change (and the conductivity) is governed by the scattering processes for electrons within the crystal.

2.04.0 EFFECTIVE MASS

A study of the dynamics of electrons in crystals shows that electrons behave as if possessing an effective mass m*, which is a direct result of the exchange of momentum between the electron and the lattice. The value of the effective mass for a general anisotropic energy surface is a tensor

$$\left(\frac{m}{m^*}\right)_{ij} = \frac{m}{\hbar^2}\,\frac{\partial^2 E_k}{\partial k_i\,\partial k_j} \qquad 2.04.1$$

It is apparent even in a simple two dimensional case that the value of m* varies through any energy band. Near the bottom of a band m* is positive, and if the band there is parabolic, its magnitude will be close to the true value m. As $\underline{k}$ is increased m* becomes infinite in the middle of the band, and then negative until at the top of the band it is negative and again close to the free electron value.

Any empty states at the top of a band are termed holes, they can be shown ([1] - [4]) to behave as electrons with negative effective mass or as electrons with positive charge and positive effective mass. In an electric field the holes drift in opposite direction to the electron.

2.05.0 INTRINSIC AND EXTRINSIC SEMICONDUCTORS

For the perfect, semiconducting crystal the electron states are those in the allowed bands. The material is able to conduct because of the

electron hole pairs thermally generated. Any material which at the absolute zero of temperature is an insulator can show this behaviour, known as "Intrinsic Conduction", if the temperature can be raised sufficiently high. The temperature necessary for the number of carriers to be appreciable will depend on the width of the forbidden gap E_g.

If however imperfections, usually taking the form of impurities and situated substitutionally in the lattice, are introduced, then their electron states may have energies lying in the forbidden region. If these states are occupied and electrically neutral at $T = 0^{\circ}K$, they are termed donors, and if empty and neutral, termed acceptors, fig. 2.2. At finite temperatures, donor states may donate their electrons to the conduction band (again the process is activated thermally), or if acceptors are present they may accept electrons from the valence band leaving holes behind. Conduction entailing these processes of charge carrier production are termed "Extrinsic" or "Impurity" conduction.

It is often the case that both donor and acceptor states are present, in which case the respective densities of the two sets of states will usually be different. Such a material is then referred to as a compensated semiconductor.

2.05.1 TRAPS

The localized electron states introduced above can act in another way. If an empty, neutral (acceptor) site is situated near or above the middle of the energy gap, then an electron in the conduction band, instead of recombining directly with a hole in the valence band, may first fall into this acceptor level. It then recombines with a hole in the valence band from this level. If the transition probability for the second stage of this process is lower than the first, then the state is referred to as an electron trap. The converse argument can be applied to describe hole trapping states.

2.06.0 DENSITY OF STATES, AND DISTRIBUTION FUNCTION

The density of states N(E) for free electrons is calculated (see for example [1] - [4]) to be

$$N(E) = \frac{4\pi(2m)^{3/2}}{h^3} E^{\frac{1}{2}} \qquad 2.06.1$$

However for the case of electrons moving in a periodic potential, and hence in energy bands of finite width, this may not be a good approximation. As described in 2.04.0 the movement of an electron, or more precisely an electron wave group, is governed by an effective mass tensor. This will vary considerably over an energy band, although experiment shows that at the band edges its value is close to that of the free electron [2].

The density of energy levels in an actual solid is difficult to calculate, and therefore equation 2.06.1, with m* substituted for m is assumed a reasonable approximation. This is most likely to be the case in the vicinity of the band edges, and as will be discussed in the next paragraph, in the case of semiconductors we are in fact mainly concerned with electrons and holes at the band edges.

The manner in which the electrons are distributed over the allowed levels is governed by Fermi-Dirac statistics. Hence the probability of occupation of a discrete non-degenerate state is governed by

$$P(E) = 1 / \left[1 + \exp (E - E_F) / kT\right] \qquad 2.06.2$$

where E_F, the Fermi level, equal to the chemical potential is the energy at which the probability of occupation is one half. For the intrinsic case the position of E_F is close to the centre of the energy gap being given by

$$E_F = \frac{1}{2}(E_c + E_v) + \frac{1}{2} kT \log \frac{m_p^*}{m_n^*} \qquad 2.06.3$$

where E_c = energy of the conduction band edge

E_v = energy of the valence band edge.

m_p^* m_n^* are effective masses of holes and electrons respectively.

In general its position will be governed by the occupation of the states in the forbidden gap.

The number of electrons occupying the available levels in an energy range dE is then

$$dn = N(E)\, P(E)\, dE$$

In particular the number of free electrons in the conduction band n_e is

$$n_e = \int_{E_c}^{\infty} N_c(E)\, P(E)\, dE \qquad 2.06.4$$

and the number of holes in the valence band

$$n_p = \int_{-\infty}^{E_v} N_v(E)\, [1 - P(E)]\, dE \qquad 2.06.5$$

where $1 - P(E)$ is the probability of hole occupation.

For E_F more than 4kT away from the band edges equation 2.06.2 may be approximated to $P(E) = \exp - (E - E_F)/kT$ which introduces with respect to the true distribution function an error of less then 4%.

It can also be seen from the approximate expression that the probability of occupation diminishes rapidly as $E - E_F$ increases, and it is for this reason that only states near the band edges are important in calculating n_e or n_p.

2.07.0 EFFECTS OF NON-HOMOGENEITY

Before continuing further with the experimental theory some important points are briefly made. They concern the effects of heterogeneity and poly-crystallinity on the electronic structure of materials, which up till now have been considered ordered crystals of uniform composition. These phenomena are expected to play an important role in amorphous semiconductors

and should be bornein mind in the comparison of experiment and theory.

If for example there are variations in concentrations of impurities throughout a specimen there will be a corresponding variation in the densities of free carriers. The region containing the excess will lose some of its charge to the relatively deficient region producing a charge double layer. The process continues until the concentration gradient is balanced by the field due to the double layer. The net effect is the production of a potential difference between the two regions which will obviously affect the transport of charge carriers.

Similar arguments may apply to the equilibrium between different grains of a crystal with different impurity concentrations, and this case may be further complicated by trapping states at the grain boundaries.

It would be expected that excessive non-homogeneity would appreciably modify the properties of semiconductors to be discussed, and the consideration of such materials may indeed provide a link between crystalline and amorphous phases.

This topic is discussed again in a little more detail in chapter 6.

2.08.0 ELECTRICAL CONDUCTIVITY

Commencing from the Boltzman equation (general transport equation for charge carriers of long mean free paths in solids) it can be shown [4], that the conductivity in an isotropic semiconductor is

$$\sigma = n_e \cdot e \cdot \mu_e + n_h \cdot e \cdot \mu_h \qquad 2.08.1$$

where n_e and n_h are the number of free electrons and holes respectively per unit volume, as given by equations 2.06.4 and 2.06.5, μ_e and μ_h are the mobilities of the respective carriers defined as

$$\mu = \frac{v}{E}$$ where v is the drift velocity in a field E.

or $$\mu = \frac{|e| \gamma}{m}$$ where γ is the average time between collisions.

2.08.2

The temperature dependence of σ will be governed primarily by the temperature dependence of n_e or n_h. As could be shown from equations 2.06.4 and 2.06.5, the principal temperature dependent term is simply exp ($-E_g/2kT$) for the intrinsic case, where E_g is the width of the forbidden gap $E_c - E_v$. When donor or acceptor sites are present and are not completely ionized this activation term is slightly modified.

The mobility also depends on temperature. The actual dependence will be a function of the scattering mechanism or mechanisms responsible for the finite mean free path and hence mobility. The magnitude of the dependence is much smaller than that of n_e or n_h and can also in principle be distinguished from it by separate measurments of mobility as in the Hall effect.

The main information then to be obtained from conductivity measurements is the activation energy for carrier production, and an indication of whether the conduction is intrinsic or extrinsic.

2.09.0 HALL EFFECT

Consider a rectangular parallelapiped of semiconductor material with mutually orthogonal axis x,y,z. If an electric and magnetic field are applied along two of these axes, an electric field is generated along the direction of the third axis. The study of this effect, the Hall effect, yields considerable information concerning the electronic properties of the material.

The Hall constant for a material is defined as

$$R = \frac{E_y}{j_x B_z} \qquad \text{2.09.1}$$

j_x = current density in x direction

B_z = magnetic induction in the z direction

E_y = the Hall field.

Writing the conductivity

$\sigma = jE$ and using equation 2.08.1 (assuming a majority carrier) gives

$$R\sigma = \frac{E_y}{E_x B_z} = \mu_H \qquad \text{2.09.2}$$

the Hall mobility

The Hall constant R may be either negative or positive according to whether electrons or holes dominate in the conduction process. The mobility as determined from Hall effect measurements, (equation 2.09.2) is not the same as that used in the conductivity. The Hall mobility μ_H requires a different averaging of relaxation times than the drift mobility, since the actual Lorentz force is dependent on γ, for its magnitude and also for the length of time for which it acts.

For a simple isotropic solid the Hall constant is shown to be [5]

$$R = \frac{-3\pi^{\frac{1}{2}}}{4} \cdot \frac{1}{n_e} \cdot \frac{\Gamma(2p + 5/2)}{\Gamma^2(p + 5/2)} \qquad \text{2.09.3}$$

$$\text{and } \mu_H = R\sigma = \frac{e}{m^*} \omega (kT)^p \frac{\Gamma(2p + 5/2)}{\Gamma^2(p + 5/2)} \qquad \text{2.09.4}$$

These results are derived from the Boltzman equation with γ written as $\gamma = \omega E^p$.

Defining the mean free path to be independent of energy gives, [5] $p = -1/2$ so that R becomes

$$R = \frac{-3\pi}{8} \frac{1}{n_e}$$

These expressions for R also assume a majority carrier and will be seriously affected if in fact both electrons and holes are present. If for example, a material is intrinsic and the mobilities and effective masses of electrons and holes are equal, then their combined effect can reduce E_y and R to zero. A more general expression for R is then [5]

$$R_{INT} = \frac{3\pi}{8} \frac{n_e C^2 - n_h}{(n_e C - n_h)^2} \quad \text{where} \quad C = \frac{\mu_{H\ ELECTRONS}}{\mu_{H\ HOLES}}$$

There are other important aspects of the Hall Effect not mentioned here since this is only meant to serve as an outline. Such additional factors as are relevant are mentioned in the discussion on the effect in amorphous semiconductors and in the section dealing with experimental results in chapter 8.

2.10.0 SPACE CHARGE LIMITED CURRENTS

In this section a little more than an outline is given, since the semi-quantitative theory presented is directly applicable to the case of amorphous semiconductors as well as crystalline. This theory will be used in the interpretation of the results of 8.03.0. The analysis is preceded by a brief explanation of the effect.

When ohmic contacts,(see 8.03.1) are made to an ideal large band gap semiconductor, injected carriers may result in currents far in excess of the equilibrium value. In fact, no really large currents are realised in a real material, because of the effect of localized states, acting as traps, which reduce the predicted current by several orders of magnitude. However depending on their density and distribution these states can influence the behaviour in another way.

When a voltage is first applied to the specimen, space charge in the form of free electrons (similar arguments will apply for hole injection) is

forced into the conduction band, causing an initial rapid increase in the current. Most of this charge condenses into the traps at a rate which depends on the capture cross section, and the current is subsequently reduced. Because the trap density is likely to be large compared with the density of the free charge it is safe to assume that all of the charge condenses into traps. This consequent large increase in the density of occupied sites raises the Fermi level towards the conduction band.. To preserve a proper statistical equilibrium the density of electrons in the conduction must now be increased in accordance with the shift in the Fermi level. The net effect of the states in the forbidden gap is then not only to reduce the size of the current but also to introduce a non linear aspect to the I - V characteristic, since as V is increased the position of the Fermi level changes to give a larger number of free carriers in the conduction band.

It is possible, for certain distributions of states to obtain closed forms for the relationship between I and V and for two cases, (both relevant to the result of chapter 8) a linear distribution, and an exponential distribution, this relationship is now obtained.

The analysis for the two cases, presented here side by side, is based on the approach of Lanyon [8].

Transport is considered to be by positive holes, and the electrodes, hole injecting.

The density of states in the gap for the two cases is given by

<u>uniform distribution of states</u>

$$N(E) = N_T \, cc^{-1} \, e.v^{-1}$$

<u>exponential distribution of states</u>

$$N(E) = N_o \exp - E/\Delta \qquad 2.10.0$$

(See figure 2.3) Δ characterises the "fall off". N_o is the density of states at the band edge.

The edge of the valence band E_v will be taken as the zero of energy, and the initial position of the Fermi level E_{Fo} is assumed to be somewhere above E_v in the 'tail' of states.

Applying a voltage V, a density $\triangle V$ of holes is assumed to be injected into the valence band. Provided $\Delta \gg kT$ it can be assumed that all the charge is condensed into traps. The density of trapped charge is then

$$P_t = \bar{P}_t + \triangle V \quad \Big| \quad P_t = \bar{P}_t + \triangle V \qquad \text{2.10.2}$$

where $\bar{P}_t$ is the density of trapped holes before any field is applied. A quantity V_a is defined by $\bar{P}_t = \triangle V_a$ so that

$$P_t = \triangle (V_a + V) \quad \Big| \quad P_t = \triangle (V_a + V) \qquad \text{2.10.3}$$

The trapped holes will cause the Fermi level to be moved to a lower energy say E_{Fl} in fig. 2.3. The total number of trapped holes $\triangle V$, is approximately the total number of states in the tail above E_{Fl}, and therefore given as

$$P_t = (E_o - E_{Fl}) \cdot N_T \quad \Big| \quad P_t = \Delta N_v e^{-E_{Fl}/\Delta} \qquad \text{2.10.4}$$

E_o is some energy at which the distribution N_T finishes.

Also, the density of free carriers in the valence band is

$$P = N_v e^{-E_{Fl}/kT} \quad \Big| \quad P = N_v e^{-E_{Fl}/kT} \qquad \text{2.10.5}$$

Where N_v is the density of states at the valence band edge,

Combining 2.10.4 and 2.10.5 gives

$$P = B e^{\frac{P_t}{kT N_T}} \quad \Big| \quad P = C P_t^{\Delta/kT}$$

$$B = N_v e^{-E_o/kT} \quad \Big| \quad C = N_v/(N_v\Delta)^{\Delta/kT} \qquad \text{2.10.6}$$

Both relations are independent of the position of E_F.

Now using 2.10.3 we can write

$$P = B \exp \frac{\Delta}{N_T kT} (V + V_a) \quad \Big| \quad P = \Delta C (V + V_a)^{\Delta/kT} \qquad 2.10.7$$

and in the absence of any applied voltage the number of free carriers is simply

$$\bar{P} = B \exp \frac{\Delta V_a}{N_T kT} \quad \Big| \quad \bar{P} = \Delta C \left(V_a\right)^{\Delta/kT} \qquad 2.10.8$$

Writing $\sigma = P e \mu$, where μ is the hole mobility, and $J = \sigma \frac{V}{L}$, where L is the specimen thickness, the expressions for current density become

$$J = \frac{B \cdot \mu \cdot e}{L} \exp \frac{(V_a + V)}{N_T kT} \quad \Big| \quad J = \Delta \frac{C \cdot \mu \cdot e}{L} V (V + V_a)^{\Delta/kT}$$

$$J = \text{CONSTANT } V \exp \frac{\Delta V}{N_T kT} \quad \Big| \quad J = \text{CONSTANT } V (V + V_a)^{\Delta/kT} \qquad 2.10.9$$

As might be expected both relations shown an ohmic behaviour for small values of V, until the number of injected carriers exceeds the number $\bar{P}$ predicted by the initial equilibrium conditions.

For the first case the ohmic dependence is then followed by an exponential dependence, and in the second case the high voltage region is described by the power law $J \propto V^{(\Delta + kT)/kT}$. In each case information about materials showing these behaviours will be obtained from log I vs. V and log I vs. log V respectively.

The discussion is taken up again in chapter 8.

2.11.0 OPTICAL ABSORPTION

For semiconductors there are five separate processes contributing to the absorption of radiation. These are (1) electronic transitions between different energy bands (2) lattice vibrations (3) electronic

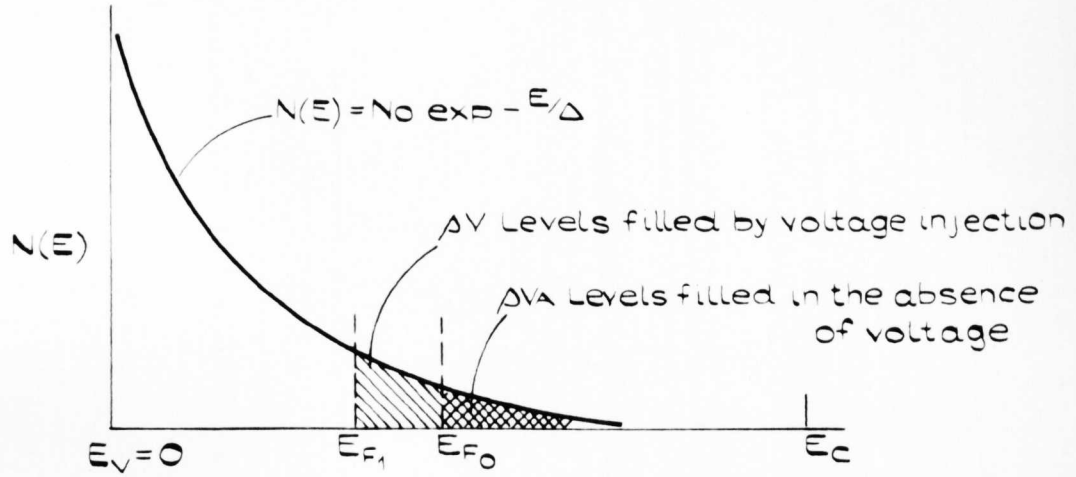

FIGURE 2.3.

PROPOSED EXPONENTIAL DISTRIBUTION OF STATES SHOWING MOVEMENTS OF FERMI LEVEL AFTER INJECTION OF HOLES

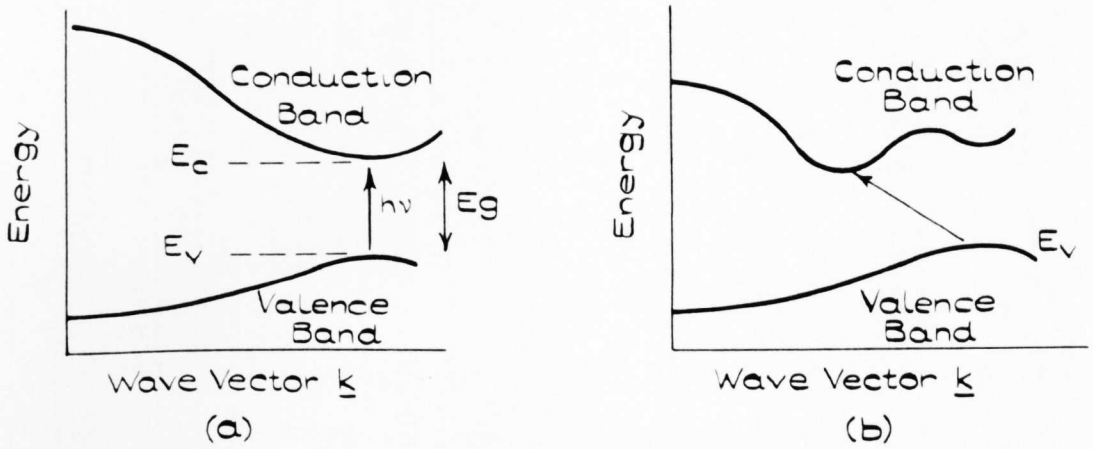

FIGURE 2.4

POSSIBLE ENERGY BANDS IN SEMICONDUCTORS SHOWING (a) DIRECT OPTICAL TRANSITION (b) PHONON ASSISTED INDIRECT TRANSITION.

transitions within energy bands (4) electronic transitions to localized states of impurity atoms (5) vibration of impurity atoms. Mechanism (1) and (4) are those entailed in the so called, fundamental absorption edge, the phenomenon studied in this project, and only these are discussed.

Theoretically these two processes and the resultant absorption edge are not well understood [22]. There are of course notable exceptions, e.g. Macfarlane et. al. on germanium, but a universal theory that can be applied to the edge of any material does not exist. Certain general principles do however prevail and the discussion commences with these.

Consider a hypothetical one dimensional semiconductor with E vs $\underset{\sim}{k}$ for the conduction and valence bands as shown in figure 2.4. In fig. 2.4(a) a photon of energy $h\nu \geq E_g$ would excite an electron from the top of the valence band to the bottom of the conduction band. Momentum is conserved during the process so that $\underset{\sim}{k}_i + \underset{\sim}{q} = \underset{\sim}{k}_{final}$ where q = wave vector of the photon. For photons of the required energy $\underset{\sim}{q} \ll \underset{\sim}{k}_i$, or $\underset{\sim}{k}_f$ so that

$$\underset{\sim}{k}_i = \underset{\sim}{k}_f \qquad \text{2.11.1}$$

Transitions obeying 2.11.1 are termed direct (or vertical) transitions and 2.11.1 is the selection rule for the transition.

There will be a sharp increase in absorption coefficient K as photon energies of $h\nu = E_g$ are approached, so information concerning E_g, which is also the activation energy for conduction process is available from the K vs photon energy data. In the more general case, as will now be seen E_g is not so easily obtained from absorption data.

Fig 2.4(b) shows the case where the maxima and minima of the two bands do not coincide. "Indirect" transitions now occur being the result of an electron phonon interaction during which a phonon is either absorbed or emitted by the electron. The selection rule for this process is then

$$\underline{k}_i = \underline{k}_f + \underline{g} \qquad \text{2.11.2}$$

where $\underline{g}$ is the wave vector of the phonon.

At finite temperatures the commencement of absorption will be more gradual, until direct transitions become important, and the photon energy involved will not be easily related to the activation energy E_g.

Even for simple mechanisms of absorption it is not possible to calculate exactly the form of the absorption edge. The absorption coefficient is given by Fan [9] as

$$K = \frac{\pi e^2}{nm} f_{ij} \; N(E)$$

$N(E)$ = density of states function

f_{ij} is the oscillator strength for the transition.

For direct transitions from and to plane wave states he shows

$$K = \frac{2e^2(2m_r)^{5/2}}{3m^2\hbar^2 cn} \cdot \frac{(h\nu - E_g)^{3/2}}{h\nu} \qquad \text{2.11.3}$$

For the case of indirect transitions first treated by Hall, Bardeen and Blatt [10] it was shown that

$$K \propto (h\nu - E_g)^2$$

The involvement of the phonon is shown explicitly in the expression used by Macfarlane and Roberts [11] who used

$$K = \frac{(h\nu - E_g + k\theta)^2}{\exp\left(\theta/T\right) - 1} + \frac{(h\nu - E_g - k\theta)^2}{1 - \exp - \theta/T} \qquad \text{2.11.4}$$

where the first term concerns the absorption and second term the emission of a phonon. Equation 2.11.4 has been applied to silicon [12] and in a modified form to germanium.

The above predictions in fact apply in only a few cases. The absorption edges of most materials very rarely follow these shapes over any appreciable range of K, and in all cases are spread over much larger energy ranges than

they predict. For many materials the edge is well described by an empirical rule first introduced by Urbach [13]. This rule shows the edge to have an exponential dependence and can be written as

$$K = K_o \exp \frac{\gamma}{kT} (h\nu - E_o) \qquad 2.11.5$$

where γ and K_o are constants.

The rule applies over several decades of K to a diversity of materials including amorphous and crystalline semiconductors ([14] - [17]) and ionic insulating crystals ([18] [19] [13]). Because of the wide applicability there is as yet no universal theory to explain the edge but several models do predict the behaviour, these include, the finite temperature edge of an exciton ([21]) the effects of tails of states ([8] [17]) and finally electric field broadening of an exciton [20].

Equation 2.11.5 commonly breaks down at low temperatures viz $< 200^{o}K$ when K_o and E_o become temperature dependent. A complete description of the dependence on temperature would entail the effects of lattice dilatation on the band structure of the material, Fan [9] considers such an approach.

In the discussion of the fundamental absorption edge in amorphous semiconductors these and other aspects of absorption processes will be considered further.

REFERENCES CHAPTER 2

(1) Kittel C., Introduction to Solid State Physics, John Wiley & Sons.

(2) Hanney N.B., Semiconductors, Reinhold Publishing Corporation, 1959.

(3) Shockley W., Electrons and Holes in Semiconductors, D. Van Nostrand Co. Inc.

(4) Ziman J.M., Principles of the Theory of Solids, Cambridge University Press.

(5) Putley E.H., The Hall Effect and Related Phenomena, Butterworths.

(6) Mott N.F., Gurney R.W., Electronic Processes in Ionic Crystals, Oxford University Press.

(7) Rose A., Phys. Rev. 97, p. 1538, 1955.

(8) Lanyon H.P.D., Phys. Rev. 130, p. 134, 1964.

(9) Fan H.Y., Reports on Progress in Physics 19, p.111, 1956.

(10) Hall L.H., et al, Phys. Rev. 95, p. 559, 1954.

(11) Macfarlane G.G., and Roberts V., Phys. Rev. 97, p. 1714, 1955.

(12) Macfarlane G.G., and Roberts V., Phys. Rev. 98, p. 1856, 1955.

(13) Urbach F., Phys. Rev. 92, p. 1324, 1953.

(14) Siemson K.J., Fenton E.W., Phys. Rev. 161, p. 632, 1967.

(15) Dutton D., Phys. Rev. 112, p. 785, 1955.

(16) Marple L., Phys. Rev. 150, p. 728, 1966.

(17) Panklove J.L., Phys. Rev. 140, p. 2059, 1965.

(18) Martienssen W., J. Phys. Chem. Sols., 8, p. 294, 1959.

(19) Kobyashi K., Tomiki T., J. Phys. Soc. Japan 15, p. 1892, 1960.

(20) Dow J.D., Redfield D., Phys Rev. 1970, to be published.

(21) Mahr H., Phys. Rev. 132, p. 1880, 1963.

(22) Hopfield J.J., Comments on Solid State Physics 1, p. 16, 1968.

CHAPTER 3.

AMORPHOUS SEMICONDUCTORS

3.01.0 INTRODUCTION

Theoretically the problem of predicting the behaviour of valence and conduction band electrons in amorphous materials is formidable. One is called upon to predict the wavefunctions of electrons moving in a spatially non-periodic potential, with wells, of random depth, and even this is an idealized situation. In practice there may be further complications in that materials designated as amorphous by various physical tests may contain small regions which are ordered and/or of different composition. Such structures would be difficult to detect but would strongly influence the electronic behaviour. As will be seen later this longer range disorder is not always included in the approach.

All approaches to date have started with the standard band theory of crystalline solids and have assumed perturbations to this model, the perturbation taking the form of annihilating the long range order, say over a few atomic spacings, whilst maintaining the short range order. Such an approach would seem valid on the majority of experimental results thus far published for amorphous semi-conductors.

To provide a basis for this chapter some of the experimental evidence is now cited.

1. Electrical conductivity. The magnitude of the electrical conductivity shows that chalcogenide based amorphous semiconductors can cover the range "good insulator" to "good semiconductor", and are of conductivity 10^{-2} ohm^{-1} cm^{-1} to 10^{-16} ohm^{-1} cm^{-1}, and are electronic, (rather than ionic) conductors over the whole range. The dependence on temperature is always governed by a positive temperature coefficient of

conductivity and usually reported to show a characteristic activation energy, which is constant over a large temperature range. More recent work begins to show that this activation energy, as derived from the slope of $\log \sigma$ vs $\frac{1}{T}$. may be temperature dependant, see references [1], [2] and Chapter 6 of this thesis. General references are [2], [3] and [4].

2. Optical Absorption. If the activation energy for intrinsic conduction is considered half the forbidden band gap, (as in theory of crystalline solids), then there is an optical absorption edge corresponding to a value slightly lower than the complete gap. The behaviour of the edge as a function of photon energy follows Urbachs' rule (see 2.11.0) over large regions of the edge, and its behaviour with temperature is also similar to that for crystalline materials, the whole edge moving to shorter wavelength with decreasing temperature (see for example [2], [5] and [6]).

3. Thermoelectric power. In magnitude and temperature dependence this is again very similar to crystalline semiconductors (general references [5], [7]). With very few exceptions (see [1].) the sign of the carrier determined from thermoelectric power measurement is positive. The obvious conclusion that all amorphous semiconductors have a majority of positive holes over electrons is discussed in Chapter 6. This result is in apparent opposition with information from Hall effect data which shows the majority carrier to be negative.

4. Hall effect. Few Hall measurements have been made to date, due possibly to the experimental difficulties involved. However its existence at all provides evidence for at least some short range order. Mobilities derived to date are in the range 10^{-1} - 10^{-3} $cm^2\ V^{-1}\ sec^{-1}$, indicating very small mean free paths or highly intrinsic materials or even very small crystallites. The very small mobilities and the inferred small mean free paths are currently throwing doubt on the interpretation of

Hall data, but this is unlikely to throw doubt on the approach to the problem as a whole, general references [4] and [8].

Although this work is not concerned with the liquid phase, it is worth mentioning that for many materials the value of certain properties, which rely on band structure for their interpretation are maintained as the materials melt, examples of this are discussed by Gubanov [9].

Having established the possibility of a band structure model being applied to amorphous semiconductors, more specific, current ideas on the subject are now presented. Amongst these theoretical ideas it is possible to determine three separate approaches to the problem, these are that of Gubanov, Mott, and thirdly the Cohen Fritzche Ovshinsky school. The current ideas of each are outlined and to some extent the methods used to attain their predictions are also given.

The first model presented is that due to the Cohen Fritzche Ovshinsky group.

3.02.0 COHEN MODEL OF AMORPHOUS SEMICONDUCTORS

The authors emphasise the generality of the approach, and working from the universal features of perfect crystals, through imperfect crystals try to establish the universal features of disordered materials.

3.02.1 ORDER AND DISORDER

The most general material requires three types of order to be satisfied to render it perfect, these being structural, compositional and magnetic. Elementary excitations; phonons, electrons in conduction band etc., are not included and it is also convenient to exclude the magnetic disorder. The common distinction is made between long (several 100 Å) range and short range order; pointing out that, for a disordered

material short range order can be satisfied in the absence of long range order, but for an imperfect crystal the converse applies, i.e. the long range order is maintained whilst the short range order is destroyed, as at a crystal imperfection.

3.02.2 CONSEQUENCE OF IMPERFECTIONS IN THE PERFECT CRYSTAL

The salient features of the electronic structure of perfect crystalline solids have been presented in 2.01.0 - 2.05.0 and assuming these understood, the discussion of the model is continued.

The introduction of a single imperfection destroys the nature of the Bloch functions, so that they now play the part of incident waves in a scattering process. The crystal potential V is changed at the imperfection to ΔV_I. For small ΔV_I resonant scattering occurs near a band edge, and as ΔV_I increases above a certain value, a state is split off from the conduction band (for ΔV_I negative), producing a localized electron state. The density of states N(E) of the system will suffer very little change.

The argument is extended to consider the effect of a random distribution of imperfections of density N_I, the ΔV_I associated with each one being too weak actually to produce localization. The wave functions are now more severely changed. In travelling the distance of the mean free path ℓ

$$\ell = \frac{1}{N_I \alpha} \qquad \alpha = \text{scattering cross section} \qquad \text{3.02.1}$$

the electron is scattered and the wavefunction becomes the sum of Bloch type functions $\psi_{\underline{k}}$

$$\Psi(\underline{r}) = \sum_{n\underline{k}} a_{n\underline{k}} \psi_{n\underline{k}}(\underline{r}) \qquad \text{3.02.2}$$

where the coefficients $a_{n\underline{k}}$ have random phases.

To display the relevant properties of the wave function conveniently the correlation function C(R) is introduced.

$$C(R) = \langle \psi^*(r + R)\, \psi(r) \rangle \propto \frac{e^{-R/\xi}}{R} \qquad 3.02.3$$

ξ is the phase coherence length, differing from ℓ by a numerical factor due to averaging over all configurations. For ξ finite, there will only be short range order for these non-localized, or extended states.

For a single imperfection the change in the density of states can be written $\Delta g_I(E)$ and will be of order $\frac{1}{N}$ where N is the number of atoms in the crystal. For a number N_I of imperfections the total change $\Delta g(E)$ can be written

$$\Delta g(E) = \sum_I g_I(E) \qquad 3.02.4$$

and will be expected to be of order N_I/N. In general the band for the perfect solid as in fig. 3.1, curve 1 , will, as a result of equations 3.02.1 be changed to curve 2. In particular the square root singularities will be rounded off and the band edges may shift, but will remain sharp. These conclusions are expected to apply universally to imperfect solid crystals.

3.02.3 SIMPLE MODEL OF A DISORDERED SOLID

The transition from imperfect to disordered solid is made for the case of a Binary Alloy A-B. The potential will be of the form

$$V(r) = \sum_\ell U_{\alpha_\ell}(r - R_\ell) \qquad 3.02.5$$

where α_ℓ is randomly A or B. A is considered the majority constituent and the potential written

$$V(r) = V_A(r) + \sum_\ell X_{\alpha_\ell}\, \omega(r - R_\ell) \qquad 3.02.6$$

x_{α_ℓ} is zero if A is on ℓ and 1 if B is on ℓ.

$$\omega(R) = U_B(R) - U_A(R) \qquad 3.02.7$$

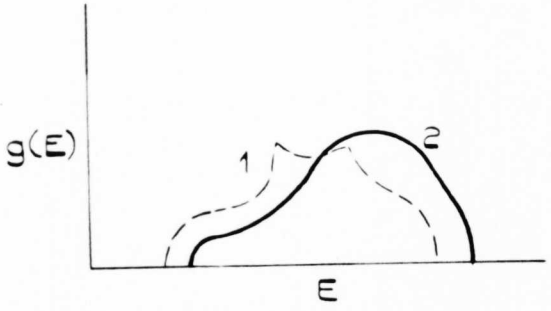

FIGURE 3.1.

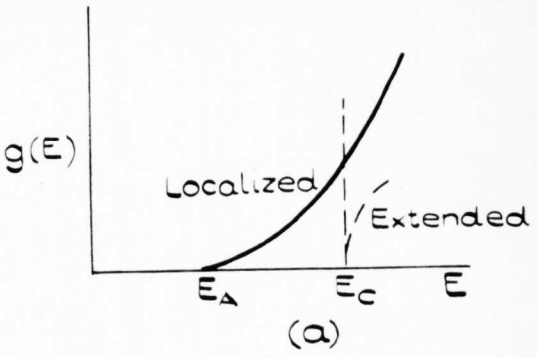

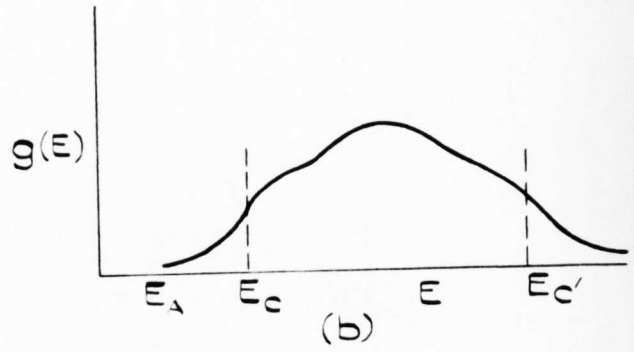

FIGURE 3.2.

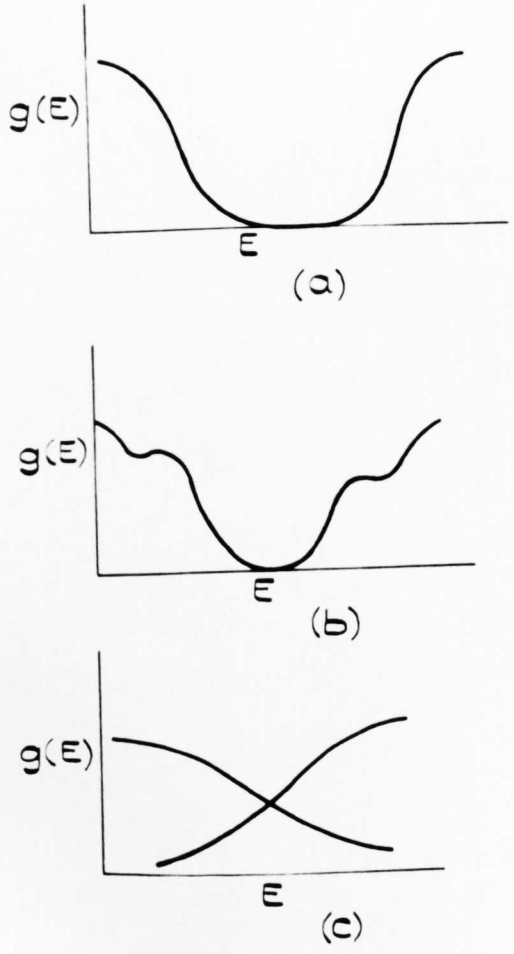

FIGURE 3.3.

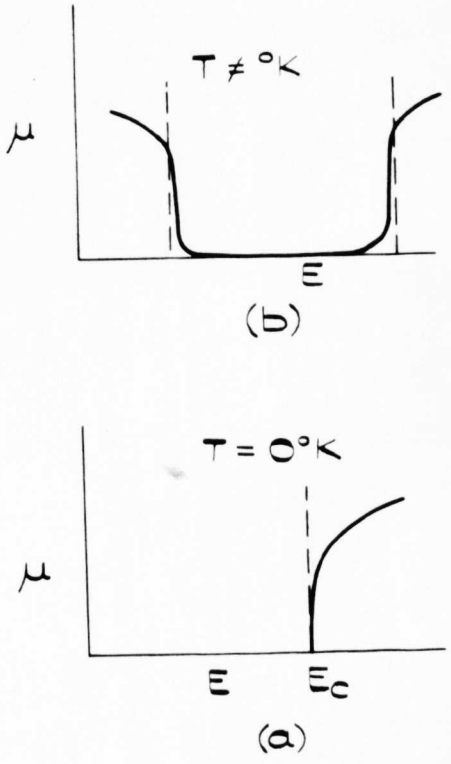

FIGURE 3.4.

FIGURES APPLICABLE TO SECTION 3.02.

A parameter λ is introduced, where $0 \leqslant \lambda \leqslant 1$, so that V becomes

$$V(r,\lambda) = V_A(R) + \lambda \sum_i \chi_{k_i} \omega(r - R) \qquad \text{3.02.8}$$

$\lambda = 0$ corresponds to the perfect crystal of A and $\lambda = 1$ to the alloy. The parameter λ is introduced so that the effects of concentration and potential strength on the structure can be examined separately. For general C and λ the problem is very difficult, but can be simplified if they are small, when two effects predominate.

Firstly for arbitrary λ it is shown that the bottom of a band shifts by an amount

$$\Delta E_c = \frac{\hbar^2}{2m} \cdot 4\pi \cdot N_B a \quad a = \text{scattering length} \qquad \text{3.02.9}$$

which for small λ is proportional to λ [10].

A second effect is that the Bloch states now have a finite life time τ where

$$\frac{1}{\tau} \propto g(E) \qquad \text{3.02.10}$$

for a particular N_B, and expectation value of ω. This implies no broadening of the band edge when $g(E) = 0$. Hence the combined effect is as before, a rounding off of $g(E)$ curve, and a shifting of the edges.

However, the effect of random fluctuations in the density of B atoms has thus far been overlooked, these are shown to have a major effect.

The concentration fluctuations allow the finite probability P(R) of finding no B atoms in a region of radius R. This probability is

$$P(R) = (1 - C)^{4/3\pi R^3 N} \simeq e^{-4/3\pi R^3 N_B}$$

N = density of lattice sites $\qquad$ 3.02.11

Suppose then that the shell of pure A is surrounded by one of radius R' in which the density of B is close to the average, then the potential in R differs from that of the surroundings by $-\lambda \langle w \rangle$. Providing R and R' are many atomic spacings so that the effective mass theorem can be used, then for $R > R_c$ where

$$R_c = \frac{1}{2}.\pi \left(\frac{2m^* V_o}{\hbar^2}\right)^{-\frac{1}{2}} \qquad \text{3.02.12}$$

V_o is the depth of the potential well.

there will be at least one state of energy E bound to the potential fluctuation, which will satisfy the condition $E_A < E < E_c$ in fig 3.2(a). There will be a range of R and hence of E so that there will be a contribution to the density of states below E_c given by

$$g(E) = Ne^{-R^3(E)N_B}.\ 4\pi R^2(E)\ \frac{dR}{dE} \qquad \text{3.02.13}$$

This probably represents a minimum value, because concentration fluctuations of lesser amplitude, and those of non-spherical shape have been ignored. Because the overlap between wavefunctions bound on neighbouring fluctuations is neglected the expression for g(E) for $E < E_c$ breaks down at E_c. It is obviously in this region that the overlap becomes important, the region is shown dotted in fig. 3.2(a). For concentration fluctuations with $R \leqslant R_c$ there are resonant states just above E_c, so that the g(E) is enhanced in this region. At the transition E_c, the wavefunctions are expected to change smoothly from localized to extended states.

The final postulated density of states curve for a band in a disordered solid is shown in fig. 3.2(b). The tail in g(E) above the band will be due to regions containing an excess of B atoms, where similar arguments apply. Because of the accompanying decrease in mean free path as λ and C are increased E_c and E_c' will be expected to move further into the bands as disorder increases.

3.02.4 BAND MODELS FOR MORE PARTICULAR CASES

The case described above, shown again in fig. 3.3(a) may be modified in several ways, but two in particular are considered.

For elemental and compound semiconductors a more accurate representation is considered to be that of fig. 3.3(b). For these materials there is probably some degree of short range order, so that it is possible to consider particular, recurring structural defects (e.g. broken bonds, chain ends, vacancies, etc.). These would have quite well defined energies and are expected to appear in the density of states curve as shown.

Fig. 3.3(c) is thought to apply to amorphous covalent alloys, such as the chalcogenide glasses. As first suggested by Mott [11], it is postulated that in these materials the structure changes with local composition so that each atom has its valence requirements satisfied. The production of the conventional localized acceptor and donor sights is then severely restricted. Now in addition to compositional disorder there will be considerable translational disorder due to the satisfying of all "local requirements" and causing further broadening of the energy bands. The tails of the valence and conduction bands may be sufficiently broadened as to overlap.

The overlapping of the bands may be of extreme importance. The topmost valence states will empty into the lowest conduction band states until the Fermi Level is established in the region of overlap. Now valence band states and their associated localized levels (in this case the tail) are neutral when full and positively charged when empty, and those of the conduction band neutral when empty, negatively charged when full. Hence the above emptying and filling of localized valence and conduction states will produce a large density of charged electron and

hole traps respectively below the conduction band and above the valence band. The consequences of these traps on conduction processes may be of some importance.

3.02.5 MOBILITY

The ideas thus far developed are confirmed to a certain extent by some work of Williamson and Matthews [12]. They consider an aperiodic crystal, and study for this case the average momenta

$$\bar{p} = \int_a^b \psi^* \frac{\hbar}{i} \frac{\partial}{\partial x} \psi \, dx \Big/ \int_a^b \psi^* \psi \, dx \qquad \text{a-b = length of 1-D chain} \qquad \text{3.02.14}$$

as a function of energy. This is done in preference to considering the relation between energy and wavenumber k, since in this case k is a function of position, and hence not easily defined.

Their main result is that the energy spectrum is divided into alternating bands with $\bar{p}$ close to its value for periodic structure in one band and in the other extremely small. The difference in the value of $\bar{p}$ depends upon the size of the crystal but $\bar{p}$ in the 'forbidden' band is generally 10^{-25} -10^{-10} smaller than in the 'allowed' bands.

Cohen extends and modifies slightly this theory and further concludes that for $\bar{p}$ very small, the state is either localized or does not exist at all. States are then either extended or localized. This leads to the conclusion, at least for the one-dimensional case, that the E_c' and E_c already introduced are energies demarking regions of localized and extended states. The conductivity can be written (Ref. [10] p.34) in the form

$$\sigma(E) = B \, |p(E)|^2 \, g^2(E) \qquad \text{L = length of the 1-D crystal; B = constant.} \qquad \text{3.02.15}$$

so that the conductivity per unit energy range decreases rapidly at E_c and E_c' where $p(E)$ becomes small. Comparing the above with σ written as

$$\sigma = \sum_b dE \cdot g_b(E)\, e\, \mu_b(E)\, f_b(E) \qquad \text{3.02.16}$$

indicates that $\mu(E) = B\ p(E)^2\ g(E)$. 3.02.17

Hence the mobility exhibits edges at E_c and E_c'. These are illustrated in fig. 3.4.

The exact form of the mobility edge at $T = 0^oK$ for a real amorphous semiconductor is not certain but is thought to be (a) in fig. 3.4. At finite temperature these edges are expected to be modified slightly: E_c and E_c' may move into the forbidden gap, the amount slightly depending on the exact shape of the g(E) curves. Also the mobility of the localized states below E_c' and above E_c will become finite, because of the possibility of phonon assisted hopping between localized states.

The mobility of phonon assisted hopping is estimated to have a maximum value of 10^{-2} cm^2 $volt^{-1}$ sec^{-1}, whilst the minimum value for propogation in extended states, propogation with occasional scattering is estimated to be 5 cm^2 $volt^{-1}$ sec^{-1}. This would indicate a discontinuous change in μ at E_c of something approaching two and a half orders of magnitude. However this apparent gap can be accounted for and 'filled in' by considering transport just on the extended sides of the mobility edges.

It is shown using a Greens Function method (Ref.[10] page 36) that motion within kT of E_c is best characterized by a Brownian type motion. Instead of transport with occasional scattering, the situation is more scattering with occasional transport. This hopping between centres is purely electronic, so that it will persist down to $T = 0^oK$. The estimated maximum value for the mobility of this process is approximately 5 cm^2 $volt^{-1}$ sec^{-1} so that the gap in the mobility is now bridged. This result was anticipated in drawing fig. 3.4 where the curve for $T = 0^oK$ drops continually to zero at E_c.

This concludes the essential feature of the Cohen model. Some of its implications are discussed further in 3.05.0.

3.03.0 MOTT MODEL OF AMORPHOUS SEMICONDUCTORS; INTRODUCTION

The general approach is to consider the electronic structure and transport in an impurity band, in which conduction is metallic. Disorder is introduced into the band and the possible changes in N(E) and σ (E) discussed. Having thus established certain principles concerning disordered systems, the ideas are extended to amorphous semiconductors, and in particular the behaviour at the band edges.

3.03.1 ANDERSON BAND

This model is suitably approached via a description of the relevant features of compensated semiconductors.

Consider an 'n' type compensated semiconductor, such that N_D (density of donors) > N_A (density of acceptors), at some low temperature with all the acceptor sites ionized and $N_D - N_A$ of the donor sites occupied. At sufficiently low concentrations the overlap of wavefunctions between different donor sites is small and the resonance energy between them less than the energy difference due to variation of local electric fields (caused by the essentially random arrangement of charged acceptor sights). The electrons are then well localized and neighbouring sites nondegenerate. Miller and Abrahams [14] discuss the conduction in such a band in terms of electrons hopping from occupied to unoccupied levels, the energy difference being made up by the absorption or emission of a phonon. The conductivity in such a band will obviously go to zero with absolute temperature.

If, however, N_D is sufficiently large, then the wavefunctions on the donor sites may overlap such that the electron states lose their localized

DAMAGED TEXT IN ORIGINAL

character. An impurity band is thus formed with Fermi Energy in the band. From the tight binding theory the width of this band is shown to be

$$J = 2zI \qquad \text{3.03.1}$$

$$I = w \exp(-\alpha R_o).$$

$$w' = cR_o^{-1} H \propto \upsilon. \qquad \text{(see fig. 3.5)}$$

z is the coordination number, and I the overlap integral between nearest neighbours. The wavefunction for a single well will fall off as $\psi = \frac{\text{constant}}{R} \exp(-\alpha R)$

The model of Anderson can be considered ([15] - [17]) to discuss the effect on N(E) and σ (E) of introducing some random potential on each of the donor sites. Such a potential would be produced by increasing the number of acceptors. The two cases, before and after the introduction of the random potential, together with the postulated N(E) for each, are shown in fig. 3.5.

Anderson studies the effect of varying the width V_o of the random potential and shows that for a particular value of $\frac{V_o}{J}$ the states in what was an impurity 'band', become localized. Localization here means that there will be zero probability of diffusion in finite time. The estimation is that for $z = 6$ localization occurs when $\frac{V_o}{J} = 5$.

Mott extends the argument to consider the electrical conduction in the Anderson band. Localization is re-defined to mean that localized states make no contribution to d.c. conductivity $\sigma(0)$ at absolute zero of temperature. If $\frac{V_o}{J} > 5$ then the conductivity of the band is zero at absolute zero. An important feature of this consideration is that even if E_F lies in the middle of a range of localized states, as it will for the Anderson band, for $\frac{V_o}{J} > 5$ the d.c. conductivity is still zero. This point is now discussed further.

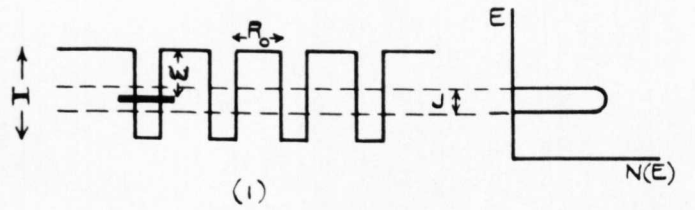

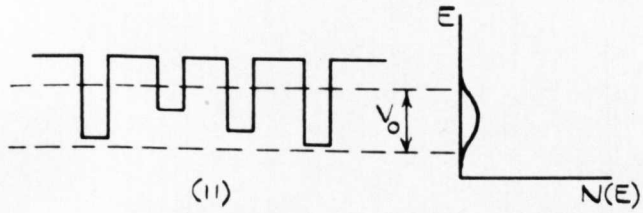

FIGURE 3.5.

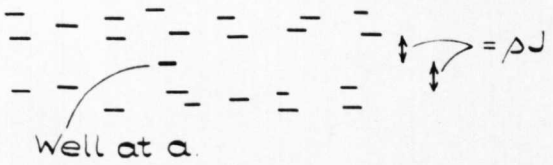

FIGURE 3.6.

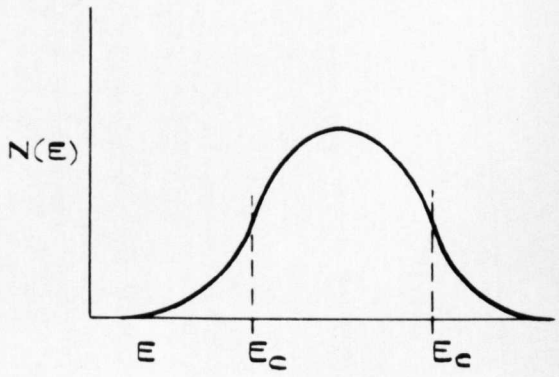

FIGURE 3.7.

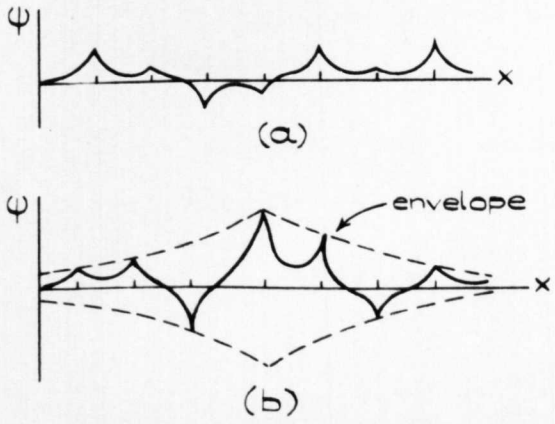

FIGURE 3.8.

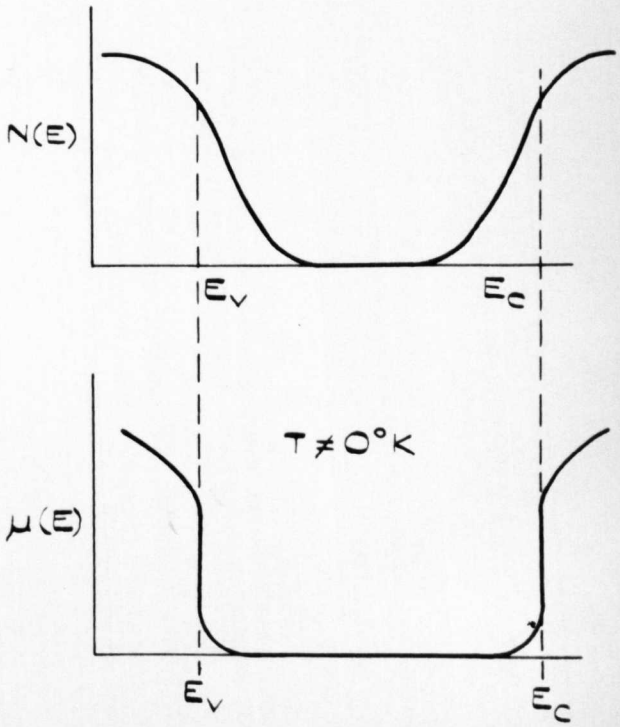

FIGURE 3.9.

FIGURES APPLICABLE TO SECTION 3.03.

3.03.2 D.C. CONDUCTIVITY IN THE ANDERSON BAND

A convenient form of the Kubo Greenwood formula for conduction is given as (see p. 9 of [17]).

$$\sigma(\omega) = 2\pi e^2 \Omega \hbar \omega^2 |x_{ij}|_{av} \{N(E)\}^2 \text{ for small } . \qquad 3.03.2$$

$$x_{ij} = \frac{\hbar}{m\omega} D_{ij}$$

$$D_{ij} = \int \psi_i^* \frac{\partial}{\partial x} \psi_j \, d^3x$$

Ω = specimen volume

and in the limit as $\omega \to 0$

$$\langle \sigma_E(0) \rangle = \text{constant} \quad \langle |D_{ij}|_{av}^2 \rangle \, N^2(E) \qquad 3.03.3$$

It is pointed out that for long mean free paths this leads to a result almost identical with that deduced from the Boltzman formulism where in particular the result is finite at absolute zero.

Equation 3.03.2 is used to estimate $\sigma(0)$ for the case of a short mean free path. A limit of ℓ was suggested by Ioffe and Regel [18] to be equal to the interatomic distance or more exactly $\frac{1}{\hat{k}}$. They suggest that values of ℓ less than this are impossible. For $\ell = \frac{1}{\hat{k}}$ the situation in the Anderson band is one where there is a random change of phase from site to site. This will correspond to a minimum metallic conductivity for the band.

It is estimated that in the middle of the Anderson band as

$$\ell \to \frac{1}{\hat{k}} \qquad \sigma(0) = \left(\frac{8\pi^3 e^2}{\hbar a}\right)\left(\frac{I}{V_o}\right)^2 \qquad 3.03.4$$

I is as in 3.03.1

a = distance between sites.

By assuming a value of $V_o \simeq 5$ at which localization of all states is considered to occur, the minimum value of the conductivity for the Anderson band is

$$\sigma(0) = .06 \left(\frac{e^2}{a}\right)\left(\frac{6}{z}\right)^2 \qquad 3.03.5$$

a, is the distance between wells and is discussed later in applications of equation 3.03.5.

3.03.3 LOCALIZED STATES AND $\sigma(0)$

The existence of localized states in the Anderson band is demonstrated and proved by the following argument.

Consider an electron in a well (a) at an energy V_a below the band of fig. 3.5. (i), its state will be a localized one if (see fig. 3.6)

$V_a > \beta J$ where β is a constant of order unity.

However in this problem, it will be the potentials V of all the other states in the "band" of fig. 3.5 (ii) which will be important and must be considered. Mott argues that if in this situation the well at (a) was at least $(\mp)\beta J$ from any other states in the band, then the removal of well (a) would create a band gap with no states in it. The band gap width he estimates to be $2(\beta - 1)J$. The well (a) can therefore be imagined to be sitting in a band gap and is therefore localized. Hence for some configurations of the states, localized states will exist.

Now consider configurations of the system limited to those which will produce two wells (a) and (b) say, a distance R from each other. They will be situated in the "gap", in the sense introduced in the preceding paragraph. The wavefunctions in the two states will resonate so that the energy separation will not be less than

$$I' = w \exp -\alpha' R. \qquad \alpha' < \alpha \text{ but } > 0.$$

α' = Value of α in the 'gap' ____3.03.6

For a frequency ω, wells (a) (b) will make no contribution to σ unless R is greater than R_ω given by (see [16]).

$$w \exp(-\alpha' R_\omega) = \hbar\omega \qquad \text{____3.03.7}$$

$$\text{so } R_\omega = \frac{1}{\alpha} \log_e \frac{w}{\hbar\omega} \qquad \text{____3.03.8}$$

The x_{ij} will obviously depend on R and it is shown that

$$x_{ij} \simeq R_{\omega}$$

Using this, $\sigma(\omega)$ is found to tend to zero as $(\omega^2 (\log \frac{w}{\hbar\omega})^4$

_____3.03.9

i.e. dc conductivity (when $\omega = 0$) is zero.

Now the fraction of the total possible configurations for which (a) and (b) are further than $(\mp) \Delta J$ from all other sites is small and tends to zero as N (the number of atoms) increases. However this restraint can be relaxed so that this fraction of configurations remains finite. The effect of a third well (c) is considered.

It is estimated that the probability of the electron from (a) being near to (c) is B^2 where

$$B \simeq \left(\frac{\alpha'}{\alpha}\right)^{3/2} \cdot \frac{w}{V_a - V_c} \exp(-\alpha' R) \qquad \text{_____3.03.10}$$

So long as $V_a - V_c \gg w \exp(-\alpha' R_{ac})$ the probability is small, and if B^2, summed for all states in the gap is small, then the localization of (a) is not affected. Hence only wells near to (a) in space, and within the energy range

$$I' \simeq w \exp(-\alpha' R_o) \qquad R_o = \text{distance between nearest neighbours.} \qquad \text{_____3.03.11}$$

need be considered. The number of such configurations and their effect on $\sigma(0)$ must be estimated.

The number of clusters of 'n' wells each within energy I' of each other will be given approximately by

$$N \left(\frac{I'}{V_o}\right)^n \qquad \text{_____3.03.12}$$

It is considered that the possibility of a 'channel' of such clusters existing throughout the material tends to zero as N becomes large, and also that the contribution to $\sigma(0)$ from electrons tunnelling from cluster to cluster will tend to zero in the same way. More explicitly we can consider the energy separation of the wells in such a cluster. The average separation will be J/n, so that conduction as given by equation 3.03.4 will only be possible if $h\omega \gtrsim J/n$ or $n > \frac{J}{\hbar\omega}$. The number of such clusters using equation 3.01.12 is then

$$N \left(\frac{I'}{V}\right)^{J/\hbar\omega} \qquad \text{which} \to \text{zero as } \omega \text{ tends to zero.}$$

It is concluded then, that localized states for which $\sigma(0) = 0$ can exist.

3.03.4 CRITICAL ENERGY

While the Anderson criterion may not be satisfied for states in the energy range of the middle of the band, the nature of N(E) will very likely be such that it is satisfied for a range near the band edges. This implies that in a region near the middle of the band states are non localized, but may well become localized near the edges of the band. A critical energy E_c will then exist demarking the two regions, as illustrated in fig. 3.6. For samples with large N, $\sigma(E)$ is expected to change discontinuously through E_c, this follows from the arguments of the last section.

Just on the conducting side of E_c the wavefunctions are expected to be as in fig. 3.8 (a). Fig. 3.8 (b) is the expected form of ψ in the localized region. The conductivity at T = 0°K jumps discontinuously from zero to a value given by an equation of type 3.03.5 with an appropriate value of 'a'. This value of 'a' is the jump distance given by

$$a_E = a_m + \frac{1}{\alpha} \log \frac{V_c}{V_o'} \qquad \text{3.03.13}$$

a_m = middle of band value of 'a'.

V_c is the given value of V_o for the energy range about E_c, and V_c the critical value of V_o' at which localization will occur. It is also shown that the value for N(E) at E is

$$N(E)_{E=E_c} \geq \frac{1}{a_E^3 V_o} \qquad \text{3.03.14}$$

It is shown in the next section that 3.03.5 with a_E substituted for 'a' is a useful and experimentally determinable property of amorphous semiconductors.

3.03.5 APPLICATION TO AMORPHOUS SEMICONDUCTORS

So far the discussion has been concerned essentially with a disordered metallic band, but the ideas thus far developed are expected to be applicable to amorphous semiconductors. The band edges in such materials are expected to contain localized states. This would imply again the existence of a critical energy E_c, E_v near the band edges of fig. 3.9. Since the discontinuous change in σ at E_c and E_v, cannot be attributed to such a change in N(E) it would seem pertinent to think of the mobility as acting in this discontinuous manner. The sudden drop in μ at E shown in fig. 3.9, Mott refers to as a mobility shoulder. For finite temperatures μ will not drop to zero on the localized side of E_c, E_v because of the contribution to μ from thermally activated hopping.

If the conduction takes place principally in the states on conducting side of E_c and E_v then the usual semiconductor expression for

$$\sigma = \sigma_o \exp -\left(E_g/kT\right)$$

$$\text{where } E_g = \frac{E_c - E_v}{2}$$

for wide band gap semiconductors is expected to apply. The constant

is especially significant, written as

$$\sigma_o = e.\mu.kT.N(E)_{E=E_c}$$

it is seen to be the conductivity of the extended states within kT of E_c , E_v. This is exactly the value given by equation 3.03.3 with a_E of section 3.03.4 substituted for a.

This value of σ_o, with some experimentally determined values is discussed further in chapter 6.

3.04.0 GUBANOV THEORY OF AMORPHOUS SEMICONDUCTORS

In his book [9], Gubanov discusses many aspects of amorphous (solid and liquid) semiconductors, and metals, not all of which are relevant to the materials discussed in this thesis. This section will only deal briefly with his approach to determining the band structure of amorphous solid semiconductors.

A large amount of evidence is put forward in an attempt to show that the band structure of solids is generally maintained in the liquid state. Most of this is in the form of conductivity data of a diversity of materials, measured through the melting point. Having thus established that there is a band structure in the liquid phase of a material, perturbation theory is used to determine details.

3.04.1 DISORDER PARAMETER

The case of a one-dimensional chain of atoms is first considered.

On melting, the long range order of an initially periodic chain of atoms is destroyed, while the short range order is only slightly affected. This is best described mathematically in the following way.

For the crystalline case the N+1 atom is at a distance $(N_a + y)$ from the first atom, where $y \ll a$ and long range order exists. The small departure is due to thermal vibrations. When the crystal melts, the distance between each pair of atoms will become

$$a(1 + \varepsilon\gamma), \qquad \varepsilon \ll 1 \qquad \text{3.04.1}$$

where ε is a constant parameter for a particular material. The quantity γ is different for each pair of neighbours and is of random nature. Assuming no expansion or contraction of the array $\bar{\gamma} = 0$. The probability of a given value of γ is assumed to be given by a Gaussian distribution.

The distance of the N + 1 atom is now given by

$$N_a + y' \qquad \text{3.04.2}$$

where y' is εa times the sum of N values of γ. The root mean square value of y' is shown to be

$$\sqrt{\bar{y}^2} = \varepsilon a\sqrt{N} \qquad \text{3.04.3}$$

If $N > 1/\varepsilon^2$, then the probability of finding the (N + 1) atom is smeared out over a region greater than a lattice constant. Hence the long range order is lost if the number of atoms is

$$G \gg 1/\varepsilon^2$$

The effect of destroying the strict periodicity of the chain on the potential energy seen by an electron is twofold. Firstly, the maxima and minima are displaced in real space following the displacement of the atoms. Secondly, due to the random nature of the displacements the depth of the wells is altered an amount ΔV, which will also be a random quantity, but will be small as ε is small.

It is estimated that the effect of the second type of distortion will be much less than the first. It is however taken into account regardless in the following way. A coordinate scale ξ deformed in the same way as the maxima and minima is introduced using the relation

$$\frac{d\xi}{dx} = \frac{1}{1 + \varepsilon\gamma} \qquad \text{3.04.4}$$

so that the potential correct to within distortions of the second kind is still periodic. The potential can then be split into a part $V_o(\xi)$ periodic in ξ, and a part due to the second kind of distortion. This perturbing potential is expected to be proportional to ε. Hence

$$V = V_o(\xi) + \varepsilon V'(\xi)$$

The Schroedinger equation in the cartesian coordinate x is then transformed into the coordinate ξ and written as

$$(H_o + \varepsilon V' + \varepsilon W + \varepsilon^2 w \ldots)\psi = E\psi \qquad \text{3.04.5}$$

the values of w and W are given in terms of γ and ε

The solutions $\phi(\xi)$ for the perturbed case are assumed to be linear combinations of the Bloch Functions $\psi'^{o}_{nk}(\xi)$ of the unperturbed case i.e.

$$\phi(\xi) = \sum_{nk} C_{nk} \psi^{o}_{nk}(\xi) \qquad \text{n refers to the band} \qquad \text{3.04.6}$$

With the problem set out in this way the details of the energy spectra of the band are calculated. The same thing is done for the three dimensional case.

3.04.2 RESULT FOR ONE AND THREE DIMENSIONAL CASES

In the one dimensional case the two principal effects of the disordering are that the band as a whole is broadened by ΔE, and that the edges of the band become diffuse.

$\Delta E \triangleq E_1 (\varepsilon)^{4/3}$ where E_1 is the width of the initial unperturbed band. ____3.04.7

An estimate of the effect of interband interactions shows this to give a contribution to ΔE which is much less than $E_1 (\varepsilon)^{4/3}$.

In the three dimensional case where the same basic methods are used the edges are again found to be diffuse but the spread of the band is less, being given by

$$E = E_1 \varepsilon^2 \qquad \text{____3.04.8}$$

On the other hand the effect of interband interactions is greater, although for large ε this interaction impedes the closing up of the energy gap, i.e. it reduces ΔE.

The approach for more real cases is taken from this point. In particular the expansion or contraction of the lattice is taken into account, as is the smoothing out of the E(k) curves for the valence and conduction bands.

3.04.3 LOCALIZED STATES

In the amorphous case the wavefunctions were taken to be linear combinations of Bloch functions. Localized states can then in principle exist since such states can be produced by the appropriate combinations of Bloch functions.

Such states could be associated with a potential well of sufficient size, and are thought of as being produced by a large short range order fluctuations. Then density of such levels for a covalently bonded semiconductor is shown to be

$$N = N_o \frac{\varepsilon \sqrt{z}}{2\ 2} \exp - \left(\frac{2}{\varepsilon^2 z \phi^2} \right) \qquad \text{____3.04.9}$$

z is the number of neighbouring bonds, and the coefficient Ø depends on the degree of overlap of the bonding functions. These levels are expected to be in the form of acceptor levels split off from the conduction band or donor levels split off from the valence band. Hence the band edges will tail off exponentially.

Gubanov is able to compare some of his results with numerical calculations of other workers and the agreement is generally good. This is especially so for the band shape and spread, of the one dimensional liquid.

3.05.0 SUMMARY AND DISCUSSION

The theoretical approaches to the problem of amorphous semiconductors, very briefly described in this chapter, although in some ways quite different, have a unifying feature in the results they predict. This is the conceptually simple one of a smearing of the band edges, the states associated with which then probably tail off exponentially into the forbidden gap, and are localized in nature. The consequences of the localized states are only touched upon by the various theories in their present form. Cohen deals briefly with the consequence of the tails overlapping when possibly large densities of charged traps will be created, which will affect the conductivity. Gubanov mentions similarly briefly that the nature of the states will be acceptor and donor like, lying below the conduction band and above the valence band respectively.

Now a simple calculation shows that tails, exponential in form and stretching a few tenths of an electron volt into the gap would produce densities of localized states of approximately $10^{18\text{-}19}$ cc^{-1}. In a crystalline semiconductor such a density of acceptor or donor site would give extrinsic conduction over a reasonably large range of

conductivity and temperature. It is therefore rather surprising that single values of activation energy, presumably associated with $E_c - E_v$ (in say figure 3.6) have always been claimed to describe σ over large temperature and conductivity ranges. Chapter 6 deals with this point and shows that careful measurement of σ reveals considerable changes in activation energy with temperature. The dependence $E_g(T)$ will be seen to be explained by calculations based on the general model of semiconductors drawn again in figure 6.1.

It is interesting to raise the question: what is, or what gives rise to a localized state ? Cohen predicts the tails of states solely on the basis of density fluctuations in a random structure, but also suggests such things as chain ends in selenium. This is thought to be similar in nature to the "dangling bond" concept used by various authors. This "dangling bond" is assumed to be similar in nature to the excess valence electron associated with for example an arsenic atom in the germanium lattice. However donors in a crystal lattice are generally just below E_c so that in fact the analogy may not be a good one.

Contrasting with the agreements of the theory are the disagreements or differences. Apart from the concepts of the exact nature of the localized state, is the more fundamental question of the form of the potential which describes the amorphous semiconductor.

Both Williamson and Matthews, and Gubanov use a potential where depth of wells and distance between them vary randomly. In contrast Mott, and Anderson neglect variation in spatial separation considering only the depth of the wells to be random in size. Gubanov in fact considers this aspect of the disorder to be the less important of the two. However Gubanov's result is also idealized in that he considers no overall change in density of the lattice so that his conclusions are only correct to within this assumption.

There is also a slight difference in the form of the 'mobility edge' as discussed by Mott, and Cohen. The latter favours a continuous change at E_c whilst Mott suggests the change to be discontinuous. The difference in implications for charge transport would not be expected to be great.

REFERENCES CHAPTER 3

(1) Stuke J., Ref. (11) of chapter 1, p. 1.

(2) Male J.C., Warren B.E., New Scientist, 1970.

(3) Kolomiets B.T., Phys. Stat. Sol. 7, p.713, 1964.

(4) Male J.C., Brit. J. Applied Physics, 18, p. 1543, 1967

(5) Edmond J.T., Brit. J. Applied Physics, 17, p. 979, 1966

(6) Siemson K.J., Fenton E.W., Phys. Rev. 161, p. 632, 1967.

(7) Owen A.E., Glass Industry, p. 637, November 1967.

(8) Peck W.F., Dewald J.F., J. of Electrochem Soc. 111, p.501, 1964.

(9) Gubanov A, Quantum Theory of Amorphous Semiconductors, Consultants Bureau, New York, 1965.

(10) Cohen M.H., Electronic Structure of Amorphous Materials, Lectures presented at N.A.T.O. Summer School on Amorphous Semiconductors, University of Ghent, Belgium, 1969.

(11) Mott N.F., Advances in Phys. 16, p. 49, 1967.

(12) Williamson F.W., Matthews N.F.J., Phys. Rev. 180, p. 804, 1969.

(13) Cohen M.H., Ref. (10) of chapter 1, p. 400.

(14) Miller A., Abrahams E., Phys. Rev. 120, p. 745, 1960.

(15) Mott N.F., J. Non Crystalline Solids, 1, p. 1, 1969.

(16) Mott N.F., Phil. Mag. 17, p. 1259, 1968.

(17) Mott N.F., Phil. Mag. 22, p. 7, 1970.

(18) Ioffe A.F., Regel A.R., Ref. (9) of chapter 1.

CHAPTER 4.

MATERIAL AND SPECIMEN PREPARATION

4.01.0 INTRODUCTION

In the past very little information has been given in the literature about the preparation of these materials, and not a great deal of attention given to the point. It has been said [10] [11] that impurities do not play a very significant role in amorphous semiconductors, although on the other hand Mackenzie [12] and Owen [13] have shown that certain impurities do have an effect and are therefore important. To remove the doubt that still persists about this question from the analysis of the results, the method of production was designed to yield as pure materials as possible. Also, the same method was used for all the different glasses produced, so that even though impurities might be present they should be the same impurities and present in similar concentrations in all glasses. It is unfortunately impossible to say what the impurity level is in each material, although the starting elements in each case were claimed 99.999% pure.

Some method had also to be found for determining, other than by qualitative methods, whether or not the materials were amorphous. This was found to be very important since it was shown that the qualitative test of conchoidal fracture was not necessarily indicative of a completely amorphous structure.

The main difficulty in specimen fabrication from the produced materials was an apparent inherent mechanical weakness. This seemed to be a universal feature which could only be dealt with by care in the fabrication techniques employed.

4.02.0 CHOICE OF METHOD

In chapter 1 there was some discussion as to whether this study of amorphous semiconductors should deal with bulk materials or thin films

and the conclusion reached was to work on bulk materials. This choice, having been made, the subsequent question of method of preparation is basically straightforward. It consists of preparing a melt of the glass and quenching, sufficiently rapidly to prevent it crystallizing. However, in order to be able to contrast the end products of thin films and bulk produced materials, the standard methods of thin film production are very briefly outlined.

The method of simple evaporation has been used extensively for the production of thin films [1] [2]. The material is melted in vacuum and the vapour deposited onto a substrate whose temperature ideally is controllable. This basic method has received refinements of late [3] [4], enabling the final composition of the film to be accurately controlled, and reducing the number of impurities in the film arising from residual gases in the evaporator.

Flash evaporation is an extension of the above, the material being dropped directly onto a hot surface and the vapour then condensing onto the substrate.

In the third method, referred to as splat cooling, the molten material is dropped or projected onto a cold surface and thus cooled rapidly [5].

Finally the method of reactive sputtering [6] [7], where the chemical reaction takes place in an r.f. discharge instead of being promoted thermally.

4.03.0 DESCRIPTION OF METHOD

The exact procedure adopted for material preparation was governed by the objective of producing specimens as free as possible from unwanted contamination.

The starting elements were all obtained commercially* and claimed to

* From Koch Light Ltd. and Johnson Matthew Ltd.

be better than 99.999% pure.

The fused silica tubes in which the materials were melted were given a rigorous cleaning procedure. This consisted of washing with a solvent, generally acetone, followed by a further wash with a 2% solution of hydrofluoric acid. The tubes were finally washed with distilled water before being heated to approximately 400°C, and cooled slowly, to remove all water from the surfaces. Details of the dimensions of the tubes are given in fig. 4.1.

The silica ampoules, starting elements, and balance were all contained within a glove box and, before any weighing out of materials was commenced, a constant flow of dry nitrogen was maintained to the box, for at least twenty four hours. After this time, it was considered that the quantity of oxygen remaining was negligibly small.

The appropriate amounts of the starting elements were then weighed out on a balance which allowed weighings to be made with an accuracy of 0.5% for 1gm weight, and 0.05% for 10gm weight.

The starting elements were used in the form in which they were delivered, with the exception of selenium. This was obtained in pellet form and had to be ground into slightly finer grained particules, approximately 2 mm. maximum dimension, in order to facilitate tipping into the ampoules. It was not possible to use the powder form of selenium otherwise easily available, for reasons explained in 4.05.0.

Effectively three weighings were required for each sample, and the estimated maximum error in any constituent of a melt was 1.0%, and typically 0.5%. The ampoule and contents whilst still in the glove box, was then sealed temporarily and removed to a pumping unit. At this stage the ampoule was evacuated and refilled with argon, the processes being repeated three or four times. This was a further precaution taken, to prevent contamination from oxygen. The ampoule and contents were then

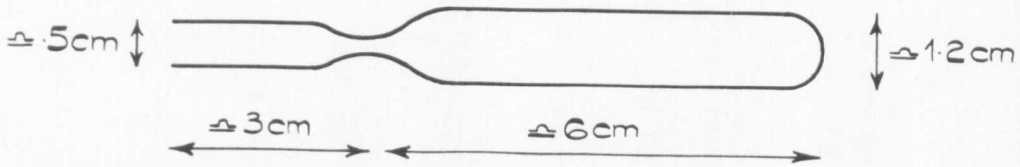

FIGURE 4.1.

TYPICAL SILICA AMPOULE IN WHICH GLASSES WERE MELTED

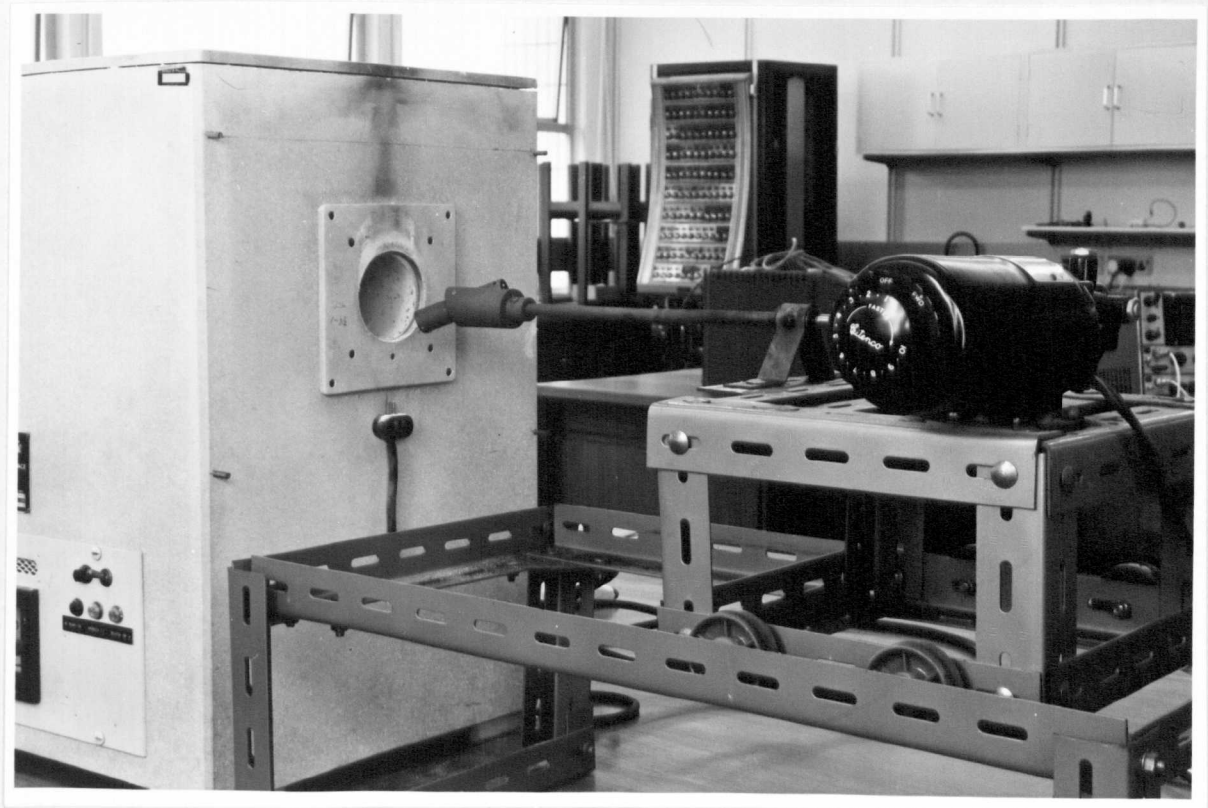

FIGURE 4.2

FURNACE ARRANGEMENT.

baked out at a temperature of approximately 120°C, and pressure 10^{-4} torr, to remove any water from the surfaces of the elemental powders. Following this, the ampoule and contents were again flushed out with argon, prior to final pumping down and sealing. This final sealing off was achieved by heating the neck of the tube until the glass was soft enough to collapse under atmospheric pressure.

The evacuated tube and contents were then fixed into a stirrer mechanism and subsequently, into a furnace. The experimental arrangement of stirrer and furnace are shown in fig. 4.2. The stirrer consists of a hollow stainless steel tube in which the ampoule is slotted and held, attached at an angle of 20° to a stainless steel rod. As the rod turns, the ampoule is made to rotate about an axis, not equal to its own, causing constant agitation of the contents.

The furnace, made to order by the Carbolite Company, consisted of a heated tube, 16" long and 3" in diameter, with a hot zone, some 8" long. A stainless steel 'liner' was added to the inside of the tube, to protect it from exploding ampoules. The temperature of the tube was controllable to within 10°C of any desired temperature between 100°C and 1200°C. The stirrer was mounted on a simple trolley and rail system, to allow easy access to the furnace.

All melts were stirred continuously whilst in the furnace. The As-Se and As-Te glasses were melted at a temperature of 820°C for between 8 and 20 hours, the Se-Te melts at 600°C for similar lengths of time. (The reason for different melting times, is explained later.) At the conclusion of the melting time, the ampoule was removed from the furnace, still at the temperature of melting, and quenched in air. It was found necessary for some materials, for reasons explained in 4.05.0, to subject them to an annealing process. This was suitably achieved by allowing the melt to cool until it was effectively solid, and then placing it in a furnace at a

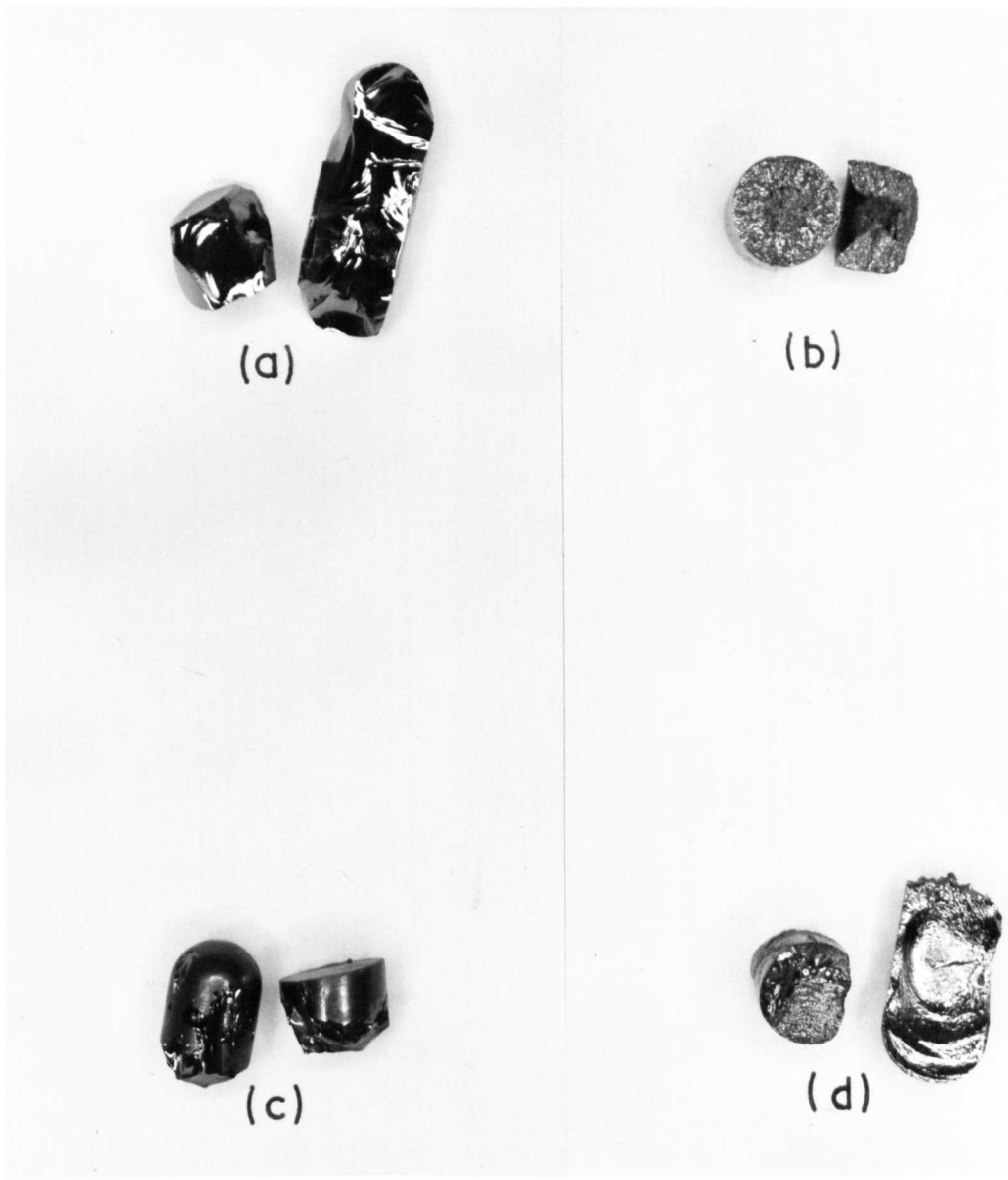

FIGURE 4.3.
TYPICAL AS-QUENCHED SPECIMENS.
(a) SHOWING CONCHOIDAL FRACTURE.
(b) CRYSTALLINE FRACTURE SURFACE.
(c) MECHANICALLY WEAK SPECIMEN SHOWING TENDENCY TO SHATTER.
(d) AMORPHOUS MATERIAL WITH 'MATT' FRACTURE SURFACE.

temperature estimated to be close to the softening temperature of the glass. The furnace, which had been stabilized at this temperature, was then allowed to cool at its natural rate. This effected a suitable annealing process.

After attaining room temperature, the ampoule was opened and the ingot of material removed.

4.04.0 TESTS FOR AMORPHOUSNESS

Before measurements were made on any of the materials produced, they were subjected to examination to determine whether they were crystalline or amorphous. Two tests were applied. The first and more simple test was by examination of the fracture surface. Amorphous solids can be characterized by their so-called conchoidal fracture. The fracture surface consists of convexities and concavities, this is best appreciated by reference to fig. 4.3, in which (a) shows the fracture surface of an amorphous solid and (b) is the fracture surface of the crystalline phase of the same material. This test is useful for a first examination, but the material can more definitely be said to be amorphous or not, by means of the second test used, that of X-Ray diffraction.

It was most suitable for these materials, to use the Debye Scherrer method, employing a finely powdered specimen. The specimen was contained in a fine capillary tube and rotated in a beam of Copper K_{α} X-Rays. The apparatus used was a Phillips PW 1009 X-Ray generator, with matching Debye Scherrer camera. The tube current was typically 20 mA and exposure of the Ilford G film was for 4 hours. As an example fig 4.5 shows the result for the glass 20 At% Te 80 At% Se. (a) is the diffraction pattern of the amorphous phase, and (b) that of the crystalline phase. This test clearly distinguishes the crystalline and amorphous phases, and was made for each material.

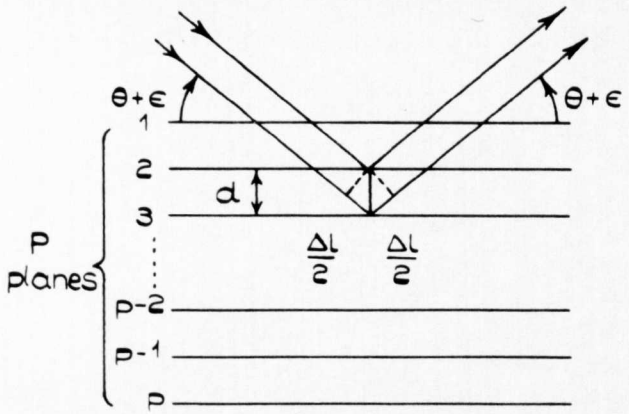

FIGURE 4.4.

X-RAY DIFFRACTION PATTERNS FOR AMORPHOUS AND CRYSTALLINE 80Se 20Te.

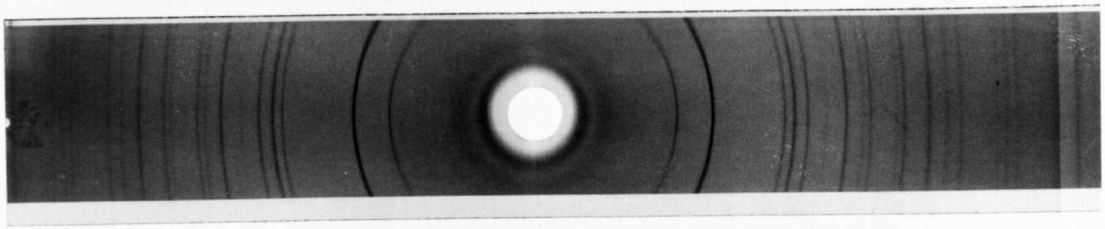

X-RAY DIFFRACTION PATTERN OF PARTIALLY DEVITRIFIED 80Se 20Te

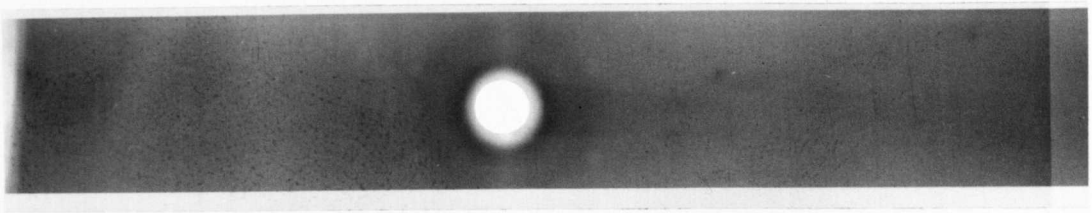

X-RAY DIFFRACTION "PATTERN" OF AMORPHOUS 80Se20Te

FIGURE 4.5.

However the test has a limit of resolution. It would be possible for the material to consist of very small crystallites and for both of the above tests to show the material to be amorphous. A simple analysis is therefore made, so that an upper limit can be placed upon the size of any crystallites.

4.04.1 RESOLUTION OF X-RAY TEST

The following simplified argument is due to Klug [9].

Assume a crystallite has p atomic planes (h.k.l) fig.4.4, and radiation incident at an angle θ. The amplitude of the diffracted ray is a maximum for $\Delta\ell = 2d\sin\theta = n\lambda$ ____ 4.04.1

If the glancing angle becomes $\theta + \epsilon$

then $\Delta\ell = 2d\sin.(\theta + \epsilon)$.

which simply becomes using 4.04.1 $= n\lambda + 2\epsilon\, d\cos\theta$ for small ϵ.

The corresponding phase difference $\frac{2\pi\Delta\ell}{\lambda} = 2\pi n + \frac{4\pi}{\lambda}\epsilon\, d\cos$

$$= \frac{4\pi\epsilon\, d\cos}{\lambda} \quad \text{____ 4.04.2}$$

Using a simple theory of optics if n equal vectors of amplitude 'a' alter in phase by successive uniform increments the phase difference of the first and p^{th} planes is

$$a_n \frac{\sin\alpha}{\alpha}$$

α being one half the phase difference of the first and the last vectors. Now the phase difference between the first and p^{th} planes is

$$\phi = \frac{4\pi\, p\epsilon\, d.\cos}{\lambda}$$

Hence the amplitude of the reflected wave is

$$A = ap\, \frac{\sin\left(\frac{2\pi\, p\,\epsilon d.\cos}{\lambda}\right)}{\left(\frac{2\pi\epsilon\, d\,\cos}{\lambda}\right)}$$

when $\epsilon = 0$ the maximum amplitude A_o is then

$$A_o = ap.$$

At half maximum intensity

$$\frac{A^2}{A_o^2} = \frac{1}{2} = \frac{\sin^2 \phi_{\frac{1}{2}}}{\left(\frac{\phi}{2}\right)^2} \qquad 4.04.3$$

4.04.3 is satisfied when $\frac{\phi}{2} = 1.4$

Then $$\frac{2\pi p \epsilon_{\frac{1}{2}} d \cos\theta}{\lambda} = 1.4$$

The full angular width at half maximum intensity of the reflection

$$4\epsilon_{\frac{1}{2}} = \frac{4 \times 1.4 \lambda}{2\pi pd \cos\theta}$$

$$= \frac{.89\lambda}{D_{hkl} \cos\theta} \qquad 4.04.4$$

This is a relationship which gives an estimate of the size of the crystal (normal to the h.k.l. planes) in terms of the half width of diffraction line.

4.05.0 PARTICULAR PROBLEMS IN MATERIAL PREPARATION

Ideally, the procedure outlined in 4.03.0 produced ingots of non-crystalline material, as defined by the tests applied and discussed in 4.04.0. They would also be mechanically strong enough to withstand the cutting procedure required in the fabrication of experimental specimens. That these points were satisfied, was however more often the exception than the rule. If a material did not appear in this ideal state, it was generally found to be in one of three other "states". Firstly, and most simply, the material was crystalline, or more exactly polycrystalline. This was a common result in trying to prepare materials near the glass-forming limit of a system, but as will be described, it could appear elsewhere. Secondly, the material was in all but one respect ideal, the exception being that it was mechanically weak. This would typically mean that the specimen would break up on removal from the silica ampoule, although in other cases it

was not manifest until an attempt was made to cut the ingot. The third type of defect was for the ingot to have, what is adequately described as a matt finish to the fracture surface. This was often accompanied by a large number of small bubbles, those in the centre usually being larger than those at the edge of the ingot. It was also common in such cases to find a 'slag' on top of the ingot, rather resembling sintered material. Examples of some of these defects are shown in Fig. 4.3.

The causes of these defects were never clearly understood and indeed only the vaguest idea of the controlling factors of the first and third type of defects was obtained. Analysing the causes and effects was made particularly difficult because of the apparently large number of variables having an influence on the final product. However, there was evidence for certain controlling factors and these are now outlined.

The most straightforward defect, that of mechanical weakness is dealt with first. It was reasonable to believe that this was due in the major part to the rapid cooling of the melt, particularly below the softening temperature. This, together with a finite thermal coefficient of expansion, caused strains to set up in the ingot, leading to cracking and fracture. The most obvious remedy was to anneal the specimen. This was generally successful, though not in every case. The most suitable form of annealing, was to stop the rapid quench at a temperature just below the liquidus temperature, and from then on to cool slowly to room temperature. How this was achieved experimentally is described in 4.03.0. This defect affected in the main the As-Te system and the As-Se system above 30 At% As.

The defect of crystallinity, especially in the As-Te system, was in many ways the most difficult to overcome. It would obviously always appear beyond the glass-forming region of a system, but it was not possible to define this clearly for the As-Te and Se-Te systems. For the second of these two systems, melts containing 20-30 At% Tellerium were liable to

produce crystalline or non-crystalline solids. It is possible here to rule out the effect of melting temperature on the state, (i.e. glassy or crystalline) of the final product, since this was kept constant for all melts in any one system. The melting temperatures were:- As-Te and As-Se systems, 820°C, Se-Te system 600°C. The purity of the selenium was possibly a factor. This was found to influence the quality of the As-Se melts and it may have affected the Se-Te melts to the extent of causing crystallinity.

For the As-Te system the final result , i.e. amorphous or crystalline, for compositions containing between 45 and 60 At% Arsenic were entirely unpredictable. Outside this region the resulting material was always crystalline.

A factor which appeared, surprisingly, to have no effect was the speed of cooling. If a glass was not formed by quenching in air it was not 'formable' from that melt, even by very rapid cooling to say liquid nitrogen temperatures.

A factor for which there was some evidence, was that of contamination of the arsenic with oxygen. If initially pure arsenic was contaminated (presumably with oxygen) by a brief exposure to the atmosphere, or even by a long exposure to the controlled atmosphere of the glovebox, then it was much less likely to form a glass with an appropriate amount of tellurium. On the other hand, in the early stages of the work, glasses were quite easily obtained using 'Analar' arsenic (purity 99%), but the impurities involved, although probably metallic, were not known.

This dependence on purity, of the glass forming ability is worthy of comment. It has been reported in the literature (e.g. Refs [14] and [9] of of chapter 3) that impurities do not effect the electronic properties of amorphous semiconductors. The above result however shows that the

structure is affected by certain, not clearly defined impurities. If the structure is affected in such a fundamental manner, then in these cases one would expect that the electrical properties are also affected. Since in fact little work has been done on this point it should only be concluded at the present that some impurities do affect the general properties of the materials and some do not.

The third type of defect, that described as giving bubbles and a matt finish, was in part understood. If a successful procedure for producing a selenium containing glass were repeated, replacing the pelleted form of selenium generally used with a finely powdered form, then the final product would contain defects of the third class. The same effect would occur if the pelleted selenium were exposed to the atmosphere for some length of time, probably several hours. The cause would again seem to be oxygen, although in what sort of quantities it is impossible to estimate* accurately.

As well as the above causes of defects it was also possible to speculate on the effect of the condition of the surface of the quartz ampoules, especially with regard to whether the cleaning procedure had been adequate. Also, the taking out procedure, the effectiveness of flushing with argon, and the quality of the vacuum in which the materials were melted could have affected the quality of the final product.

It would be possible only to say with certainty that oxygen impurities in starting element reduces the glass forming ability, but it most certainly is not the only factor. Following all reasonable precautions to prevent contamination by oxygen did not in these systems automatically ensure a good defect free product.

* A very crude estimate from assuming the red oxide film observed on the surface of a pellet 2mm in diameter is 1μm thick which is enough to cause the effect, implies the presence of .1% Oxygen.

4.06.0 PREPARATION OF EXPERIMENTAL SPECIMENS.

The materials on removal from the silica ampoules were in the form of ingots 1 - 1.2 cm. in diameter and from 1 - 4 cm in length. The first stage in producing a specimen for any of the experiments, was most conveniently to obtain a disc of the material, so that it was required to slice the ingots normal to their axis. The most suitable available instrument for this was a 'CAPCO Q.35 High Precision Cutting Machine". The essential features of the machine were a thin (.008") annular blade, diamond impregnated on its inner edge, which rotated at $\triangleq$ 1000 r.p.m. The sample to be cut was mounted on a horizontal table, which could be moved parallel to and normal to the plane of the blade. The speed of the movements parallel to the blade (i.e. the cutting speed) was variable. With this arrangement the ingots were easily sliced into parallel sided discs.

4.06.1 A.C. AND D.C. CONDUCTIVITY

These specimens were discs cut as described above to a thickness of 1mm. Both surfaces were ground with the equivalent of 600 mesh Carborundum and subsequently cleaned and dried. Gold eletrodes were then applied to the sample which was achieved using a standard evaporation technique. The chamber containing the sample was evacuated to approximately 10^{-4} torr and the gold evaporated from a tungsten filament at a distance of 5 cm or so. The electrode configurations used (they are explained in 5.02.) are shown in fig. 4.6 The thickness of the electrodes is estimated at .1 - 1μ .

4.06.2 OPTICAL ABSORPTION

For measurement of optical absorption, up to values of absorption coefficient of $10^{1} - 10^{2}$ cm^{-1} a disc of thickness 1 mm was again suitable.

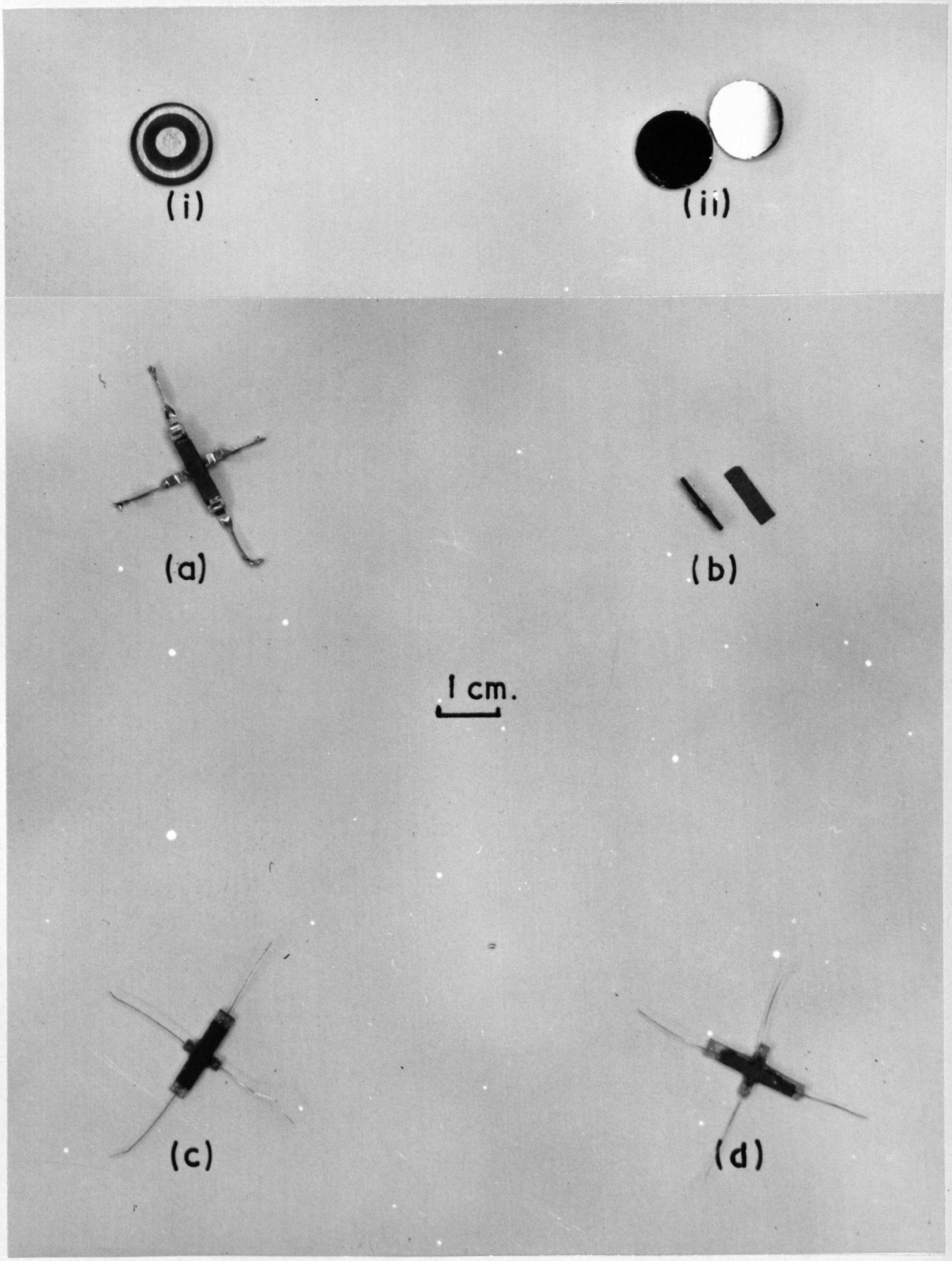

FIGURE 4.6.

EXPERIMENTAL SPECIMENS

(I) ELECTRICAL (II) OPTICAL (a) - (d) HALL EFFECT.

To obtain measurement of higher values of absorption coefficient thinner specimens are required. Very little further information will however be obtained unless the specimen is at least an order of magnitude thinner. Information can then be obtained about absorption coefficients of between 10^2 and 10^3 cm^{-1}.

To produce thin specimens by mechanical polishing was difficult since a characteristic of the materials was their mechanical weakness, even of those specimens having undergone the annealing process described in 4.05.0. Methods of chemically thinning samples were investigated, but no suitable etchant or procedure was found.

A second method that was tried, was to produce a fine powder of the material suspended in K.Br.discs. Transparent discs could be easily obtained by using finely powdered (200 mesh) K.Br. powders, and compressing these at pressures of approximately 50 tons/sq.in. However on introducing even very small amounts of the powdered specimen the discs become opaque. It was deduced that the loss of light was due to scattering from the particles which were all $< 38\mu m$, and from scratches on the surface of the particles.

The method finally found was simple, and also very suitable for measurements of optical transmission. A slight modification also made electrical measurements of thin samples (see chapter on space charge limited currents) possible. The method is now described.

A disc of approximately 1 mm thickness has one face polished (this polishing procedure is described later in this section), before being glued, polished face down, to a microscope slide. The ideal glue for this purpose was Durofix, since it provides a mechanically strong bond, and possesses suitable optical properties. Once set firmly the specimen could then be ground down to a thickness of $100\mu m$, the microscope slide providing adequate support. It was often the case that hairline cracks would appear

across a specimen during this procedure. However they remained very thin and did not affect the absorption measurements as long as the thinning stopped at approximately 100μm. The freshly ground surface was then optically polished.

The final product was a composite layer, consisting of 100μm of specimen, approximately 10μm of glue and 1 mm of microscope slide. The glue and microscope slide were found to have completely constant transmission over the range of the absorption edges. This meant these absorptions were automatically accounted for in the procedure used (see 5.03) to deduce absorption coefficient from transmission data. The actual thicknesses of the specimens was simply measured with a micrometer, the measurement at 100μ being within 5%.

The surfaces of all specimens, after being ground to the equivalent of 600 mesh were polished using a suspension of alumina particles in water. The polishing was best effected using the suspension on a damp velvet pad (trade name Metallurgical Services Dormax Alumina Suspensions) fixed to a rotating disc. A good polish was achieved using a coarse alumina suspension followed by the fine suspension.

This method of thinning is considered very useful, and it is estimated that with care specimens could be obtained only 10μm thick. This would mean a large amount of the fundamental absorption edge can be investigated without resorting to the methods of 4.02.0 to produce thin films. This is very desirable since there is a strong possibility of these materials having different structure to bulk produced glasses.

4.06.3 HALL EFFECT SPECIMENS

In the past a large number of different specimen shapes have been used in Hall effect measurements [8]. The governing factors of specimen

shape are, size of signal, edge effects, strength of material and ease of electrical contact. In the first instance the overruling factor for the materials being investigated here was the strength of sample, or more exactly the weakness. This meant overlooking at first the problem produced by edge effects. The first samples were then simply plane parallelepipeds typically 1.2 cm by .3 x .08 cm with gold evaporated on to the two ends and at opposite points on the long edges, see fig. 4.6(b). Electrical contact was made by pressing brass pins onto the evaporated gold. The result was unsuitable for two reasons, (1) the offset voltage (due to Hall electrode mis-alignment) was generally too large and (2) the contacts were very susceptible to mechanical failure. These points were improved by mounting specimens on glass crosses as shown in fig. 4.6(a). The evaporated gold is 'trailed' onto the glass and contact made from there by silver clips. There was still however the problem of offset voltage, and also this voltage became distorted if too large a field was applied (typically greater than 50 volts/cm). The cause of signal distortion was never conclusively determined.

A further improvement was made and fig. 4.6(c) shows this. The contact to the specimen is made by platinum wires. The wires were heated to a temperature just above the softening temperature of the specimen (this was most suitably effected by contact with a soldering iron). Quickly touching the hot wire on the specimen and removing the source of heat, resulted in the wire being bonded into the specimen. The contact was strengthened with a small bead of araldite holding the wire onto the glass. The problem of signal distortion was overcome in this way, but the problem of offset voltage remained.

It was at this point when it became obvious that the offset voltage would have to be overcome elsewhere than at the specimen itself and it was decided to back off this voltage in a difference amplifier. This is described in 5.04.0 and was, at least in part, successful.

The reason that a Hall voltage could now not be seen was attributed to edge effects at the Hall probes, and to reduce this effect specimens of the type shown in fig. 4.6(d) were produced. A very tedious procedure was required in producing these specimens which were cut from discs using the CAPCO cutting machine, a total of 10 cuts being required for each specimen. The difficulties were also increased by a large failure rate due to the weak materials. However such specimens were produced for the four materials in the As-Te system, and these are the ones from which the results quoted were obtained.

4.06.4 SPECIMENS FOR SPACE CHARGE LIMITED CURRENT MEASUREMENTS

These specimens were a simple extension of the procedure for producing the thin optical specimens. Before glueing the disc to the glass slide a hole 3 - 4 mm was ultrasonically drilled through the slide. A surface of the discs ground to 600 mesh is then glued over the hole, so that both sides of the disc are still accessible. After being ground down to the required thickness gold electrodes were evaporated onto both surfaces. Contacts were made to these electrodes using a silver paste compound.

REFERENCES CHAPTER 4

(1) Holland L., Vacuum Deposition of Thin Films, Chapman and Hall.

(2) Chopra K.L., Thin Film Phenomena, McGraw Hill.

(3) Howson R.P., Malina V., J. App. Physics D, 871, 1970.

(4) Ferrier R.P., Herrell D.J., Phil. Mag. 19, 853, 1969.

(5) Dwez P., Willens R.H., Trans. Met. Soc. A.I.M.E., 227, p. 362, 1963.

(6) Chittick R.C., et al, J. Elec. Chem. Soc., 116, p. 78, 1969

(7) Sterling H.F., Swan R.C., Solid State Electronics 8, p. 653, 1969.

(8) Putley E.H., Hall Effect and Related Phenomena, Butterworths.

(9) Klug H.P., Alexander L.E., X-Ray Diffraction Procedures, John Wiley.

(10) Ref (9) of Chapter 3.

(12) Mackenzie H., J. of Non. Cryst. Sols. 3, 1970.

(13) Ref (7) of Chapter 3.

(14) Fagen E.A., Fritzche H., J. of Non. Cryst. Sols., 2, p. 180, 1970.

CHAPTER 5

EXPERIMENT

5.01.0 INTRODUCTION

As stated in chapter one, it was decided to undertake several complementary experiments. The object was to gain information which could be compared and contrasted, with the aim of increasing the information and understanding of the electronic behaviour and structure of the materials. The choice of the experiments was also explained in the first chapter, and in this chapter the experimentation concerned with each is described, in the following order: (i) conductivity, (ii) optical absorption, (iii) Hall effect, (iv) Supporting experiments. The last group of experiments, as the title suggests, were carried out to support certain ideas, and in general were not made on glasses from all systems.

A description of the actual experimental specimens and their fabrication is given in chapter 4.

5.02.0 D.C. CONDUCTIVITY

At the time of the commencement of the project, no measurements of conductivity had been reported below room temperature, and very rarely below conductivities of 10^{-12} ohm^{-1} cm^{-1} (see for example refs. [1] - [4]). It was considered necessary to make a more exhaustive measurement of conductivity than this, and therefore the apparatus was designed to be as sensitive as possible, and to cover as wide a range of temperature as possible.

5.02.1 THE ELECTROMETER AND MEASURING CIRCUIT

The basic instrument used in this measurement was an Electronic Instruments Ltd. 62.A vibrating reed electrometer. This is a standard

instrument for the measurement of d.c. potentials from high source impedancies.

The electrometer was used to determine the current passing through a specimen, by measuring the potential drop across a known resistance in series with the specimen. The known resistance was always at least two orders of magnitude smaller than the specimen resistance, so that the latter was simply determined from

$$R_{Spec} = \frac{V \cdot R_k}{V_{Elec}}$$

R_k = known resistance

See fig. 5.1.

The instrument had an input impedance greater than 10^{16} ohms, and an approximate detection limit of 10^{-16} amperes.

The experimental arrangement is shown in fig. 5.1. The d.c. voltage was obtained most conveniently by using dry cell batteries; these provided good stable voltages, the only disadvantage being that to vary the voltage, batteries had to be switched in and out of the circuit which caused unwanted transients. The switch S.1 allowed any capacitance associated with the specimen to be discharged.

5.02.2 THE CRYOSTAT AND SPECIMEN HOLDER

A special cryostat and specimen holder were designed which allowed the temperature of the specimen during measurement to be varied from 77°K to approximately 500°K. (500°K was above the softening point of all the materials investigated.)

Details of the cryostat and specimen holder are shown in figs. 5.2 and 5.3. All leads in the measuring circuit were passed through P.T.F.E. lead-throughs in the top of the cryostat and specimen holder to give good electrical insulation. The whole cryostat was necessarily "gas tight" to

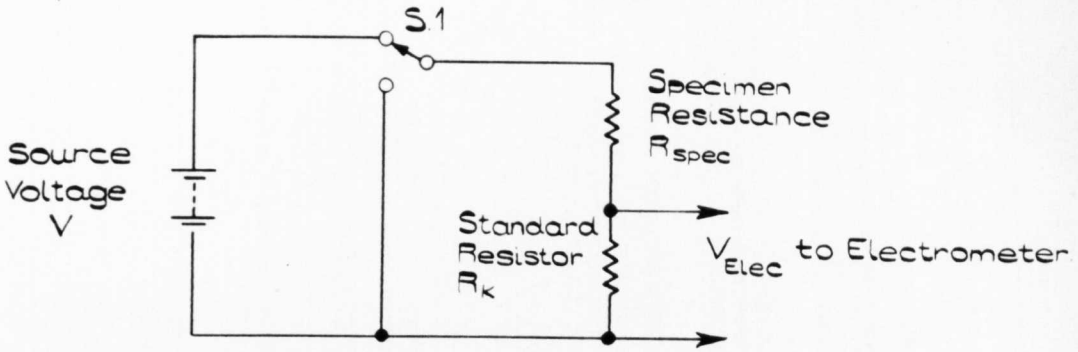

FIGURE 5.1.
ELECTROMETER CIRCUIT.

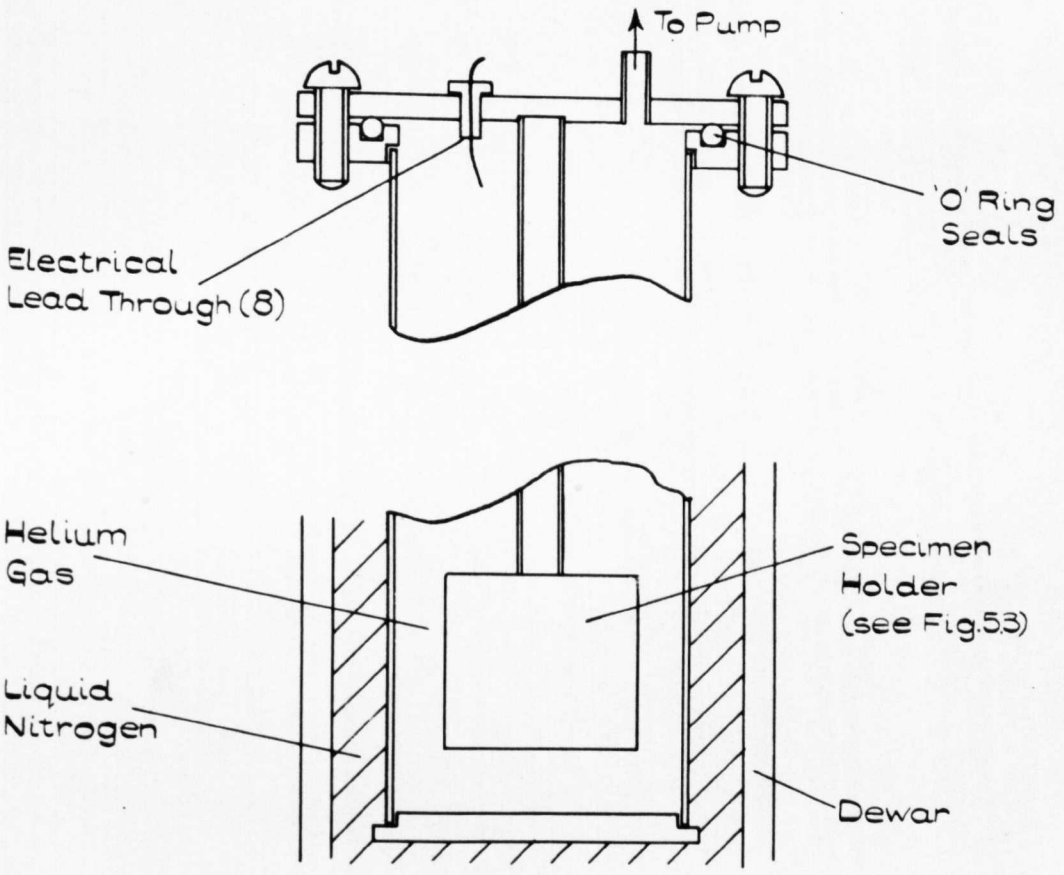

FIGURE 5.2.
D.C. CONDUCTIVITY CRYOSTAT.

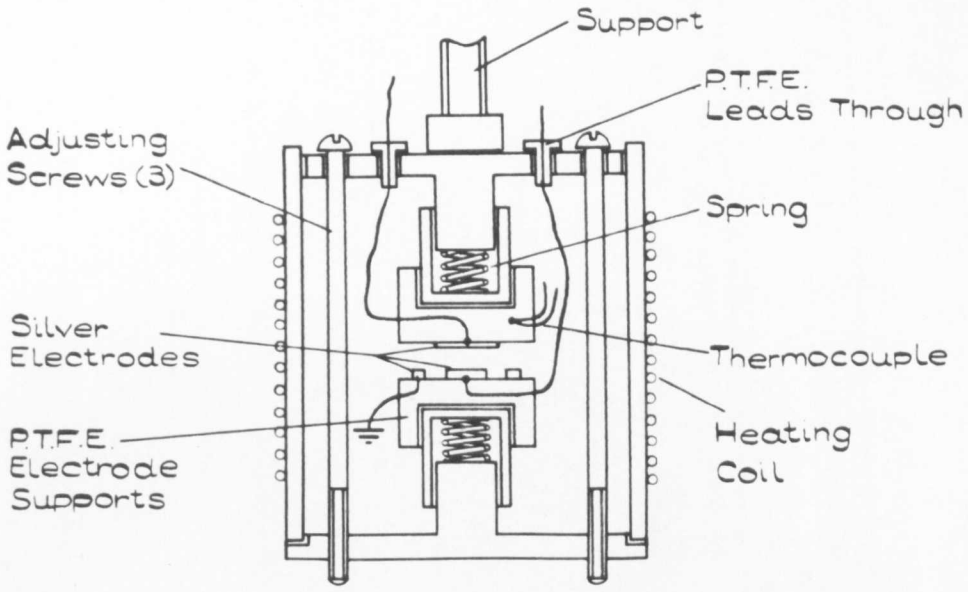

FIGURE 5.3.
SECTION THROUGH SPECIMEN HOLDER.

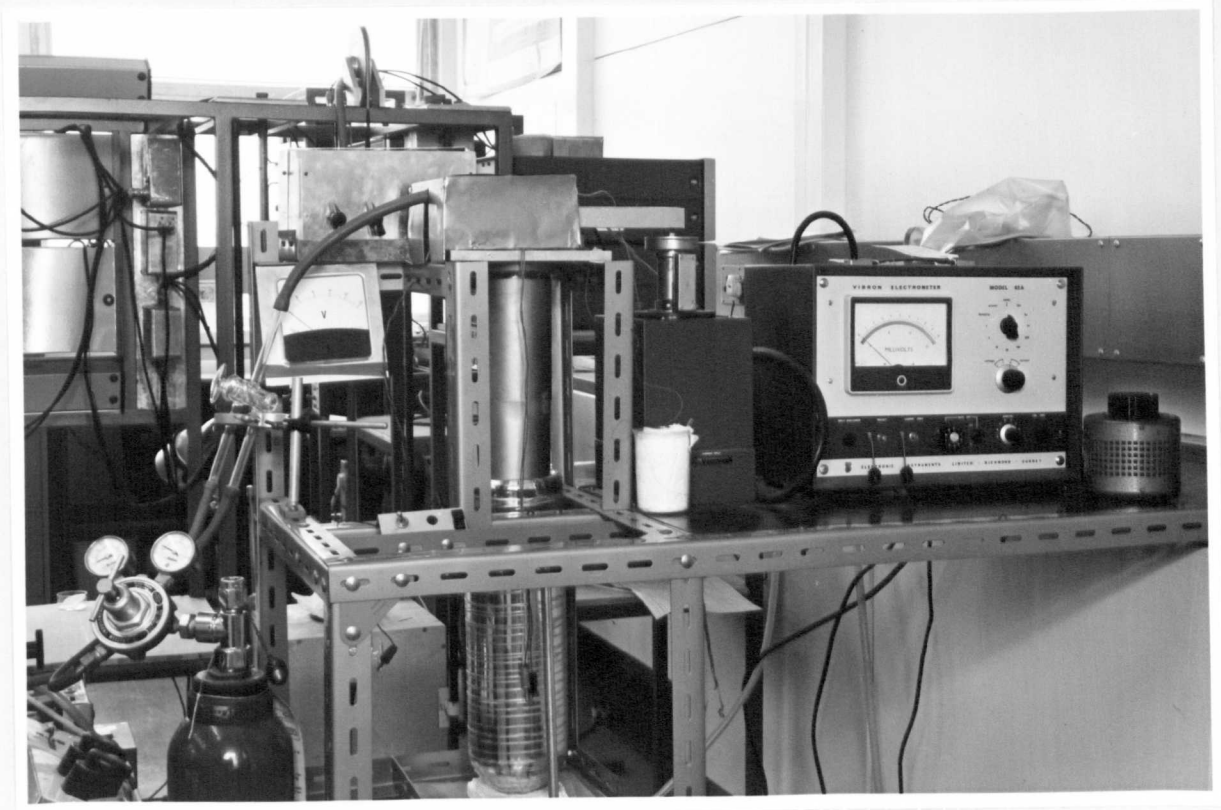

FIGURE 5.4.
PHOTOGRAPH OF D.C. CONDUCTIVITY APPARATUS.

allow the removal of air and replacement with an exchange gas, which in each case was helium.

With the exception of the electrode mounts, springs, and supporting screws, the whole of the specimen holder was made from copper to ensure a reasonably constant temperature throughout. The electrodes were made from silver and mounted in P.T.F.E. There were three electrodes in all, providing high and low terminals and a separate earth, matching with the electrodes evaporated onto the specimen. The springs provided the pressure for contact with the specimen.

Temperatures down to 77°K were obtained by heat exchange with a jacket of liquid nitrogen around the cryostat. A simple resistance heater, powered via a variable step-down transformer from the A.C. mains, allowed the temperature of the holder to be increased up to 500°K. The temperature of the specimen was measured using a copper-constantan thermocouple, which had been calibrated at 77°K 273°K and 373°K. The reference junction during measurements was melting ice and the thermocouple voltage was measured with a Pye thermocouple potentiometer. The thermocouple was placed as near as possible to the specimen (approximately 1 m.m. distant) to obtain as true a specimen temperature as possible.

Measuring small currents associated with high source impedances is made difficult by stray electromagnetic and electrostatic fields which produce transient currents far in excess of that being measured. To reduce the effects of these fields all leads from the cryostat to the electrometer were shielded. This was most suitably effected using some form of low noise screened cable with the outer screen earthed. The top of the cryostat was capped with a high susceptibility metal shield, to screen the inevitable short lengths of unscreened leads at the junctions. Fig. 5.4 is a photograph of the apparatus.

5.02.3 EXPERIMENTAL PROCEDURE

Before making any measurements the air in the cryostat was flushed out and replaced with helium, which provided a suitable heat exchange between specimen holder and the liquid nitrogen jacket.

Some preliminary measurements, using very low applied voltages were first required on a new material to obtain an approximate value of the specimen resistance. The electrometer was very sensitive and would be damaged if R_k were chosen incorrectly so that a large voltage was applied to the input. This being established suitable values of the applied voltage and R_k were selected.

The A.C. supply to the heater provided a small problem in that the associated e.m. waves induced A.C. voltages in the sample leads inside the cryostat, and the frequency of these voltages was within the pass band of the electrometer. This could obviously be overcome by only making measurements as a function of decreasing temperature. Some accuracy is however sacrificed by not being able to take any result as the average of two (obtained as the temperature increased and decreased), but the temperature was varied slowly, of the order of 1-2^{o}C per minute so that the error in the value of specimen resistance for any value of temperature is not expected to be significant.

Measurements then, were made from a temperature, close to that of the softening point of the material, at intervals of 1^{o}C or 2^{o}C, down to a temperature at which the voltage across R_k, as recorded by the electrometer could not be distinguished from noise. A typical specimen resistance at this point would be $\simeq 10^{15}$ ohms, which for a typical specimen configuration would represent a conductivity $\simeq 10^{-16}$ ohm^{-1} cm^{-1}.

The conductivity of a material is calculated from the specimen resistance R_{Spec}, and specimen and electrode geometry, simply using

$$\sigma = \frac{R_{Spec} \cdot L}{A} \qquad 5.02.1$$

L = thickness of specimen, A = area of central electrode.

The estimated error in any absolute value of σ , due to errors in electrometer reading, R_k L, and A is 10%. The errors in relative values for any system are however reduced since the same values of R_k and of A are used in each case.

This measurement was carried out on each material investigated and the results, presented as plots of log.σ vs. $\frac{1}{T}$ are presented in chapter 6.

5.03.0 INFRA-RED ABSORPTION

The transmittance of specimens was measured over the wavelength range of the absorption edge, and the measurement repeated at several temperatures from room temperature down to 4.2°K. The apparatus, experimental procedure, and calculation of absorption coefficient from experimental data are described.

5.03.1 THE SPECTROPHOTOMETER

The instrument employed for determining the transmission of a specimen was a Grubb Parsons Spectromaster Spectrophotometer, covering the wave number range 12500 to 400 cm^{-1} (wavelength range .8μm to 25μm). In this instrument, radiation from a Nernst filament is split into two beams, one being a reference beam, while the specimen is placed in the other. After absorption by the specimen, the two beams are brought together and made to follow the same optical path, but at different intervals of time, any one interval being $\frac{1}{10}^{th}$ sec. After passing through a monochromator the radiation falls upon a detector, in this case a thermocouple. If the sample is absorbing, an alternating component is produced in the output from the detector. This signal is amplified,

rectified, and used to control a servo motor, which drives an attenuater into the reference beam until balance is restored. A potentiometric recorder, records essentially the position of the attenuater in the reference beam, which is directly proportional to the percentage absorption of the specimen.

5.03.2 THE CRYOSTAT AND SPECIMEN HOLDER

To measure the absorption over a range of temperatures, the specimen had to be contained in a cryostat in which it was possible to have I.R. transparent windows. No such device was commercially available so that one was designed and built in the School of Physics. It was designed by the author and Dr H. Harper, although principally by the latter. Fig. 5.5 shows the essential features. The entire dewar, with the exception of the specimen holder was made of glass, an unusual feature in cryostat design, but which was in the event very successful. The inner dewar is surrounded by vacuum jacket, liquid nitrogen jacket, and a further vacuum jacket. The walls of the vacuum jackets were silvered to provide further thermal isolation. With liquid nitrogen in the appropriate jacket, and a vacuum better than 1×10^{-5} torr, helium could be contained in the inner jacket for a considerable time.

The copper block had a heater wound on it, to assist in warming the dewar from cold. The temperature of the block was measured using a copper constantan thermocouple fixed into a small hole close to the specimen. The reference junction was melting ice and the thermocouple potential was measured using a Pye thermocouple potentiometer. The thermocouple was "calibrated" at liquid nitrogen temperature and was accurate to within .002 mV. It was not used to measure temperature exactly, below 77^{o}K since it was not sufficiently sensitive. However, it served to indicate when the copper block was actually in contact with liquid helium. This was

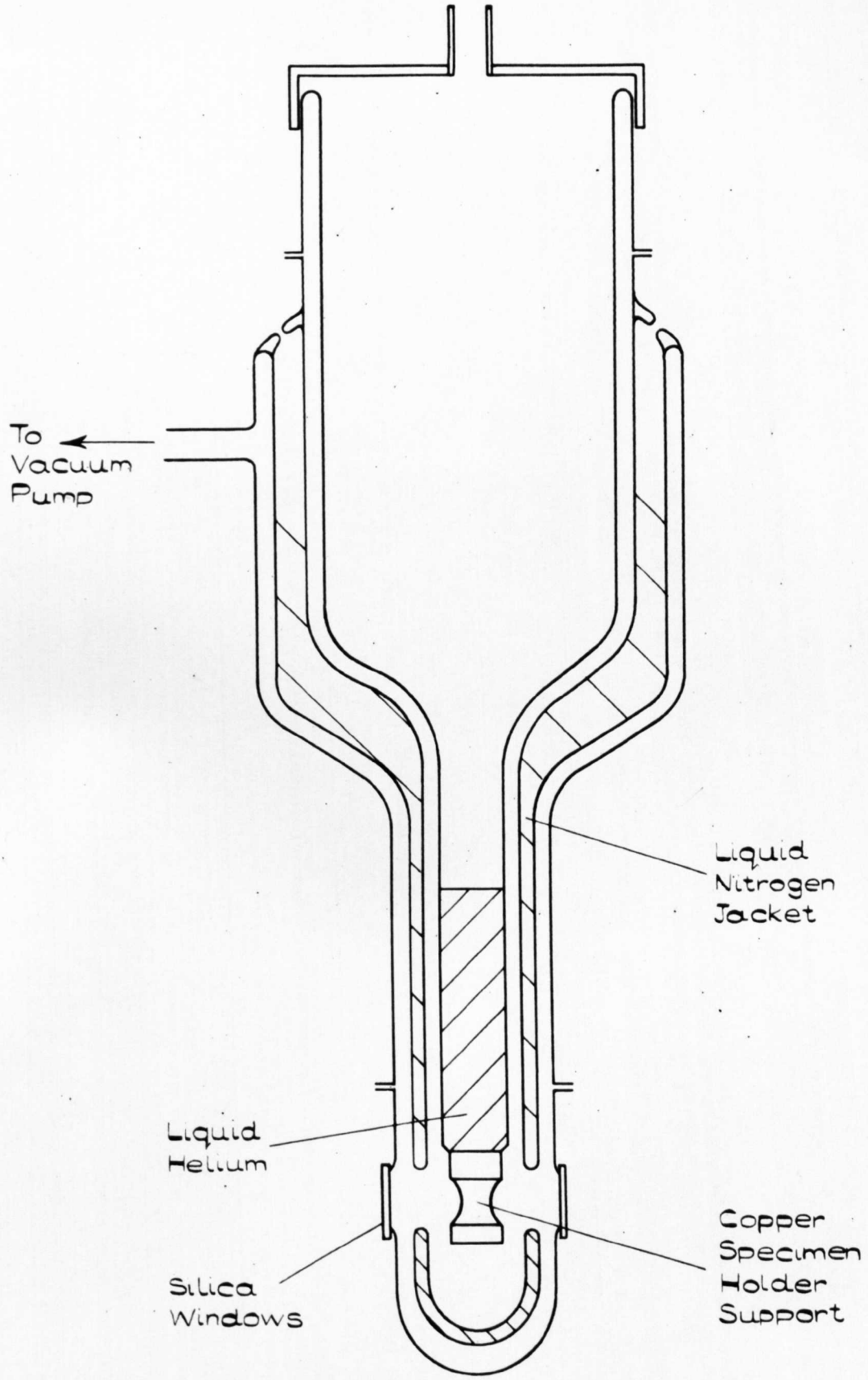

FIGURE 5.5.

CRYOSTAT FOR OPTICAL MEASUREMENTS AT LIQUID HELIUM TEMPERATURE.

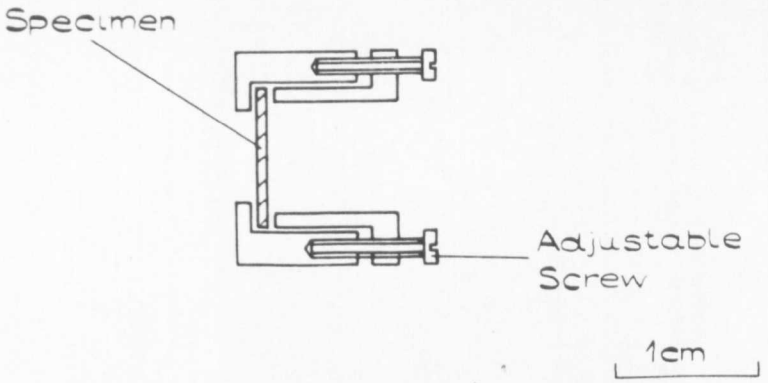

FIGURE 5.6.

OPTICAL SPECIMEN HOLDER

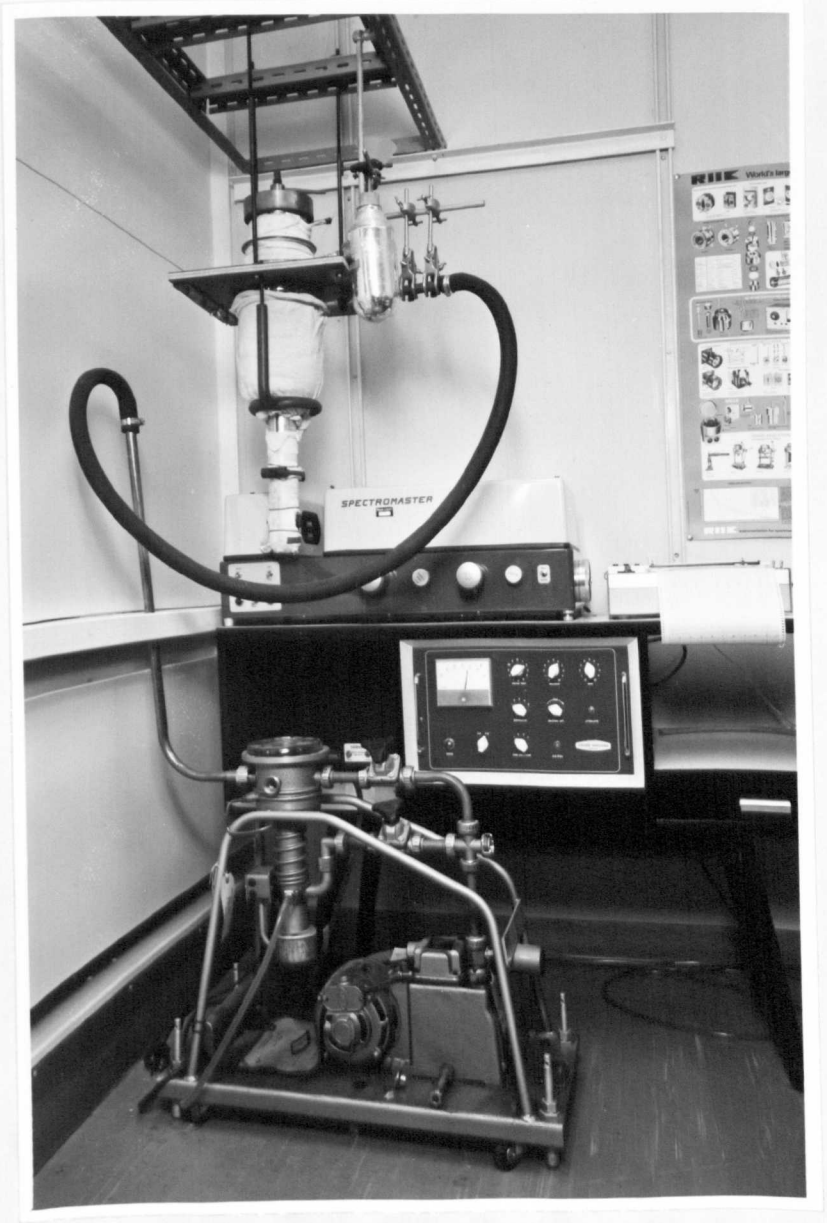

FIGURE 5.7.

PHOTOGRAPH OF CRYOSTAT AND SPECTROPHOTOMETER

manifest by the thermocouple-voltage being close to the correct value for liquid helium, but also being stable after a sudden rapid drop. t was also possible to detect the presence of the helium by visual inspection. The temperature of the sample and block were then taken as $4.2^{o}K$.

The actual specimen mount was also made of copper and was designed to be a close fit into the hole running through the block. This is shown in fig. 5.6.

The pumping system was a standard general $\frac{3}{4}$" rotary and diffusion pump unit, and the pumping technique similarly standard.

The dewar was mounted in a trolly above the spectrophotometer and the tolly in turn mounted on a simple rail system. The cryostat could then be moved in or out of the spectrophotmeter sample beam as required. The whole apparatus is shown in fig. 5.7.

5.03.3 EXPERIMENTAL PROCEDURE

The sample to be investigated was placed into the specimen holder, and then the holder slid into the copper block of the cryostat. The lower outer section of the cryostat was then placed in position, and the dewar pumped down. It was necessary to exercise some caution in 'roughing' out the dewar to ease the mechanical shock on the dewar. Pumping was continued until a pressure, better than 2×10^{-5} torr was achieved. The cryostat was then moved into position in the sample beam.

After first determining that the zero absorption line was quite "flat" the absorption of the specimen was scanned over the wavelength range of the absorption edge.

It was usual practice to attenuate the reference beam to such an extent, that beyond the bottom of the absorption edge, when the absorption

is low and constant, the recorder reads zero or near zero absorption. This simply means that between the sample being transparent and opaque the whole of the recorder scale is used. If this were not done, then when the specimen was transparent, the recorder indicated an apparent absorption of $\simeq$ 60%, this being the sum of reflection losses and reduction of area of the sample beam by the specimen holder. The effect of expanding the remaining 40% to cover the whole scale is simply to increase the resolution of the edge. The decrease in sensitivity was not significant.

Reflection losses due to the silica windows of the dewar were compensated for by placing an empty cell, consisting principally of two exactly similar silica windows in the reference beam.

When the room temperature run was completed, the liquid nitrogen jacket was filled approximately three quarters full with liquid nitrogen. The copper block and specimen holder were cooled to any desired temperature down to 77°K by pouring the appropriate quantity of liquid nitrogen into the inner dewar. The thermal insulation of the block was sufficient for any such temperature to be maintained for the duration of a scan of the absorption edge.

This was the method of cooling down to a temperature of 77°K. To obtain lower temperatures than this liquid helium was employed.

Helium was transferred to the inner dewar using the standard method of a 'U' shaped vacuum jacketed transfer tube, passing from inside the inner dewar to the liquid helium reservior. A slight pressure applied to the surface of the helium in the reservior forced the liquid up through the transfer tube and into the cryostat. Helium gas that boiled off from the cryostat was allowed to pass through the valve in the lid of the cryostat.

The method of measurement of the absorption at these lower temperatures was precisely the same method as that already described for room temperature.

5.03.4 CALCULATION OF ABSORPTION COEFFICIENT FROM EXPERIMENTAL DATA

The absorption coefficient K for any media, is defined by the condition that the energy in the wave falls off by $\frac{1}{e}$ in a distance $\frac{1}{K}$ cm. As the energy flow is given by the Poynting vector, it is thus proportional to the product of the amplitudes of electric and magnetic vectors, and since each contain the term $e^{\frac{-\omega k x}{c}}$ the attenuation is $e^{\frac{-2\omega k x}{c}}$ (see 7.02.0)

$$\therefore \qquad K = \frac{2\omega k}{c} = \frac{4\pi k}{\lambda}$$

and the attenuation is e^{-Kx}

units of K are cm^{-1}

Consider a plane slab of material. When K is small, $< 1\ cm^{-1}$, a specimen only 1 mm thick will be effectively transparent (< 8% of light is absorbed), so that for light falling normally onto the surface the transmission of the specimen, t is

$$t = \frac{T^2}{1-R^2} \qquad \text{5.03.1}$$

and the reflected fraction r

$$r = \frac{2R}{1+R} \qquad \text{5.03.2}$$

where R and T are the reflection and transmission coefficients for the interface between the material and the atmosphere.

When K is $> 1\ cm^{-1}$ absorption must be taken into account and equation 5.03.1 becomes

$$t = \frac{(1-R)^2\ e^{Kx}}{e^{2Kx} - R^2} \qquad \text{5.03.3}$$

With the Grubb Parsons Spectrophotometer, it was not possible to measure reflectively at normal incidence, and the measurement that could be made at 12° incidence could only be made accurately with some difficulty. Also, this measurement could not be undertaken at anything other than room temperature, since this would have required development of further specialised experimental techniques. It was therefore necessary to devise a method of determining K from transmission data only.

Now equation 5.03.3 could only be used for deducing values of K so long as R (determined using 5.03.1 for some wavelength below the edge, or the above reflectivity measurement) remained constant over the wavelength range of interest, and also constant with temperature. Due to the suitable properties of the materials this was possible. The method of determining R, and of ensuring that the two conditions are fulfilled is now described.

To be able to use 5.03.1 to determine R it was first necessary to ensure that K was in fact very small below the absorption edge. This was most easily done by placing a sample of material in each beam of the spectrophotometer, that in the reference beam being thinner than that in the sample beam. Then, at the bottom of the edge when absorption was constant, a constant output was shown on the recorder. If K was small, each sample would have absorbed equal amounts and the recorder would show effectively zero absorption. This was usually the case.

Thus knowing the value of λ say λ_T at which K became zero (or effectively zero) and constant, a zero absorption line could be drawn on any trace of specimen transmission against wavelength, i.e. the recorder output, an example of this is shown in fig. 5.8.

Hence if the transmission at λ_T and larger wavelengths is referred to as 100%, the fraction of the light transmitted at any other (shorter) wavelength, (with respect to that transmitted at λ_T) is given by

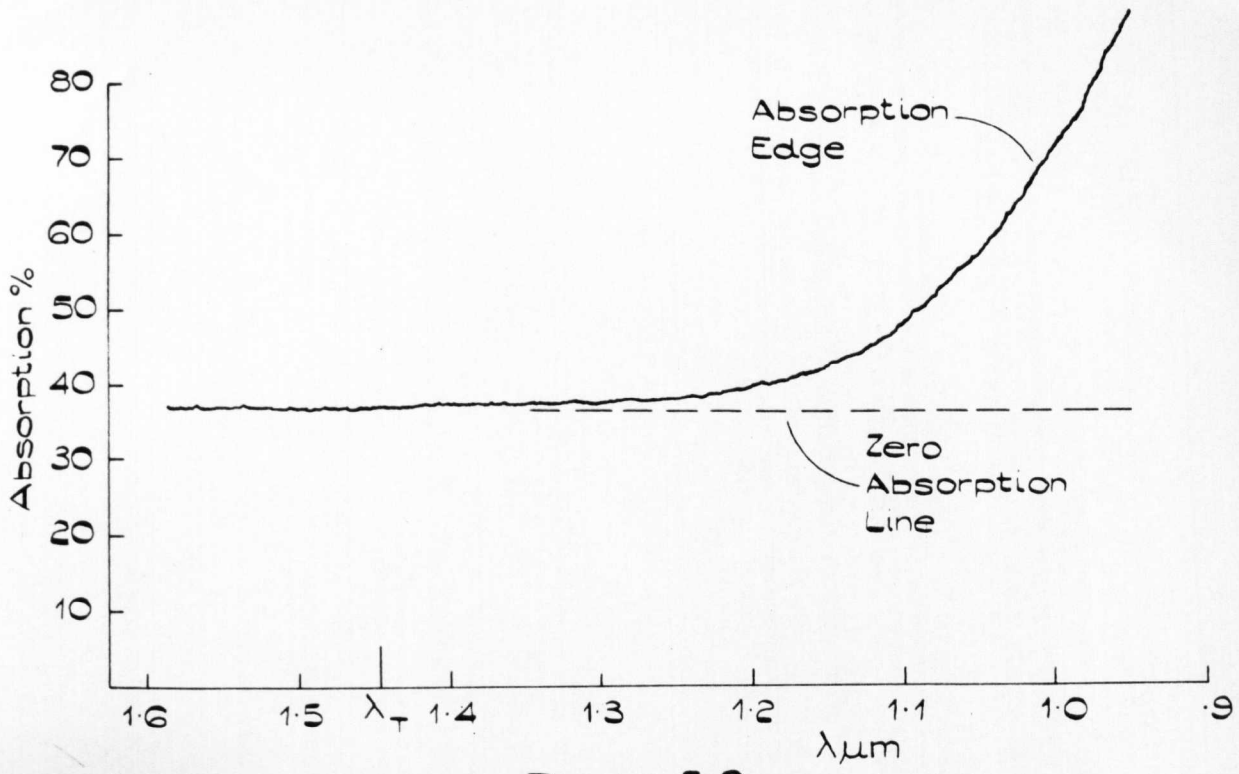

FIGURE 5.8.

ABSORPTION VS WAVELENGTH

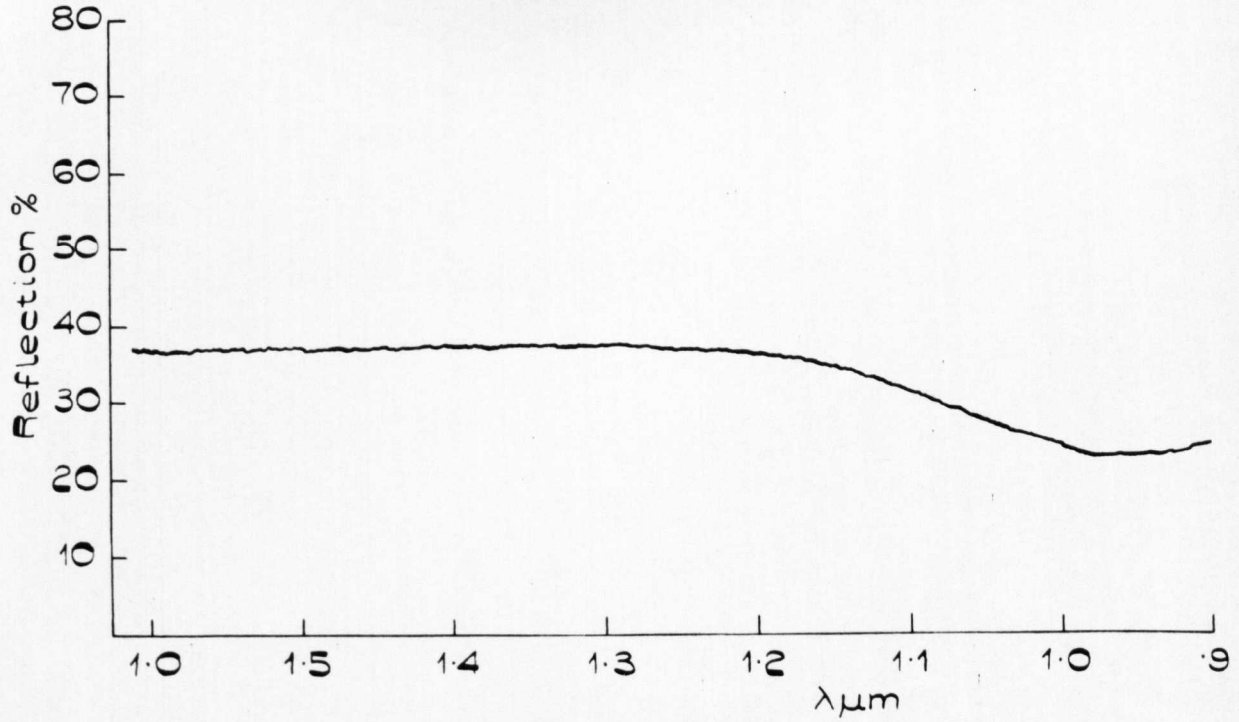

FIGURE 5.9.

REFLECTION VS WAVELENGTH.

$$\text{Relative transmission} = \frac{t_\lambda}{t_{\lambda_T}} = \frac{\left(\frac{T_\lambda^{\,2} e^{Kx}}{e^{2Kx} - R_\lambda^{\,2}}\right)}{\frac{T_{\lambda_T}^2}{1 - R_{\lambda_T}^2}} \times 100 \qquad 5.03.4$$

x = sample thickness

It has already been emphasised that R and T should be constant (and equal to the long wavelength values) and this equation clearly shows why. Unless this is the case, determining K from this equation requires a separate measurement of R at each wavelength. If the condition is satisfied it becomes more simply

$$\text{Relative transmission} = \frac{(1 - R^2) e^{Kx}}{e^{2Kx} - R^2} \qquad 5.03.5$$

The relative transmittance is simply obtained from the recorder output and R can be measured using equation 5.03.1. It must now be shown that R did remain constant over the wavelength range of interest, and also with temperature. How this was determined for each glass is illustrated by reference to a particular case, namely 20Te80Se. What is reported was applied to all glasses.

5.03.5 THE VALIDITY OF THE ASSUMPTION R =CONSTANT

Figure 5.8 shows absorption against wavelength for a 1 mm. thick specimen of 20Te80Se. The apparent absorption below the edge is due entirely to reflection losses, as would be shown by placing a thinner sample in the reference beam, in the manner already described. For λ greater than 1.5 μm, K is very small, and the specimen can be considered transparent. The value of the transmission beyond this wavelength is .63 which, using equation 5.03.1 gives R = .225.

Figure 5.9 shows reflectance at 12° incidence against wavelength for the same sample. Fresnels equations show that 12° incidence is sufficiently close to normal incidence for the normal incidence value of R to be used. For wavelengths longer than 1.5μm the reflection is obviously expected to be .37 and to approach .225 at the absorption edge. (The value of k which will enter the expression for R vis $R = \left[(n-1)^2 + k^2\right] / \left[(n+1)^2 + k^2\right]$ will be negligible up to values of $K = 10^3$ cm^{-1}). These values agree with those of fig. 5.9 to within the expected error.

In this way it was ascertained that R could be considered constant over the beginning of the absorption edge, and hence equation 5.03.5 could be used for calculating values of K.

That R remained constant with temperature was easily seen when on decreasing the temperature, the long wavelength transmission remained constant.

5.03.6 SPECIAL DIFFICULTY WITH THE AS-SE SYSTEM

It was found that the above approach had to be modified to a certain extent to deal with data for the materials in the As-Se system. This system was peculiar in that with the exception of pure amorphous selenium the value of K at the bottom of the absorption edge remained high, typically between 10-100 cm^{-1}. Again, using specimens of different thicknesses, one in each of the two beams, the wavelength at which K became relatively constant was found. The value of K at this point was found simply using

$$\% \text{ transmitted} = \frac{e^{Kd_1}}{e^{Kd_2}} \times 100 \qquad \text{5.03.6}$$

d_1 and d_2 are specimen thicknesses, $d_2 > d_1$

This simple formula neglects multiple reflections, but with a high value of K, and small values of R (always less than .2) for this system, the approximation does not introduce a prohibitive error.

The value of K found as above was then used with the value of transmittance for the thinnest specimen in formula 5.03.2 to determine the value of R. The value was checked by making the reflectivity measurement at 12° incidence, and was found to agree to within 5%. It was also found to be constant over the wavelength range of the edge.

With the above information it was then possible to draw the zero absorption line, and then values of K were found using 5.03.3 as before.

5.03.7 PRESENTATION OF RESULTS

The values of log K plotted against photon energy are presented in chapter 7. For each of the materials in the As-Te and Se-Te system on which measurements were made, a plot of log K vs photon energy represents the information gained from two specimens, one approximately 1000 μm and the other approximately 100 μm in thickness.

5.04.0 HALL EFFECT:- INTRODUCTION

The measurement of Hall Effect in materials of high resistivity and low mobility, is made difficult due to the high scource impedance, small signal, and large thermal drift. The last factor for example can produce resistivity changes of 4% per °C temperature change. Because of these difficulties the decision as to whether or not to attempt the experiment was held in question for some time. However, after some experience of material preparation it was thought that two systems had sufficiently high conductivity for there to be a good chance of the experiment proving successful. And of course, the possibility of being able to apply a

successful Hall Effect experiment to materials of higher resistivity was a further incentive. (The information to be gained from Hall effect studies is discussed in chapters 2 and 8.) For these reasons it was decided to attempt the experiment.

5.04.1 CHOICE OF METHOD

There are four basic methods which can, and have been used to measure Hall Effect (references [1] [2] [5]). These are:

(1) D.C. magnetic and electric fields,

(2) A.C. electric and magnetic field,

(3) A.C. magnetic field and D.C. electric field,

(4) D.C. magnetic field and A.C. electric field.

Method (1) is the most obvious choice in most cases because of the relative ease of experiment. But the method is limited for measurements on low mobility materials by noise, since the ratio $\frac{E_{Hall}}{E_{Drift\ field}}$ is directly proportional to mobility.

The signal to noise ratio that can be tolerated is greatly decreased by employing A.C. methods. Very briefly the improvement arises because the alternating voltage at the probes can be phase sensitively detected.

Method (2) where the Hall voltage appears at the beat frequency of the alternating electric and magnetic, requires some complex experimentation. Rejection filters are required in the detecting circuit for the two fundamental frequencies involved. Also, there are other signals appearing at mixed frequencies as well as the Hall signal, and distinguishing between them adds further complications.

For the third method a low frequency magnetic field is required. To obtain fields of the necessary strength with the standard type of electromagnet available, a large amount of power would have been required at the

low freqency. This would need either expensive equipment, or an appreciable amount of time to produce the power supply in the laboratory. Neither could be afforded.

For these reasons method (4) was chosen. The major disadvantage of this method is having to deal with a large offset voltage at the probes, since the Hall voltage when produced is exactly in phase with the offset signal. This offset arises because of the inevitable probe mis-alignment. It was compensated for experimentally by backing off the total signal at the probe with an exactly out of phase signal.

5.04.2 DESCRIPTION OF APPARATUS

A block diagram of the apparatus is shown in fig. 5.10. The pre-amplifier, and difference amplifier were the only non-commercial pieces of apparatus, the circuits of each of these are shown in fig. 5.11.

The signal from the probes, one of which provides the 'earth' of the secondary circuit, was fed into the high impedance pre-amplifier, set to a gain of one. The purpose of the pre-amplifier was to act as an impedance transformer between the high sample impedance and lower input impedance of the difference amplifier. The signal was "backed off" in the difference amplifier against an out of phase signal. The backing off signal was initially generated at the signal generator (which produced two independent coherent signals). Its phase relative to that of the probe signal could be varied with the phase shifter 2

It was found during the development of the apparatus that this backed off signal contained two unwanted frequencies. One was at 50 c/s the other being the first harmonic of the frequency being used. It is thought that both of these signals originated in the signal generator rather than being induced elsewhere. However they were effectively reduced (by 40 dB) by

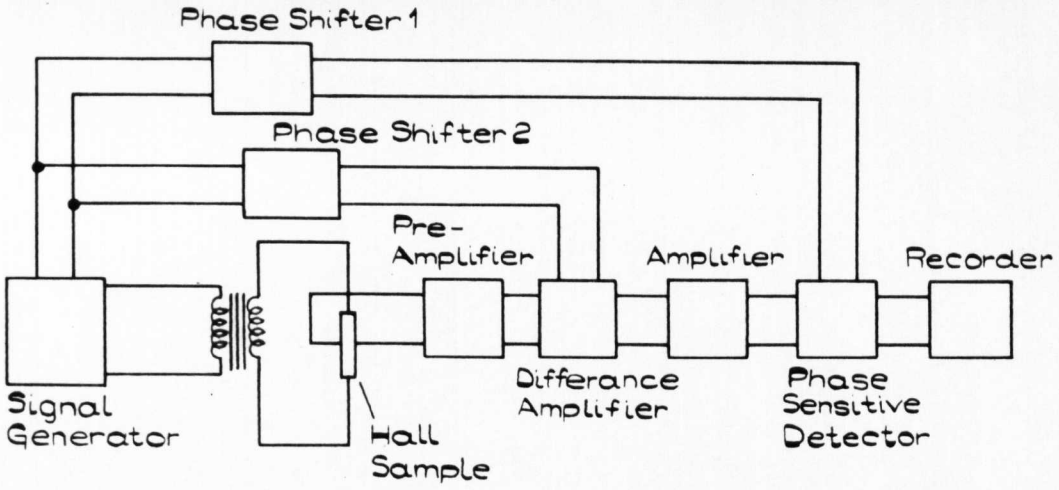

FIGURE 5.10.
BLOCK DIAGRAM OF HALL EFFECT APPARATUS.

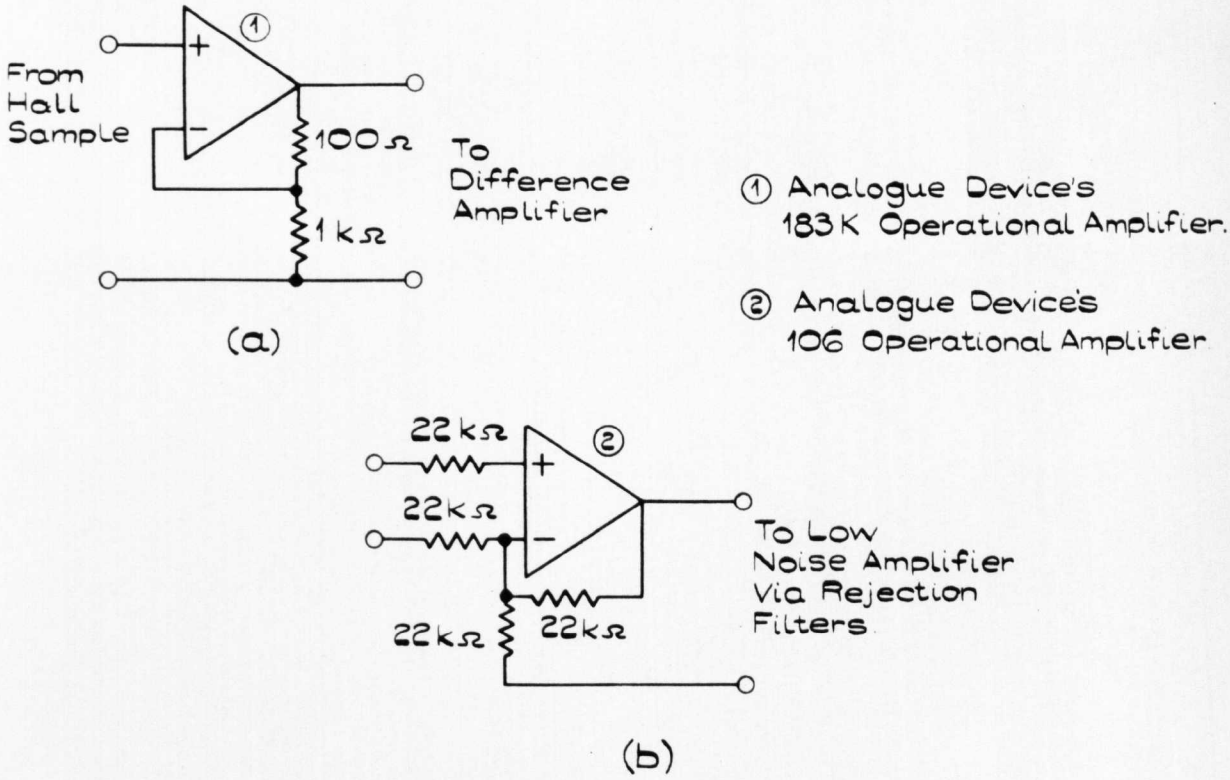

FIGURE 5.11
(a) PRE-AMPLIFIER (b) DIFFERENCE AMPLIFIER.

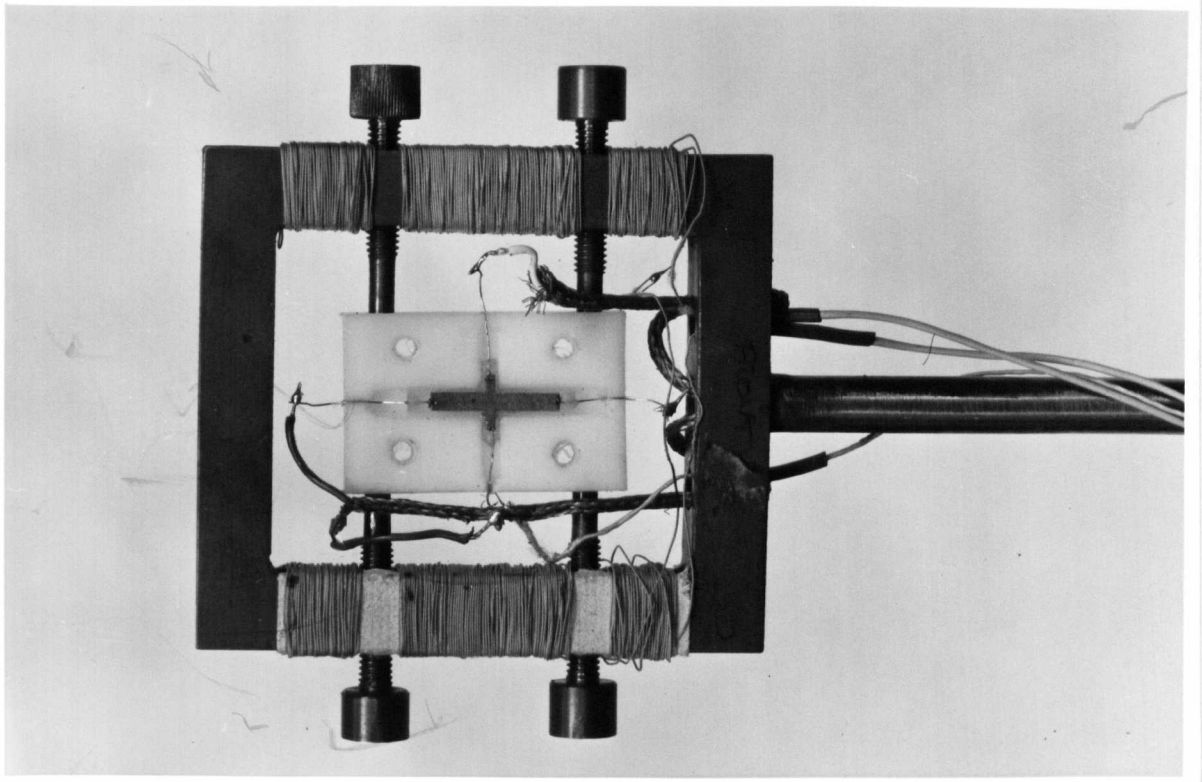

FIGURE 5.12.

HALL SPECIMEN SAMPLE HOLDER

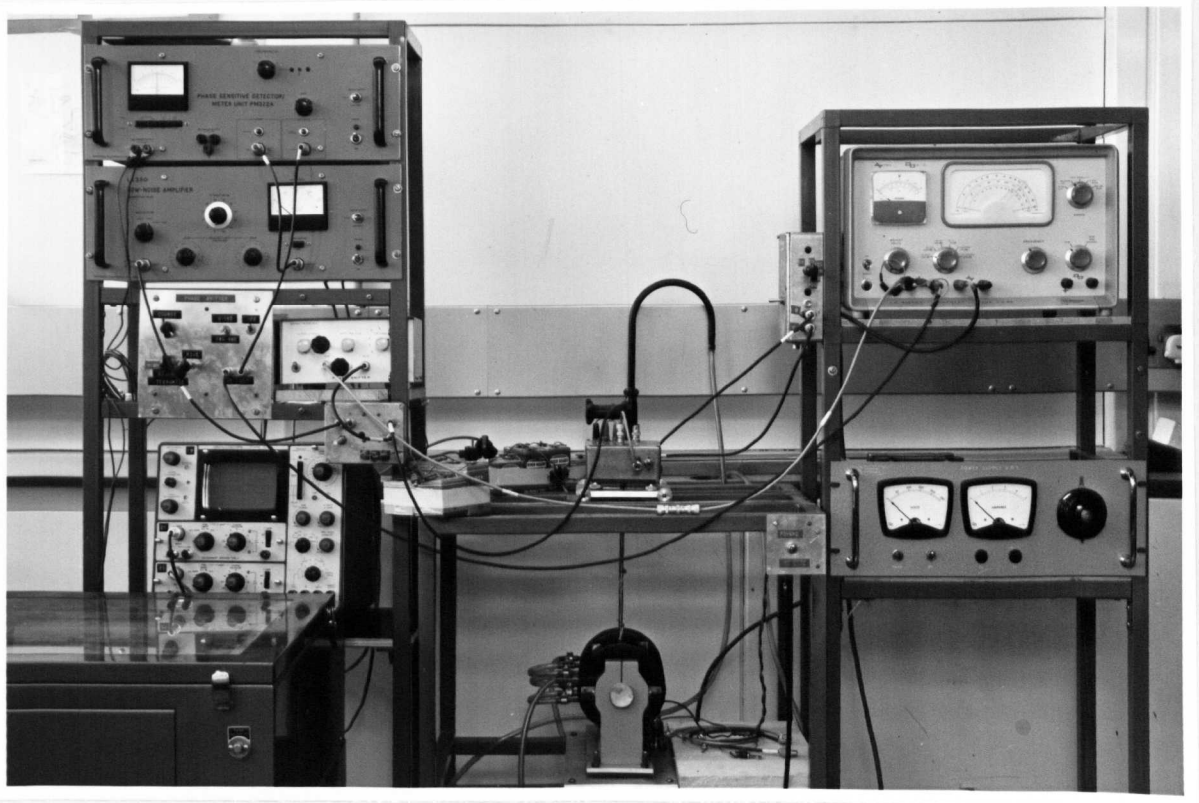

FIGURE 5.13.

PHOTOGRAPH OF HALL EFFECT APPARATUS.

the insertion of two simple band stop filters after the difference amplifier. An effect of the filters was also to attenuate the wanted signal, but only by about 5 dB which produced no problem and was easily accounted for.

The backed off signal with unwanted components attenuated was then amplified to the level required for input into phase sensitive detector, where it was subsequently phase-sensitively detected. The rectified output of the P.S.D. was fed into a pen recorder.

The magnetic field was produced with a Newport Type C Magnet and matching power supply VR3. With a pole separation of 1 cm., a field of 8 Kilogauss could be produced, uniform over an area of one sq. cm.

5.04.3 CALIBRATION OF APPARATUS AND MAGNETIC FIELD

The calibration of the apparatus was achieved by producing a small known signal across a resistance comparable with a typical specimen resistance, and applying this to the input of the pre-amplifier.

The known potential was produced by feeding the signal from the generator into the input of a potential divider, and calculating from the values of resistance in the dividing chain, the potential across the relevant resistance. The voltage at the input of the divider was measured using a voltmeter of input impedance comparable to that of the potential divider.

The magnetic field was simply calibrated with a flux coil and flux meter.

5.04.4 SPECIMEN HOLDER

Owing to the small space available between the poles of the magnet,

the design of the specimen holder was considerably restricted. The requirements were that the specimen and electrical contacts could be mechanically supported, that there should be good electrical insulation and that the temperature should be maintained constant, or at worst only drift slowly. It was also desirable to be able to vary the specimen temperature to values above room temperature, because of the extra information to be obtained from values of mobility as a function of temperature.

Fig. 5.12 shows the essential details of the specimen holder. A reasonable temperature stability was achieved simply by surrounding the holder with a draught proof shield. Heat was transferred to the p.t.f.e. insulator and sample by the copper support screws, and the temperature measured using a chromel alumel thermocouple, and potentiometer.

The sample holder was suspended underneath a trolley which was constrained to move along a simple rail system. This enabled the whole unit to be moved smoothly into or out of the poles of the magnet. The pre-amplifier was placed as close as possible to the sample, to prevent the high input impedance of the amplifier being compromised by capacitance in the leads. Fig. 5.13 shows a photograph of the arrangement.

5.04.5 EXPERIMENTAL PROCEDURE

The apparatus was arranged as described in the above paragraphs with the sample fixed in position between the poles of the magnet, but without at first the field being applied. The 120 Hz. electric field was measured by replacing the sample with a voltmeter of equal input impedance. Values of the drift field used varied between 10 - 100 volts/cm.

The size of the offset signal was typically .1 - 1 volt. By adjustment of the phase shifter 2, a signal was arranged to be of similar size to

the offset signal, and 180° out of phase with it. The two signals were then applied to the difference amplifier, and final adjustment made to make the 120 Hz. component of the output of the difference amplifier as small as possible. A typical signal size after back off would be $\simeq$ 100 μV. The low noise amplifier was then used to bring the signal to the level necessary for input into the p.s.d. The signals from the low noise amplifier and phase shifter I were first adjusted to be in phase before application to the p.s.d. The rectified, phase sensitively detected signal from the output of the p.s.d. was then fed into the pen recorder. Using the calibration curves the 'backed off' sample signal is obtained. When the recorder output was steady, the magnetic field was switched on. The new signal that resulted would be the sum of several signals, namely that due to remaining offset voltage, capacitive and inductive pick up and the Hall voltage.

Of these various signals only the Hall voltage would have its phase determined by the direction of the magnetic field, so that reversal of the magnetic field produced a difference in the recorded signal proportional to twice the Hall voltage. Hence the Hall voltage could be determined and unwanted signals discriminated against.

5.04.6 RESULTS

Despite considerable persistence with the above described apparatus and procedure, in attempts to further increase sensitivity, no positive results could be obtained.

Of course it was possible to place a maximum size on the Hall voltage that could be obtained, this being somewhat below the limit of detection of the apparatus, and this was done.

The implications of this negative result are discussed in chapter 8.

5.05.0 OTHER EXPERIMENTS

A number of other experiments were undertaken. These were on a smaller scale than those described earlier because they were relatively simple, or that experimental difficulties rendered further development not worthwhile.

The procedure for the X-ray diffraction has already been described in chapter 4, and is not repeated here.

5.05.1 THERMOELECTRIC POWER

Measurement of thermoelectric power was intended from the outset to be part of the experimental investigation. A cryostat, measuring circuit and experimental specimens were prepared and two or three preliminary runs made. The results of these early attempts suggested that a great deal of development of the apparatus would be required in order to produce accurate results. The principal problems were the mode of heating, and again the high specimen impedance and associated problem, of isolating the detecting circuit from stray electromagnetic fields.

Because of the time that would have been required to resolve these difficulties the experiment was abandoned.

5.05.2 SPACE CHARGE LIMITED CURRENTS

This experiment entailed the measurement of d.c. current voltage characteristics of thin (typically $< 80\mu m$) specimens of large band gap amorphous semiconductors. For reasons described in 2.10.0 the measurement had to be completed with the specimen in the dark and with large time intervals between separate measurements.

The measuring circuit was a simple extension of that shown in

fig. 5.1. In particular the battery power supply was replaced by a continuously variable supply, and a Kiethly 602 electrometer replaced the E.I. 62A instrument.

The results for this experiment on three specimens are presented and discussed in 8.03.

5.05.3 DENSITY

The size of the specimens were such that it was only necessary to employ the simple method of Archimedes. A suitably dense liquid, namely ethylene dibromide, was used to increase the accuracy of the results.

5.05.4 CHEMICAL ETCHING

With the intention of studying the microstructure of the material using an electron microscope, several attempts were made to establish suitable etchants and etching procedures.

With the exception of As-Te glasses which were rapidly etched with HNO_3 - HF mixtures, all glasses were highly resistant to attack by the common compounds used in etching procedures. Since there were no other means of thinning or etching samples available, this investigation was ceased.

5.05.5 A.C. MEASUREMENT

The measurements that were made employed two separate A.C. bridges which between them covered the frequency range 100 Hz to 10 M.Hz. For the range 100 Hz to 100 K.Hz a modified form of Lynch Bridge was used and from 100 K.Hz to 10 M.Hz a Wayne Kerr B.602. Both Bridges were essentially transformer ratio arm types.

A cryostat and specimen holder were designed (and built) to match the bridges, and to enable measurements to be made from room temperature down to 77°K. The temperature was varied and measured in the same way as described in 5.02.2.

REFERENCES CHAPTER 5

(1) See (3) of Chapter 3.

(2) See (4) of Chapter 3.

(3) See (7) of Chapter 3.

(4) See (9) of Chapter 1.

(5) See (8) of Chapter 3.

CHAPTER 6

D.C. CONDUCTIVITY

6.01.0 INTRODUCTION

This chapter deals first of all with the implications for conduction of the proposed model of amorphous semiconductors introduced in chapter 3.

Such a model requires for its basis a random atomic structure, but it has been suggested (see for example [1][2][3]) that amorphous semiconductor materials may be made up in a compound way, consisting of two or more phases, or small crystallites ($< 80^{\circ}A$). Such structures have been observed in oxide glasses [4][5] and also possibly in amorphous semiconducturs [25].

In the light of this possibility the experimental results are looked at in terms of the model proposed in chapter 3, but also keeping in mind the properties that will apply to compound structures.

6.02.0 CONDUCTION IN A RANDOM STRUCTURE

This section extends some of the ideas introduced in chapter 3. In that chapter a general form for the density of states in amorphous semiconductors was introduced, and we now consider d.c. conduction based on this density of states curve.

6.02.1 THE EXTENDED STATES

Figure 6.1 represents the density of states curve and is derivable from any of the three approaches of chapter 3. The extended states above E_c and below E_v (the mobility "edges" or "shoulders") behave as conduction and valence band states in crystalline semiconductors, although the mean free path and mobility will be reduced due to scattering.

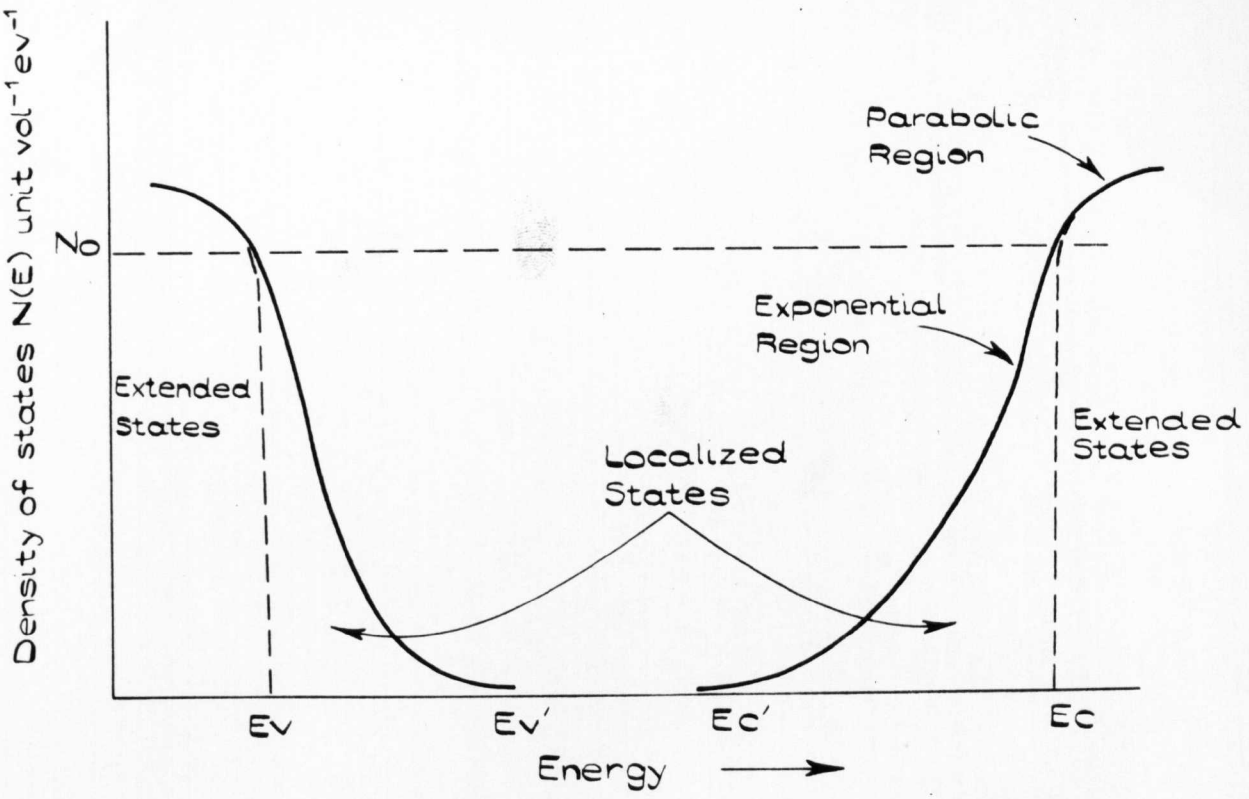

FIGURE 6.1.

SCHEMATIC DENSITY OF STATES CURVE.

CURVE	Ec - Ev	α_c ev.$^{-1}$	α_v ev^{-1}	$N_{c}^{o'}$ $N_{v}^{o'}$	$N_{E=Ec}(E)$	$N(E)_{E=Ev}$	Ec'	Ev'
I	1·0 ev	90	230	10^{20}	1	1	0·5 ev	0·2 ev
II	1·0	72	180	10^{20}	10^{5}	10^{5}	0·5	0·2
III	1·0	60	150	10^{20}	10^{7}	10^{7}	0·5	0·2
IV	1·0	90	190	10^{20} 10^{17}	1	1	0·5	0·2
V	1·5	72	180	10^{20}	10^{5}	10^{5}	1·0	0·2
VI	1·5	51	118	10^{20}	10^{5}	1	0·7	0·4

For the purposes of this table and the calculations, Ec' and Ev' are the limits of intergration in equ. 6·02-9.

TABLE 6.1.

SUMMARY OF DATA USED IN DEDUCING CURVES OF FIG. 6.2.

The conduction band tail is indicated as being longer than that of the valence band, since this is expected to be the case. The reasons are as follows; (1) that the valence bands are generally narrower than conduction bands and (2) that the structure or configuration of the disordered material will be arranged so as to minimize the energy of the occupied valence states [6].

The conductivity due to the extended states within kT of E_c may be written [6]

$$\sigma = \sigma_o \exp - (E_c - E_F)/kT \qquad \text{6.02.1}$$

and similarly for E_v

The conduction for these amorphous solids is often assumed intrinsic and can hence be written

$$\sigma_{int} = \sigma_o \exp - (E_c - E_v)/2kT \qquad \text{6.02.2}$$

with σ_o slightly modified

Since in wide band gap non-degenerate semiconductors, conduction takes place within kT of the band edges, σ_o can be written as

$$\sigma_o = N(E)_{E=E_c} \cdot kT \cdot \mu \qquad \mu = \text{mobility}$$

However σ_o can also be equated to the minimum value of conductivity in an Anderson type band (see 3.03.5), since the states within kT of E_c would become localized if the disorder were further increased, just as the Anderson band will become completely localized when V_o becomes greater than 5 J (for the case discussed in 3.03). The intersite distance must however, be modified as discussed in 3.03.4 so that the expression for σ_o (see 3.03.4) becomes

$$\sigma_o = .06\left(\frac{e^2}{\hbar a_E}\right)\left(\frac{6}{z}\right)^2 \qquad \text{6.02.3}$$

e.g. with $a_E = 4\ \mathring{A}$ and $z = 6$ $\quad \sigma_o \simeq 200\ \Omega^{-1}\ cm^{-1}$

Obtaining true values of σ_o experimentally from the intercept of the ordinate of a plot of $\log \sigma$ vs $1/T$, is made difficult since E_c and E_v may be temperature dependent. This could arise simply from the variation of the 'lattice constant' with temperature. A simple and relevant case can be illustrated here but the question will be raised again when the form of the $\log \sigma$ vs $1/T$ curves are discussed.

If we suppose

$$E_c - E_v = E_{g_o} - \Delta T \qquad 6.02.4$$

then substitution in equation 6.02.2 gives

$$\sigma_{int} = \sigma_o \exp\left(\frac{\Delta}{2k}\right) . \exp - \left(\frac{E_{go}}{2kT}\right) \qquad 6.02.5$$

so that the value of the pre-exponential constant as measured would be $\sigma_o \exp(\Delta/2k)$ and not σ_o.

It is noted that a dependence such as 6.02.5 still gives a simple exponential dependence of σ on $1/T$.

6.02.2 THE LOCALIZED STATES

The effect of the localized states is twofold. First, those states between E_c and E_c' will act as acceptors, and possibly electron traps, and those above E_v and below E_v', as donors, or hole traps. Secondly at finite temperatures there will be thermally activated hopping, between ionized and un-ionized sites in both conduction and valence band tails. The action of the states as donors and acceptors is first considered.

EXTRINSIC CONDUCTION

The lengths of the tails $E_c - E_c'$ and $E_v - E_v'$ will govern to what extent the conduction is extrinsic, and also determine how the position of E_F varies with temperature. To obtain precise information concerning these points some calculations of n(T) (number of free carriers) and $E_F(T)$ were

made for various cases of the model of figure 6.1.

The calculations were made on an Elliott 1430 computer; the programme was written by the author.

The top of the valence band E_v is taken as the zero of energy, so that the two tails of states are described as (see also 7.04.0)

$$E_v < E < E_v' \quad N(E) = N_o' \; e^{-\alpha_v E} \qquad 6.02.7$$

$$E_c' < E < E_c \quad N(E) = N_o' \; e^{-\alpha_c (E_c - E)} \qquad 6.02.8$$

For energies greater than $(E_c - .01)$ev and less than $(E_v + .01)$ev., the bands are assumed to follow the commonly proposed parabolic form for crystalline semiconductors. Hence for the extended states of the conduction band

$$N(E) = N_o \, (E - E_c + .01)^{\frac{1}{2}}$$

The method of calculation was as follows: Assuming that at absolute zero all states up to E_v' are filled then at any subsequent temperature

n_{FH}	+	n_{ID}	=	n_{IA}	+	n_{FE}
number of free holes below E_v		number of ionized donor sites between $E_v - E_v'$		number of ionized acceptor sites between $E_c - E_c'$		number of free electrons above E_c

i.e.

$$N_o \int_o^{-\infty} E^{\frac{1}{2}} \cdot F_h(E,T) + N_o' \int_o^{E_v'} \exp - (\alpha_v E) \cdot F_h(E,T) =$$

$$N_o' \int_{E_c'}^{E_c} \exp - \alpha_c (E_c - E) \cdot F_e(E,T) + N_o \int_{E_c}^{\infty} (E - E_c)^{\frac{1}{2}} \cdot F_e(E,T)$$

N_o and N_o' are chosen such that the two sections of the curve match. 6.02.9

It is assumed that $m_e = m_h = m$, the mass of the free electron, so that

$$N_o = \frac{4\pi (2m)^{3/2}}{h^3}$$

$F_e(E,T)$, and $F_h(E,T)$ are the Fermi-Diracdistribution functions for electrons and holes respectively.

A value of E_F above $E_{F_{T=0^oK}}$ was given to the computer, which was programmed to integrate numerically equation 6.02.9 for increasing values of T until the equation was satisfied. The value of E_F, n_{FH}, n_{ID}, n_{IA}, n_{FE} and T were then printed out according to the programme. The process was repeated for as many steps in E_F as required, up to the value of E_F at $T = 1000^oK$. The whole programme could be repeated with a series of values of α_c, α_v and $E_c - E_v$.

Now the Fermi Dirac distribution function is valid, only if the probability of the level E being occupied is independent of the state of occupation of neighbouring levels. For localized states of high density, neighbouring electrons may interact and the condition not be satisfied. It was not possible to take this into account, so the results should be interpreted taking this possible approximation into consideration.

The method and programme were tested against some of the results of Hutner et al [7] who calculated n(T) and $E_F(T)$ for a number of hypothetical extrinsic semiconductors, the results agreed exactly.

DISCUSSION OF CALCULATIONS

In figure 6.2 the results of n(T) of the calculations are shown as plots of log n(T) vs $1/T$. n(T) is the total number of free carriers, holes plus electrons. Several curves are drawn for different values of α_c α_v and $E_c - E_v$.

In figure 6.3 the results for $E_F(T)$ are drawn as E_F vs T for some of the cases of figure 6.2.

FIGURE 6.2

Log n and log σ vs. the reciprocal of absolute temperature for the model of figure 6.1

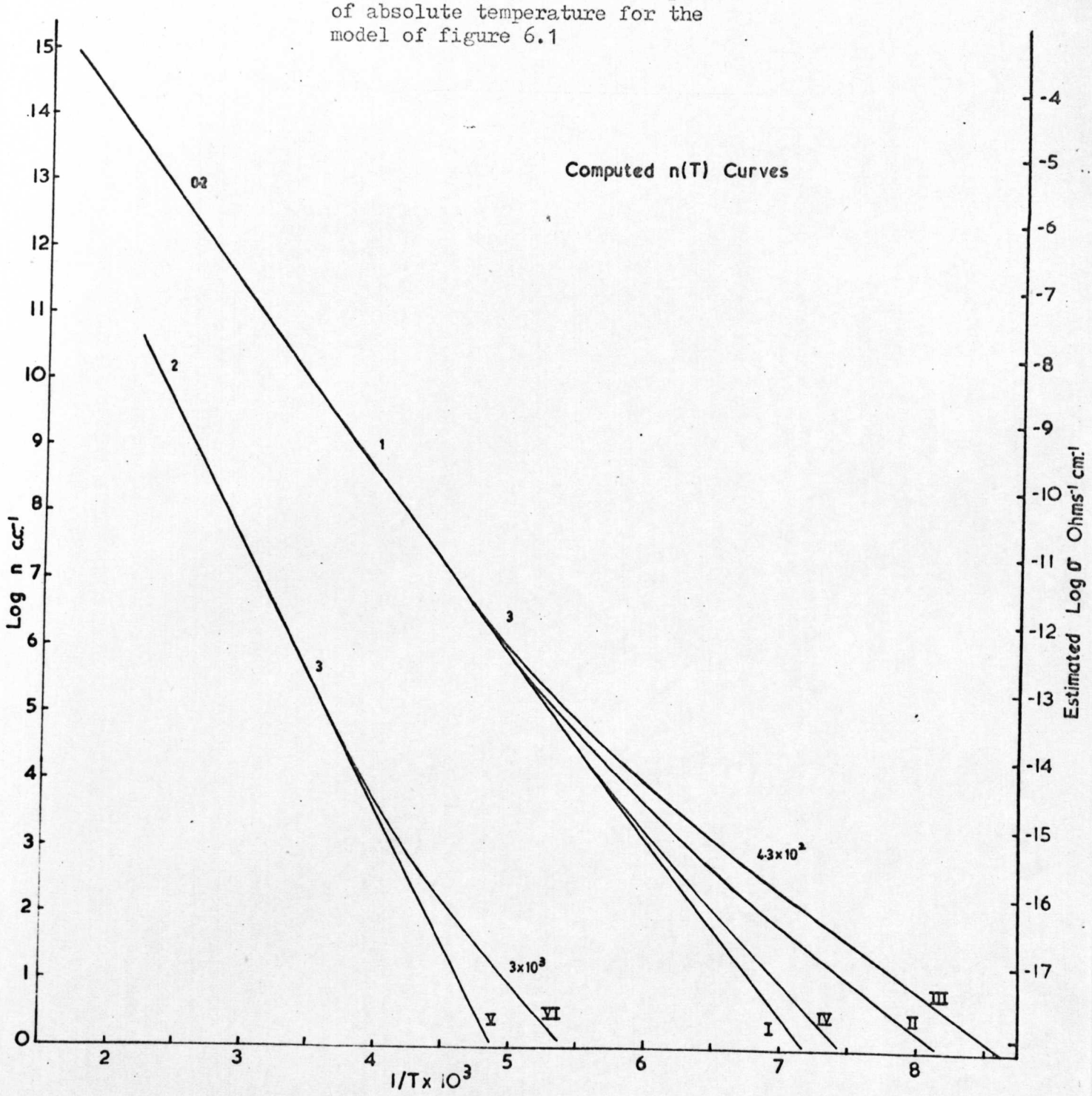

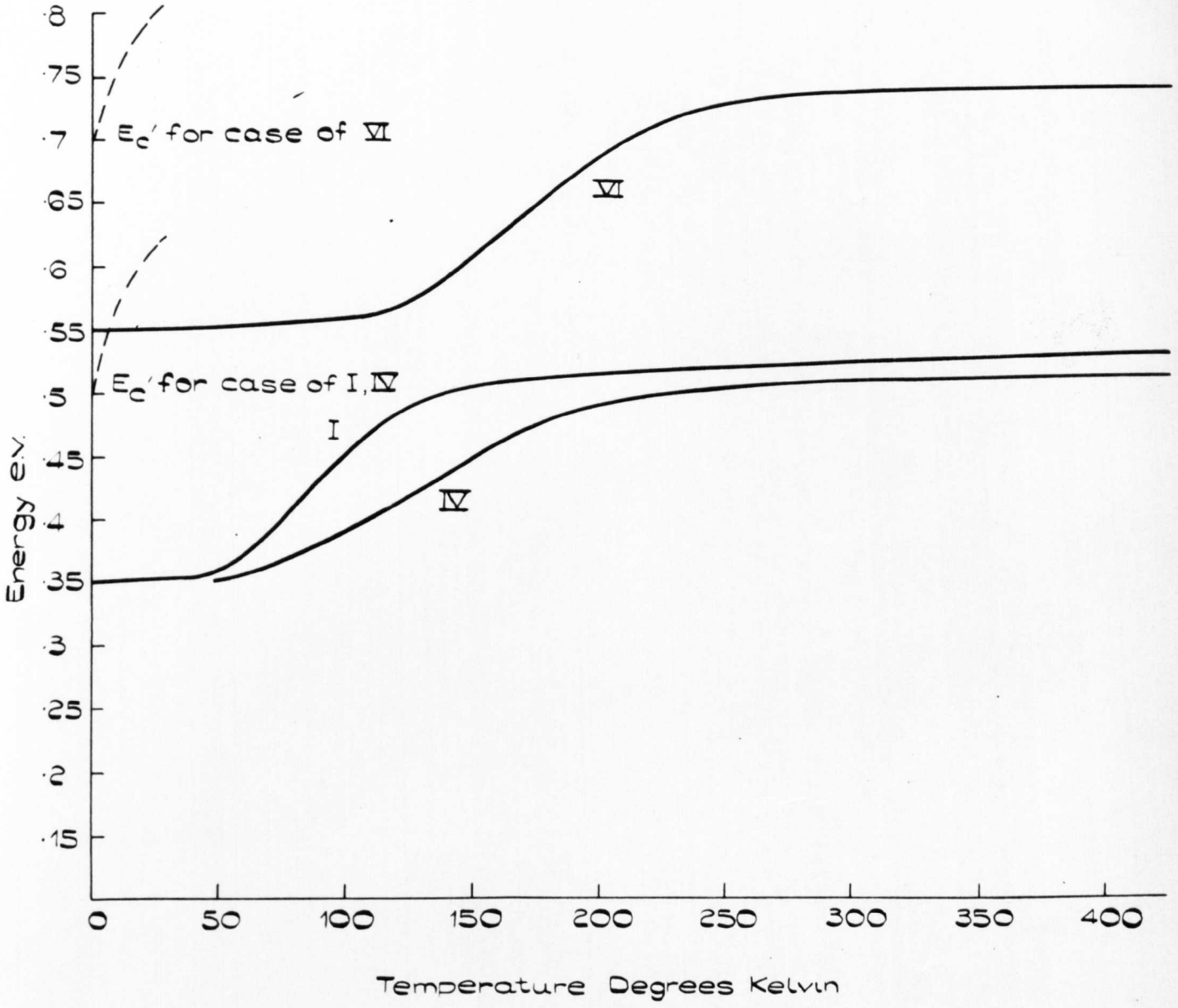

FIGURE 6.3.

E_F AS FUNCTION OF TEMPERATURE FOR MODEL OF FIG. 6.1.

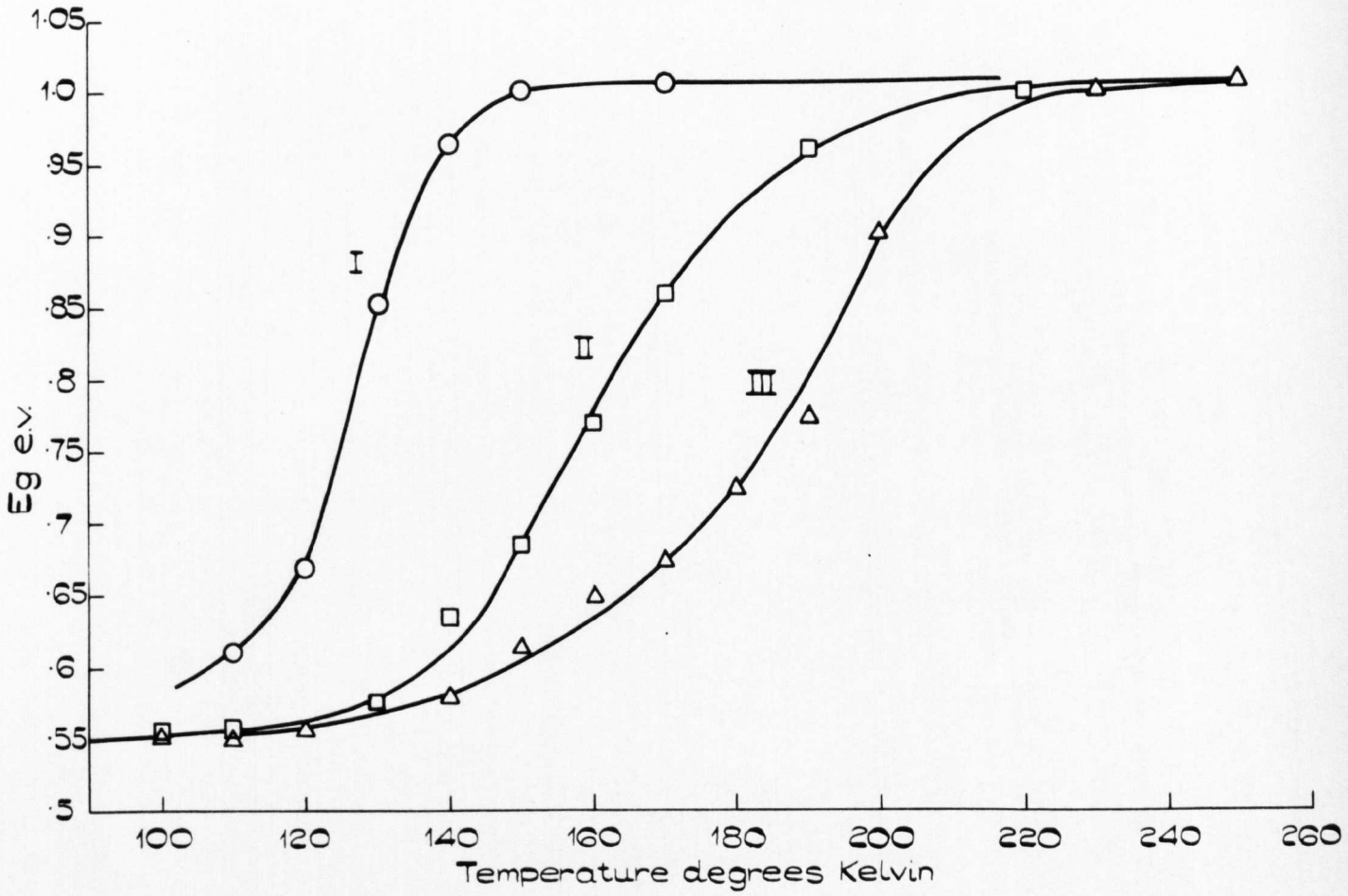

FIGURE 6.4

APPARENT ACTIVATION ENERGY AS A FUNCTION OF TEMPERATURE FOR CURVES OF FIGURE 6.2.

In table 6.1 the various values of the variables are summarized. In the calculations E_c' and E_v' are the limits of integration in 6.02.9, and not necessarily (as in figure 6.1) the energies at which N(E) becomes unity.

It will obviously be more useful to think in terms of conductivity and therefore the right hand ordinates of figures 6.2 are thus calibrated. The conductivity is simply based on

$$\delta = n(T) \cdot e \cdot \mu .$$

assuming $\mu = 10\ cm^2\ volt^{-1}\ sec^{-1}$, and to be constant with temperature. The value of 10^{20} for N_o used in the calculation is according to Lanyon [20] reasonable. He estimates such a value at the valence band edge in amorphous selenium.

With the exceptions of I and VI all the plots show some curvature which should be seen within the temperature, and (predicted) conductivity ranges available to experiment.

Curves I, II, III with α_c and α_v decreasing, show the increasingly high temperatures and conductivities to which extrinsic conduction persists. The majority carriers are of course holes, and the actual values of the ratio n_h / n_e are shown as numbers against the curves. Even for long tails of states (such as would produce some overlap of the tails) the conduction has become intrinsic at room temperature. At very high temperatures there is in fact a slight majority of electrons, a consequence of the conduction band tail being the longer of the two.

The form of the curvature is of interest, and will be discussed again later in comparison with the experimental results. The activation energies derived from the slope assuming

$$n(T) \propto \exp \frac{-E_g}{2kT}$$

are plotted against temperature for a number of cases in figure 6.4.

At low temperatures this is equal to $\triangleq .5$ ev as expected and corresponds to holes excited from E_c' to E_v. It increases up to a value equal to $E_c - E_v$, the value for intrinsic conduction, at a rate determined by the number of acceptor sites available. (For curves other than I, E_g should decrease to smaller values in accordance with values of α. But in the calculations E_c' (=.5 ev) is the limit of intergration in 6.02.9 for curves I-IV, and hence the minimum activation energy will be $E_c' - E_v = .5$ ev. However what is important is the temperature to which extrinsic conduction persists for a particular α, and not the value of E_g at such low conductivities as cannot be measured.)

Figure 6.3 shows how the Fermi Energy varies with temperature for three cases. It is interesting to note that it enters the tail of acceptor states, a result which will have consequences for hopping conduction, since the possible large number of ionized sites may make a significant contribution to the conductivity.

It can be concluded from the calculations that if n(T) is the dominant temperature dependent quantity in the conductivity, then measurements of conductivity below approximately $300^{\circ}K$ and conductivities below $10^{-12\ -13}$ $ohm^{-1}\ cm^{-1}$, should not show constant activation energy, i.e. log vs $1/T$ is not linear.

This conclusion will be seen to be verified by the experimental results.

6.02.3 LOCALIZED STATES - HOPPING (IMPURITY) CONDUCTION

For the hypothetical amorphous semiconductor of fig. 6.1, the general expression for the d.c. conductivity in the localized states will contain two activation terms. One is associated with the excitation of electrons to the energy range E_c to E_c', (or holes to the range E_v to E_v') and a

second term

to account for the energy difference ΔW between sites. The conductivity, say for the conduction band tail could then be written [12]

$$\sigma_{loc.} = \int_{E_c'}^{E_c} \sigma_{OL} \exp - (E - E_F)/kT . \exp - (\Delta W/kT) \, . \, dE \qquad 6.02.10$$

σ_{OL} (the effective σ_o for localized states) and ΔW will both be functions of energy.

The term σ_{OL} willinvolve the tunnelling probability and the jump distance. Those states farthest away from E_c will be highly localized so that the probability of hopping (essentially thermal excitation plus tunnelling) will be very small. Only those states close to E_c where the localization is weak (the overlap finite) will make a significant contribution to $\sigma_{loc.}$. Theoretically estimated values of σ_{OL} have not yet been published.

As discussed in chapter 3, for certain cases N(E) may contain a peak in the localized region which would 'pin' E_F. The first activation term in equation 6.02.10 would then be lost, and hence

$$\sigma_{loc.} = \sigma_{OL} \exp - (\Delta W/kT) \qquad 6.02.11$$

In discussing the temperature and field dependence of $\sigma_{loc.}$ the principal variation will be via ΔW, since the tunnelling probability will not be expected to vary significantly [9]. The value of ΔW may vary as the density of occupied sites increases, simply because of coulombic interaction. Local polarization around an ionized site will also affect the value. In this very brief outline of temperature and field dependence these last two points are not considered explicitly.

In Miller and Abrahams theory [10], the hopping frequency (for sites at E_F) is of the form:

$$\nu_{ph} \exp (-2 \alpha R_o) \exp (-W_a/kT) \qquad 6.02.12$$

α describes the fall off, of the wave function on a localized site.
R_o is inter-site distance.

Mott [6] deduces that at low temperatures an electric field F will cause sites a distance R apart to be made level (so that tunnelling can occur) if

$$eFR \geqslant W_D \left(\frac{R_o^3 \alpha}{R^2} \right) \qquad \text{6.02.13}$$

and therefore the current will be of the form

$$j \propto \nu_{ph} \exp - (2\alpha C / F^{\frac{1}{3}}) \qquad \text{6.02.14}$$

C is a constant

At finite temperatures the jump frequency is expected to follow

$$\nu_{ph} \exp (-2\alpha R_o) \exp \left\{ - (W_D - eR_oF) / kT \right\} \qquad \text{6.02.15}$$

and the current governed by whichever is the larger of 6.02.14 and 6.02.13.

The activation energy at low temperatures should decrease with decreasing temperature since only jumps for which ΔW is small can occur. Mott [11] shows that in this region the hopping probability is proportional to

$$\exp - \left\{ \text{constant} . (\alpha R)^{\frac{3}{4}} (W_D / kT)^{\frac{1}{4}} \right\} \qquad \text{6.02.16}$$

and such a dependence has been observed [16] [17].

Hopping conduction is discussed again in the results section later in this chapter.

6.03.0 CONDUCTION IN A NON-HOMOGENEOUS STRUCTURE

This is a very large topic which cannot be dealt with here in all its aspects. It is only required to note the salient features, so as to be able to determine whether or not on the basis of d.c. conductivity, one can distinguish this type of structure from that of 6.02. In particular, temperature and low field dependence are looked for.

Figures 6.5(a), and 6.6(a) show the types of structure that might reasonably be expected. Figure 6.5(a) is a simple two phase structure

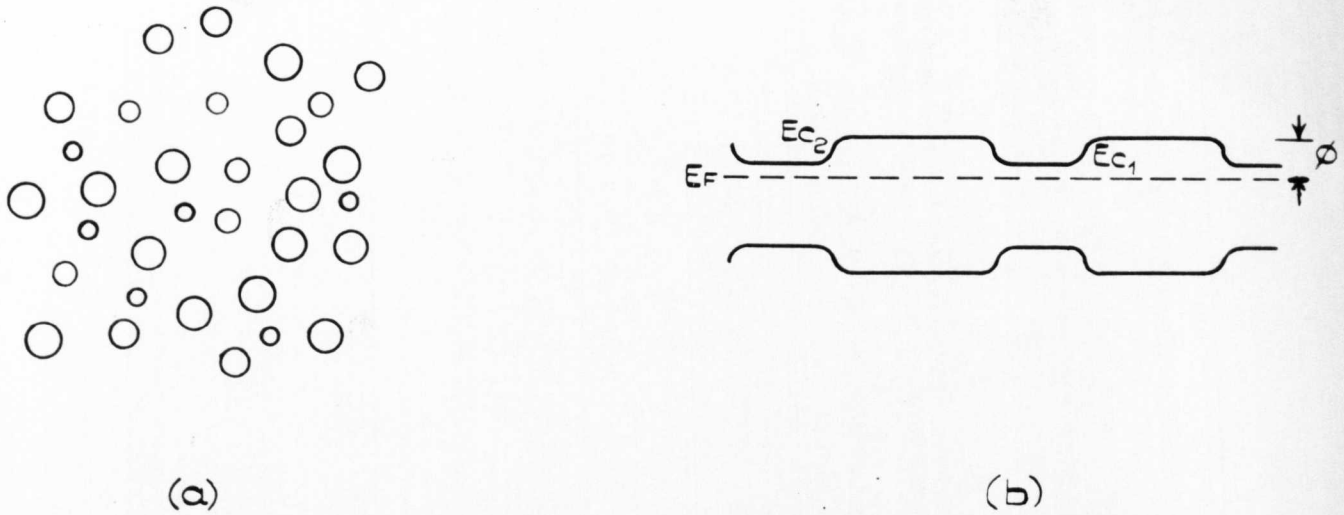

FIGURE 6.5

SCHEMATIC TWO PHASE STRUCTURE, AND CONSEQUENT ENERGY LEVEL DIAGRAM.

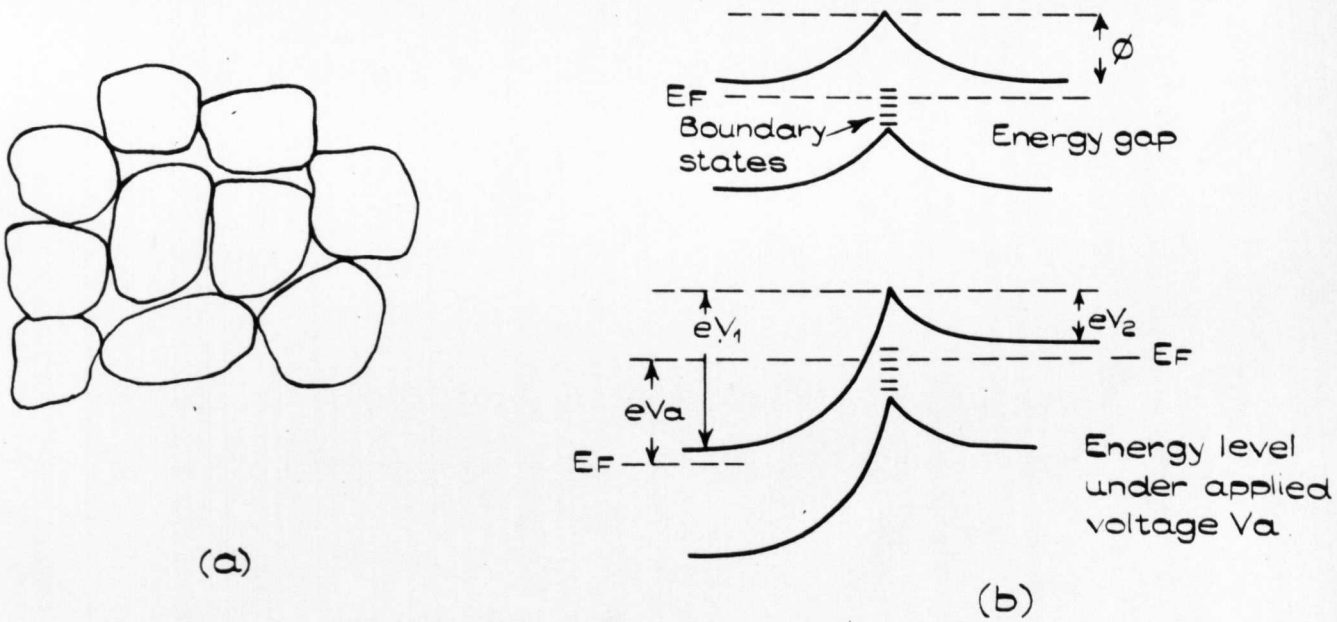

FIGURE 6.6

SCHEMATIC GRAIN STRUCTURE AND CONSEQUENT ENERGY LEVEL DIAGRAMS

where it will be assumed that the discontinuous phase is more conducting, and in figure 6.6(a) potential barriers due to grain boundaries are expected to limit the conductivity.

As regards d.c. conduction the most important consequence of these structures is the potential barrier that the more insulating phase or grain boundary will produce. The general form for these barriers are shown in figures 6.5(b) and 6.6(b). In figure 6.6(b) the composition in the grain boundary is obviously different, and the figure is drawn assuming these states to act as traps for the carriers in the grains.

CASE OF FIGURE 6.5

In this situation, the conductivity of a sample will be greater than that of the continuous phase if, (a) carriers can tunnel between sections of the discontinuous phase, (b) the mean free path of carriers in the continuous phase is longer than the mean separation of second phase particles, since then carriers can be thermally excited across the more resistive regions [13].

The probability for tunnelling in (a) will be of the form, [14]

$$\exp \left\{ - \left(\frac{8\pi x}{3h} \right) (2m^*)^{\frac{1}{2}} (\phi - E)^{\frac{1}{2}} \right\}$$

where $E \triangleq E_{c1}$

$\phi = E_{c2} - E_F$

For distances **x** more than a few atomic spacings, which are envisaged in figure 6.5, this term becomes negligibly small and must be discounted.

For case (b), even if the condition is satisfied which is unlikely for amorphous semiconductors, the number of carriers being thermally excited out of the second phase, will only be of similar magnitude to those from the continuous phase at E_{c2}, and therefore this is an unlikely mechanism for increasing the conductivity.

The height of the barrier will be approximately

$$E_{c_2} - E_{c_1} = \frac{kT}{e} \log \left(\frac{n_1}{n_2}\right)$$

which is independent of temperature if n_1 and n_2 (the density of free carriers in each phase) are governed by $\exp (E_c - E_F)/kT$ terms. There will however be a field dependence of the barrier height which will be similar to that of Schottky barriers, i.e.

$$\phi_{Field} = \phi - \beta F^{\frac{1}{2}}$$

since all the potential drop can be associated with the resistive phase. However the large number of barriers over which the potential must be shared will mean that the potential drop for any one barrier is small, and the effect will be negligible.

CASE OF FIG. 6.6

It has been shown for this case [15] that the current across the barrier varies as

$$- \exp \left(\frac{-eV_2}{kT}\right) \cdot \left\{1 - \exp \frac{-eV_a}{kT}\right\}$$

which for high fields approximates to

$$\exp -\left(\frac{eV_2}{kT}\right) .$$

However, more important than the field dependence is the size of potential needed at each boundary before any non-ohmic behaviour is observed. This was shown to be $\triangleq$ 10 volts [15]. Many barriers are envisaged as occurring in the materials, and therefore except in the case of very thin specimens the effect is again negligible.

The height of such barriers will not depend on temperature [14]. But it should be remembered that it will depend on the thickness of space charge region λ_o and the density of localized states as, [14]

$$V \propto \frac{N_D \lambda_o^2}{K}$$

K = dielectric constant

and therefore in amorphous semiconductors may be quite small (λ_o will be small).

These brief considerations show that such structures will not be detected by measurement of d.c. conductivity as a function of temperature or as a function of electric field unless very high fields are employed.

6.04.0 RESULTS

The d.c. conductivity was measured as a function of temperature, and in a few cases as a function of electric field, for compositions throughout the glass forming regions of the three systems.

The sets of figures 6.7, 6.8 and 6.9 sum up the results of the d.c. measurements. Figures (a) in each case, show Log σ vs $1/T$, (b) the activation energy vs composition, (c) conductivity (at $20^{\circ}C$) vs composition and (d) σ_o vs composition.

The error in any value of σ, arising from uncertainties in measurement of electrode diameter, specimen thickness, and meter readings, are shown by the error bars in figures (c).

The value of σ_o shown in figures (d) is that obtained from extrapolating the tangent of the curves of log σ vs $1/T$ at the high temperature end (see 6.02). These σ_o values are not corrected for the term $\exp \frac{B}{k}$ as equation 6.02.5 suggests they should be. The reason for not doing so is that even if equation 6.02.5 does apply, B is not known accurately for each case. It may however be helpful to note that a typical value, based on the shift of the absorption edge with temperature, is $\simeq 10$.

Before commencing with the discussion, certain pertinent remarks are made concerning each set of results.

FIGURE 6.7 (a)

Log σ vs the reciprocal of absolute temperature for glasses from the selenium arsenic system.

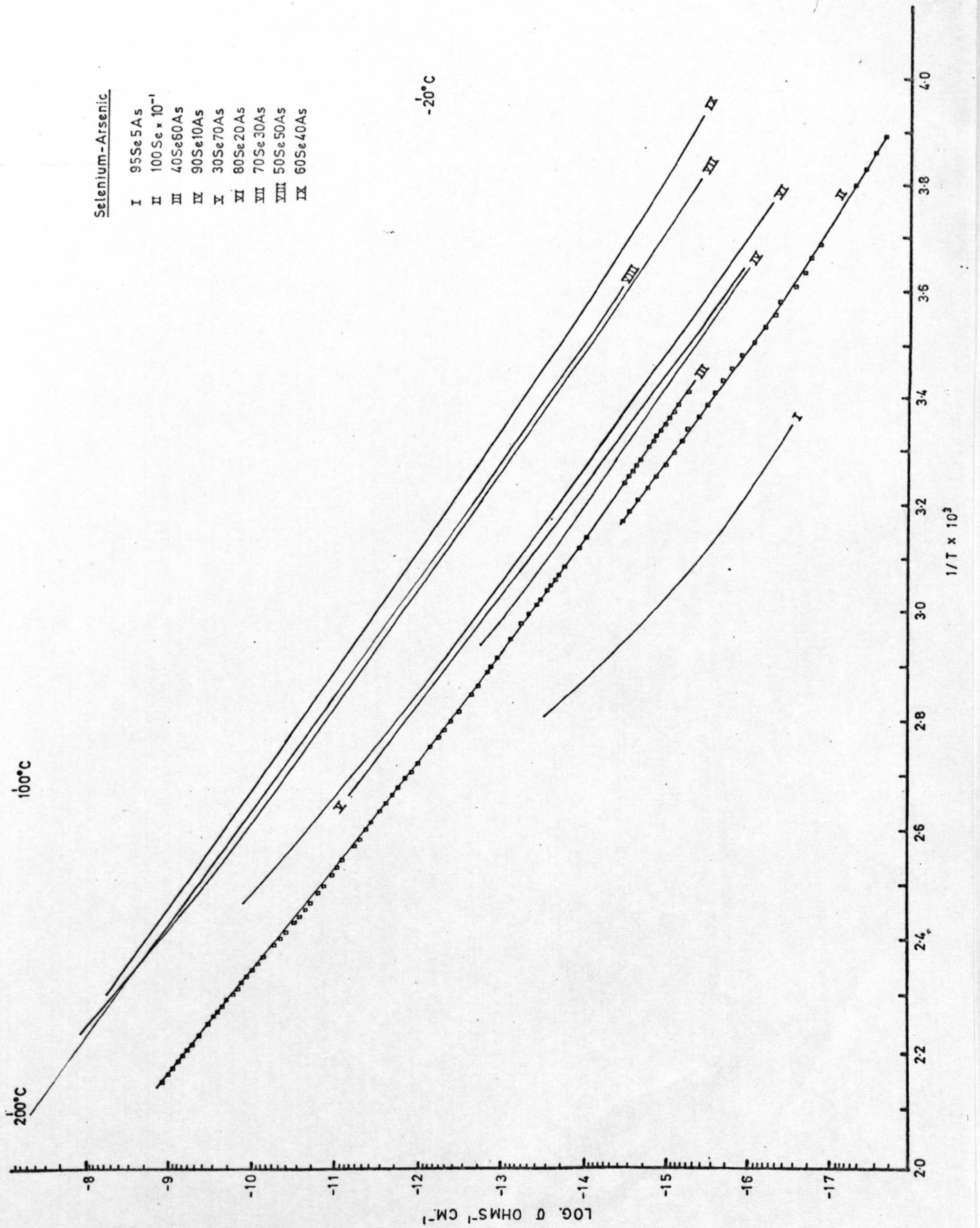

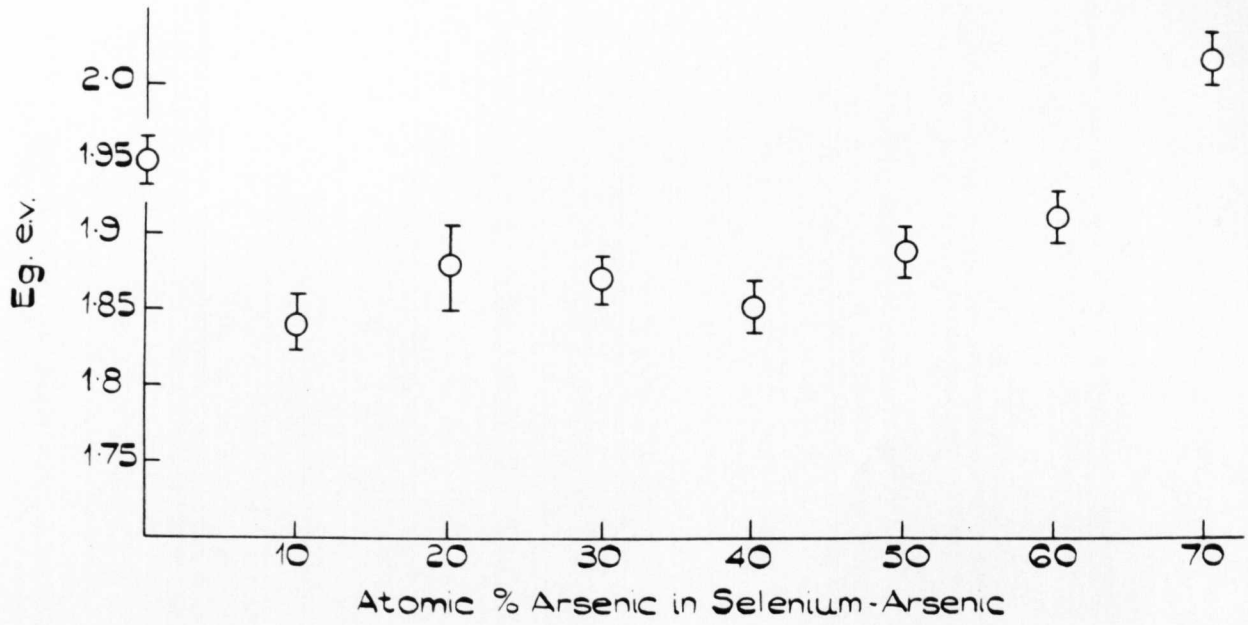

FIGURE 6.7.b.

ACTIVATION ENERGY Eg VS. COMPOSITION FOR THE SELENIUM-ARSENIC SYSTEM.

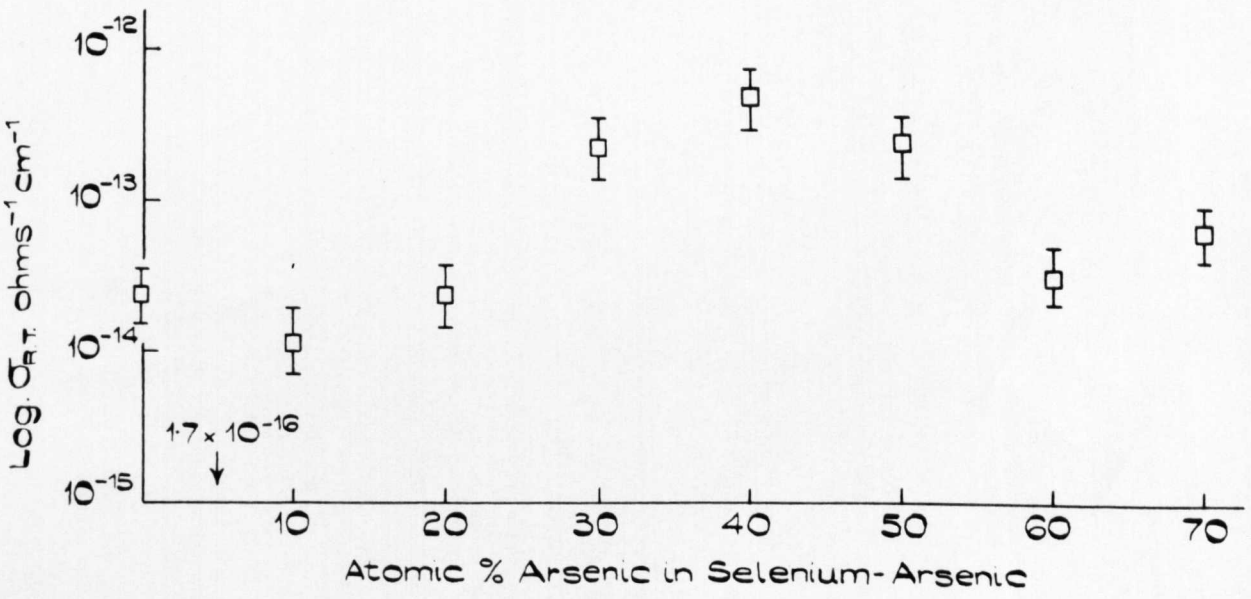

FIGURE 6.7.c.

LOG. ROOM TEMPERATURE CONDUCTIVITY σ_{RT} VS. COMPOSITION FOR THE SELENIUM-ARSENIC.

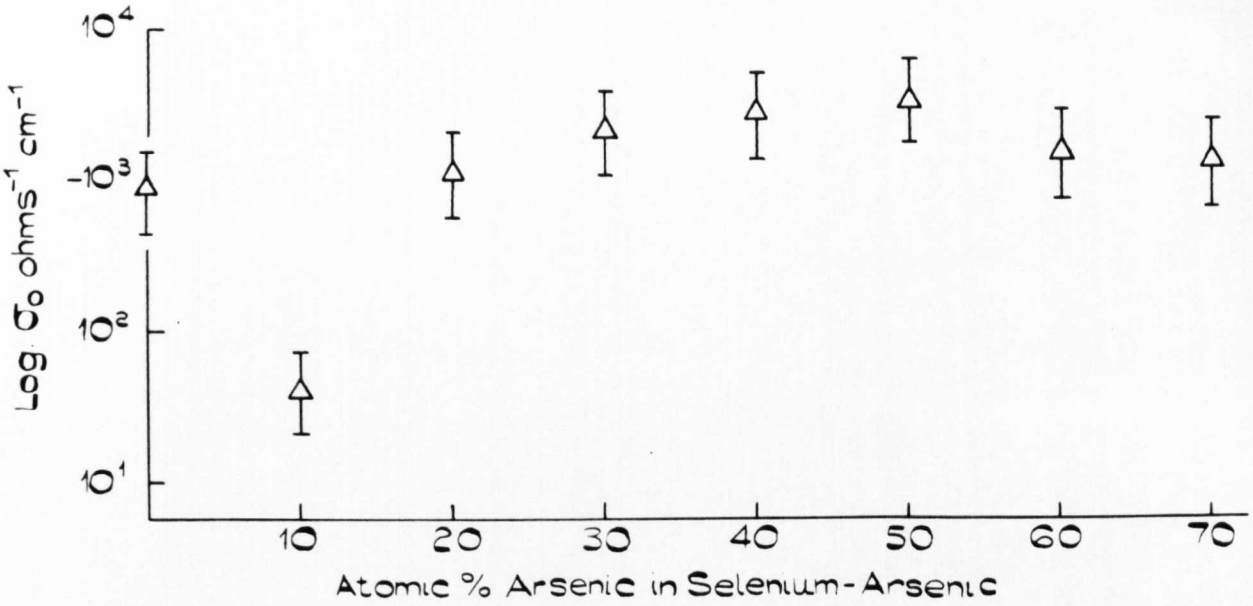

FIGURE 6.7.d.

LOG. σ_o VS. COMPOSITION FOR THE SELENIUM-ARSENIC SYSTEM.

COMPOSITION Se-As	Eg e.v.	σ_{RT}	σ_o
100-0	1·95	$2{\cdot}4 \times 10^{-14}$	9×10^2
95-5	Large Variation	$1{\cdot}7 \times 10^{-16}$	
90-10	1·84	$1{\cdot}1 \times 10^{-14}$	$4{\cdot}4 \times 10^1$
80-20	1·88	$2{\cdot}3 \times 10^{-14}$	$1{\cdot}05 \times 10^3$
70-30	1·865	$2{\cdot}2 \times 10^{-13}$	$2{\cdot}3 \times 10^3$
60-40	1·85	$3{\cdot}0 \times 10^{-13}$	$3{\cdot}0 \times 10^3$
50-50	1·89	$2{\cdot}5 \times 10^{-13}$	$3{\cdot}9 \times 10^3$
40-60	1·91	$5{\cdot}5 \times 10^{-15}$	$2{\cdot}6 \times 10^3$
30-70	2·04	$1{\cdot}1 \times 10^{-14}$	$1{\cdot}4 \times 10^3$

TABLE 6.7.

SUMMARY OF DATA OBTAINED FROM FIGURE 6.7.a. FOR THE SELENIUM-ARSENIC SYSTEM.

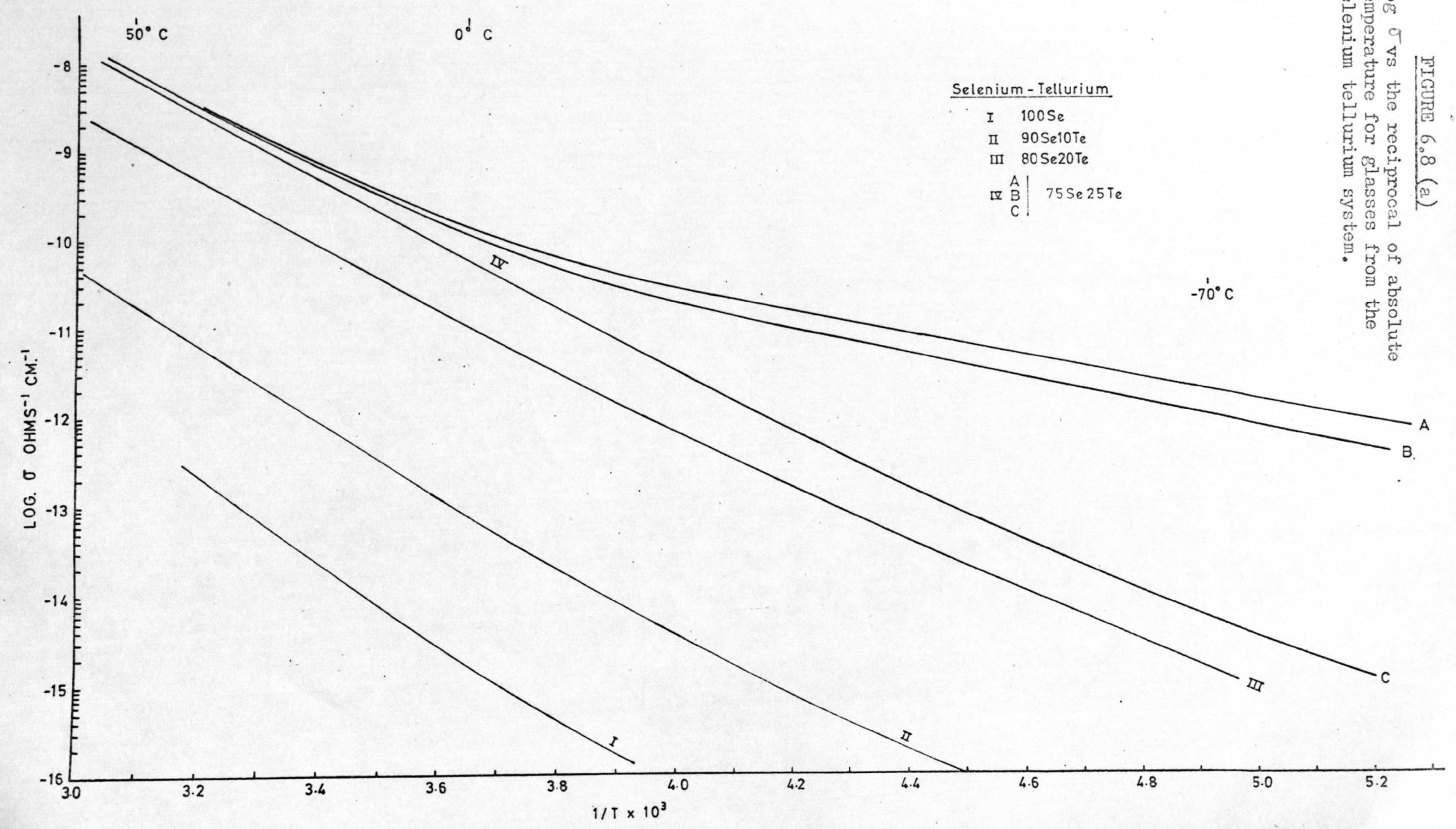

FIGURE 6.8 (a)

Log σ vs the reciprocal of absolute temperature for glasses from the selenium tellurium system.

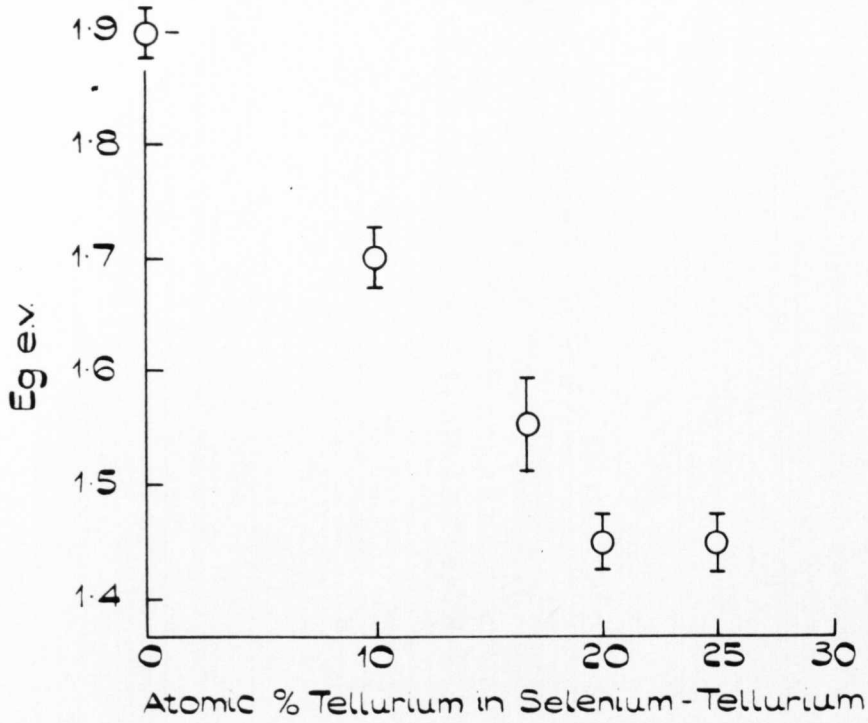

FIGURE 6.8.b.

ACTIVATION ENERGY Eg VS. COMPOSITION FOR THE SELENIUM - TELLURIUM SYSTEM.

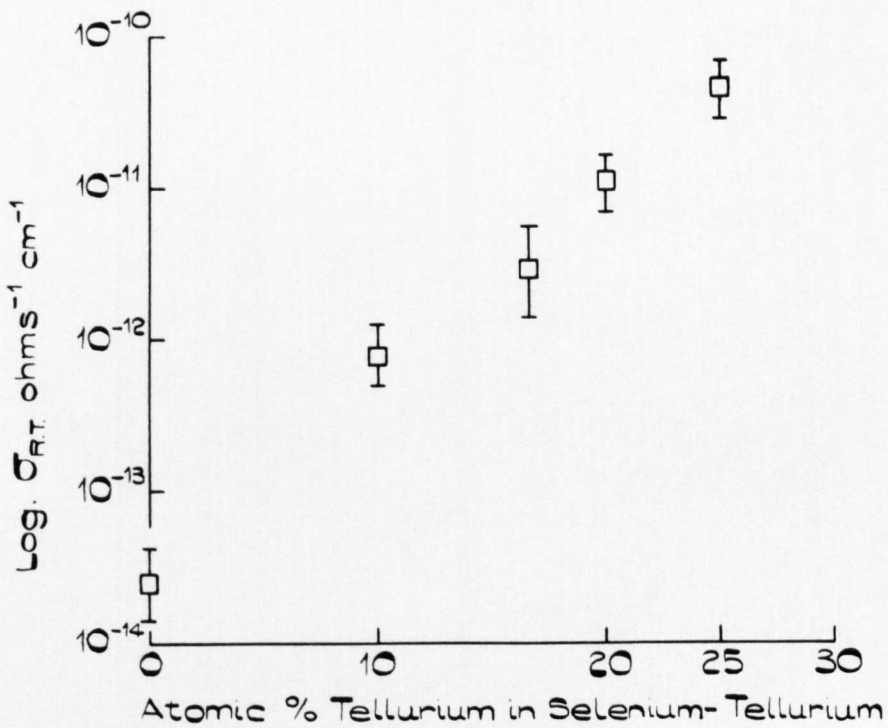

FIGURE 6.8.c.

LOG ROOM TEMPERATURE CONDUCTIVITY $\sigma_{R.T.}$ VS COMPOSITION FOR THE SELENIUM - TELLURIUM SYSTEM.

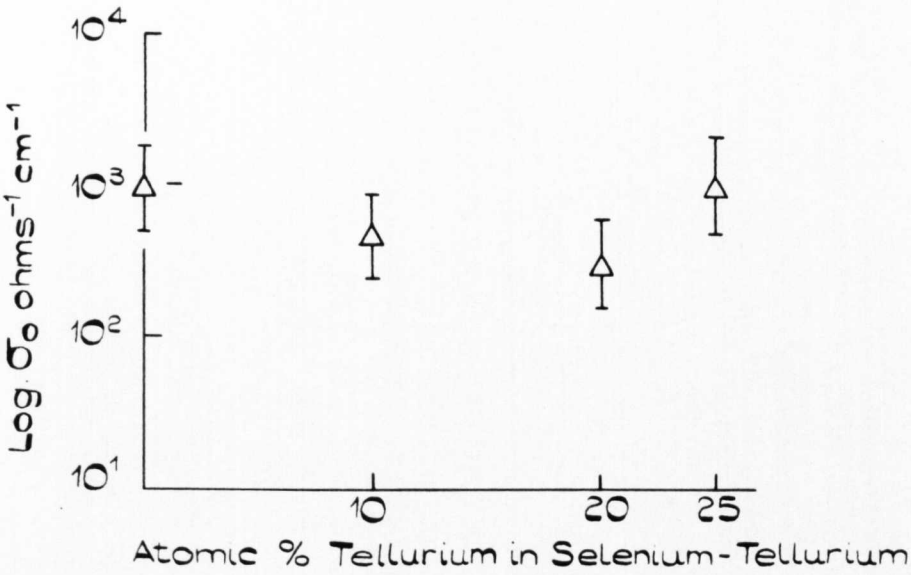

FIGURE 6.8.d

LOG. σ_o VS. COMPOSITION FOR THE SELENIUM-TELLURIUM SYSTEM.

COMPOSITION Se-Te	Eg e.v.	$\sigma_{R.T.}\ \Omega^{-1}\,cm^{-1}$	$\sigma_o\ \Omega^{-1}\,cm^{-1}$
100-0	1·90	$2{\cdot}4\times10^{-14}$	$9{\cdot}0\times10^{2}$
90-10	1·75	$8{\cdot}0\times10^{-13}$	$5{\cdot}1\times10^{2}$
83-17	1·55	$2{\cdot}0\times10^{-11}$	
80-20	1·46	$1{\cdot}1\times10^{-10}$	$2{\cdot}5\times10^{2}$
75-25	1·46	$4{\cdot}4\times10^{-10}$	$1{\cdot}0\times10^{3}$

TABLE 6.8.

SUMMARY OF DATA OBTAINED FROM FIGURE 6.8.a FOR THE SELENIUM-TELLURIUM SYSTEM.

FIGURE 6.9 (a)

Log σ vs the reciprocal of absolute temperature for glasses from the tellurium arsenic system.

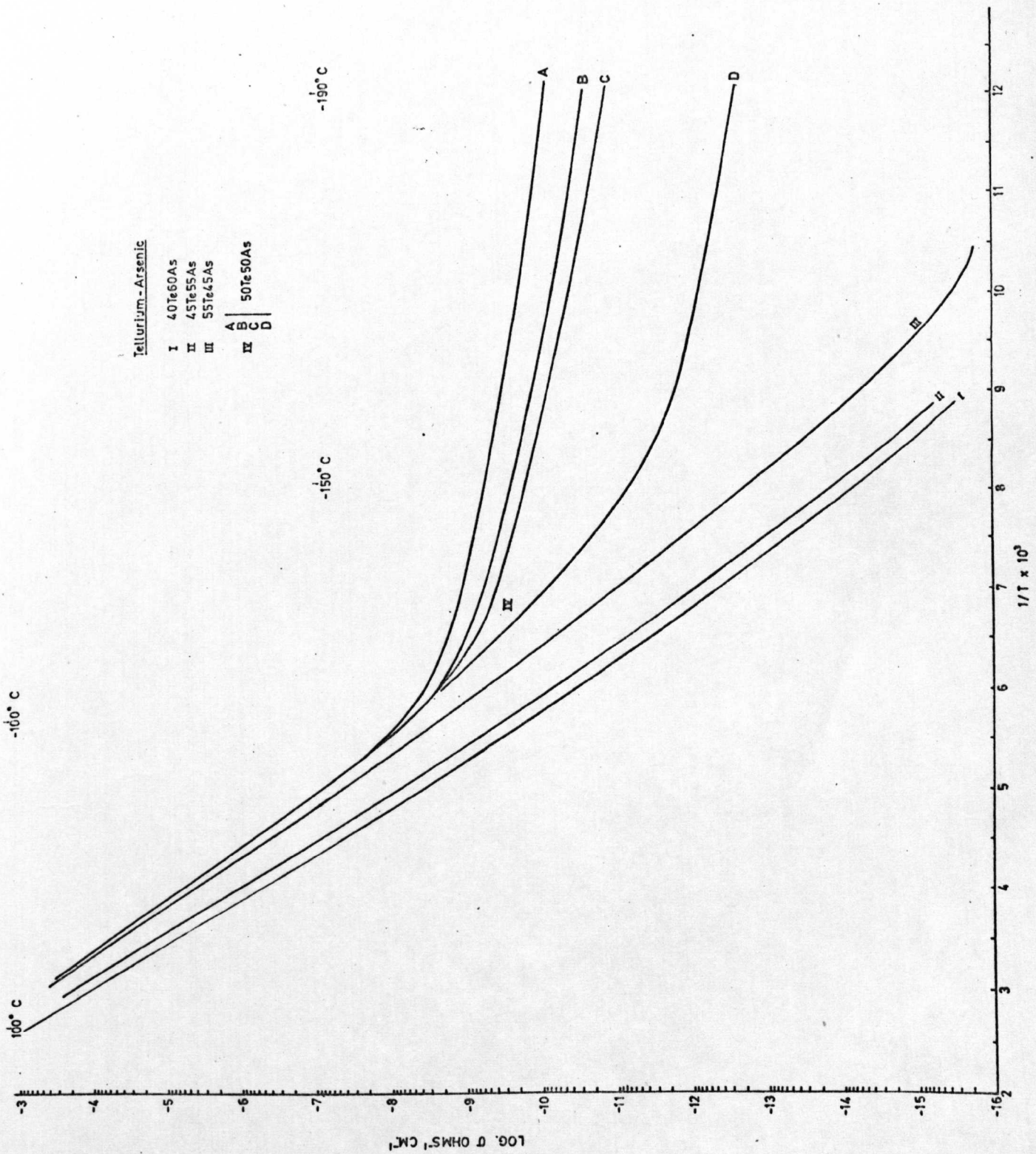

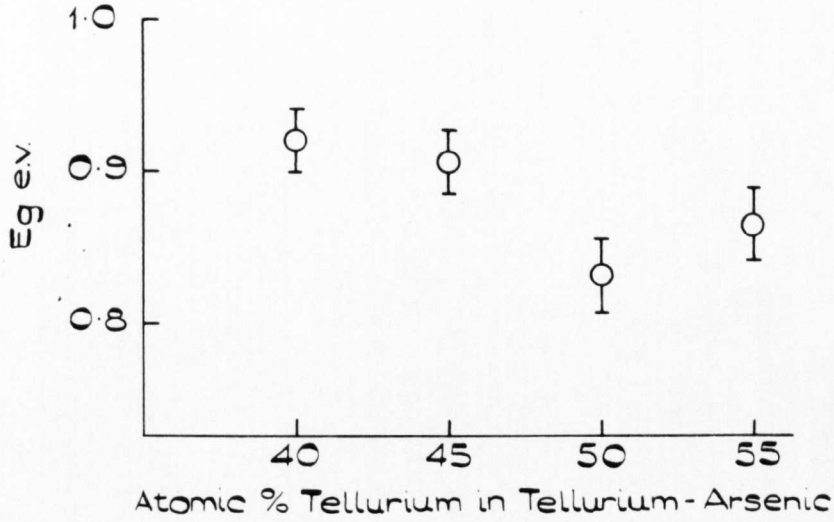

FIGURE 6.9.b.

ACTIVATION ENERGY Eg VS COMPOSITION FOR TELLURIUM-ARSENIC SYSTEM

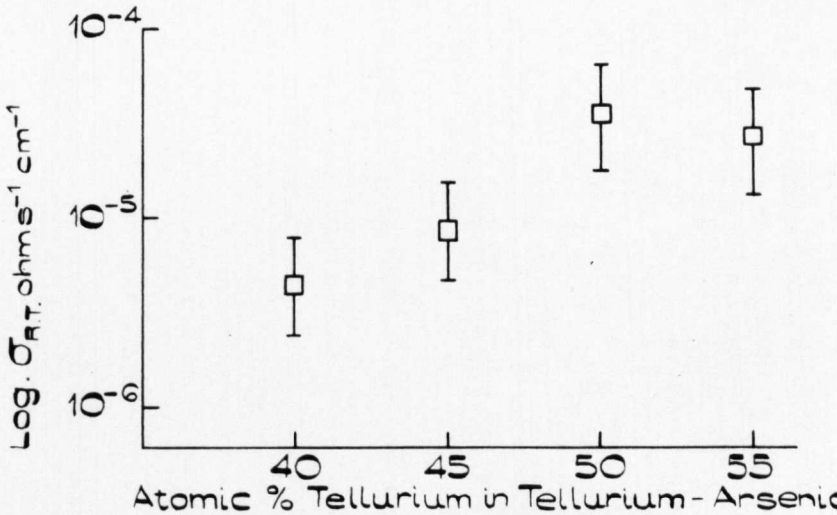

FIGURE 6.9.c.

LOG. ROOM TEMPERATURE CONDUCTIVITY $\sigma_{R.T.}$ VS COMPOSITION FOR THE TELLURIUM-ARSENIC SYSTEM.

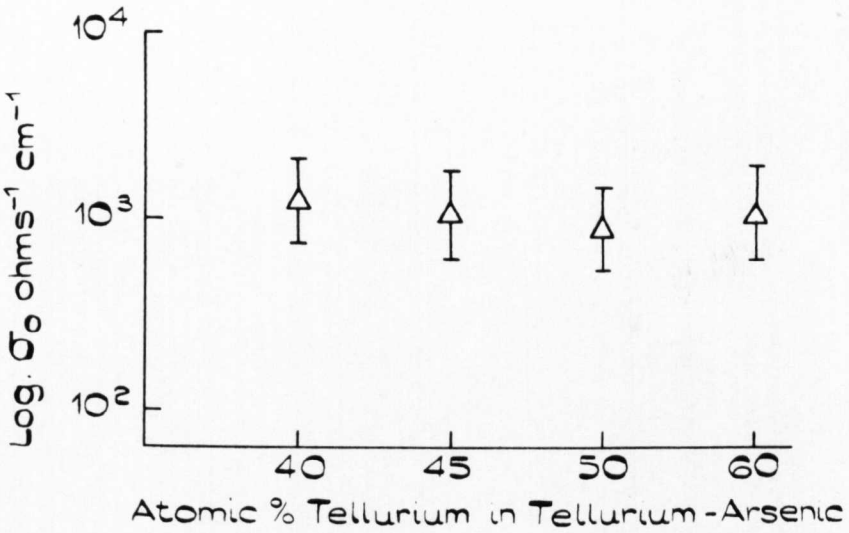

FIGURE 6.9.d.

LOG σ_o VS. COMPOSITION FOR THE TELLURIUM-ARSENIC COMPOSITION.

COMPOSITION Te-As	Eg e.v.	σ_{RT} ohms^{-1} cm^{-1}	σ_o ohms^{-1} cm^{-1}
40-60	0·92	4.4×10^{-6}	1.3×10^{3}
45-55	0·907	8.4×10^{-6}	1.15×10^{3}
50-50	0·83	3.5×10^{-5}	8.8×10^{2}
55-45	0·804	2.8×10^{-5}	1.15×10^{3}

TABLE 6.9.

SUMMARY OF DATA OBTAINED FROM FIGURE 6.9.a. FOR THE TELLURIUM-ARSENIC SYSTEM.

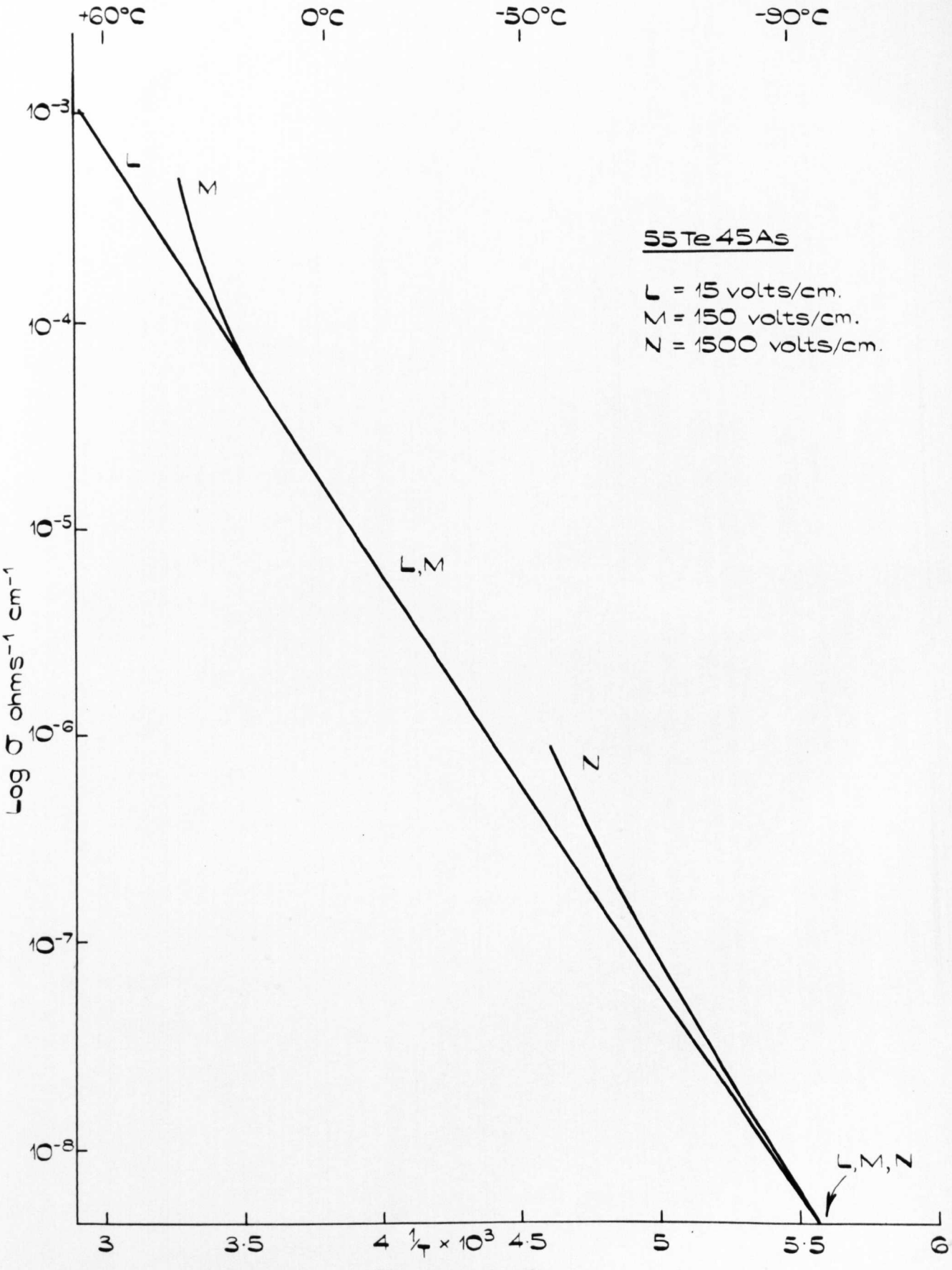

FIGURE 6.10.

LOG σ VS 1/T FOR 55Te45As GLASS FOR THREE DIFFERENT ELECTRIC FIELDS.

6.04.1 THE Se-As SYSTEM: FIGURES 6.7(a) - (d)

For three materials in this system, conductivity vs. temperature was measured as a function of electric field. These three glasses, 100 Se, 80Se 20 As and 40Se 60As, showed no field dependence up to a field of 2000 volts/cm. In another experiment reported in chapter 8, there was found to be no field dependence for the 60Se 40As glass up to fields of 80,000 volts/cm.

The curvatures of the plots for 80Se 20As and 70Se 30As in figure 6.7(a), are seen to increase at higher temperatures. These increases may be attributable to the specimen softening. Consequent distortion of the specimens will mean that the error in the high temperature measurement is greater (and biased to give higher values of σ) than over the rest of the temperature range. However, no data has been published for measurements of conductivity into the softening region, and they may be valid.

The curve for 100Se is drawn an order of magnitude too low, to prevent confusion with other curves.

6.04.2 THE Se-Te SYSTEM: FIGURES 6.8 (a) - (d)

The curves for glasses containing 0, 10, 20 At.% tellurium and curve A for that containing 25 At.% tellurium are field independent up to fields of 2000 volts/cm. The curves A and B were produced for the same specimen of 75Se 25Te that gave curve C. The new behaviour at temperatures below -20°C was found after the specimen had been held at 70°C for approximately ten minutes. Curve B was produced with a field of 20 volts/cm, and curve A a field of 2000 volts/cm.

6.04.3 THE Te-As SYSTEM: FIGURES 6.9 (a) - (d)

Apart from the 50Te 50As composition each of the materials in this

system were found to have field independent conductivities over most of the temperature range.

However at higher temperatures all of the glasses (including 50Te 50As) were capable of showing a more rapid increase of conductivity with temperature. The temperature at which this occurred was a function of the voltage across the specimen. This is shown in figure 6.10. It was found that these branches were the prelude to some form of switching, when the current jumps very rapidly, many orders of magnitude. Rapid removal of the voltage restored the specimen to its initial state.

Curve D in fig. 6.9(a) was obtained using an electric field of 15 volts/cm, after the specimen has been annealed at 150°C for approximately 15 mins. Curves A, B and C were obtained after a second anneal at 150°C again for approximately 15 mins, the magnitudes of the fields used were 1500, 150 and 15 volts/cm respectively.

DISCUSSION

6.05.0 THE FORM OF THE LOG σ vs $^{1}/_{T}$ CURVES

It will be noticed immediately on inspection of figures 6.7(a) - 6.9(a) that the majority of log σ vs $^{1}/_{T}$ plots are curved with the slope increasing with temperature.

Before discussing this, it is pointed out that the $T^{3/2}$ term which appears as a pre-exponential factor in σ for crystalline semiconductors, does not explain this effect. Neither the magnitude of the curvature nor its temperature dependence are explained by such a term.

There are several possible causes for the curvature. Two of these are looked at in detail, and some others considered more briefly.

6.05.1 EXTRINSIC CONDUCTION

The possibility of localized states, acting as donors and acceptors

was introduced in 6.02.2. In that section computer calculations of n(T) were given and attention drawn to the fact log n vs $^{1}/_{T}$ did not give a straight line. It will now be shown that there is considerable agreement between the curves of fig. 6.2 and 6.7(a) - 6.9(a).

In figure 6.4, activation energy was drawn against T for the theoretical curves. The same relationship, deduced from the conductivity curves is drawn in fig. 6.11(a), (b) and (c), for glasses from each of the three systems. It is seen that there is reasonable agreement in the form of the curves of figures 6.4 and 6.11. The high temperature sections of the curves agree particularly closely. It is also noted that the conductivity ranges for which the theoretical and experimental lines are curved are similar.

This agreement implies the following. First, if the materials can be adequately described by the model of figure 6.1, then the localized states can be considered as acting as acceptors and donors. The second point is that the lengths of the tails as inferred from experimental curves, will be similar to those considered in the calculations, i.e. N(E) for each tail becomes unity somewhere in the gap.

The latter of these two points is made without considering the effect of band overlap. Since this may lead to false deductions, some estimate should be made of the effect of such an overlap. For example, consider $E_c - E_v$ 1.5 ev, and $\alpha_c = \alpha_v = 20$ ev^{-1} (a value which gives considerable overlap, and one which is relevant to the results of the next chapter). The Fermi level at absolute zero will be at .75 ev (E_v = 0 ev) where N(E) for both tails of states is 10^{14} cc^{-1} ev^{-1}. The number of conduction band tail states between E_F and E_c is 5×10^{18} cc^{-1} and the number of valence band states, which according to Cohen [18] will maintain their character and therefore act as charged traps, will be 5×10^{11}. Such a large difference would suggest that n(T) as calculated would still be

dominated by the conduction band tail states. However the charged traps would be expected to limit the mobility and it may no longer be possible to compare n(T) and σ (T), assuming a simple, temperature independent mobility.

Despite this a calculation was made with $\alpha_c = 20\ ev^{-1}$. The form of the curve of n(T) was the same, but the extrinsic conduction dominated up to a conductivity of $\simeq 10^{-5}$ ohm^{-1} cm^{-1} and temperature of $\simeq 300^{\circ}C$, compared with $10^{-10} - 10^{-13}$ ohm^{-1} cm^{-1} and $\simeq 0^{\circ}C$ for the experimental cases. Such large differences can obviously not be accounted for by the mobility term.

The curvatures of figs. 6.7(a) - 6.9(a) can therefore be explained by considering the conduction and valence band tails to provide a density of states distribution giving extrinsic conduction. The results also suggest that N(E) for the tails became unity between E_c and E_v .

6.05.2 TEMPERATURE DEPENDENCE OF E_v AND E_c

The effect of any temperature dependence of $E_v - E_c$ is now considered.

One type of dependence has already been considered in 6.02.1, but a more general case is now investigated, namely, let

$$E_g = E_c - E_v = E_{go} - BT^x \qquad 6.05.1$$

From the results of optical absorption (chapter 7), B is seen to be a positive quantity (E_g decreases with increasing temperature). Also, x is not expected to differ greatly from +1 over the range of temperature under discussion. This fact is again derived from chapter 7, and also from other published results for both amorphous and crystalline semiconductors (see chapter 7 for references).

Substituting 6.05.1 into 6.02.2, taking the logarithm, and then differentiating gives

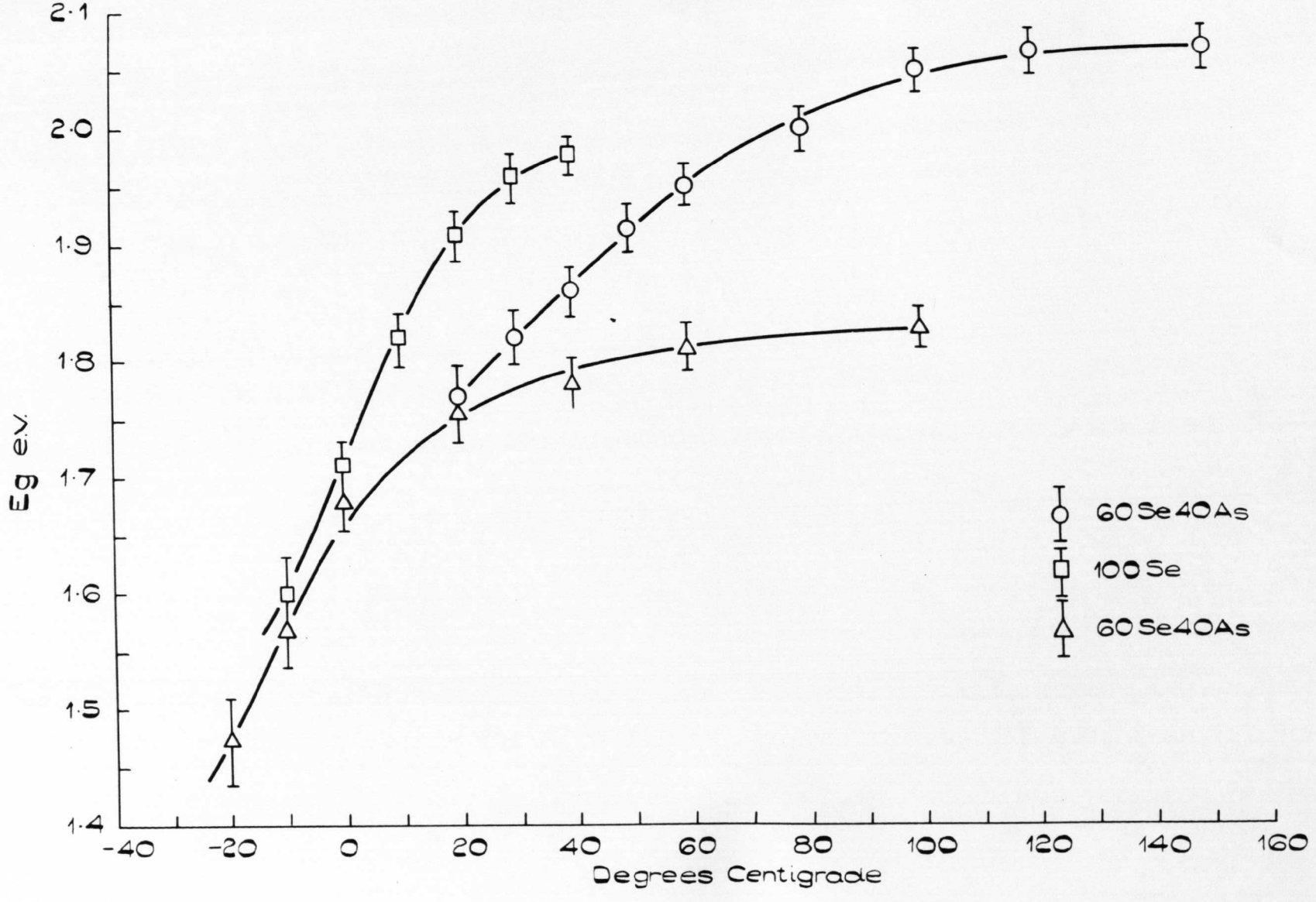

FIGURE 6.11.a.

ACTIVATION ENERGY VS TEMPERATURE FOR THREE SELENIUM ARSENIC GLASSES.

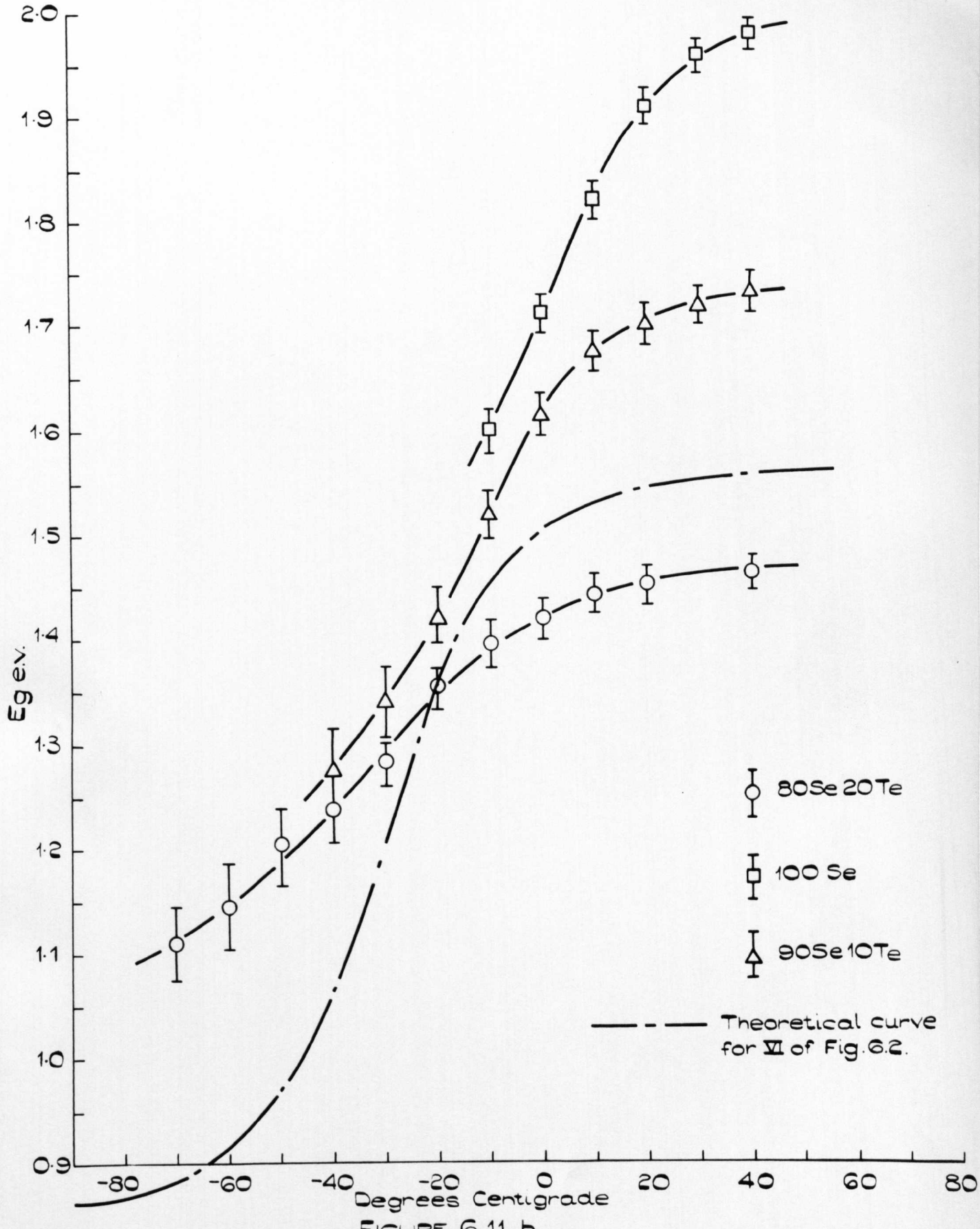

FIGURE 6.11.b.

ACTIVATION ENERGY VS TEMPERATURE FOR THREE GLASSES FROM THE SELENIUM TELLURIUM SYSTEM.

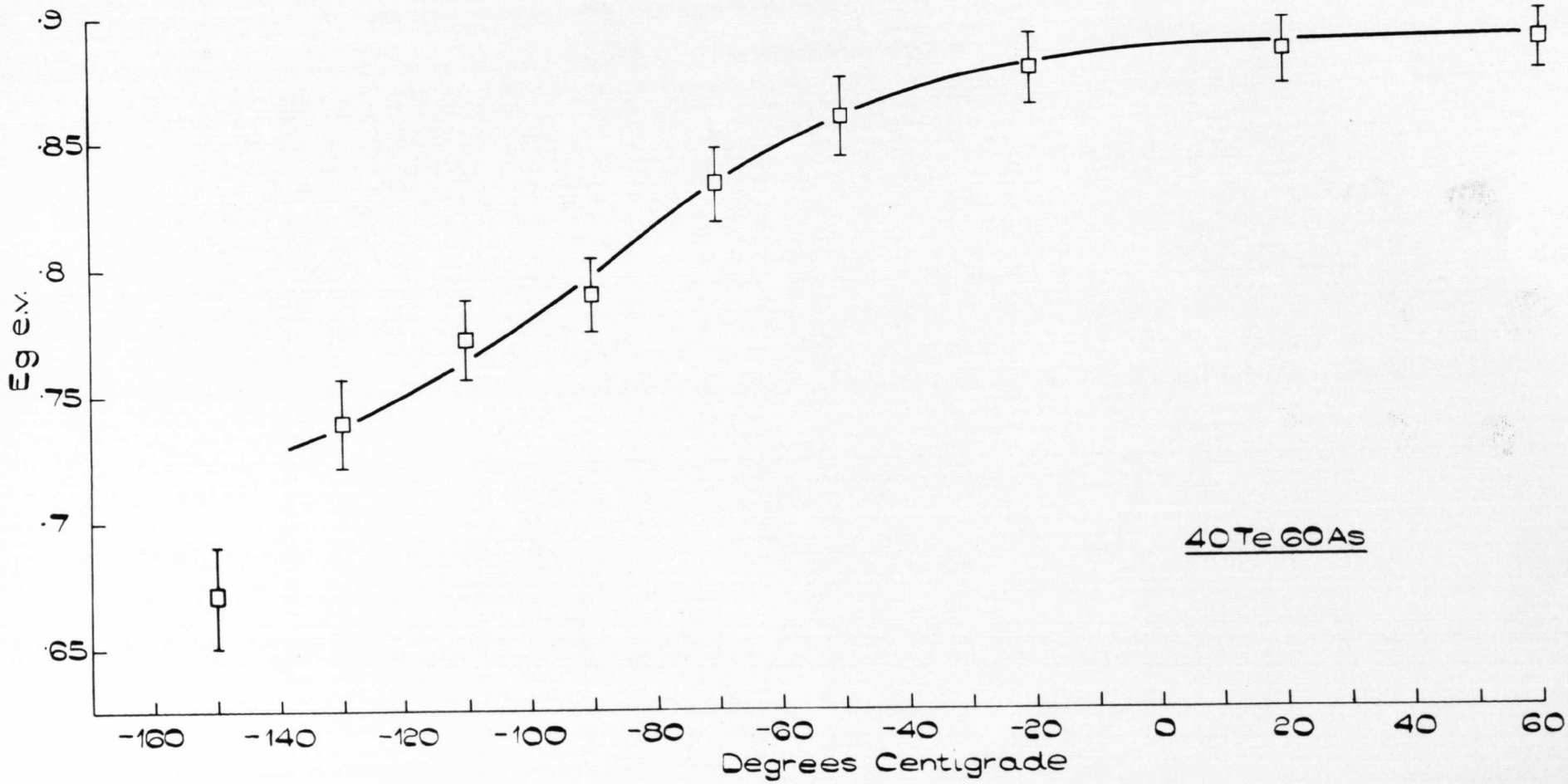

FIGURE 6.11.c.

ACTIVATION ENERGY VS TEMPERATURE FOR TELLURIUM ARSENIC GLASS.

$$\frac{d(\log \sigma)}{d(1/T)} = -\left[\frac{E_{go}}{k} + \frac{B}{k} (x-1)\, T^{x} \right] \qquad 6.05.2$$

and differentiating a second time

$$\frac{d^2 \log \sigma}{d(1/T)^2} = \frac{B}{k} x(x-1)\, T^{x+1} \qquad 6.05.3$$

Over the temperature range of measurement, the L.H.S. of equation 6.05.3 (which is the slope of figures 6.11(a) (b) (c)) is always positive, and hence it can be deduced that x would be greater than unity.

Equation 6.05.3 also shows that the slope of the log vs $1/T$ should increase continuously with temperature and not level off as do the curves of figures 6.11. Also the curvature should be greater at higher temperatures, i.e. figures 6.11 should be concave upwards and not downwards as is the case.

These discrepancies make it apparent that if 6.05.1 does apply, it is not significant in determining the form of $\sigma(T)$ over the temperature ranges of figures 6.7(a) - 6.9(a).

This can also further be seen from the following rough estimate of B. If it is assumed that at the edge of the relevant Brillouin zone

$$E \propto \frac{\pi}{a}^{2}$$

then $$\frac{dE}{E} = -2 \frac{da}{a}$$

assuming a thermal coefficient of expansion of 10^{-5} unit length^{-1} $^{\circ}C^{-1}$

then $$B = \frac{dE}{E} = 2 \times 10^{-5} \text{ /ev/}^{\circ}C$$

If x in equation 6.05.1 is close to unity, then substituting B into 6.05.1 shows that it is only at high temperatures that the change in $E_c - E_v$ becomes significant.

6.05.3 OTHER CAUSES

As well as the above, it would be possible to put forward other causes for the form of $\delta(T)$:

There will obviously be other localized state distributions which will produce the effect.

There are also the consequences of the metal-semiconductor contact to consider. This is thought however to be an unlikely cause since the effect is universal to all the glasses studied here, and also it will be shown in chapter 8 that the quality of the contacts used was good, and not expected to produce potential barriers.

It may also be that E_v, and E_c are dependent on temperature in that as the lattice constant decreases, states which were weakly localized may become non-localized, hence E_v and E_c would move into the bands as the temperature increased.

6.06.0 DISCUSSION FOR INDIVIDUAL SYSTEMS

An attempt must now be made to understand the groups of curves in figures 6.7(a), 6.8(a) and 6.9(a), and the information derived from them shown in the other figures 6.7 - 6.9 and summarized in tables 6.7 - 6.9 respectively.

6.06.1 THE ARSENIC SELENIUM SYSTEM

Attention is first drawn to figure 6.7(d) which shows σ_o values. Over almost the entire range, the values, within the limits of experimental error can be made to agree at a value of 1.8×10^3 ohm^{-1} cm^{-1}. (If the correction implied by equation 6.02.5 is applied this becomes 1.8×10^2 ohm^{-1} cm^{-1})

The first point made about this result is that there is agreement, of σ_o, over almost the whole composition range. In as much as the composition changes, so also must the short range order which will determine N(E). The similar values would imply, if the model of figure 6.1 is in each case applicable, that N(E), at least at E_c and E_v is in all cases similar.

The second point, is that the value of σ_o agrees closely with that predicted by equation 3.03.5 of Mott's theory. Not too much significance should be placed on this agreement immediately, since several factors used in arriving at the theoretical estimate are approximations; in particular, the value of a_E taken to be 4 Å, the coordination number taken to be 6, and the value of V_J at $E = E_c$, which is derived for this coordination number, to be 5. As a consequence of these approximations the agreement is simply noted.

The results of figure 6.7(b) and 9.1 (density vs composition) are now considered. From 6.7(b) it is seen that the activation energy varies markedly for additions of arsenic (up to 20 atomic %) but from 20 - 60 atomic % the variation is small, although there is a minimum at the stoichemetric composition $As_2 Se_3$. From figure 9.1 the density shows a pronounced maximum at the stoichemetric composition where the value is very close (within 2%) to that of the crystalline phase of the material.

It will be shown in chapter 9 that the density result can be explained, at least on the selenium rich side of 60Se 40As, by considering the material to have a two phase structure, the constituents being $As_2 Se_3$ and Se. The amorphous arsenic-triselenide would be the continuous phase. If this were the case then σ_o and E_g would be expected to remain constant over the two phase region. Small variations in each could be attributed to excess material in the continuous phase. However, as will be seen in chapter 9 there is another explanation of figure 9.1 which would lend no support to this argument.

Finally some comments are made concerning the results for small additions of arsenic in selenium. From the fluctuations in density, σ , and E_g at low concentrations, it is obvious that some other structure must prevail in this region. It is well known that small additions of arsenic causes cross linking between Se chains, which increases viscosity and makes recrystallization more difficult to achieve. Such cross linking would increase the disorder and decrease the mobility, hence causing the drop in the conductivity. The curve for 95Se 5As in 6.7(a) has changed considerably from that for selenium. The curvature suggest a very large value for $E_c - E_v$ in figure 6.1 and hence also for σ_o, which is difficult to account for simply by cross linking of selenium chains.

Similarly the result for 90Se 10As is not understood. The further addition of arsenic has decreased the density, which result suggests an even more disordered network. On the other hand conductivity has increased and become more nearly exponential with $E_g/2kT$, which from the 95Se 5As result would mean a re-ordering of the structure.

6.06.2 THE SELENIUM TELLURIUM SYSTEM

It will again be instructive to include the results of the density measurements, from fig. 9.2.

From figs. 6.8(b) - (d) and 9.2 it is observed that replacing selenium by tellurium, up to 20 atomic % causes the respective properties to vary, in a manner approximately proportional to the quantity of tellurium. The glass 75Se 25Te does not follow this proportionality. The reason for this is expected to lie in the fact that it is at the very end of the glass forming region, so that its structure may be different to other glasses in the system.

It is apparent then that increasing the proportion of tellurium in a

random Se-Te network has the effect of decreasing the band gap. However it can be shown that at the same time the length of the tails of states remains approximately constant.

Consider the results of E_g vs T for the three glasses 100Se, 90Se 10Te, and 80Se 20Te as shown in fig. 6.11(b) (the dashed curve is from the theory see 6.02.2). The fact that in each of the three experimental curves, intrinsic conduction begins to dominate at the same temperature, is thought to be of some significance. The following simple argument produces one consequence.

It will be assumed that the conduction band tail is dominant, and also that these states can be represented by a single narrow band of acceptor states at an energy E_A, and of number $N_A\ cc^{-1}$. N_A will increase as the length of the tail increases, i.e. as α_c decreases, and also $E_c - E_A < E_A - E_v$.

Over the temperature range of extrinsic conduction the number of free holes n_h, will be equal to the number of ionized acceptor sites, i.e.

$$n_h = \frac{N_A}{1 + \exp \frac{(E_A - E_F)}{kT}} \qquad \text{6.06.1}$$

and n_h will be much greater than n_e, the number of free electrons at E_c. Now when the conduction becomes intrinsic the number of free electrons

$$n_e = \frac{N_o}{1 + \exp \frac{(E_c - E_F)}{kT}} \qquad \text{6.06.2}$$

will become equal to n_h. If it is assumed that E_F does not come within kT of E_A, then from equating 6.06.1 and 6.06.2 we obtain

$$E_c - E_A = kT \log \frac{N_o}{N_A} \qquad \text{6.06.3}$$

Now in figures 6.11(b), E_c is decreasing as the tellurium content is increased. Also, the temperature at which the conduction becomes intrinsic

remains constant. For equation 6.06.3 to be satisfied, $E_c - E_A$ must remain constant, since if $E_c - E_A$ (the length of the tail) decreased, so also (from the way the equivalent set of states has been defined above) will N_A and therefore the right hand side of 6.06.3 would increase.

This result therefore suggests, that, if the tail of states can be considered as equivalent to some discrete set of acceptor states, then whilst decreasing the band gap, tellurium does not reduce the lengths of the tails of states. A similar result has been observed in the computer calculations of figure 6.2.

6.02.3 THE TELLURIUM ARSENIC SYSTEM

It is obvious that this system is quite different from the two previously discussed. It does not contain selenium which is the majority constituent in most of the other glasses, and also the glass forming region occurs in the middle of the composition range. This second property is not peculiar to this system, (see for example Rawson [4] Hilton [19]).

In view of the gross compositional and hence possibly structural differences it is interesting to again find σ_o values very close to 10^3 ohm^{-1} cm^{-1}. The variation across the system is small (the 50Te 50As glass may not be typical as discussed below) so that it is once again possible to conclude that this parameter is very little dependent on short range order and also that $N(E)_{E = E_c}$ is constant.

It is believed that the results for 50Te 50As should be considered separately. The one electrical specimen which was produced, was, during the first measurement taken to a temperature of 150°C, which temperature it is thought, was sufficient to modify the structure and consequently N(E) sufficiently, to produce the different low temperature behaviour of the conductivity. A subsequent heat treatment at similar temperatures

enhanced the behaviour. The same result was produced, by similar treatment of the 75Se 25Te glass. In this second case there was a slight (fig. 6.8a) increase in room temperature conductivity, which is a factor supporting the argument that a material so treated is not typical of the as quenched glass. These results are discussed separately in 6.07.

In view of the above comments, in considering the system as a whole the result for 50Te 50As is not included. It is then apparent, that, as in the selenium-tellurium system, the addition of tellurium decreases the band gap. This decrease in E_g can also again be associated with an increase in density as shown in figure 9.3.

The log σ vs $1/T$ plots maintain similar curvatures so that the tails of states for each of the glasses will be expected to be of similar length.

In figure 6.11(c), E_g is drawn against temperature for the 40Te 60As glass. It is evident that the transition from extrinsic to intrinsic conduction takes place over a much larger temperature range than is the case for other glasses. Such a behaviour could be associated (taking into account the actual temperatures involved) with a tail of states which falls off more slowly than exponentially.

6.07.0 THE EFFECTS OF ELECTRIC FIELD IN CERTAIN GLASSES

In general the conductivity of these binary chalcogenide glasses was not field dependent, at least up to field strengths which will now be described.

The maximum fields used for the Se-As and Se-Te glasses was 80,000 volts/cm, which was applied to specimens of 60Se 40As and 80Se 20Te. In the first of these, no dependence at all was found, and in the second case, the field dependence was attributed to the effects of space charge limited currents. In fact in both cases the object of the

experiment was to look for this phenomenon, the results of which are discussed in chapter 8. Since the glasses are quite representative of their respective systems it is expected that there is no field dependence of conductivity, for quenched specimens, in the Se-As and Se-Te systems up to fields of approximately 10^5 volts/cm.

There was however, a field dependence applying to all Te-As glasses, and a second type which appeared in annealed specimens of 75Se 25Te and 50Te 50As.

The first effect is known to be associated with the Pearson-Ovshinsky switching (see for example [20] [21]), and studied in these glasses by Nesvádba [22]. This is very much a subject in its own right, and therefore no comment is made, except to suggest that information derived from such measurements as recorded in figure 6.10, may be useful, in that it gives a very precise relationship between temperature, current, and electric field, at which non-ohmic behaviour commences.

This section then is only concerned with the field dependence of conductivity, as produced by annealing, or heat treating of the material.

6.07.1 ANNEALING, AND CONSEQUENT FIELD DEPENDENT CONDUCTIVITIES

The results on conductivity of annealing specimens of 50Te 50As and 75Se 25Te are shown by the curves ABCD of 6.9(a) and AB of 6.8(a) respectively. In figure 6.9(a) curve D was obtained after taking the specimen to 150°C for approximately 15 mins. and curves ABC after a second similar heat treatment. Field dependence after the first anneal was not looked for. All the curves coincide over the high temperature region.

In figure 6.9(a) curves A and B were obtained after the specimen which gave C was heated at approximately 70°C for ten minutes.

CURVE	FIELD VOLTS cm^{-1}	Eg e.v.	σ_0 OHMS^{-1} cm^{-1}	HEAT TREATMENT
D	15·5	·128	10^{-10}	Approx. 150°C for 15 mins
A	1500	0·0625 - 0·118	10^{-6}	Approx. 150°C for 30 mins.
B	150	0·077 - 0·124	10^{-8}	Approx. 150°C for 30 mins.
C	15·5	0·1 -- 0·133	10^{-8}	Approx. 150°C for 30 mins

Data for 50 Te, 50 As

(a)

CURVE	FIELD VOLTS cm^{-1}	Eg e.v.	σ_0 OHMS^{-1} cm^{-1}	HEAT TREATMENT
A	2000	·492	10^{-8}	70°C for 10 mins
B	20	·55	10^{-7}	70°C for 10 mins

Data for 75 Se, 25 Te

(b)

(Two values of Eg are given where this varies over the temperature range of measurement.)

TABLES 6.10 (a), (b).

SUMMARY OF DATA OF FIELD DEPENDENT CONDUCTIVITY IN ANNEALED SPECIMENS OF 50 Te 50 As, 75 Se 25 Te.

The data derived from the curves is summarized in table 6.10(a) and (b). Before commencing a discussion of the effect the following points are made.

(1) The effect appears only after some form of heat-treatment.

(2) For the 50Te 50As sample, annealing increased the density by approximately 8%. This measurement was not made on the 75Se 25Te glass.

(3) For the 75Se 25Te specimen the X-ray diffraction pattern after (as well as before) the heat treatment, showed no indication of devitrification.

(4) Equal changes in electric field for the two cases produce equal changes in the activation energies, although the actual magnitudes are quite different.

On the basis of these experimental points two assumptions are made. First, quite obviously some change in the microstructure occurs and secondly, that the cause of the effect is the same in both glasses.

The most obvious explanation for this new mode of conductivity, is that it is associated with the production of a set of donor or acceptor sites, possibly such that N(E) takes the form shown in figure 3.3(b). These sites could then act simply as donor and acceptor sites as in crystalline semiconductors or alternatively, if there is adequate compensation then impurity band conduction can occur.

It seems unlikely that these sites are acting simply as donors or acceptors, because the field dependence of E_g, persists down to very low electric fields (1 volt cm^{-1}). The field dependence that would be associated with this type of extrinsic conduction, is field emission from

the sites, and this requires much larger fields than are the case here.

Considerable data has been published on impurity band conduction in crystalline semiconductors (see for example [23] [24]) but to the author's knowledge field dependence of the activation energy has not been observed. Also in these crystalline cases E_F lies in the impurity band and hence E_g is very small, usually of the order of 10^{-3} ev.

The activation energy in this phenomenon is comparatively large, so that E_F is expected to be some way from the band. For conduction to take place carriers must first be thermally excited into the band. The conduction could therefore be described by 6.02.10, i.e.

$$\sigma_{low} = \sigma_{OL} \exp (E_B - E_F)/kT \quad \exp - (W_D/kT) \qquad \text{6.07.1}$$

E_B = Energy at which the band occurs.

The two activation energies have been discussed in 6.02. The suggestion is that W_D (the average separation between adjacent localized levels) is effectively field dependent. The question is then posed, how is it dependent and what magnitude of field can effectively reduce it ?

Unfortunately there appears at the present time to be no published work which will provide an answer, and it is not possible from the small amount of experimental data to establish an empirical relationship - Mott [6] has in fact suggested certain field dependent effects for hopping conduction in an Anderson band, but it is not thought that these apply here. One dependence simply allows for the reduction of W_D by the electric field, i.e. by a term $e.F.R_o$, where R_o is the distance between adjacent sites, but again this requires high fields. A second dependence, already discussed in 6.02 is associated with the aligning of energy levels of localized states some distance greater than R_o apart, but this effect will only dominate at low temperatures. It is not clear what magnitude of field is required.

The increase in room temperature conductivity is thought to be associated with the observed increase of density, which in 6.02.2 and 6.02.3 has been seen to be associated with decreases in the high temperature activation energy.

The possibility that the field dependence of E_g was due to some contact phenomenon has been overlooked. It was not possible to repeat the measurements using different electrodes and eliminate the possibility, and it should therefore be considered in any full investigation of the effect.

6.08.0 SUMMARY

Considerable evidence has been put forward to show that the model of figure 6.1 is valid for all the amorphous semiconductors studied here. The evidence has come principally from the form of the $\log\sigma$ vs $1/T$ relationship which in all cases is similar. The form of this curve has been predicted by calculations of n(T) based on the density of states curve shown in figure 6.1, and assuming conduction band tail states to act as acceptors and valence band tails as donors. The agreement between experiment and theory is good. The calculations also make it clear why making measurements only above room temperature will in most cases lead to the erroneous conclusion that only one value for E_g exists.

In that the overall features of the model should be applicable to all cases then the values of σ_o (see equation 6.02.2) should also be the same in each case. This fact has also been borne out by experiment and further than this, its value of 10^3 ohm^{-1} cm^{-1} is in agreement with that predicted by Mott (see chapter 3).

A low temperature, field dependent conductivity was found in annealed specimens of certain glasses. The conduction mechanism producing this is not understood but it has been suggested that it is due to 'hopping' conduction in an impurity type band.

REFERENCES CHAPTER 6

(1) Eaton D.L., Journal of the American Ceramic Soc., Vol. 47, No.11.

(2) Owen A.E., The Glass Industry, November 1967.

(3) Edmond J.T., J. of Non Crystalline Sol. 1, p. 39, 1969.

(4) Rawson H., Inorganic Glass Forming Systems, p. 141, Academic Press, 1967.

(5) See Ref (10) of Chapter 3.

(6) Mott N.F., Phil. Mag. 22, No. 175, p. 7, 1970.

(7) Hutner R.A., Rittner E.S., Du-Pre F.K., Philips Res. Rep. 5, p. 188, 1950.

(9) Frenkel J., Phys. Rev. 36, p. 1604, 1930.

(10) Miller A., and Abrahams E., Phys. Rev. 120, p. 745, 1960.

(11) Mott N.F., Phil. Mag. J. Non. Crystalline Sol. 1, p. 1, 1968.

(12) Davis E.A., and Mott N.F., Phil. Mag. 1970, to be published.

(13) Hill, R.M., Proc. Roy. Soc., A. 309, p. 397, 1969.

(14) Henisch H.K., Rectifying Semiconductor Contacts, Oxford, 1957.

(15) Taylor W.E., Odell N.H., Fan H.Y., Phys. Rev. 88, p.807, 1952.

(16) Clark A.H., Phys. Rev. 154, p. 750, 1967.

(17) Walley P.A., Jonscher A.K., Thin Solid Films 1, p. 34, 1968.

(18) Cohen M.H., Journal of Non Crystalline Solids, 4, p. 391, 1970.

(19) Hilton A.R., Texas Instruments Report No. 08-65-121, 1965.

(20) Pearson D., et al, Adv. in Glass Tech. 6th Int. Cong. on Glass, 1962.

(21) Ovshinsky S.R., Phys. Rev. Letters 21, p. 1450, 1968.

(22) Nesvadba P.N., MSc Thesis, University of Warwick, 1970.

(23) Davis E.A., Compton W., Phys. Rev. 140A, p. 2183, 1965.

(24) Fritzche H., Phys. Rev. 125, p. 1552, 1962.

(25) Phillips, S.V., Booth R.E., McMillan P.W., J. of Non-Crystalline Solids 4, p. 510, 1970.

CHAPTER 7

INFRA-RED ABSORPTION

7.01.0 INTRODUCTION

This chapter presents a report of the measurements of absorption coefficient as a function of wavelength, and in some cases as a function of temperature, for the three systems under discussion.

The principal mechanism of absorption is expected to be intrinsic absorption, i.e. the excitation of valence electrons to the conduction band across the forbidden gap. The $\underline{k}$ conservation rule is assumed to be relaxed, so that the absorption coefficient becomes simply proportional to the density of states product for the valence and conduction bands. Some justification for the assumption is given and calculations of the density of states product based on model of figure 6.1 are made. These enable a relationship to be established between the edge shape and the length of the tails of states. Assuming the model to be applicable to the materials under discussion the relationship enables estimates to be made for the actual lengths of the tails of states.

7.02.0 FUNDAMENTAL THEORY

The optical properties of a material can be described by the complex refractive index n* written as

$$n^* = n - ik \qquad \text{where } n=\text{refractive index},\ k=\text{extinction coefficient} \qquad 7.02.1$$

The significance of n* is that a plane electromagnetic wave of frequency ν travelling through the medium in the x direction has the form.

$$A_x = A_o \exp.\left(2\pi i\nu \left[t - \frac{n^* x}{c}\right]\right) \qquad 7.02.2$$

A, can be either the electric or magnetic field vector.

Also, from Maxwells equations the wave equation can be written as

$$\nabla^2 \underline{A} - \sigma\mu\mu_o \frac{\partial \underline{A}}{\partial t} - \mu\mu_o\epsilon\epsilon_o \frac{\partial^2 \underline{A}}{\partial t^2} = 0 \qquad \text{7.02.3}$$

Equation 7.02.2 is a solution of 7.02.3 provided

$$\frac{1}{v^2} = \mu\mu_o\epsilon\epsilon_o - i\sigma\mu_o\mu/2\pi\nu = \left(\frac{n^*}{c}\right)^2$$

Hence $$n^{*2} = \mu\epsilon - \frac{i\sigma\mu}{2\pi\nu\epsilon_o} \qquad \text{7.02.4}$$

using $c^2 = \frac{1}{\epsilon_o\mu_o}$

and from 7.02.1 and 7.02.4, assuming $\mu = 1$

$$n^2 - k^2 = \epsilon$$

$$2nk = \frac{\sigma}{\omega\epsilon_o} \qquad \text{7.02.5}$$

where $\omega = 2\pi\nu$

It is clearly seen from substituting equation 7.02.1 into 7.02.2 that A_x is attenuated by a term exp. $\frac{2\pi\nu k}{c} x$. More relevant than the amplitude is the energy in the wave given by the square of equation 7.02.2. The energy is obviously attenuated by

$$\text{exp.} \frac{4\pi\nu k}{c} x$$

The absorption coefficient for the medium as defined in 5.03.4 is seen to be given by

$$K = \frac{4\pi\nu k}{c} \qquad \text{7.02.6}$$

or, written in terms of the conductivity σ , from equation 7.02.5

$$K = \frac{\sigma}{c.n.\epsilon_o} \qquad \text{7.02.7}$$

Various mechanisms contributing to the absorption were introduced in 2.11.0, but only the absorption corresponding to band to band transitions was considered in any detail, since this is assumed to be the principal mechanism in this work. Two different expressions were given for $K(h\nu)$

assuming direct or indirect transitions, so that it is obvious for crystalline semiconductors that the conservation of the wave vector $\underline{k}$ or more generally, momentum, during the absorption process, plays a very important role in determining the shape of the absorption edge.

Briefly, the absorption coefficient due to band to band transitions is proportional to the transition probability, which will depend on the photon energy, $\underline{k}_{initial}$, and $\underline{k}_{final}$, and the product of the densities of initial and final states integrated over all possible transitions. The evaluation of K ($h\nu$) would be simplified if the selection rule could be relaxed, and it is possible in the case of amorphous semiconductors to argue for the relaxation of the rule. Since this is an important point some of the argument is briefly dealt with.

7.03.0 RELAXATION OF THE SELECTION RULE

The $\underline{k}$ selection rule is easily seen to be relaxed if the uncertainty in $\underline{k}$ becomes large.

In amorphous semiconductors this is the case. The wave number $\underline{k}$, interpreted as the phase change of the envelope of the wave function per unit length of the crystal, becomes, due to frequent scattering, a function of position, and is therefore no longer a good quantum number. Transitions from $\underline{k}_{initial}$ to any $\underline{k}_{final}$ can then occur, to a reasonable approximation, with equal probability. The photon energy then truly represents the energy difference between initial and final states, whilst the difference in momentum will be taken up by the lattice.

This argument can only apply to the extended states above E_c and below E_v, and possibly to the weakly localized states. Transitions from localized to extended (non-localized) states are assumed to occur with the same probability as those from extended to extended states. The probability

of transitions from localized to localized states will depend on their relative positions in real space, and will contribute far less to the absorption coefficient.

7.04.0 DENSITY OF STATES PRODUCT

On the basis of the above argument it is assumed that momentum is not conserved in the optical transitions, and that the transition probability is independent of the photon energy. The absorption coefficient is thus proportional to the product of the densities of initial and final states, integrated over all possible transitions [4], i.e.

$$K \propto \int_{\text{all transitions}} N_v(E) \cdot N_c(E + h\nu)\ dE \qquad 7.04.1$$

N_v refers to the valence band

N_c refers to the conduction band.

Davis and Mott [13] have shown that for the case of amorphous semiconductors this can be written

$$K = \frac{1}{2} \frac{\pi e^2 h^3 a}{m^2 . n . c} \cdot \int_{\text{all transitions}} \frac{N_v(E)\ N_c(E + h\nu)\ dE}{h\nu} \qquad 7.04.2$$

where a^3 is the atomic volume

n is the refractive index.

From the form of the equation it is obviously implied that E_F is some way from the band edges.

Using equation 7.04.2, $K(h\nu)$ was calculated for the model of Fig. 6.1. The calculations were made to investigate further the validity of the model, by comparing the calculations of $K(h\nu)$ with experimentally determined $K(h\nu)$ curves.

The calculations were made on an Elliot 4130 computer using a programme written by the author.

Both the conduction and valence bands for the purpose of the calculation are considered to be made up of two matching sections; an exponential tail of localized states, and parabolic bands of extended states above E_c and below E_v. Hence for example the valence band edge is described by

$$\text{for } E < E_v + .01 \quad N(E) = N_o(E_v + .01 - E)^{\frac{1}{2}} \qquad 7.04.3$$

$$\text{for } E > E_v \quad N(E) = N_o' \exp - \alpha_v(E - E_v)$$

The relative values of the constants N_o, N_o' are chosen so that the two sections join smoothly. The constants $\alpha_{v,c}$ describe the rate of fall off, of the exponential tail.

In the calculations, the probability for transitions from localized to localized states was considered to be equal to that for other transitions (i.e. extended-extended, extended-localized, localized-extended). This will not be the case in a real material, but the error introduced will be negligible, since the number of such transitions occuring (as deduced from an analysis of the results of the calculations) was far less than the number of transitions which involve an extended state.

The limits of the integration were from E_v' down to $E_v - .2$, and the values of photon energy $h\nu$ employed, varied from approximately .5 less than $E_c - E_v$, to a value sufficiently greater than $E_c - E_v$, for the absorption coefficient to have ceased rising sharply, and to have begun levelling off.

The results of the calculations given as K cm^{-1} against photon energy in electron volts, are presented in Fig. 7.1(a) and Fig. 7.1(b). The values of the constants used are, $N_o = 10^{20}/cc/ev^{-1}$, $n \simeq 2$, $a = 3 \times 10^{-8}$, and $E_v - E_c = 1.5$ ev.

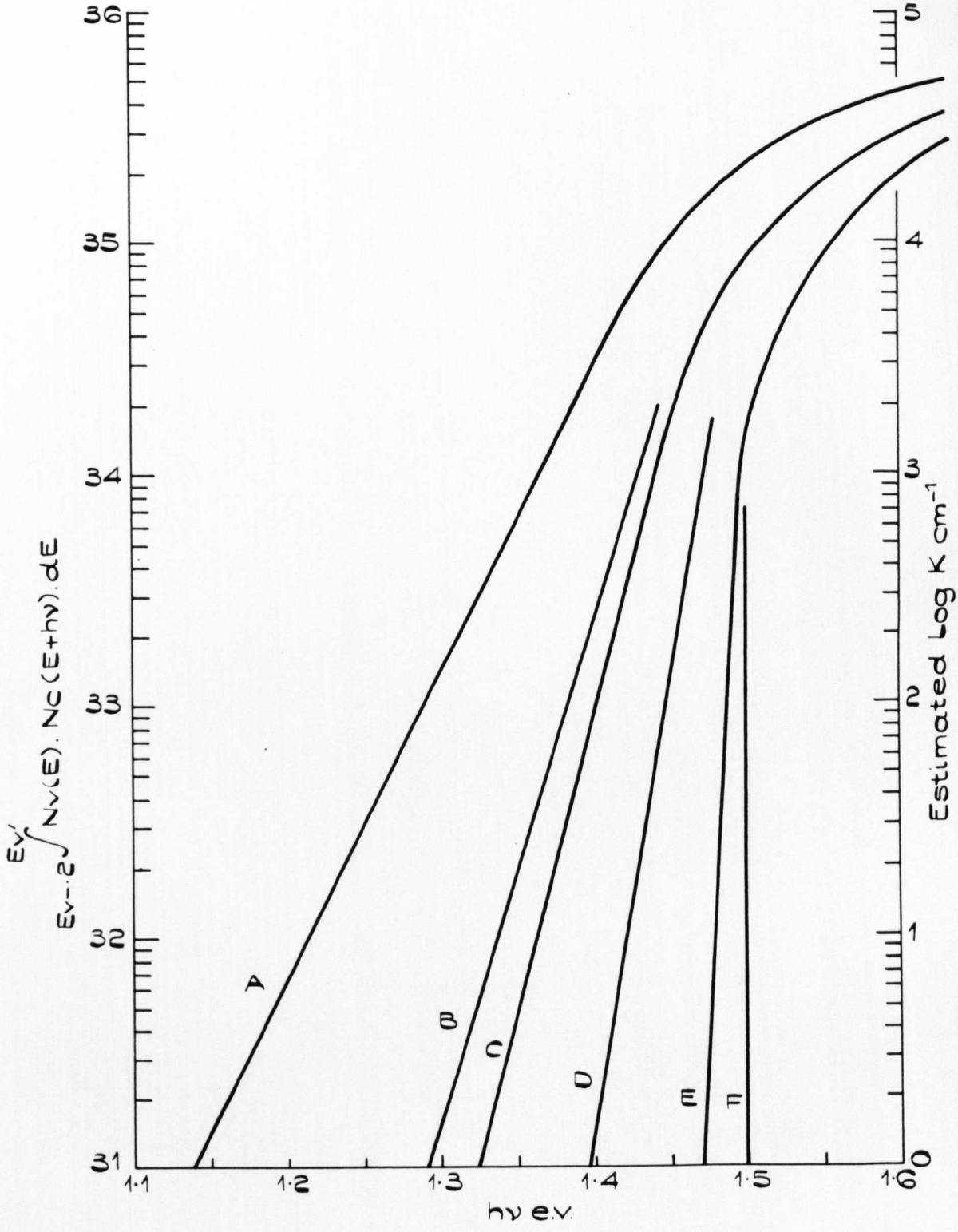

FIGURE 7.1.a.

DENSITY OF STATES PRODUCTS FOR MODEL OF FIGURE 6.1.

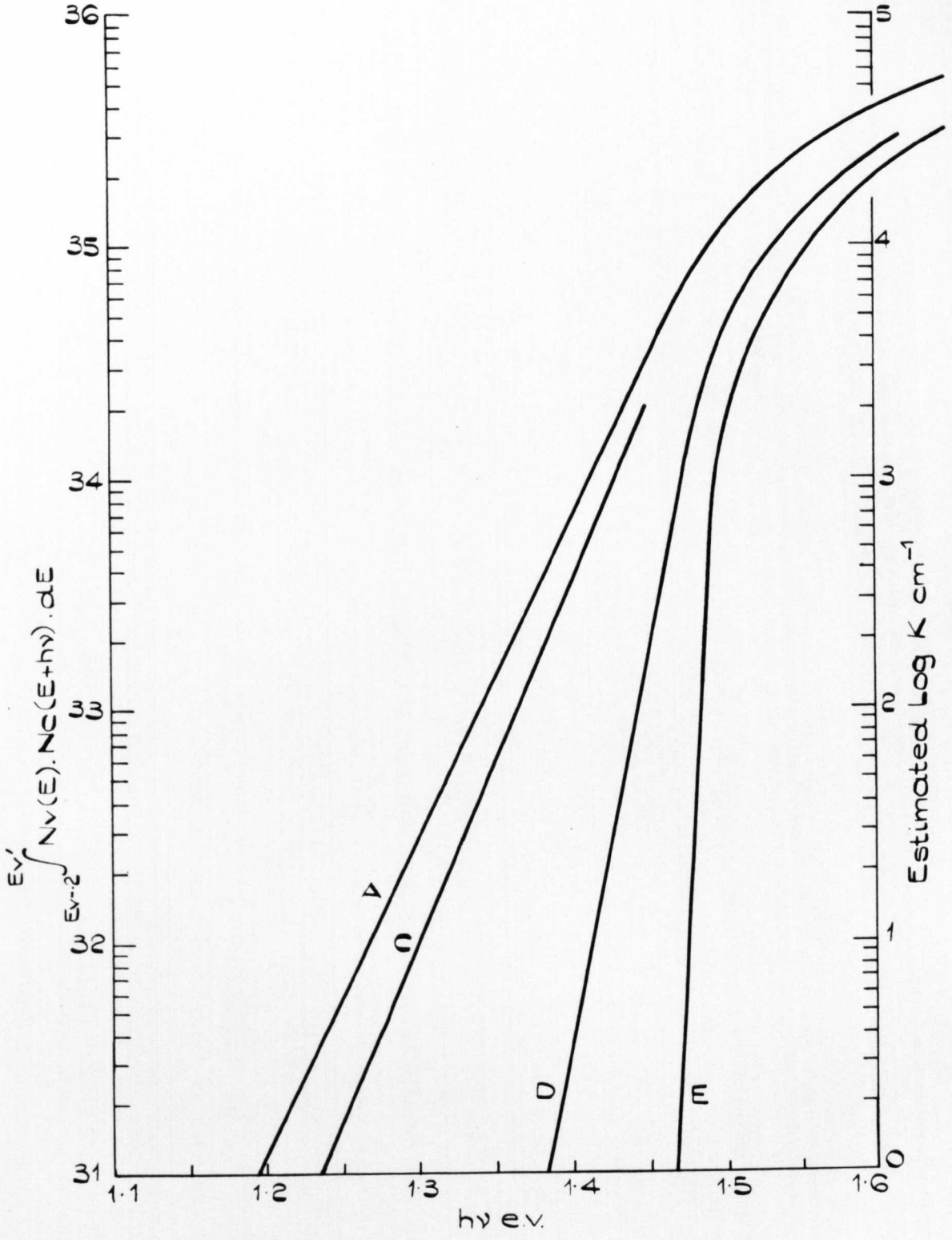

FIGURE 7.1.b.

DENSITY OF STATES PRODUCTS FOR MODEL OF FIGURE 6.1.

CURVE	α_v ev^{-1}	α_c ev^{-1}	Ev'	Ec'	d log K/dhν
A	46	31	1	0	13 ev^{-1}
B	77	51	·6	·6	22·5 ev^{-1}
C	90	60	·5	·7	26·4 ev^{-1}
D	230	90	·2	1·0	38·5 ev^{-1}
E	600	295	·1	1·3e	128 ev^{-1}
F	Parabolic Bands Only				

For each case Ev = 0
Ec = 1·5

TABLE 7.1.a.

CURVE	α_v ev^{-1}	α_c ev^{-1}	Ev'	Ec'	d log K/dhν
A	31	600	1·5	1·4	13
C	39	600	1·2	1·4ev	17
D	77	600	·6	1·4	33·5
E	295	600	·1	1·4	128·5

For each case Ev = 0
Ec = 1·5

TABLE 7.1.b.

The curves A-E in each figure are those obtained for different values of the constants α_v and α_c. The appropriate values for each curve are listed in tables 7.1(a) and 7.1(b). The values of $\alpha_{v,c}$ are chosen such that N(E) for the tails of states becomes unity somewhere between E_v and E_c. E_c' and E_v' are the values of E at which this occurs, and these values are also given in the table, as are the gradients of the resulting absorption edges.

Curve F in fig. 7.1(a) is the curve expected for a crystalline semiconductor with parabolic bands [2]. It will be noted from table 7.1(b) that in the case of fig. 7.1(b) only α_v is varying.

It will also be noticed that for the case of curves A the conduction and valence band tails overlap, so that the model becomes that suggested by Cohen, (see chapter 3) and shown in figure 3.3c. This model was not dealt with in the calculations in chapter 6, because of the possible consequences of band overlap. The implications of curves A will be discussed later in this chapter.

7.04.1 DISCUSSION OF COMPUTED ABSORPTION EDGES

Since exponential tails of states were used in the calculations, it is not surprising that all of the calculated 'edges' in figures 7.1a and 7.1b are also exponential at least up until some high value of K. At higher values, the edges level off and approach, in a manner governed by the parabolic portions of the bands, a value $\simeq 10^5$ cm^{-1}. Of course this final value is to some extent arbitrary, since it depends on a number of parameters the values of which could only be estimated. It is however the slope of the exponential edge which is the important factor rather than the final value of K.

It is of particular interest to determine whether there is some

simple relationship between the gradient of the edge and α_V and α_C. If a relationship exists, and the model and assumptions are valid for amorphous semiconductors, then from the value of the gradient of absorption edge of any material, and this relationship, an estimate can be made of the length or effective length of the tails. It will now be shown that such a relationship does exist.

Referring to tables 7.1 it will be seen that for each pair of curves in figures 7.1(a) and 7.1(b) with the same identifying letter, the value of $(E_V' - E_V) + (E_C - E_C')$ is equal. The last column of the tables shows however that the gradients are not equal, and indeed in plotting the above sum of the lengths of the tails, against the gradients, no simple relationship between them is found. This was an expected result and merely emphasises that the contributions to K from states low down in the tail are negligible. Hence, if one tail is longer (i.e. its value of α smaller) than the other tail, it will dominate in the density of states product, and it is in fact in the length of the longest tail that the relationship exists.

In figure 7.2 the gradients of all the curves of figures 7.1, (plus data from two other calculations not shown in fig 7.1), are plotted against α_V or α_C, whichever is the smaller. All the points are seen to lie on a straight line passing through the origin. The slope of the line is found to be $\log_{10} e$. Hence the very simple relationship

$$\frac{d\,(\log K)}{d(h\nu)} = \alpha \qquad \text{7.04.4}$$

$h\nu$ is in electron volts.

α is in ev^{-1}, and is α_V or α_C whichever is smaller.

If the model and assumptions are valid 7.04.4 will give α for the longest tail knowing $\frac{d(\log K)}{d(h\nu)}$ for any specimen. The same expression has been obtained by Panklove [2] and Lanyon [3] who considered approximations of the model used here.

The expression 7.04.4 holds regardless of the value of $E_c - E_v$, so long as α is not too small. It is also independent of temperature:- The calculations of $E_F(T)$ described in chapter six showed that E_F moves into the longest tail of states, as the temperature is increased. Using those results the calculations of 7.04.2 were repeated using appropriate values of E_F and T and the Fermi Dirac distribution function . At 300°K the edge was only slightly altered, and then only at values of $K < 10^{-4}$ cm^{-1}, where the gradient was increased.

The relationship 7.04.4 will be used later in interpreting results.

COMPARISON WITH THE URBACH RULE

In as much as each line is exponential, it could be said that the model abeys Urbach's rule (see 2.11.0 and [13] of chapter 2). But as the temperature changes, E_o . in equation 2.11.5, which is $E_c - E_v$ of the model, would be expected to change due to lattice dilatation. If the disordering effect due to thermal motion is significant, in a network already structurally disordered, then $\alpha(T)$ might be such that the slope followed the Urbach rule, i.e. be proportional to $^1/_{kT}$, and the rule to this extent would be followed. As will be shown later no indication of a significant change in slope was found for temperatures below 300°K, although the edge does shift.

7.05.0 RESULTS

The results of $K(h\nu)$ as obtained are given in figures 7.3 a.b.c.d. (Te-As system), figures 7.4 a.b. (Se-As) and figures 7.5 a.b. (Se-Te).

The approximate error in any given value of K is shown in each figure and is made up from errors in specimen thickness, in approximations used to determine K from transmittance data, and in the slight non-linearity of

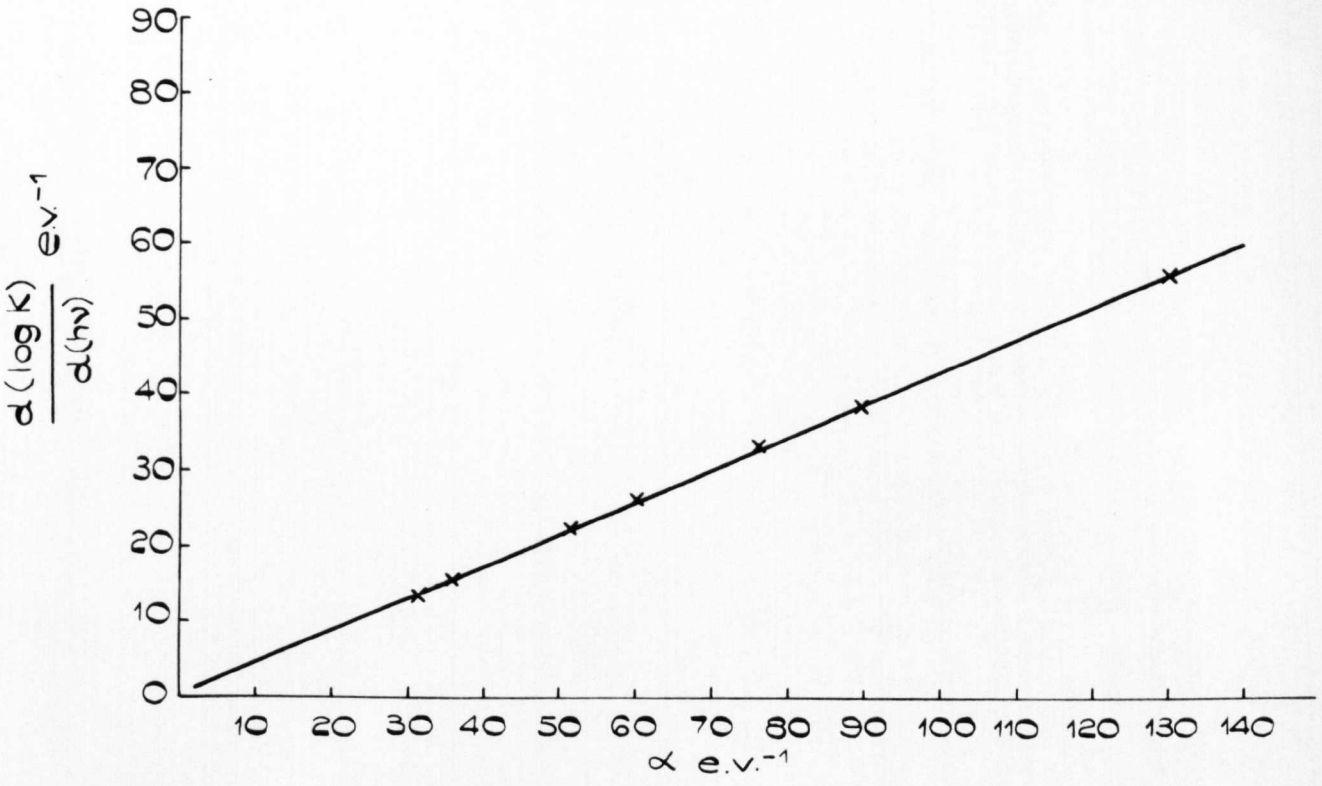

FIGURE 7.2.

SLOPE VS α VALUES FOR COMPUTED ABSORPTION EDGES.

As–Te	$\frac{d(\log_{10} K)}{d(h\nu)}$	α ev⁻¹	Eg* ev	SHIFT 300°K-42°K
45-55	9·18±·01	21·2	·77±·007	·1025
50-50	9·51±·01	22·2	·79±·007	·138
55-45	8·9±·01	20·5	·807±·007	·090
60-40	8·2±·01	18·9	·83±·007	·105

TABLE 7·2(a).

Se-Te	$\frac{d(\log_{10} K)}{d(h\nu)}$	α ev⁻¹	Eg* ev	SHIFT 300°K-4·2°K
100-0	7·07±·01	16·3	1·77±·005	·100
90-10	8·37±·01	19·4	1·56±·003	—
80-20	10·43±·01	24	1·4±·003	—
75-25	7·38±·01	17	1·47±·003	—

$Eg^* = h\nu$ for $K(h\nu) = 10^2\ cm^{-1}$

TABLE 7·2(b).

SUMMARY OF RESULTS FOR As-Te AND Se-Te SYSTEMS

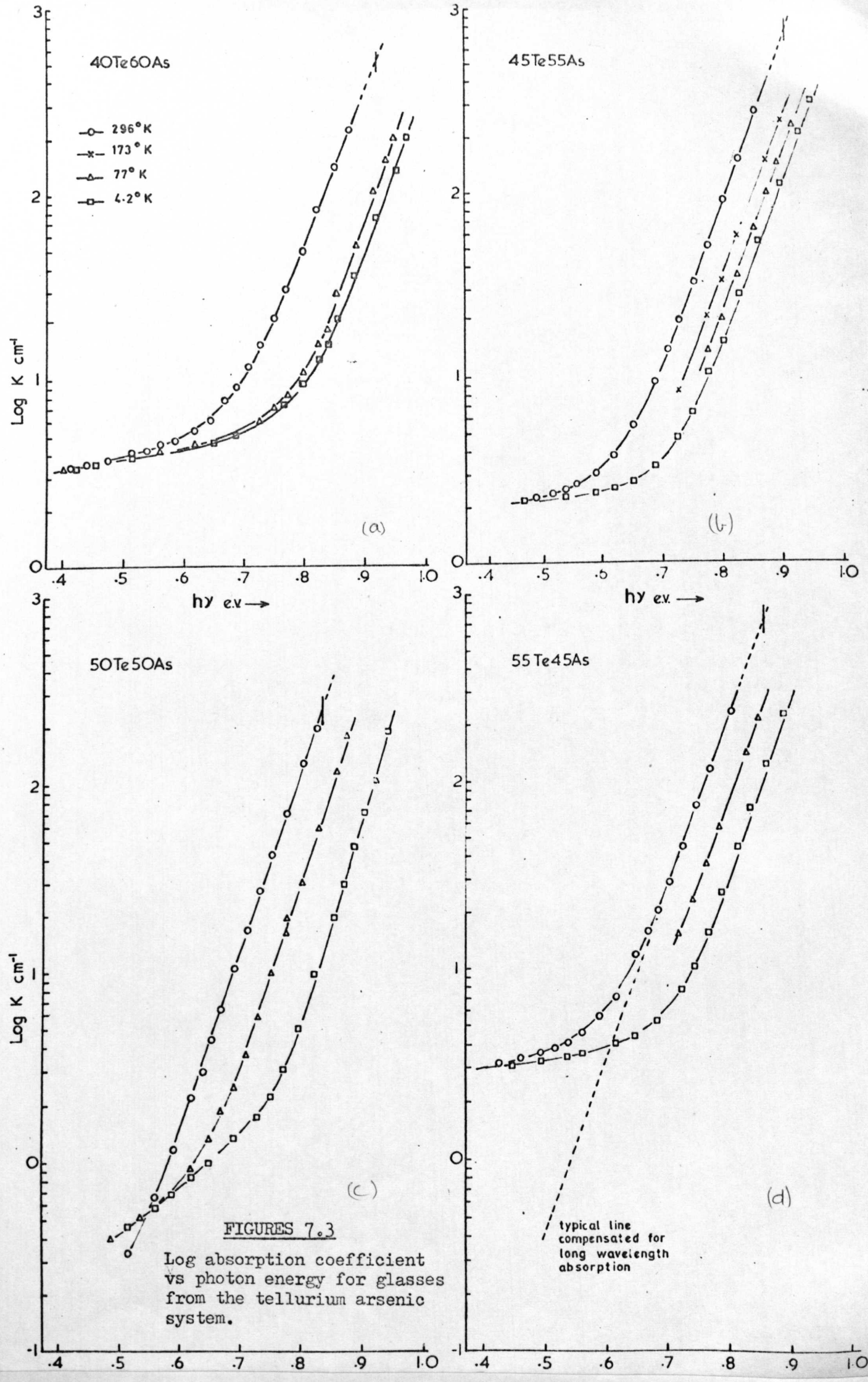

FIGURES 7.3

Log absorption coefficient vs photon energy for glasses from the tellurium arsenic system.

FIGURES 7.4

Log absorption coefficient vs photon energy for glasses from the selenium arsenic system.

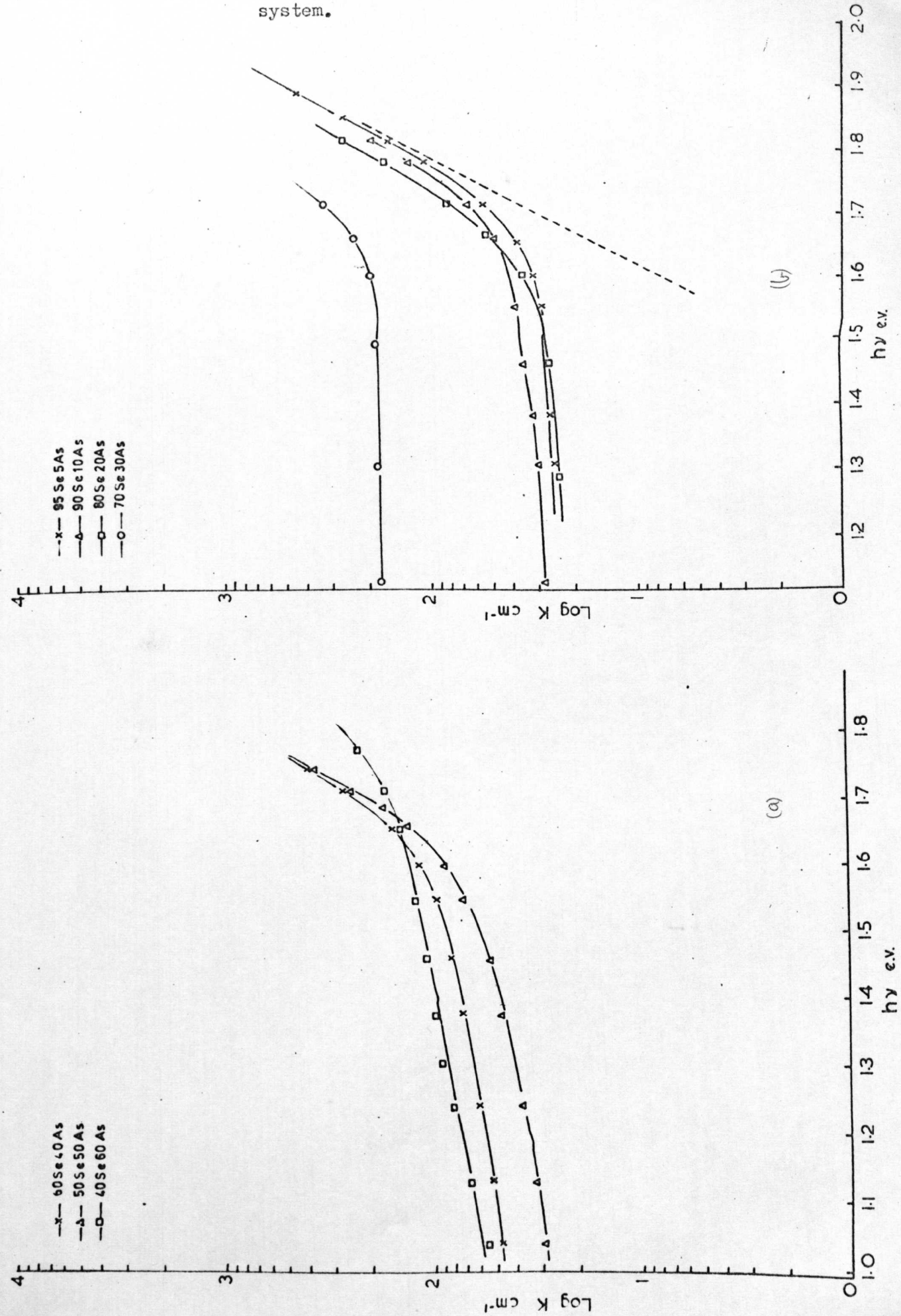

FIGURES 7.5

Log absorption coefficient vs photon energy for glasses from the selenium tellurium system

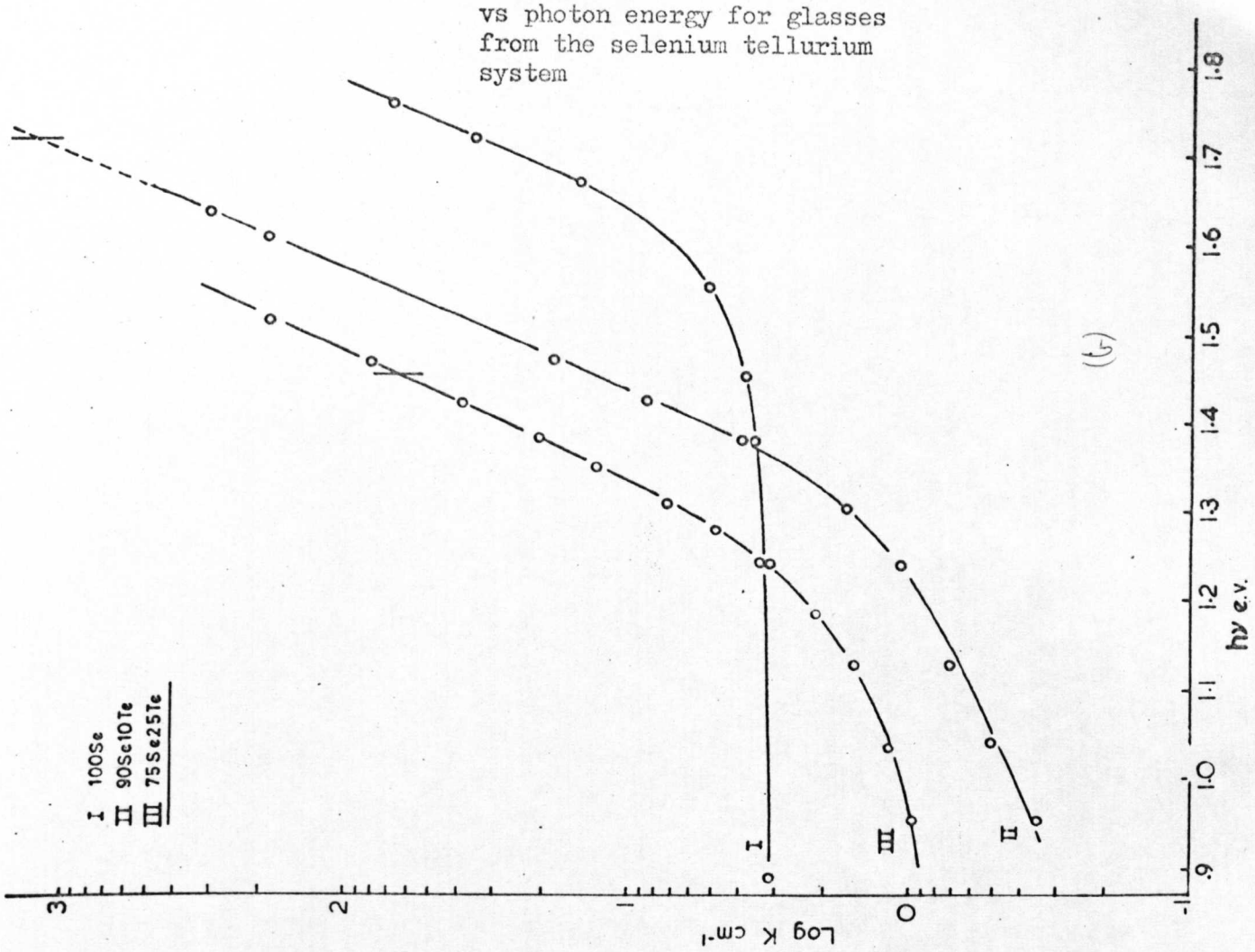

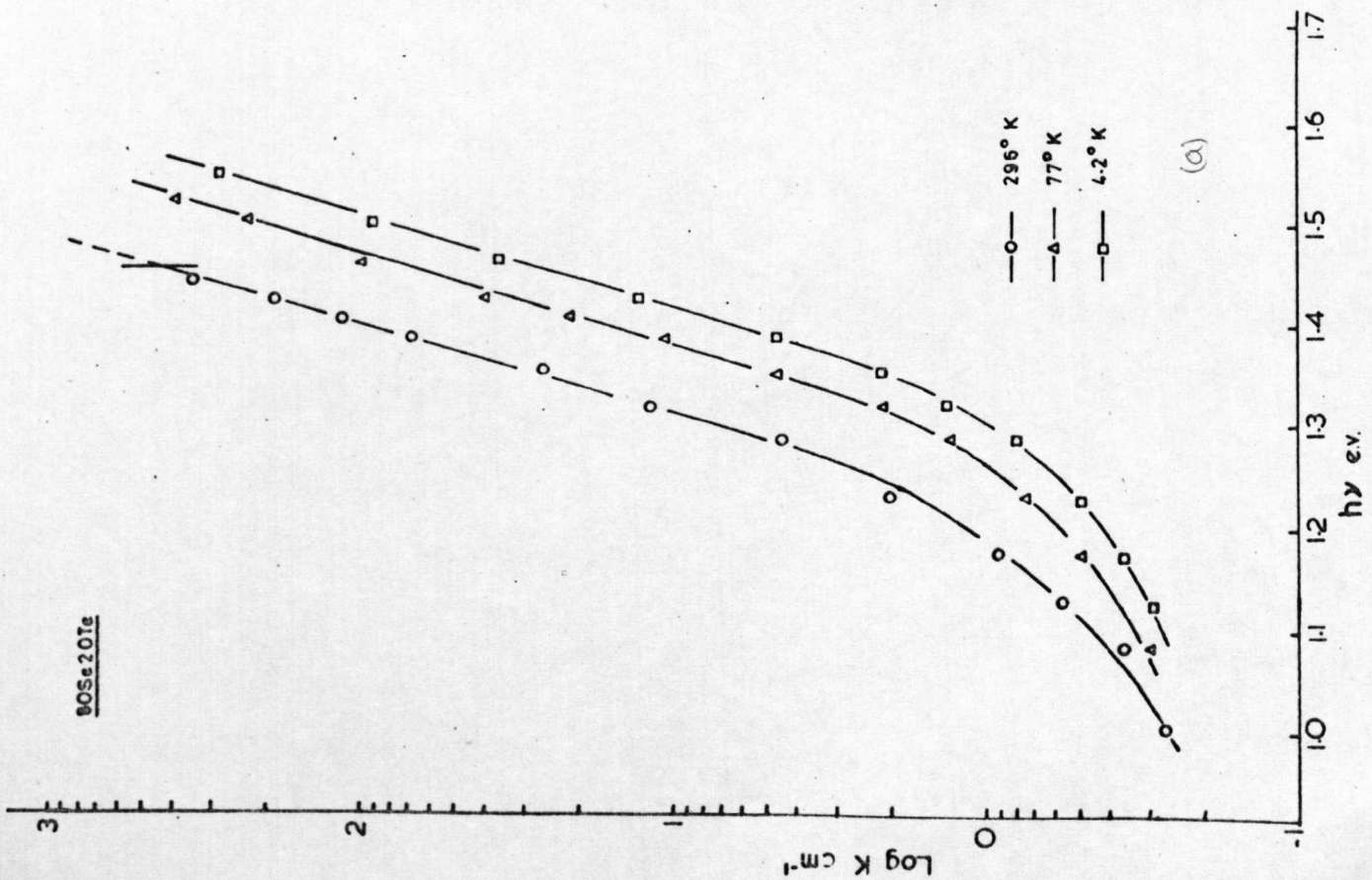

transmittance scale, as given by the spectrophotometer. For any single line, the same uncertainty in specimen thickness, and the same approximations prevail, and therefore the relative error between points on any line is much reduced, hence the gradient of any line will be accurately determined from these plots.

The short vertical intersecting line on each plot corresponds to the value of the activation energy E_g as deduced from d.c. conductivity measurements.

7.06.0 DISCUSSION

The first part of the discussion deals with the results interpreted on the basis of the calculations of 7.04. This is followed by a discussion of the general form of the curves, and finally the results for separate systems are surveyed.

7.06.1 COMPARISON WITH THE THEORETICAL MODEL

For the As-Te and Se-Te systems large sections of the measured absorption edges were exponential, so that equation 7.04.4 could be used to determine values for α. These values together with those of the gradients $d(\log_{10}K)/d(h\nu)$ are given in table 7.2(a) and 7.2(b). The error limits in tables 7.2 for α, allow for the values of α found when taking into account the constant long wavelength absorption (see for example the dashed line in fig. 7.3d).

For all materials α is in the region of 20 ev^{-1}, suggesting that at least one of the tails of states in each case is of considerable length. The range in α indicate that N(E), at 1 ev from the band edges varies from $(N_o/10^{11} - N_o/10^{7})$ cc^{-1} ev^{-1}, and in the middle of the narrowest gap (As-Te) as deduced from conductivity measurement, N(E) is only a factor of 10^4

smaller than at the band edge. The results therefore predict considerable overlap of the bands, suggesting that the model of figure 3.3c may be more applicable.

Before further discussing this point, the value of K at $h\nu = E_g$ should be noted. The values for all As-Te, and Se-Te glasses, and for the majority of the As-Se glasses, are lower (the average value for the first two systems mentioned is 7×10^2 cm^{-1}) than the computer calculations suggest they should be (see figures 7.1). This is not an uncommon result, either for amorphous semiconductors, (e.g. Fagen and Fritszche [5] show $K_{h\nu} = E_g$ to be 10^2 cm^{-1} and 10^1 cm^{-1} for the two glasses) or for crystalline semiconductors, (e.g. in the case of silicon E_g=1.21 ev[6] and $K_{h\nu} = E_g \triangleq 10^2 cm^{-1}$ [7]).

If the assumption that the conductivity is intrinsic is correct, then one explanation of the above discrepancy is easily produced. It has already been noted that α in all cases is small, so that N(E) is not falling off rapidly, therefore E_c and E_v could easily be displaced into the gap, by say x ev. Then K($h\nu$) would be expected to level off at $h\nu = E_g + 2x$. The not unreasonable values of x equal to say .1 ev would be sufficient for the two sets of data to be made to agree.

Calculations of n(T) with small, i.e. < 30 ev^{-1}, values for $\alpha_.$, were not discussed in chapter 6, because band overlap and consequent production of charged trapping centres (see chapter 3) could not be accounted for in the calculations. However, a calculation was made with $\alpha_. = 20$ ev^{-1} neglecting charged traps, to determine if $\alpha_.$ values deduced from absorption and conductivity data agreed. (See also 6.o5.1)

The temperature and conductivity at which n(T) began to be governed by the intrinsic activation energy $E_c - E_v$, was obviously higher than was the case for the results of figures 6.7(a) and 6.9(a). Hence the two experiments suggest two different values for the extent of the tails of

states and one must ask the question will the conjectured charged traps account for the difference ?

One effect of the overlap is to automatically fill a proportion of the acceptor (conduction band tail) states, and this will lower the number to be filled by thermal excitation of holes from the valence bands, i.e. in the computer calculations of $n(T)$, α_c would have effectively been increased. This will then lower the temperature at which $n(T)$ is governed by the truly intrinsic activation energy, and hence possibly partly account for the discrepancy. The effect of traps (which may be of density 10^{17} cc^{-1} ev^{-1}) on the mobility and the temperature dependence of this mobility would also have to be estimated.

A second disagreement exists concerning the values of α . In the discussion of 6.06.2 it was deduced that although E_g decreases with tellurium content in the Se-Te system, the length of the tails remains approximately constant. As will be seen in 7.06.5, results of optical absorption measurements for this system indicate that α increases (tail length decreases) with tellurium content. If the argument of 6.06.2 is correct then this disagreement would suggest that some refinement of the model or of the assumed absorption and conduction mechanisms is required.

7.06.2 LONG WAVELENGTH ABSORPTION

In all cases, figure 7.3 - 7.5, but in particular for the As-Se glasses, fig. 7.4, there is a long wavelength absorption K_{LW} which generally tends to some constant value of K. Values for K_{LW} vary between 10^{-1} and 10^{2}, and persist at least out to values of $h\nu$ = .2 ev.

From the magnitude and wavelength dependence, it is not possible to say that the absorption is due to the tails in the densities of states, since transitions from localized to localized states will have a very small

probability. Also there is generally no dependence of K_{LW} on deduced values of α.

The effect is not uncommon and has been observed in a variety of materials including ionic crystals [8] [9] and crystalline semiconductors [10] [11]. In all cases the effect has been associated with impurities, and shown to depend on the concentration, and nature of the impurity. No analysis was made of the materials under investigation, but from the claimed purities of the starting elements, and densities of the final products, the impurity content is estimated to be 1.5 - 2.0 x 10^{17} atoms/cc, and is possibly higher due to contamination during preparation. From the above mentioned works, it is seen that densities of 10^{17} atoms/cc for impurity atoms would give values of K_{LW} such as have been observed, and therefore it must be assumed that impurities do play a part.

Free carrier absorption is not expected to be significant here. The energy at which the absorption is occurring is rather high for free carrier absorption, and also the number of free carriers will be small ($E_c - E_v$ is large).

7.06.3 TEMPERATURE DEPENDENCE OF THE ABSORPTION EDGE

In general, the temperature dependence of the edge is made up from two contributions.

First, the energy levels of electrons in a lattice are functions of interatomic distance. For small dilatations Δ of the lattice an energy level can be assumed to change linearly, hence

$$E = E_o + E_1\Delta \qquad 7.06.1$$

where the coefficient E_1 will be different for different energy levels as in fig. 2.1. If E_{1c} and E_{1v} are the coefficients for the bottom and top of the valence band respectively, then

$$\Delta E_g = (E_{lc} - E_{lv}) \qquad 7.06.2$$

The coefficients can be shown [12] to be inversely proportional to the square roots of the respective band edge mobilities.

The second contribution arises from electron lattice interaction, which will depend on the intensity of vibration and hence temperature. The effect of the interaction [13], is to broaden the energy bands (cf. conclusions of chapter 3, where it was seen that structural disorder also broadens the bands) and the change in E_g is governed by an expression of the form

$$\frac{dE_g}{dT} = -A\,(m_e\,E_{cl}^{\,2} + m_h\,E_{vl}^{\,2}) \qquad 7.06.3$$

where A = constant.

Either mechanism can dominate in a crystalline semiconductor [14], and the question of the relative importance of each in an amorphous semiconductor has not yet been raised, but the answer is possibly straightforward:-

In a "lattice" already highly disordered, it could be argued that the additional vibrations due to increase in temperature would not increase the disorder significantly until some high temperature is obtained, i.e. the perturbation potential Δu will be much less than that produced by such effects as density fluctuations, and other structural defects. This would suggest that at low temperature the edge shifts only because of the lattice dilatation.

The further disordering of the "lattice" at higher temperatures would decrease α., i.e. increase the extent of the tails of states (see 3.04). Hence at higher temperatures the edge not only shifts but also the gradient decreases, whereas below a certain temperature it only shifts in accordance with equation 7.06.2. It is noted that such a behaviour has been reported in amorphous semiconductors [15] [16].

It was only in the temperature range 4.2°K - 300°K that shape, and position of the edge were measured for the materials under investigation, and only the absorption edges of glasses from two systems could be studied as functions of temperature. The results are shown in figures 7.3 a - d for Te-As glasses and 7.5 (b) for 80Se20Te.

In all cases the edge moves parallel to itself and to higher energies as the temperature decreases. The magnitude of the total shift for the entire temperature range is very similar (column three of Tables 7.2). In all cases it is approximately equal to .1 ev which is a typical result for semiconductors [1][5][2].

The temperature dependence however is not similar for all cases, and indeed there are some large differences in this behaviour, a result which is very perplexing. Especially so because of the similarity in other properties (referring now only to the As-Te glasses) namely edge shape, conductivity activation energy and density.

The two glasses, 50Te50As and 55Te45As, are those which show temperature dependences of the edges, which are quite different to those recorded for all other glasses. The only suggestion that can be made concerning this result is that it is in some way associated with the non-typical low temperature conductivity behaviour, observed principally in 50Te50As but also in 55Te45As. The effect was almost certainly associated with some characteristic density of states, and this is possibly being reflected here.

The fact that the edge moves parallel to itself with temperature is significant. As pointed out by Fritszche [5], a parallel shift of the edge is a necessary (although not sufficient) condition for claiming the transition probability to be independent of energy, as was assumed in the calculations of 7.04. Hence a little more weight is given to the calculations.

That the magnitude of the shift of the absorption edge, ΔE_g for amorphous semiconductors is close to that for crystalline semiconductors is of interest. This result again illustrates the similarities in band structure for the two cases, which further suggests that the electronic band structure is a consequence of short range, and not long range order.

7.06.4 As-Te SYSTEM

It is adequate for the purpose of comparison to define the band gap E_g as determined from absorption measurements to be the energy at which K reaches a certain value. A value of $K = 10^2$ cm^{-1} is used, and the results are shown in figure 7.6. For further comparison the values of E_g as determined from $\log \sigma$ vs $1/T$ are also shown.

With the exception of one of the results (50As50Te) it is seen that E_g as determined from the two measurements shows the same trend, i.e. it decreases as the tellurium content is increased. A possible explanation for the actual difference in the values as determined by optical and electrical measurements has already been given.

That the trend is the same in both cases further suggests that it is only the band to band transitions which are important and that other effects (see 7.07.0) are relatively unimportant. It also implies that the electronic structures of the materials are similar, which makes the result of the edge shifts for 55Te45As and 50Te50As more difficult to understand.

The long wavelength absorption follows no systematic pattern (it is notably low for 50As50Te) so that as already discussed this absorption must be attributed to impurities.

7.06.5 Se-Te SYSTEM

The results for α (see table 7.2b) show for the glasses studied in

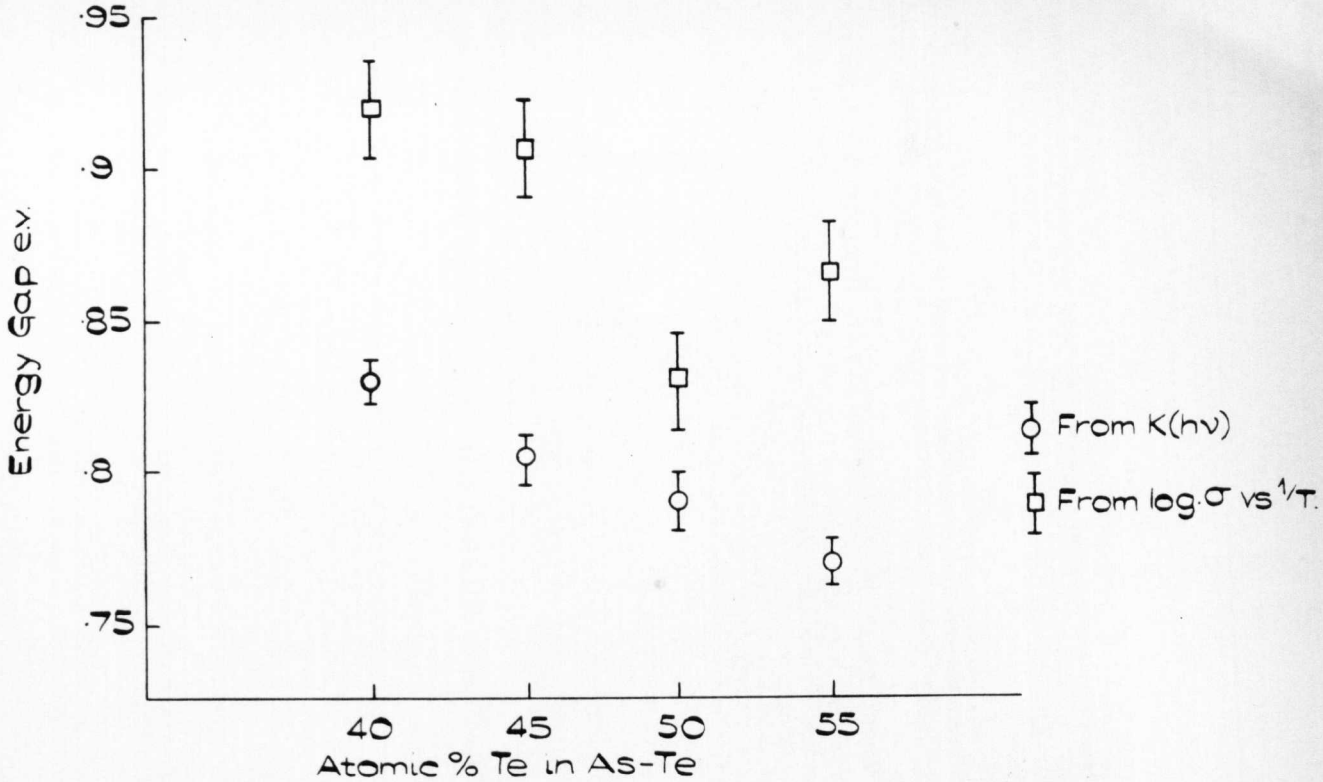

FIGURE 7.6.

ENERGY GAP VS. COMPOSITION FROM CONDUCTIVITY AND OPTICAL ABSORBTION DATA - As-Te SYSTEM.

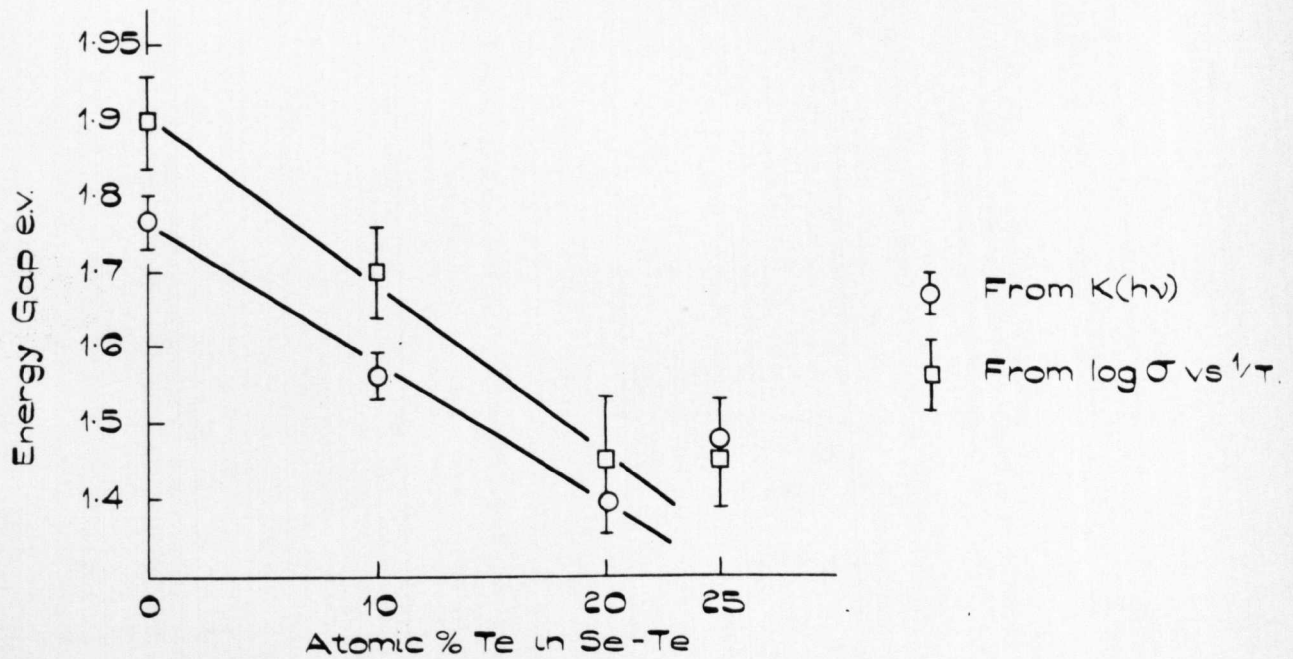

FIGURE 7.7.

ENERGY GAP VS COMPOSITION FROM CONDUCTIVITY AND OPTICAL ABSORBTION DATA - Se-Te SYSTEM.

this system, that up to 20 At% tellurium, the effect of tellurium in the structure is to decrease the extent of the densities of states tails. Also from results shown in fig. 7.7 it decreases the activation energy, a result that has been observed before in amorphous semiconductors.

Figure 7.7 repeats for this system what was shown in figure 7.6 for the As-Te system. It is of interest now to see that, when E_g changes considerably over the range so also does the difference between E_g obtained from the two experiments. This lends support to the reasoning already put forward to explain the discrepancy in 7.06.1; since one would expect, if in fact E_v and E_c do correspond to positions lower down in the tail than was assumed in n(T) calculations, that the error in the choice would be greater as α decreased.

It is possible to argue against such a conclusion (a) because only three experimental points are used in drawing the conclusion and (b) that choosing an arbitrary, fixed value of K from which to deduce E_g, may not be valid if the slope of the edge is changing significantly across the system.

The long wavelength absorption begins to show some systematic dependence, it decreasing as the tellurium content is increased, but this is thought to be of little significance.

The glass 25Te75Se for reasons discussed in chapter 6 is not thought to be typical of the system.

7.06.6 As-Se SYSTEM

With so little of the absorption edge exposed it is not possible to draw any conclusion about E_g from the data.

Again the randomness in the long wavelength absorption leads to the suggestion of impurities.

A point of interest can be raised here. All the materials were prepared identically so that the type of impurity and its density level would be expected to be similar in all cases. It is in fact seen that the long wavelength absorption differs from system to system, and to some extent from glass to glass. There is therefore the obvious suggestion that similar impurities effect the electronic structure of different glasses in different ways.

7.07.0 OTHER ABSORPTION PROCESSES

The discussion in this chapter has been exclusively in terms of band to band transitions. Effects entailing interaction of the excited electron hole pairs, namely excitons, have been entirely overlooked. Exciton absorption is well known to be of considerable importance in a number of materials particularly ionic crystals where it often covers the absorption edge due to band to band transitions. In semiconductors this situation is generally reversed, Martienssen [17].

It is possible then that excitons are important and indeed it has been shown that absorption edge of amorphous selenium can be explained as due to exciton excitation [18]. Although on the other hand the results have also successfully been interpreted in terms of the density of states product [3].

The results presented in this chapter are not considered to be due to excitons for the following regions.

(i) The absorption at $h\nu = E_g$ is not high, and this would not be the case if exciton absorption was dominating over the fundamental edge.

(ii) The edge does not change shape with temperature, and the general rule is that increase of temperature broadens the exciton band edge.

Hence although excitons cannot be dismissed they are only expected to play a minor role in the materials included in this study.

7.08.0 SUMMARY

It has been shown that the main part of the absorption edge can be explained assuming band to band transitions to be mainly responsible for the absorption, and also assuming equal probability for all transitions involving a non-localized state. Both assumptions have been to some extent justified.

By comparison with computed curves, it has been possible to estimate values for α in equation 7.04.3 for the lengths of the postulated tails of states. There was not direct agreement with values of α indicated by the conductivity results, but it was suggested that as a result of band overlap, α as deduced from absorption measurement may be effectively increased in the conductivity process.

From evidence of long wavelength absorption it has been necessary to consider the possibility of non-negligible amount of impurities affecting absorption.

REFERENCES CHAPTER 7

(1) Davis E.A., Mott N.F., Phil. Mag. 22, p. 903, 1970.

(2) Panklove J.I., Phys. Rev. 140, p. A2059, 1965.

(3) Lanyon H.P.D., Phys. Rev. 130, p. 134, 1965.

(4) Panklove J.I., Prog. in Semiconductors 9, p. 49, 1965.

(5) Fagen E.A., Fritzsche H., J. Non. Cryst. Solids.2, p. 180, 1970.

(6) Morin F.J., Maita J.P., Phys. Rev. 96, p. 28, 1954.

(7) Macfarlane G., Roberts V., Phys. Rev. 98, p. 1864, 1955.

(8) Moser F., Urbach F., Phys. Rev. 102, p. 1519, 1956.

(9) Kobayashi K., Tomiki T., J. Phys. Chem. Solids 22, p. 73, 1961.

(10) Hill D.E., Phys. Rev. 133, p. A866, 1964.

(11) Sturge M.D., Phys. Rev. 127, 768, 1962.

(12) Fan H.Y., Reports on Progress in Physics, 19, p. 108, 1956.

(13) Moss T.S., Optical Properties of Semiconductors, p. 45, Butterworths, London, 1961.

(14) Fan H.Y., Phys. Rev. 78, p. 808, 1950.

(15) Edmond J.T., Brit. J. Applied Physics 17, p. 979, 1966.

(16) Stuke J., J. Non-Crystalline Sol., 4, p. 1, 1970.

(17) Martienssen W., J. Phys. Chem. 8, p. 294, 1959.

(18) Siemsen K.J., and Fenton E.W., Phys. Rev. 161, p. 632, 1967.

CHAPTER 8

FURTHER ELECTRICAL EXPERIMENTS

8.01.0 INTRODUCTION

Two further experiments were carried out which were not applied to all glasses. These were a study of the Hall effect, in Te-As glasses, and the measurement of space charge limited currents (abbreviated to s.c.l.c.), in representative glasses from the Se-Te and Se-As systems.

The Hall effect was one of the measurements intended to be done from the outset of the project while the measurement of s.c.l.c. was made as a further confirmation of the existence of localized states, and also as a test for the quality of the electrical contacts.

The results of both these experiments are discussed in this chapter.

8.02.0 HALL EFFECT

As is well known, the Hall effect applied to semiconductors is an important measurement, which yields considerable information about the conduction processes in the material.

Also, the Te-As system of glasses is considered to be very important, since it is a very simple system compared to others producing such high conductivities, and in addition shows a form of switching, characteristic of many chalcogenide glasses. Its simplicity would be greatly beneficial in providing a quantitative explanation of the Hall effect, not only in this system, but also possibly for other amorphous solids.

However, despite continued effort to improve the detection limit of the apparatus it was never possible positively to identify a Hall voltage for any of the Te-As glasses. Hence the only result that can be claimed

is the somewhat negative one of placing a maximum possible size to the Hall signal. The discussion therefore is taken up with possible explanations for an apparently very small Hall signal.

With electric fields of up to approximately 100 V peak-peak applied to the sample, the smallest Hall voltage detectable would have been of the order of $10\mu V$. The limit was imposed by thermal drift, and could have been improved by a factor of 10^{-1} had a larger magnet been available. A typical value of magnetic field employed was 8,000 gauss.

In most of the published work on this effect in amorphous semiconductors [1] [2], the results have been interpreted simply in terms of an expression of the form

$$\mu_H = \frac{10^8 \times E_{Hall}}{B \times E_{Drift}} \qquad 8.02.1$$

where μ_H = Hall mobility in $cm^2\ volts^{-1}\ sec^{-1}$

Electric fields are in volt/cm

B is magnetic induction in gauss.

This equation is derived from elementary theory which gives

$$E_{Hall} = \frac{1}{ne} B j \qquad 8.02.2$$

using $j = nev$ 8.02.3

These equations of course assume extrinsic conduction over the temperature range of measurement, a property which has not yet been established for amorphous semiconductors.

However, using 8.02.1 μ_H is shown in both [1] and [2] to be approximately $10^{-1}\ cm^2\ volt^{-1} sec^{-1}$ for a number of quite different glasses. Also, the Hall constant is negative in both cases and there are indications that it (and hence μ_H) increase slightly with temperature, above room temperature.

This elementary interpretation shows that for the Te-As system μ_H is between 10^{-1} and 10^{-2} cm^2 $volt^{-1}sec^{-1}$, the sign of R is obviously not known.

Continuing further from this, Ioffe and Regel [3] point out that the mean free path can be written as

$$L \triangleq 10^{-8} \sqrt{m^*/m_o} \cdot \mu \qquad \text{8.02.4}$$

although μ in this equation is the drift mobility and not μ_H which may for these highly disordered materials represent a non-negligible approximation, see 2.09.0.

Such values of mobility as are mentioned above give values of L, assuming $m^* = m_o$, between 10^{-10} and 10^{-9} cm, i.e. very much less than the wavelength of conduction or valence band electrons (in crystalline materials) and much less than the interatomic spacings, and therefore a meaningless result.

Of course μ may really be very small. The large number of traps below E_c many of which according to Cohen (see 3.02) may be charged, will mean the life time, and therefore v (the average drift velocity) and μ, of a free electron are very small. Similar arguments will apply to free holes. However in the absence of any detailed, published argument which will explain the very small values of μ_H and m.f.p. other interpretations are sought. Three possible reasons are discussed, there will of course be others but in this work these appear to be the most relevant.

8.02.1 HALL MOBILITY AND DRIFT MOBILITY

Some comment should first be made on the difference between μ_H, and the mobility used in the conduction equation μ_D, the drift mobility, since these are considered equal in the estimate of L in equation 8.02.4. A detailed semi-quantitative analysis (as for example by Puttley [4]) shows

that

$$R = \frac{-3\pi^{\frac{1}{2}}}{4} \frac{1}{ne} \cdot \frac{\Gamma(2p + 5/2)}{\Gamma^2(p + 5/2)} \equiv \frac{\gamma}{ne} \qquad 8.02.5$$

where it is assumed that the relaxation time for charged carriers is given by

$$\tau = \omega E^p \qquad 8.02.6$$

(see 2.09.0)

By a similar analysis

$$\sigma = \frac{4ne^2}{3\pi^{\frac{1}{2}} m^*} \omega (kT)^p \Gamma(p + 5/2) \qquad 8.02.7$$

The Hall mobility μ_H is defined as $|R\sigma|$ so that

$$\frac{\mu_H}{\mu_D} = \frac{3\pi^{\frac{1}{2}}}{4} \frac{\Gamma(2p + 5/2)}{\Gamma^2(p + 5/2)} \equiv \gamma \qquad 8.02.8$$

The very small value of μ_H above could be explained by equation 8.02.8 if the R.H.S. could be made, say of the order of 10^{-1} or smaller.

Now, assuming that the mean free path in amorphous semiconductors is independent of energy and can be written as

$$L = v\tau \qquad 8.02.9$$

and if

$$v = \left(\frac{2E}{m^*}\right)^{\frac{1}{2}} \qquad 8.02.10$$

then p in equation 8.02.5 is $-\frac{1}{2}$. This will give a value of $\frac{3\pi}{8}$ to the R.H.S. of 8.02.8.

Obviously equation 8.02.9 may not be valid but in fact γ varies very little from unity as p varies from -1 to +1 so that the difference between μ_H and μ_D will not be great.

It is unlikely therefore that the small values for μ_H can be explained in this way.

8.02.2 INTRINSIC CONDUCTION

In chapter 2 it was mentioned that for intrinsic semiconductors, the Hall voltage and hence R could be reduced to zero or some small value. This can occur if it is assumed that in the conduction process the electrons and holes in the conduction and valence bands respectively do not interact, (in the case of the Te-As glasses $E_g \triangleq .9$ ev so that this assumption is valid). It is then possible to sum the Hall coefficients for holes and electrons. The result assuming 8.02.9 and 8.02.10 are valid is

$$R_{Intrinsic} = \frac{-3\pi}{8e} \frac{n_e C^2 - n_n}{(n_e C^2 + n_n)^2} \qquad 8.02.11$$

$$\text{where } C = \frac{\mu_{electrons}}{\mu_{holes}}$$

Now the R.H.S. of 8.02.11 passes through zero very rapidly as C passes through unity, so that there is a very limited range of C which will effectively reduce R. For example, for a non intrinsic material with $n = 10^{14}$ cm^{-3} and $\mu = 10$ cm^2 volt^{-1} sec^{-1} (the assumed minimum possible value), $R = 10^5$ cm^3 C^{-1} . To reduce this below say the limit of detection of the apparatus would mean that $n_e = n_h$ and that μ_{holes} and $\mu_{electrons}$ must be equal to within .01% . On the basis of the computer calculations of chapter 6 the first condition could be satisfied over a considerable temperature range but the second condition is unlikely. The argument which predicts that the conduction band tail of states is longer than the valence band tail, could also be used to argue that $\mu_h \neq \mu_e$ and certainly the difference would be greater than .01%. It is unlikely therefore that the small values of μ_H and R can be explained simply by assuming the material is intrinsic.

8.02.3 INHOMOGENEITY OF MATERIAL

It has been mentioned previously that the conduction processes in amorphous semiconductors may be largely determined by inhomogeneities in the structure, and examples such as crystallites, two phase materials, density fluctuations, etc. have been suggested. Now the space charge regions or potential barriers associated with the inhomogeneities will prevent a simple analysis of the Hall effect. The measured Hall mobility is now an effective mobility. A simple model of a polycrystalline material [5][6], gives the relation between the effective Hall mobility μ_{He}, and the Hall mobility in a crystal μ_{Ho}, as

$$\mu_{He} = \frac{\mu_{Ho}}{1 + \frac{\ell_2}{\ell_1}} \exp \frac{\Delta E}{kT} \qquad 8.02.12$$

ℓ_2 = 2 x barrier thickness

$\ell_1 + \ell_2$ = diameter of crystallite

ΔE = Barrier height.

On the basis of the present available data it is obviously highly speculative to try and apply this equation. However, to obtain an idea of the values of μ_{He}/μ_{Ho} it predicts, let us consider that the Te-As glasses consist of crystallites, the most likely composition being As_2Te_3, being separated by regions of excess As (see 9.03.0). In the middle of the composition range a crude estimate for the volume percentages of the two constituents gives 80% and 20% respectively, which gives a rough estimate of $\frac{\ell_2}{\ell_1} = \frac{1}{3}$ (the final result in fact depends very little on this result if barrier height is $\gg$ kT). The height of the energy barrier ΔE could take any value up to a few tenths of an electron volt, values of .05 ev, .1 ev and .2 ev are considered.

Under these conditions the following values for μ_{He}/μ_{Ho} are obtained at room temperature

$$\Delta E = .05 \text{ ev.} \qquad \mu_{He} \triangleq \frac{\mu_{Ho}}{3}$$

$$\Delta E = -1 \text{ ev.} \qquad \mu_{He} \triangleq \frac{\mu_{Ho}}{16}$$

$$\Delta E = .2 \text{ ev.} \qquad \mu_{He} \triangleq \frac{\mu_{Ho}}{1000} \qquad \text{8.02.13}$$

And it is expected that similar arguments for other types of inhomogeneities would produce similar values.

Hence under these conditions, which may very well be the case in amorphous semiconductors, the effective mobility is easily reduced by a factor of 10^3 or more. A result of $\mu_{He} = 10^{-1}$ cm^2 volt^{-1} sec^{-1} can again be meaningful.

8.02.4 OTHER EXPLANATIONS

Now there may be further explanations for small μ_H, other than outlined above. In particular Allgaier [7] suggests that the Hall effect should never be treated as simply as is usually the case, and shows that by considering closely the shape of the $E(\underline{k})$ surfaces such things as the Hall Effect - Seebock Effect sign anomoly (3.02.0) are then easily explained. The effect in the hopping region of conduction should also be studied. Finally if the mean free paths are only of the order of the inter-atomic spacings, then the major fraction of the electron path is determined by the fields of the scattering ions, and the simple Hall effect theory, again cannot be applied.

8.03.0 SPACE CHARGE LIMITED CURRENTS

For the phenomenon of space charge limited current to be observed in a specimen of semiconductor, three requirements must be fulfilled. First, the number of injected carriers must be in excess of the equilibrium

number at the temperature of the measurement. Secondly, the contact to the semiconductor must be an ohmic one. By this it is meant that at the electrode-semiconductor interface there exists a reservoir of charge carriers, which can be injected into the appropriate band, by the application of an electric field (see also [7]). This reservoir could be the conduction electrons of a metal, so long as E_F was within a few kT of the edge of the conduction band, or more generally if the work function of the metal is less than that of the semiconductor a virtual cathode will form a reservoir as occurs in a simple valve in the insulating space between cathode and anode.

The final condition is that at the temperature of the measurement E_F must be in the region of the forbidden gap where the density of traps or localized states is not too large, since the position of E_F would then be fixed (this point is seen more clearly in the derivation of the I - V characteristics as a function of trap distribution as in 2.10.0).

With the possibility of determining such important information it was obviously desirable to attempt the measurement on at least representative glasses from the systems investigated. It would give information on the suitability of the electrode material, and as well as giving direct evidence of the existence of the postulated localized states, if the I - V characteristic could be fitted to either of the closed forms, equation 2.10.8, the actual distribution would be given.

The former of the above two points is particularly important since it could be argued that the high resistances and activation energies reported in chapter 6 are attributable to a Schottky Barrier, or similar effect, at the metal amorphous semiconductor junction. This is a common occurrence in semiconductors and in making measurements on any new semiconducting material the question of electrode material is of some importance. It will in fact be shown that at least one metal commonly used for electrodes,

does show some rectifying properties. Also discussed are some other general points about contacts to amorphous semiconductors.

It was also possible to make the measurement of space charge limited current on a thin evaporated film and to be able to compare this result with that produced for the bulk material.

8.03.1 SPACE CHARGE LIMITED CURRENTS IN 80Se 20Te

The only other amorphous material on which results of s.c.l.c. have been published is selenium, where specimens were obtained as thin vacuum deposited films. Measurements have been made by Lanyon and Spear [8], Hartke [9], and Lanyon [10]. Of these Hartke used gold as the electrode, and found no difficulty in forming ohmic contacts, whilst Lanyon and Spear used tellurium and platinum and in both cases found that a large voltage had to be applied to the specimen before ohmic contacts were formed. Some explanation of the forming process is given in their work.

For the case of specimens of bulk produced 80Se 20Te using gold electrodes it was assumed that the desired contact was formed immediately, or else very rapidly once a voltage had been applied. The assumption is based on the fact that s.c.l.c. could immediately be observed on applying a voltage. Obviously no evidence can be put forward to indicate whether the contact was electron or hole injecting.

Before commencing measurements, the specimen is left in the dark for a number of hours to allow photo-generated carriers to decay, and the proper equilibrium density of free carriers to be reached. The specimens were highly photoconductive and currents would increase by several orders of magnitude on exposure to white light.

Characteristic of s.c.l.c., the current, upon increasing the voltage would increase very rapidly, and then decrease slowly to a steady value,

FIGURE 8.1

CURRENT-VOLTAGE CHARACTERISTIC FOR A 'BULK' $80Se20Te$ SPECIMEN

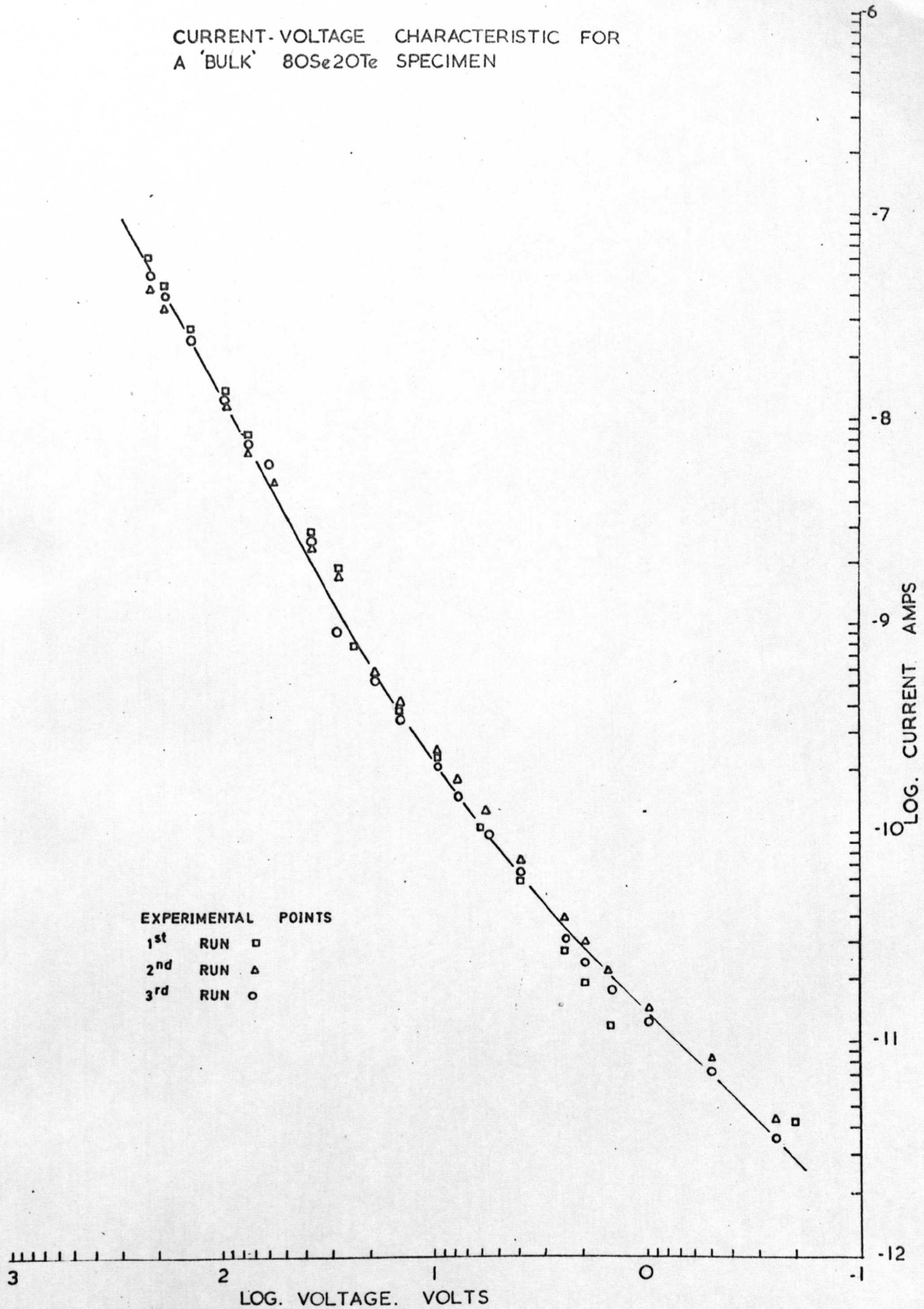

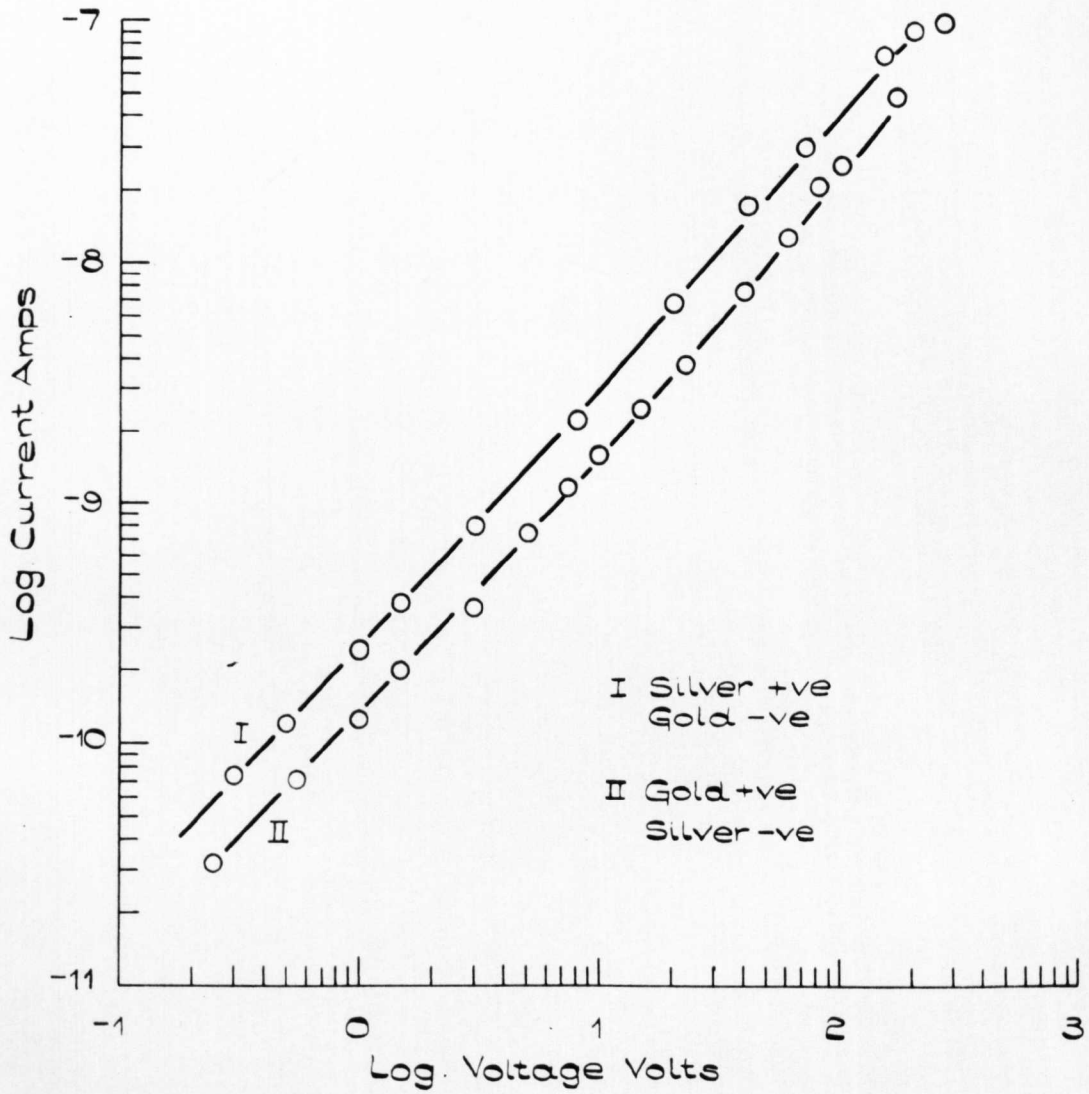

FIGURE 8.2.

LOG CURRENT VS LOG VOLTAGE FOR 80 Se 20 Te WITH GOLD-SILVER ELECTRODES.

reached after several minutes. The process is reversed following a decrease in voltage.

The results of three runs on a 50μ specimen of bulk 80Se 20Te glass are shown in figure 8.1. There is some scatter in the points due principally to not taking measurements at equal time intervals after increasing the current. The results are interpreted in terms of the analysis of section 2.10.

From figure 8.1 it is seen that at high voltages the curve on a log log plot becomes a straight line. This is the behaviour predicted by equation 2.10.8 based on an exponential distribution of states. Also the very low voltage range shows an ohmic behaviour again as predicted .

$$J = \text{Const}\ \ V(V + V_a)^{\Delta/kT} \qquad \text{2.10.8}$$

$$\text{8.03.1}$$

On the basis of this equation, several properties of the distribution can be established. The slope of the curve in figure 8.1 in the high voltage region is 1.81 which according to 8.03.1 gives

$$1.81 = \frac{\Delta}{kT} + 1 \qquad \text{8.03.2}$$

giving $\Delta = .02$ ev

The first point to notice is that for $\Delta = .02$, or α of chapter 6 = $50 ev^{-1} (\alpha = \frac{1}{\Delta})$, the tail of states extend .8 - .9 ev into the gap, which from the data of figures 6.8 is 1.5 ev wide ($E_c - E_v$ in the model of figure 6.1). Without further information it is not possible to say which tail of states is being referred to, whether conduction band or valence band. However such values allow the density of states to fall to zero in the gap as also predicted by the results of chapter 6.

Lanyon [10] in his measurements on Se found values of $\Delta = .067$ ev or $\alpha = 15\ ev^{-1}$, which implies the tail is much longer, in fact some 3.0 ev, which is far wider than the gap itself, and represents a density of states

in the middle of the gap of 10^{12} - 10^{14} states/cc/ev. Such large values of α bring into question the validity of equation 2.10.5 which requires integration from E_F to the end of the tail.

Having made this point concerning large values of Δ, it must be pointed out that values of $\Delta < kT$ are also questionable. This is again seen in the derivation of equation 2.10.4. The assumption made is that after trapping, all states above E_F are full and all those below empty, viz, the low temperature form of the distribution function has been used. This assumption is only justified if $\Delta < kT$. Unless this is fulfilled, P_t the number of trapped holes (above E_F) is in fact less than the number of free holes, as is shown by the equation 2.10.6

$$P = \frac{N}{(N\Delta)^{\Delta/kT}} P_t^{\Delta/kT} \qquad 8.03.3$$

This is exactly opposite to the assumption $P_t \gg P$ on which the analysis of 2.10 is based.

This does not mean that the assumption $P_t \gg P$ is not valid, but requires that the full form of the distribution function be used in the calculation of 2.10.4 since there will be more trapped holes below E_F than above it. The calculations rapidly become difficult since numerical methods must be used and no closed form of I - V is obtainable.

The exact value of α must therefore remain in doubt. However the s.c.l.c. were observed which was the principal object of the exercise.

8.03.2 EFFECTS OF DIFFERENT ELECTRODE MATERIALS

To determine whether or not, other metals provided ohmic contacts the above measurements were repeated using gold as one contact, and a second metal as the other contact. The experiment was completed using copper and then silver as the second contact. The results using gold-silver electrodes are shown in figure 8.2.

In neither case were the s.c.l.c. observed. For the case of silver, where forward and reverse currents were measured the specimen resistance appeared smaller, when the gold contact (and specimen) was negative with respect to the silver. This suggests that the semiconductor is 'n' type, since a forward biasing in such a material requires it to be negative with respect to the metal. However as Henisch [11] points out when the rectification is small this criterion is not reliable. Indeed the values of the work functions of the metals used suggest that gold is in fact hole injecting and during these measurements at least the semiconductor was P type.

Cohen et al [12] suggest that good (i.e. non-rectifying) contacts will always be made to amorphous semiconductors. The argument is based on the fact that any barrier width will be small, because of the large density of localized states available to accommodate the space charge. Such barriers would be easily tunnelled through with little addition to the voltage drop across the specimen.

8.03.3 S.C.L.C. IN 80Se 20Te VACUUM DEPOSITED THIN FILM

It has been mentioned several times during this work that in the author's opinion a distinction should be made between, thin film and bulk-produced materials, and it is here possible to put forward a little evidence to illustrate the point.

A thin film of 80Se 20Te was deposited over a gold contact using the method of simple evaporation described in 4.02.0. The second electrode completing the sandwich was also of gold. The starting material was bulk-produced amorphous 20Te 80Se as opposed to individual powders, and was evaporated from a molybdenum 'boat', in a vacuum of $\simeq 10^{-5}$ torr. The film was brought to atmospheric pressure before the second gold electrode was deposited so that some contamination of one interface is expected.

FIGURE 8.3

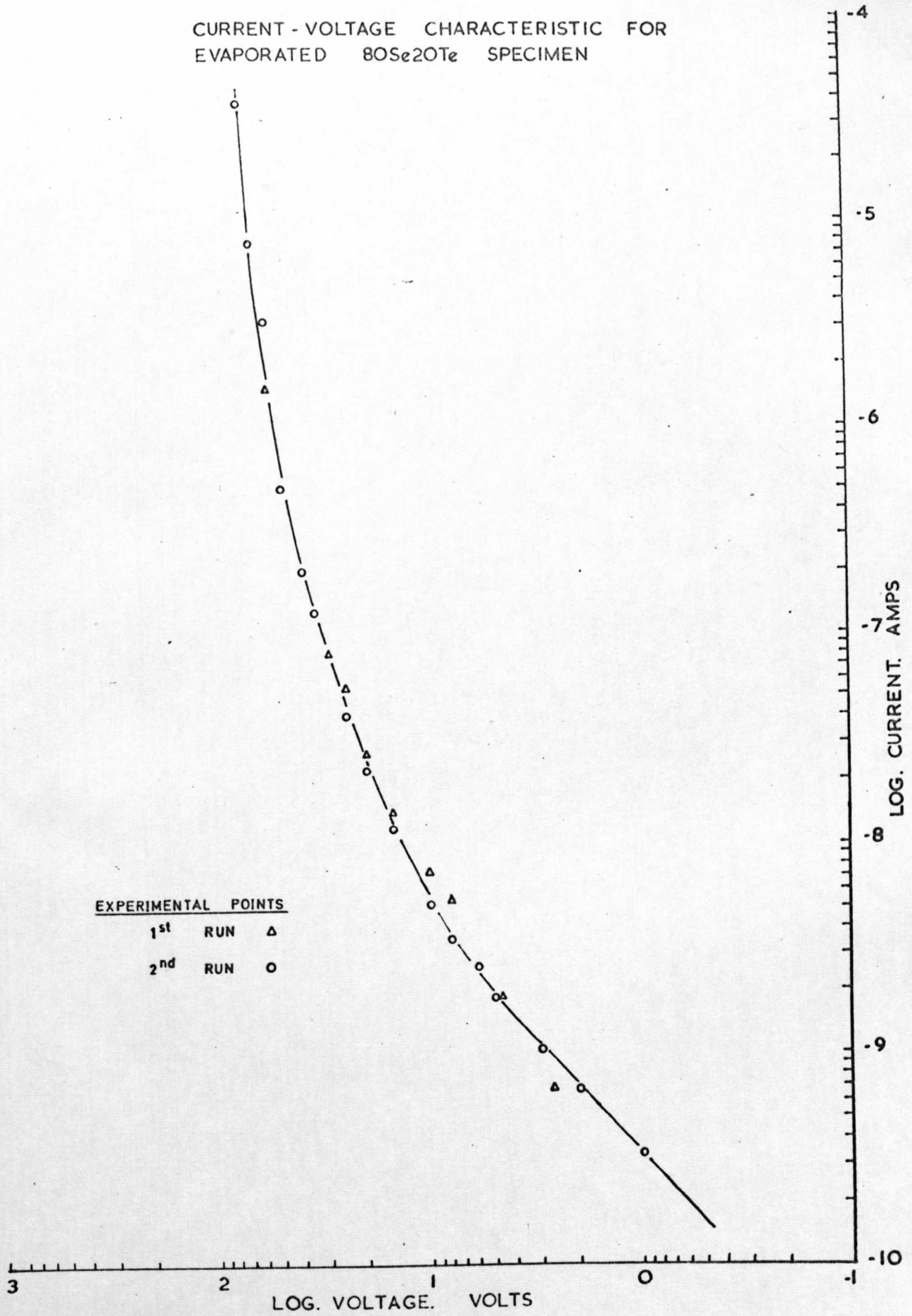
CURRENT - VOLTAGE CHARACTERISTIC FOR
EVAPORATED 80Se20Te SPECIMEN
EXPERIMENTAL POINTS
1st RUN Δ
2nd RUN O
LOG. CURRENT. AMPS
-4
-5
-6
-7
-8
-9
-10
3
2
1
0
-1
LOG. VOLTAGE. VOLTS

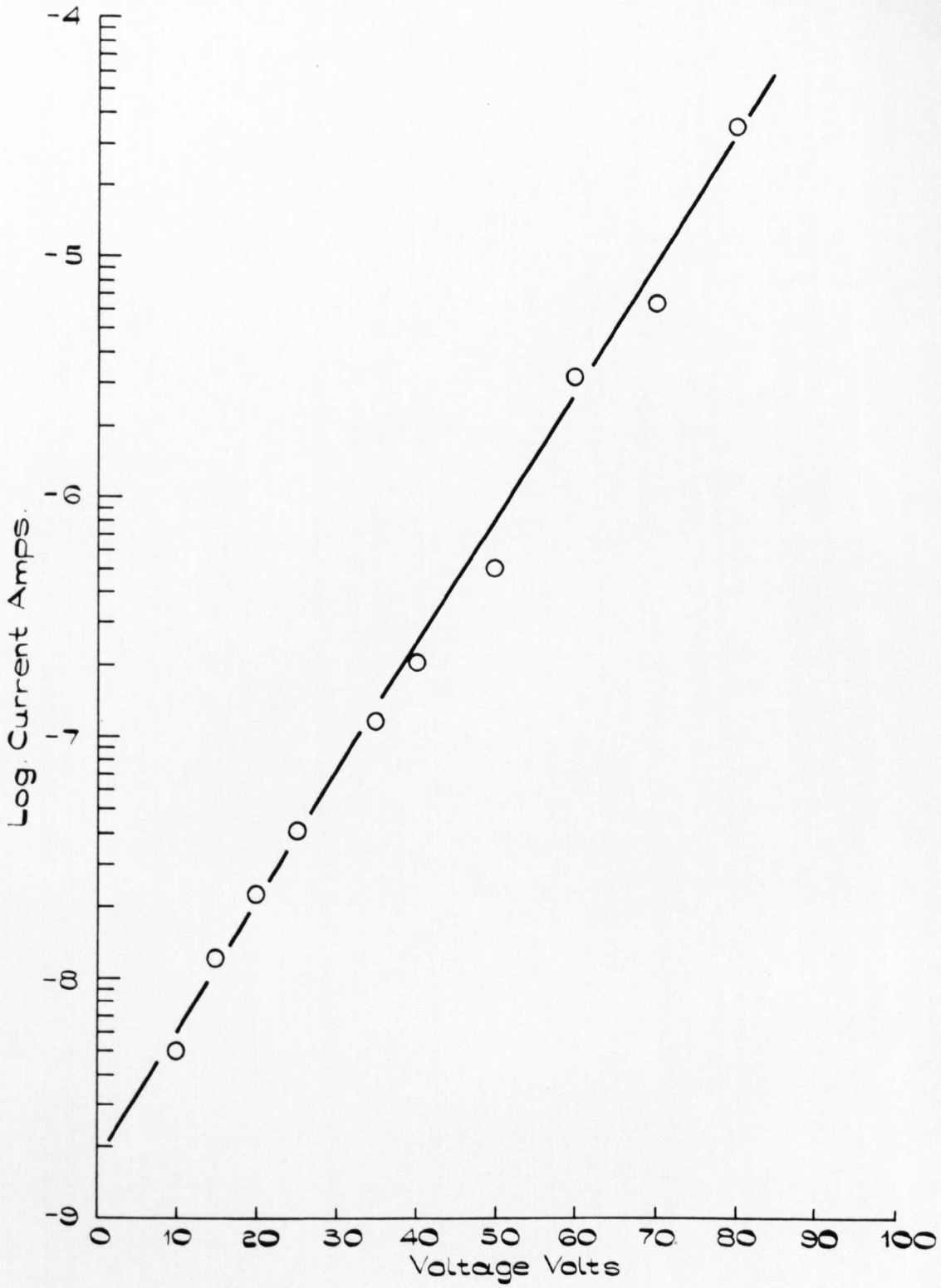

FIGURE 8.4.

LOG. HIGH FIELD CURRENT VS VOLTAGE FOR THE CURVE OF 8.3.

The current transient on increasing voltage was again indicative of s.c.l.c. The complete I - V curve is shown in figure 8.3.

At high voltages the current is increasing far more rapidly than that of figure 8.1. A close investigation in fact shows that the curve is much better described by

$$J = \text{const}\ V \exp \frac{\beta V}{N_T kT} \qquad 8.03.4$$

i.e. equation 2.10.8, which is the I - V relationship based on a continuous distribution of localized states of density N_T/cc/ev. A plot of V against log J in figure 8.4 for the high voltage points shows the exponential dependence. The slope of this line according to equation 8.03.4 is $\beta/N_T \cdot kT$, and β from the literature is given by

$$\beta \simeq \frac{\epsilon\epsilon_0}{e L^2} \qquad 8.03.5$$

assuming L = 1 and $\epsilon \simeq 2$.

$$\beta \simeq 1.2 \times 10^{14}\ cc^{-1}\ V^{-1}$$

From the slope of the line in figure 6.4, and writing kT = .025 ev N_T is given as

$$N_T \simeq 1.2 \times 10^{15}\ cc^{-1}\ ev^{-1}$$

which is not an unreasonable value.

There is therefore here, evidence that localized state distribution in the gap is different depending on the method of preparation, i.e. thin film or bulk-produced. The difference in electronic structure will be related to the difference in the short range order, which will probably be the combined effect of a slight composition change as well as a change in the structure of the network.

This result will certainly have implications as far as other properties of the materials are concerned and points out the importance of making the distinction.

8.03.4 S.C.L.C. IN 60Se 40As

The measurement of 8.03.2 and 8.03.3 was repeated on a sample from the As-Se system, namely 60Se 40As.

Using a specimen of 30μ, no non-linear dependence of I vs V was found. However two other similar characteristics were found: The specimen was highly photoconductive, and, of more importance, the characteristic transient currents were observed. The decay time of the current was however much reduced being only of the order of 1 - 2 seconds. This strongly suggests a very large density of traps, which will have the effect of pinning the Fermi level and thus preventing non-ohmic I vs V characteristics.

This result is in qualitative agreement with that from optical absorption which also predicts a large density of states in the band gap.

8.03.5 DISCUSSION AND SUMMARY

The principal object in making these measurements was to illuminate the possibility of contact resistance as a source of high impedance and activation energy, and to obtain direct evidence of the existence of localized states.

The first of the above two points, can be claimed fairly confidently for 80Se 20Te and somewhat less confidently for 60Se 40As. To extend these conclusions to other glasses in the respective systems should be done with caution, but two points would support this: (1) that gold also gives ohmic contact to amorphous Se [9] and, (2) that E_g for As-Se is constant over much of the system (here again one should be careful since electron affinity is the most important parameter).

The effect of localized states acting as traps was also observed, although exact deductions of trap distributions were not possible.

However it has been noted that non-linear I - V characteristics will only occur if E_F actually moves through the localized state distribution. It has also been stated that serious overlap of the bands (as the results of chapter[7]and Lanyon [9] imply) would act to pin the Fermi level. Since non-linearity was observed, it can be assumed that E_F is not pinned and that the band overlap is not serious. The result of conductivity as a function of temperature for 80Se 20Te (chapter 6) also predicted α values which would give only a small amount of band overlap so that the two experiments can be said to agree. One must also remember however that values of α from optical absorption measurements do not agree (see 7.06.1 and 7.06.5) with this result.

Evidence has also been given to suggest that localized sate distributions are different for bulk produced and 'thin film' produced materials, and it is recommended that some caution should be observed in generalising theories to accommodate both of these classes of amorphous materials.

REFERENCES CHAPTER 8

(1) Male J.C., Brit. J. Appl. Phys., p. 1543, Vol. 18, 1967.

(2) Peck W.F., and Dewald J.F., See (8) of Chapter 3.

(3) Ioffe A.F., Regel A.R., Prog. in Semiconductors 4, p. 237, 1960.

(4) Putley E.H., The Hall Effect and Related Phenomena, Semiconductor Monographs, Butterworths, London, 1960.

(5) Berger H., Phys. Stat. Sol. 1, p. 739, 1961.

(6) Berger H., Janiche G., Grachovskaja N., Phys. Stat. Sol. 33, p. 417, 1969.

(7) Kroger F.A., Diemer G., and Klasens H.A., Phys. Rev. 103, p. 27, 1956.

(8) Lanyon H.P.D., and Spear W.E., Proc. Phys. Soc. 77, p. 1157, 1961.

(9) Hartke J.L., Phys. Rev. 125, p. 1177, 1962.

(10) Lanyon H.P.D., Phys. Rev. 130, p. 134, 1963.

(11) Henisch H.K., Rectifying Semi-Conductor Contactors, p. 197, Oxford, 1957.

(12) Cohen, M.H., Fritzche H., and Ovshinsky S.R., Phys. Rev. Letters 22, p. 1065, 1969, and Reference (10) of Chapter 3.

CHAPTER 9

COMMENTS ON MICROSTRUCTURE

9.01.0 INTRODUCTION

Of the eighteen glasses investigated in this study, only two had been previously reported in the literature. Consequently there were no data available concerning even very fundamental and simple properties such as density, which would normally be one of the first measurements made on any new material.

This measurement would be an essential one in the study of microstructure, and it would be expected that any drastic change in microstructure which occurs on varying the composition within a given system would result in a change in the density. It was in fact for this second reason that the measurement was made. Because of its partial success in providing information about one system, it became a routine measurement.

It has been stated in chapter 4 that X-ray diffraction, using the Debye Scherrer technique was to be applied to all glasses as a test for amorphousness. The results of these tests are also discussed in this chapter. Some results concerning the structure of the devitrified materials are also given where it is thought that they might contribute to knowledge of the original glass.

9.02.0 DENSITY

The results of d.c. conductivity on the Se-As system showed a peak in certain parameters of the stoichemetric $As_2 Se_3$ composition, and in chapter six one of the suggested causes of the behaviour was that the material consisted of two phases. One of these phases was presumed to be As_2Se_3 and the other selenium or arsenic depending upon which side of the stoichemetric composition was being considered. Such a drastic change in

microstructure on passing through $As_2 Se_3$ would, it was thought, show up in measurements of density, and hence the measurements were made.

The measurement was made on all systems and results for each are discussed separately.

9.02.1 SELENIUM ARSENIC SYSTEM

The results of density versus composition are shown in figure 9.1. The form of the dependence immediately suggests something more than a continuous charge of composition occurring in a completely, and ideally random structure. Two other facts are pointed out. The density of amorphous $As_2 Se_3$ is within 2% of the density of crystalline $As_2 Se_3$, and in contrast, the densities of crystalline and amorphous Se are much further removed, the difference exceeding 10%.

The latter points made in the above paragraph are considered first: If these disordered structures can be considered as perturbations of the structure of the equivalent crystal, then the results of figure 9.1 must lead to the suggestion that amorphous $As_2 Se_3$ is less disordered than for example amorphous Se. Just what differences there are in the extent of the disorder, and what this will mean in terms of lengths of band tails cannot be said (the results on these materials in chapters 6 and 7 cannot lead to any positive conclusions about this point). It will however be shown later in this chapter that this argument of a less disordered structure is upheld by results of attempting to devitrify the glasses.

As has already been stated there is also information suggesting Se-As glasses are two phase on either side of the stoichemetric composition, and the further evidence given by density measurements is now discussed. Consider the selenium rich side of $As_2 Se_3$, and the possibility of two phases existing, one $As_2 Se_3$ and the other Se, where both are amorphous.

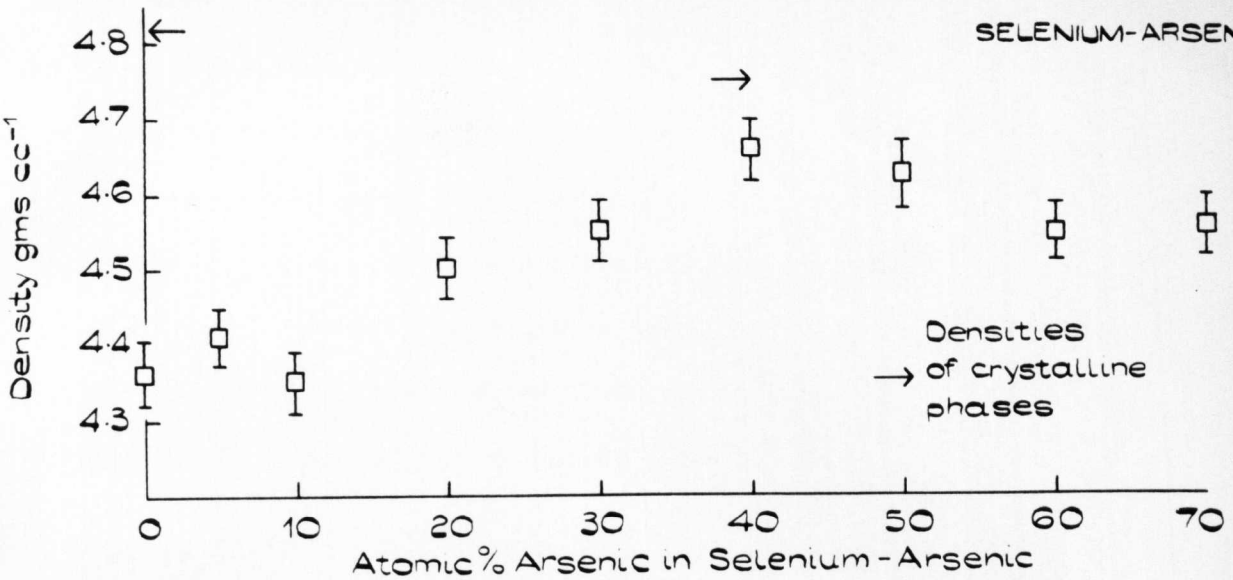

FIGURE 9.1.

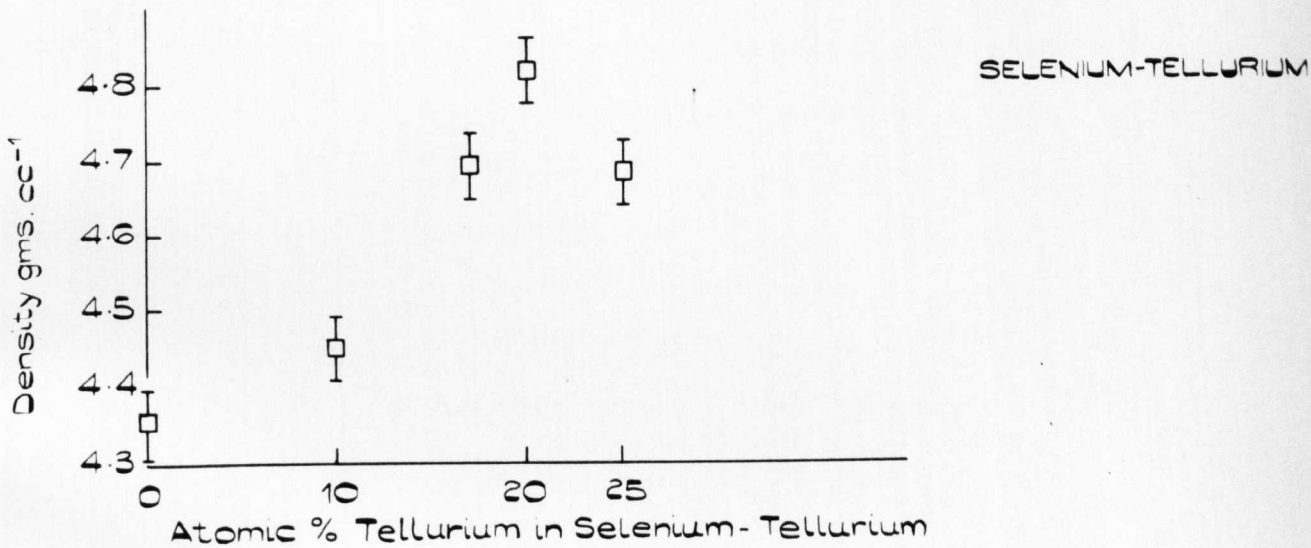

FIGURE 9.2

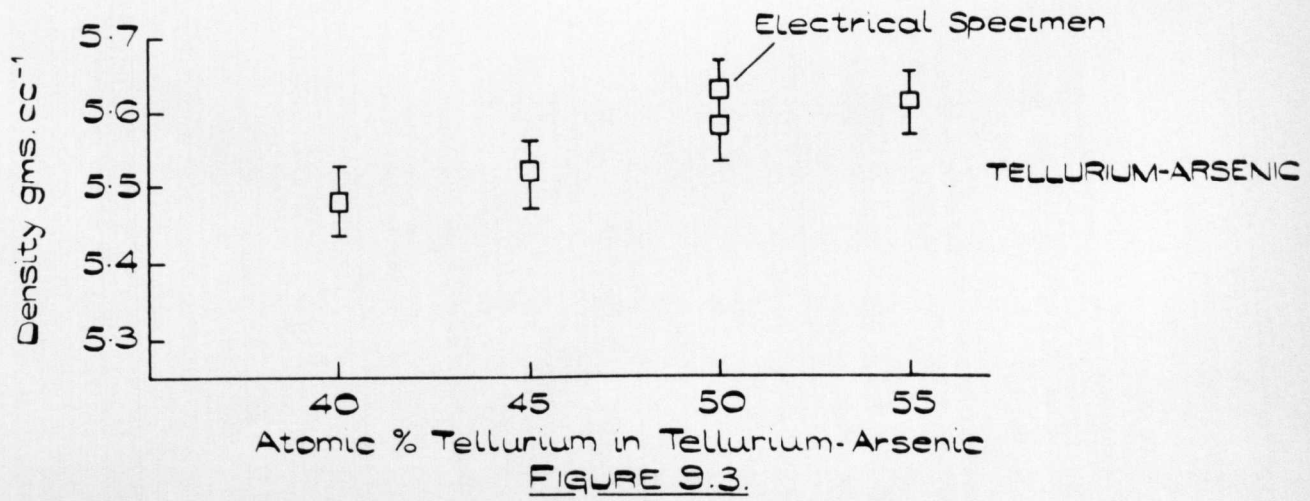

FIGURE 9.3.

FIGURES 9.1 - 9.3 DENSITY VS COMPOSITION FOR THE THREE SYSTEMS.

PAGE NUMBERING AS IN THE ORIGINAL THESIS

In this case, the densities of the resulting glasses will lie on the line passing through the points corresponding to selenium and amorphous $As_2 Se_3$. This is the case down to 80Se 20As. For glasses containing less than approximately 20 At.% arsenic this structure would appear to break down. It is known from other work (see 6.06.1) that small additions of arsenic to pure amorphous selenium are used in cross linking the chains and rings of the selenium network. From these facts it could be argued that somewhere between 10-20 At.% arsenic, a Se-As structure becomes established and is present as a second phase.

On the arsenic rich side, the density again falls off linearly with composition up to 60 At.% arsenic. The form of the excess arsenic if in fact it exists must, on the basis of X-ray results be amorphous. No report of an amorphous phase of arsenic has been published to the author's knowledge and there is no reason why it should appear as a second phase in Se-As glasses, so on this information the two phase argument breaks down.

The idea that the system at least over the range 20-60 Atomic % arsenic is two phase can obviously be considered complementary with the above, "more disordered - less disordered" argument.

9.02.2 SELENIUM TELLURIUM SYSTEM

There is little that can be deduced from the results for this system shown in figure 9.2.

In chapter 6 it was deduced that although additions of Te up to 20 At.% in selenium reduced the size of the forbidden energy gap, the lengths of the band tails remained approximately constant. The results of figure 9.2 show that up to the same composition the density increases with Te content. This will obviously be the result if the heavier tellurium atoms are simply replacing selenium atoms in a random network. This

substitution would require no further ordering of the structure, and would uphold the argument that the lengths of the band tails remain constant for additions of up to 20 Atomic % tellurium.

If density is related to disorder then the result for 75Se 25Te would indicate a more disordered structure for this glass. On this basis it has already been argued in chapter 6 that this glass is not representative of the rest of the system, and results of electrical measurements support this conjecture.

9.02.3 THE TELLURIUM ARSENIC SYSTEM

The increase in density of the as quenched material as tellurium content is increased, can again be simply associated with the replacement of arsenic by heavier tellurium atoms in some random arsenic-tellurium lattice.

There was evidence that heat treating for very short times, i.e. a few minutes, at approximately 150°C would produce increases in density. This occurred for the specimen of 50Te 50As which showed the anomolous behaviour of conductivity at low temperature. The density increased to 5.63 from 5.58 gms/cc. The experiment could not be repeated because of insufficient material, but all glasses devitrified rapidly at 250°C so that a preliminary increase in density may be expected.

The density of the crystalline phase of 60Te 40As which would be useful as a comparison is unfortunately not known.

9.03.0 X-RAY DIFFRACTION

Using copper K_α X-rays (λ = 1.541 Å) and the Debye Scherrer technique, all glasses, with one exception, showed no long range order, as deduced from the powder diffraction patterns.

This result must be interpreted in terms of the analysis of 4.04.1. In fact, for the Se-As and Se-Te glasses it was not even possible to detect the diffuse lines often associated with short range order in amorphous materials (see fig. 4.4 for typical example). If the completely diffuse patterns that were obtained, are assumed to consist of a number of lines sufficiently diffuse as to be indistinguishable then using the equation (see 4.04.4)

$$\text{Half Width} = \frac{.89 \times \lambda}{D \cos \theta} \qquad 9.03.1$$

would indicate that any crystallite would be less than approximately 50 Å in any dimension. However in these two systems the compositions were not generally stoichemetric and also from the evidence that will be given later in this section the idea of a two phase structure is refuted. Hence the probability of these materials consisting of small crystallites is made much smaller. The implication is that these compositions actually form ideal random structures.

For the Te-As glasses, some structure was suggested in the diffraction patterns, an example of one of the patterns is given in figure 9.4. This result again interpreted from the viewpoint that the material consists of very small crystallites, suggest a crystallite size of $\triangleq$ 80 Å .

The one glass for which sharp lines were seen in the diffraction pattern was selenium. Three attempts were made to produce the material free of this "defect" but it was present in each case. The lines were in fact very weak and were superimposed on the diffuse background characteristic of other selenium containing glasses, hence the volume fraction of the crystals was expected to be very small. They are not therefore suspected of affecting the electrical or optical properties of the amorphous phase. It is worth noting that such samples of selenium exhibited conchoidal fracture similar to all other glasses, a fact which illustrates the limitations of the fracture surface test.

FIGURE 8.4

DEVITRIFIED
75Se25Te
Se-Te
3·78Å
3·04
2·07Å
Se
DEVITRIFIED
60Se40As
Se-As
4·87Å
2·86Å
1·78Å
As2Se3
AMORPHOUS
55Te45As
DEVITRIFIED
55Te45As
As
2·77Å
3·25Å
3·00Å
2·32Å
1·96Å
As2Te3
DEVITRIFIED
40Te60As
Te-As

To further prove or disprove that stoichemetric selenium - arsenic glass, was less disordered than others in this system, a simple test was made on the ease of devitrification. The stoichemetric glass, plus one from either side namely 70Se 30As and 50Se 50As were heat treated at 220°C for 24 hours. After this time only the 60Se 40As glass had devitrified. Neither of the other two glasses indicated any change of structure (as determined from X-Ray diffraction). Interpreting devitrification as simply an ordering of the structure one can conclude that either (a) $As_2 Se_3$ is less disordered or (b) the structure is less complicated, which two statements could of course be considered synonymous. The idea of a two phase structure is not supported by this result, since a separate phase of amorphous $As_2 Se_3$ would presumably devitrify as rapidly as did the 100% $As_2 Se_3$ specimen.

It is seen from figure 9.4 that the devitrified $As_2 Se_3$ also has a highly distorted structure. This is deduced by the splitting of the strongest lines corresponding to the $As_2 Se_3$ structure [1], which can be attributed to variations in the crystal symmetry.

Arsenic - tellurium glasses devitrified above approximately 220°C to show the structure of arsenic - telluride $As_2 Te_3$ [2]. For the composition farthestremoved from the stoichemetric one, namely 40Te 60As, it was also possible to detect the strongest lines of the arsenic structure [3] indicating that in the devitrified material arsenic, and arsenic - telluride are present as separate phases.

Selenium - tellurium glasses devitrified rapidly above 80°C. The glass containing the highest tellurium content devitrified to show the selenium structure only (figure 9.4) [4].

9.04.0 THE GLASS FORMING LIMITS

This chapter is concluded with a statement of the glass forming

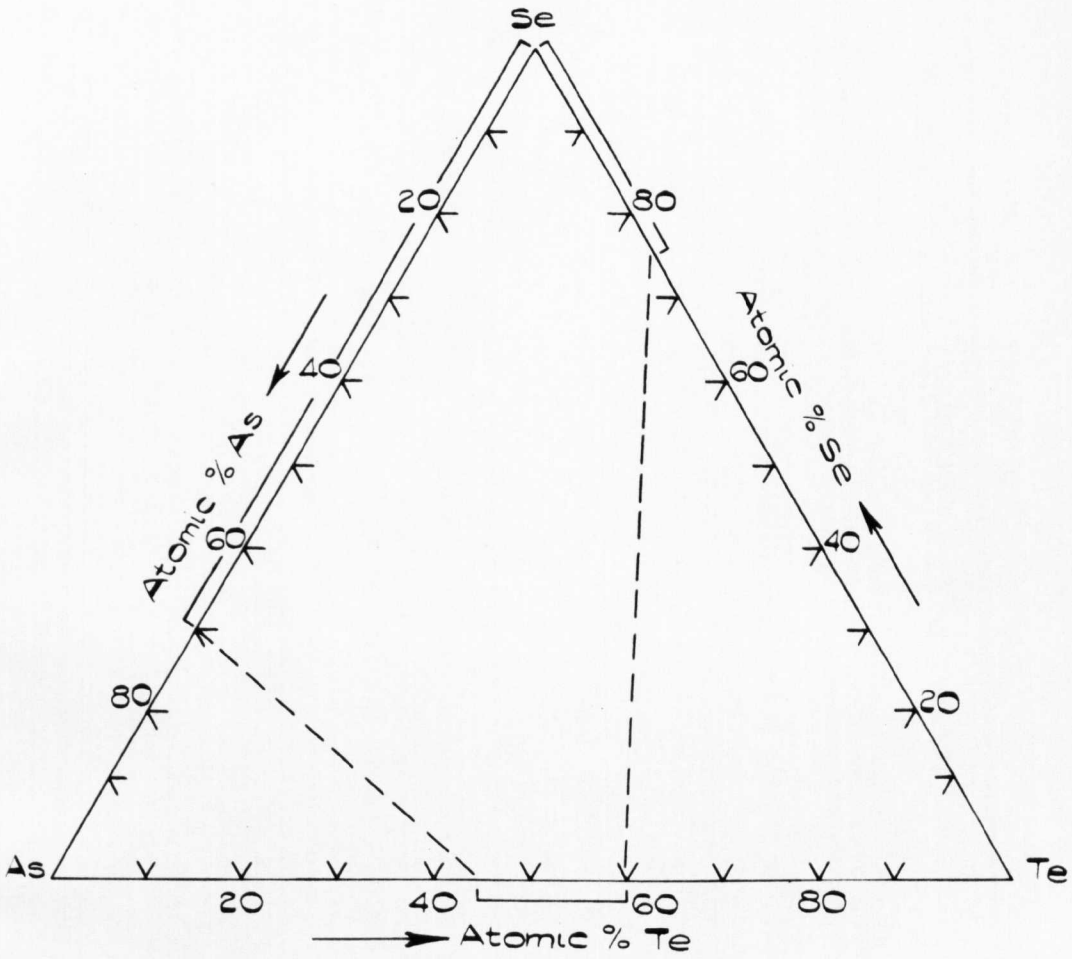

FIGURE 9.5.

GLASS FORMING UMITS FOR BINARY GLASSES FROM SELENIUM - TELLURIUM - ARSENIC

limits for binary combinations of arsenic - selenium - tellurium, as determined by this study. The statement is given in figure 9.5.

In this figure the dashed lines are not intended to represent the glass forming limits of the ternary glasses, but they would be expected to provide a good starting point in investigating the ternary system.

REFERENCES

1 A.S.T.M. Index Card No. 17-327

2 A.S.T.M. Index Card No. 15-407

3 A.S.T.M. Index Card No. 5-0632

4 A.S.T.M. Index Card No. 6-0362

CHAPTER 10

CONCLUSIONS

10.01.0 INTRODUCTORY NOTE

This final chapter summarizes only the more important (and positively identified) conclusions. It is intended to be brief, since full discussionsof the results are given in the results and discussion sections of the various chapters.

10.02.0 THE DENSITY OF STATES IN AMORPHOUS SEMICONDUCTORS

The theoretical ideas that were discussed in chapter 3, suggested that a model exists which will describe the essential features of the density of states for amorphous semiconductors. This model summarized in figure 6.1 should apply to a very large range of disordered solids.

It has been possible from the experimental results to substantiate to a large extent this model, and to show that it applies to all of the materials considered. The existence of the postulated localized states below the conduction band and above the valence band has been clearly demonstrated in conductivity, and space charge limited current measurements. These states were assumed to act as acceptor and donor states respectively. Then from the results of computer calculations and measurement, between which there was considerable agreement, it was shown that at very low conductivities the activation energy describing the conduction was associated with excitation to these localized states, i.e. the conduction was extrinsic, becoming intrinsic at higher temperatures. The calculations and measurements also clearly indicated why, in general, measurements above room temperature only, lead to the erroneous conclusion that intrinsic conduction always persists (see 1.04.1).

It was not possible from the conductivity or s.c.l.c. measurement to obtain an exact value of the lengths of tails of states. However estimates made in both cases strongly suggested they were such that N(E) became unity within a few tenths of an electron volt from the band edges.

The same general behaviour of the conductivity, in particular the temperature dependence of the activation energy, applied to all glasses. Such a result supports the conjecture that certain features of the proposed model will be applicable to a large range of materials.

Also supporting the general features of the model is the remarkably close agreement in all cases of the σ_o value. This parameter is the infinite temperature value of the conductivity σ, in the normal intrinsic semiconductor expression for the conductivity. It has been argued that this agreement suggests approximately equal values in each case for the density of states at the band edges.

The proposed model, was also used to calculate the optical absorption coefficient as a function of photon energy. (Band to band transitions were considered to be the dominant absorption mechanism.) The calculations were based on the density of states product for the conduction and valence band edges, and justification for this straightforward approach was given. Assuming the tails of states to decay exponentially the theoretical absorption edges were not surprisingly also exponential, and the results of experiment agreed with this. However as was discussed there are other explanations of exponential edges and these should not be overlooked in a close examination of the effect.

From the calculations, a law was derived which gave the length of the longest tail (i.e. conduction or valence band) in terms of the gradient of the absorption edge, $\frac{\partial(\log_{10} K)}{\partial h\nu}$. The extent of the tails as deduced from the absorption measurement using the relationship were not in agreement

with the estimates deduced from conductivity and s.c.l.c. measurement. In all cases the absorption measurements predicted longer tails. Also, in the Se-Te system, absorption measurements could be interpreted to show that the tail length decreased as tellurium replaced selenium in the lattice, implying that tellurium decreased this disorder. However from the form of the $\log \sigma$ vs $^{1}/_{T}$ curves for glasses in this system it was argued that in fact the tail length, or more exactly the number of states in the tail remained approximately constant, i.e. the degree of disorder did not change.

In the discussion it was suggested that amongst other possibilities the method of calculating $K(h\nu)$ may be brought into question to explain the discrepancy.

10.03.0 MOBILITY OF CHARGE CARRIERS

If the standard interpretation of the Hall effect as applied to crystalline materials with long mean free paths is valid here (and this has been questioned), it must be concluded that the Hall mobility and probably the drift mobility are very small $< 10^{-2}$ cm^2 V^{-1} sec^{-1} (In the model this statement applies to states above E_c or below E_v). In explanation of this result it has been pointed out that one should ascribe this value to an effective Hall mobility, which will be reduced from the real value by intrinsic conduction or a polycrystalline type microstructure.

10.04.0 OTHER CONCLUSIONS

The amorphous nature of all the materials was verified by X-ray diffraction and this, together with measurements of density and the results of devitrification experiments, suggests that the term "random structure" may well describe these glasses. The suggestions of two phase structures and polycrystallinity were not generally supported.

Experiments entailing space charge limited current measurement gave further strong evidence for the existence of localized states, and eliminated the possibility of contact phenomena being the source of the high impedances and activation energies. Comparison of thin film and bulk produced samples, ostensibly of the same composition, gave results, interpreted as showing considerable differences in the localized state distribution.

The likelihood of conduction in localized state regions, by a thermally activated tunnelling ('hopping') process was raised in chapter 3. An anomolous conductivity - temperature - electric field characteristic in two annealed glasses was thought to be associated with such a mechanism. A very low field dependence of conductivity associated with the effect could not be explained by any well established field effect.

10.05.0 SUGGESTIONS FOR FURTHER WORK

The range of experiments and materials still to be studied in the field of amorphous semiconductors is vast. It is not possible to select any preferential area in which to work. However to help answer some of the more specific questions raised in this work the following should be completed:

Firstly, the measurement of conductivity should be carried out to its lowest possible limit. It should be possible for many of the glasses studied here, to reduce the measured σ by another one or two orders of magnitude. Suitable specimen shapes and electric fields would enable this to be done. The results would help to verify whether or not at low temperatures the activation energy does in fact reach a constant value.

The question of the effect of impurities in disordered solids has from time to time been raised. Some controlled experiments to give more understanding of just what their effect is would be greatly beneficial.

Electron microscopy applied to any of these glasses would also greatly assist in the interpretation of results, and in particular the question of the microstructure would be finally solved.

Two areas of theoretical work in particular might give useful information. Firstly, a calculation of absorption coefficient based on a more refined model than that of chapter 7 would be worthwhile, since it is particularly important to know whether or not length of tails of state can be found in the manner suggested. Secondly, an understanding of the Hall effect in disordered systems will be required if this measurement is to produce the wealth of information achieved for crystalline semiconductors.